



University
of Glasgow

Stepto, Hannah (2015) *Development of adenoviral and miRNA eluting stents*. PhD thesis.

<http://theses.gla.ac.uk/7175/>

Copyright and moral rights for this thesis are retained by the author

A copy can be downloaded for personal non-commercial research or study

This thesis cannot be reproduced or quoted extensively from without first obtaining permission in writing from the Author

The content must not be changed in any way or sold commercially in any format or medium without the formal permission of the Author

When referring to this work, full bibliographic details including the author, title, awarding institution and date of the thesis must be given

Development of adenoviral and miRNA eluting stents

Hannah Stepto, MSci

Submitted in the fulfilment of the requirement of the degree of Doctor of Philosophy in the College of Medical, Veterinary and Life Sciences, University of Glasgow

British Heart Foundation Glasgow Cardiovascular Research Centre, Institute of Cardiovascular and Medical Sciences, College of Medical, Veterinary and Life Sciences, University of Glasgow

September 2015

© Hannah Stepto

Author's Declaration

I declare that this thesis has been written entirely by myself and is a record of the work performed by myself with the exception of the animal surgery at the Institute of Cardiovascular and Medical Sciences and the School of Chemistry (University of Glasgow), under the supervision of Prof A.H. Baker, Prof L. Cronin and Prof. K. Oldroyd. The pig stenting surgery was performed by Dr. S. Kennedy and Dr. R. McDonald at the Biological Procedures Unit (University of Strathclyde). The mouse stenting surgery was performed by Dr. R. Dakin at the Institute of Cardiovascular and Medical Sciences (University of Glasgow). This thesis has not been submitted previously for a higher degree.

Hannah Stepto

September 2015

Acknowledgements

Firstly, I would like to thank my excellent supervisors Professors Andrew Baker, Lee Cronin and Keith Oldroyd for providing me with support and guidance throughout my doctoral studies. When I first arrived in Glasgow I hadn't set foot in a biological laboratory, and thought when my friend's mouse died, that she was referring to her pet, so it was a steep learning curve. I therefore would like to give special thanks to Andy who has been patient, supportive and helpful, encouraging me to embrace the biology and conduct my experiments with conviction. I do not think I could have asked for a better mentor. I would also like to thank Lee, who made me feel included within the chemistry group, even when I was working in biology for large parts of my time. I think Lee's relentless enthusiasm and energy for science rubs off on everybody who works with him. Finally, Keith's expertise provided the project with a clinical overview for which I was very grateful, and I thoroughly enjoyed my insightful visit to the Golden Jubilee to watch the stenting procedure in action. I would also like to thank the University of Glasgow and the Lord Kelvin Adam Smith PhD Scholarship for funding these studies.

Secondly, I would like to thank everybody in the Level 4 Lab and the Cronin Lab that has helped me throughout my time in Glasgow, particularly Nicola Britton and Gregor Aitchison who have been great to work with, both professionally and personally. I would like to thank Dr. Robert McDonald, Dr. Simon Kennedy and Dr Rachel Dakin for conducting all the animal surgery, which has been a vital part of this research. I really appreciate all the time and effort put into those studies.

A special mention should go to Dr. Alan Parker, who was absolutely brilliant when I first arrived in Glasgow and helped me immensely to learn the ropes in my first year.

During my time in Scotland I have made some really good friends. I would like to thank Lorna and Leanne, our journey on the West Highland Way, the cheese party to end all cheese parties, lunches in the Botanic Gardens and our hilarious attempt at a triathlon with Liz are all times I will look back on with a huge smile on my face. That brings me on to Liz, who has been a brilliant friend to me. I feel like

she is my 'PhD sister. We both started on the same day in Glasgow after moving up from Bristol. Despite mistaking Liz's Geordie accent for a Welsh one and writing Elizabeth Taylor on her TC flasks, because the name sounded strangely familiar, she still made friends with me, for which I am really grateful. We have had such a laugh together! Thanks to Josie, Clare, Lesley, Jenny, Hollie, Lisa, Caroline & Chris L, who I have had a great time sharing office with, and who have all been lovely to be around. Thanks to Carla; sharing a flat with you was absolutely hilarious, you are amazing! Thanks to curry lads Nick and Jen, Banana Leaf will miss us when we are gone. I will miss John Mercer's intellectual chat and poetry. Thanks to the cycling crew, LGW, Luke, Faux, Sally, Alan, Paul & Cog, big 10! And finally thanks to Lucy and Tom my best friends from home.

Most importantly I would like to thank my family: Mum, Dad, brothers Alan and Robert and grandparents for all the help, love and support throughout the years, I think you know that I couldn't have done it without your encouragement and enthusiasm for everything that I do. In particular I would like to thank my two grandads, who have been an enormous inspiration to me.

Finally, I would like to thank my boyfriend Cogs, for being such a great friend and for cooking such nice curries. There is no one else I would prefer to walk up a mountain with. I have had so many brilliant adventures with you and Car in Scotland. You have been the person on the frontline of my PhD experience, thanks for looking after me and being a brilliant friend, I will miss you when you are in Sweden.

Table of Contents

Development of adenoviral and miRNA eluting stents	1
Author's Declaration	2
Acknowledgements	3
List of Tables	9
List of Figures	10
List of Publications	12
List of Abbreviations	13
Summary	21
1 Introduction	24
1.1 Cardiovascular disease	25
1.2 Treatment of coronary heart disease	28
1.2.1 Stent Technology	32
1.3 Mechanisms for neointima hyperplasia	40
1.4 Therapeutic strategies for prevention of in-stent restenosis	43
1.5 Vectors for cardiovascular gene therapy	47
1.5.1 Non-viral vectors	47
1.5.2 Adenoviral vectors	50
1.5.3 Adeno-associated vectors	56
1.5.4 Lenti-viral vectors	58
1.6 miRNA	59
1.6.1 Biogenesis of miRNAs	59
1.6.2 miRNAs involved in in-stent restenosis	62
1.7 Delivery of therapeutic vectors from stent surfaces	66
1.7.1 Local delivery of virus vectors from stent surfaces	66
1.7.2 Delivery of miRNA from stent surfaces	71
1.8 Project aims	73
2 Materials and Methods	74
2.1 Materials	75
2.2 Cell culture techniques	75
2.3 Production of adenoviral vectors	75
2.3.1 Adenovirus Purification	76
2.3.2 Virus Titration by End-Point Dilution Assay	77
2.3.3 Virus Particle Concentration Determination	78
2.3.4 Labelling adenovirus 5 with Alexa Fluor™ 555	78
2.4 Formation of Polyelectrolyte Multilayers (PEMs)	79
2.5 UV-visible light Spectroscopy to monitor build-up of PEMs	79

2.6	Visualisation of fluorescently tagged adenovirus on polycationic monolayers	80
2.7	Atomic Force Microscopy (AFM)	80
2.8	Adenovirus transduction <i>in vitro</i>	80
2.8.1	Transduction of A10 cells with Ad5 CMV lac Z.....	80
2.8.2	Measuring the effect of polycationic solutions on adenoviral transduction	81
2.8.3	Measuring the effect of different concentrations of acetic acid on adenoviral transduction in a chitosan solution	81
2.8.4	Measuring adenoviral transduction from SS surfaces coated with PEMs	82
2.8.5	Measuring adenoviral transduction from adenovirus encapsulated in collagen gel from PLA and SS surfaces	82
2.9	<i>Ex vivo</i> transduction of Ad5	83
2.9.1	<i>Ex vivo</i> transduction of Ad5 from stent surfaces coated with (chi-ha) ₈ chiPEMs to rat aortas.....	83
2.9.2	<i>Ex vivo</i> delivery of Ad5 CMV lacZ to mouse aorta.....	83
2.9.3	<i>Ex vivo</i> delivery of Ad5 CMV lacZ from PLA coated stents to porcine coronary arteries	84
2.10	β -galactosidase transgene quantification	85
2.11	Protein concentration determination from cell lysates	86
2.12	X-gal staining of cells and tissues.....	86
2.13	Luciferase Assay	86
2.14	Modification of PLA surface chemistry	87
2.14.1	3D printing PLA squares.....	87
2.14.2	Measuring extent of hydrolysis of PLA by %wt loss	87
2.14.3	Binding of hexamethyldiamine (HMD) to a PLA surface by EDC/NHS activation	87
2.14.4	Binding of HMD to PLA surface by direct aminolysis.....	88
2.14.5	Ninhydrin assay to test for functionalisation of PLA with primary amine groups	88
2.14.6	Derivatisation of PLA with benzaldehyde	88
2.14.7	Deprotection and detection of Fmoc from Fmoc lysine	88
2.14.8	ESI-MS	89
2.14.9	Derivatisation of PLA with Fmoc-lysine-OH	89
2.15	Methods for collagen adenovirus gel formation and coating onto stent surfaces.....	89
2.15.1	Entrapping adenovirus into a collagen gel and coating onto PLA surfaces	89
2.15.2	555-Ad5 collagen gel on PLA preparation and visualisation	90
2.15.3	Quantification of amount of virus on surface	90
2.16	PLA coating onto SS methodology	91

2.16.1	Preparation of PLA coated onto SS discs	91
2.16.2	Coating PLA onto mouse stents.....	91
2.16.3	Coating PLA onto pig stents.....	92
2.17	Transfection of miRNA <i>in vitro</i>	92
2.17.1	Transfection of rat A10 cells with cel-miR-39-3p at different concentrations	92
2.17.2	Transfection of rat A10 cells with cel-miR-39-3p from PLA and SS surfaces \pm collagen	93
2.17.3	Transfection of rat A10 cells with miR-145-5p and miR-145-inhibitor	93
2.18	Transfection of miRNA <i>ex vivo</i>	94
2.18.1	miRNA transfection from PLA squares:	94
2.18.2	miRNA transfection from stents coated with PLA.....	94
2.19	Extraction of RNA from cells and tissues	95
2.19.1	RNA sample preparation from cells:	95
2.19.2	RNA sample preparation from mouse aorta.....	95
2.19.3	RNA sample preparation from pig coronary arteries	95
2.19.4	General RNA extraction procedure	96
2.20	Reverse-transcription polymerase chain reaction (RT-PCR)	97
2.21	Taqman quantitative real time PCR (qRT-PCR).....	98
2.22	Cell Proliferation EdU Assay	99
2.23	Flow assisted cell sorting	100
2.24	<i>In vivo</i> models	100
2.24.1	Mouse stenting model.....	100
2.24.2	Pig stenting model.....	102
3	Development of methods for coating adenovirus particles to stent materials and surfaces	106
3.1	Introduction	107
3.1.1	Aims	109
3.2	Results	110
3.2.1	Poly electrolyte multilayers.....	110
3.2.2	Covalent attachment of virus to PLA surfaces	123
3.2.3	Collagen Entrapment of Virus onto PLA surfaces	133
3.3	Discussion.....	149
4	Development of methods for coating miRNA onto stent materials and stent surfaces	154
4.1	Introduction	155
4.1.1	Aims	157
4.2	Results	158
4.2.1	Transfection of miRNAs <i>in vitro</i>	158

4.2.2	Using miRNAs to inhibit SMC proliferation as a potential therapeutic for prevention of ISR	166
4.3	Discussion	171
5	Local delivery of miRNA in murine and porcine <i>in vivo</i> stenting models ...	174
5.1	Introduction	175
5.1.1	Aim	175
5.2	Results	176
5.2.1	Transfection of miRNA in murine <i>in vivo</i> stenting model	176
5.2.2	Transfection of miRNA in porcine <i>in vivo</i> stenting model	177
5.3	Discussion	181
6	General discussion	183
6.1	General discussion.....	184
	List of references.....	189

List of Tables

Table 1	miRNAs associated with neointima formation which could be targets for treatment of ISR.....	62
Table 2	Summary of virus-eluting stents for prevention of in-stent restenosis studies	70
Table 3	Results on %wt/wt PLA coating on BMS ability to be inflated and whether virus transduction was observed after the PLA coated BMS were then coated with Ad5 CMV lacZ collagen gel.	147

List of Figures

Figure 1-1	Structure of a healthy artery (left) and a diseased artery (right) showing a build-up of atherosclerotic plaque and plaque rupture.	27
Figure 1-2	Revascularisation procedures, PCI and CABG.....	30
Figure 1-3	Revascularisation by deployment of a coronary stent.	32
Figure 1-4	Cross-sectional representation of an artery undergoing in-stent restenosis.	35
Figure 1-5	Structure of Adenovirus 5.	50
Figure 1-6	miRNA biogenesis pathway.	61
Figure 3-1	Diagram of method for poly(electrolyte) multilayer formation. ...	110
Figure 3-2	Chemical structures of polycationic and polyanionic species used for the formation of PEMs.	111
Figure 3-3	UV-vis spectra of PAH-PSS and chi-ha PEMs forming on quartz slides.	112
Figure 3-4	Confocal micrographs of PEMs chi-ha and PAH-PSS incubated with fluorescently tagged adenovirus.	114
Figure 3-5	Atomic force height images of the microscope slides coated with PEMs.	115
Figure 3-6	Transduction of A10 cells with Ad5 CMV lac Z.....	116
Figure 3-7	Transduction of A10 cells with Ad5 CMV lac Z treated with polycations, chitosan and PAH.	118
Figure 3-8	Transduction of A10 cells with Ad5 CMV lac Z from Stainless Steel surfaces	120
Figure 3-9	Transduction of A10 cells with Ad5 CMV lac Z in chitosan solution with different concentrations of acetic acid.	121
Figure 3-10	Transduction of A10 cells with Ad5 CMV lac Z deposited on (chi-ha) ₈ chi PEM coated SS disc.	122
Figure 3-11	Chemical structure of PLA.	123
Figure 3-12	%wt loss of PLA after exposure to 1 M NaOH solution at different time points.	124
Figure 3-13	Treatment of PLA with ninhydrin to test for primary amines on the PLA surface.	126
Figure 3-14	UV absorbance at 220 nm of 1 M HCl solutions after exposure to PLA surface following benzaldehyde conjugation.	127
Figure 3-15	A) Chemical structure of FMOC-lysine, B) Deprotection of PLA-FMOC-lysine using piperidine.	129
Figure 3-16	ESI-MS of FMOC lysine deprotection in solution after treatment with piperidine.....	130
Figure 3-17	UV-vis of washes with EtOH of PLA surface after FMOC functionalisation.....	131
Figure 3-18	UV-vis spectra of piperidine solutions after removal of FMOC group.	132
Figure 3-19	ESI-MS of PLA after FMOC deprotection.	132
Figure 3-20	Fluorescent micrographs of PLA surfaces with fluorescently tagged Ad5.	134
Figure 3-21	Transduction of A10 cells with Ad5 CMV lac Z encapsulated in collagen and deposited on PLA surfaces.	135
Figure 3-22	Transduction of A10 cells with Ad5 CMV lac Z encapsulated in collagen and deposited on PLA and SS surfaces.....	136
Figure 3-23	microBCA assay of serial dilution of Ad5 CMV lac Z.....	137
Figure 3-24	qRT-PCR from a serial dilution of Ad5 CMV lac Z.....	138

Figure 3-25	qRT-PCR of serial dilution of Ad5 CMV lac Z and of washings from collagen coated PLA surfaces.	139
Figure 3-26	Transduction of Ad5 CMV lacZ and Ad49 from collagen coated PLA surfaces.	141
Figure 3-27	Transduction of A10 cells with Ad5 CMV lacZ encapsulated in collagen and deposited on PLA and SS and SS coated in PLA surfaces.....	143
Figure 3-28	X-gal stained mouse aorta after incubation with Ad5 CMV lac Z for 72 h.	144
Figure 3-29	X-gal stained mouse aorta after incubation with Ad5 CMV lacZ collagen gel coated onto PLA for 72 h.....	145
Figure 3-30	X-gal stained mouse aorta ± balloon damage after incubation with Ad5 CMV lac Z collagen gel coated onto PLA for 72 h.....	146
Figure 3-31	X-gal stained pig coronary arteries after Ad5 CMV lac Z collagen gel was coated onto PLA 20% wt/wt BMS for 72 h.	147
Figure 4-1	miR-39-3p expression in A10 cells transfected with miR-39-3p mimic.	158
Figure 4-2	miR-39-3p expression in A10 cells transfected with miR-39-3p mimic coated onto PLA and SS surfaces ±collagen.	160
Figure 4-3	miR-145-5p expression in A10 cells transfected with miR-145-5p mimic and miR-145-5p inhibitor coated onto PLA surfaces.	162
Figure 4-4	<i>Ex vivo</i> delivery of miR-39-3p from PLA squares to mice aorta.....	163
Figure 4-5	<i>Ex vivo</i> delivery of miR-39-3p from PLA coated stents to mouse aorta at different PLA concentrations.	164
Figure 4-6	<i>Ex vivo</i> delivery of miR-39-3p from PLA coated stents to mouse aorta.	165
Figure 4-7	EdU Assay measuring the effect of miR cluster 99b/let7e/125a on HVSMC proliferation.....	167
Figure 4-8	Relative expression of miR-99b-3p and 5p strands of HVSMC after 48 h treatment with the miRNA at 3 nM.	168
Figure 4-9	Relative expression of miR-let7e-3p and 5p strands of HVSMC after 48 h treatment with the miRNA at 3 nM.	169
Figure 4-10	Relative expression of miR-125a-3p and 5p strands of HVSMC after 48 h treatment with the miRNA at 3 nM.	170
Figure 5-1	Local delivery of miR-39-3p from PLA coated stents to mouse aorta, 48 h after deployment using murine <i>in vivo</i> stenting model.	176
Figure 5-2	Comparison of U6 and miR 103 as endogenous controls for <i>in vivo</i> porcine stenting study.	177
Figure 5-3	Local delivery of miR-39-3p from PLA coated stents to porcine coronary arteries, 48 h after deployment using porcine <i>in vivo</i> stenting model.	178
Figure 5-4	Local delivery of miR-145-5p from PLA coated stents to porcine coronary arteries, 48 h after deployment using porcine <i>in vivo</i> stenting model.	179
Figure 5-5	Local delivery of anti-miR-21 from PLA coated stents to porcine coronary arteries, 48 h after deployment using porcine <i>in vivo</i> stenting model.	180

List of Publications

Abstracts:

1st NanoFar Autumn School

University of Angers, 2012.

Development of adenoviral eluting stents for cardiovascular gene therapy, **H. Stepto**, A. Parker, M. Hutin, L. Cronin, A. H. Baker (Poster communication).

Kelvin Smith Symposium

University of Glasgow, 2013.

Biodegradable gene eluting stents*, **H. Stepto**, P. Kitson, A. Parker, K. Oldroyd, L. Cronin, A. Baker (Oral communication).

European Society for Biomaterials

ACC Liverpool, 2014.

Development of biodegradable virus and miRNA eluting stent technology, **H. Stepto**, K. Oldroyd, L. Cronin, A. Baker (Poster communication).

European Society for Microcirculation and European Vascular Biology Organisation

Polo Carmignani, Pisa, 2015.

Development of miRNA eluting stents, **H. Stepto**, R. Dakin, R. McDonald, S. Kennedy, L. Cronin, K. Oldroyd, A. Baker (Oral communication).

*Awarded first prize for best oral presentation at Kelvin Smith Symposium, 2013.

List of Abbreviations

AAV	Adeno-associated virus
ACE	Angiotensin-converting enzyme
Ad	Adenovirus
ADP	Adenosine triphosphate
AFM	Atomic force microscopy
AGENT	Angiogenic gene therapy trial
Ago II	Argonaute II complex
ANOVA	Analysis of variance
ATP	Adenosine triphosphate
β -gal	Beta-galactosidase
BCA	Bicinchoninic acid
BHF	British Heart Foundation
BMS	Bare metal stent
BrdU	Bromodeoxyuridine
CABG	Coronary artery bypass graft
cAMP	Cyclin adenosine monophosphate
CAR	Coxsackie and adenovirus receptor
CD	Cluster of differentiation

CDK	Cyclin-dependent kinases
<i>c.elegans</i>	<i>Caenorhabditis elegans</i>
CHD	Coronary heart disease
Chi	Chitosan
CR1	Complement receptor 1
CREB	cAMP-responsive element binding protein
Ct	Cycle threshold
CUPID	Calcium up-regulation by percutaneous administration of gene therapy in cardiac disease
CVD	Cardiovascular disease
DES	Drug-eluting stent
DNA	Deoxyribonucleic acid
EC	Endothelial cells
ECM	Extra-cellular matrix
EDC	1-Ethyl-3-(3-dimethylaminopropyl)carbodiimide hydrochloride
EdU	5-Ethynyl-2'-deoxyuridine
EPC	Endothelial progenitor cells
eNOS	Endothelial nitric oxide synthase
ERK	Extracellular signal-regulated kinase
ESI-MS	Electrospray ionisation- mass spectrometry

ETT	Exercise tolerance testing
FACS	Fluorescence assisted cell sorting
FCS	Foetal calf serum
FDA	Food and drug administration
FGF	Fibroblast growth factor
FMOC	Fluorenylmethyloxycarbonylchloride
FX	Factor X
G	Gap
GFP	Green fluorescent protein
GMP	Good manufacturing practice
GRB-2	Growth factor receptor bound 2
GTP	Guanosine triphosphate
h	Hours
ha	Hyaluronan
HEK	Human embryonic kidney cells
HIV	Human immunodeficiency virus
HMD	Hexamethyldiamine
HSPG	Heparin sulfated proteoglycan
HVSMC	Human vascular smooth muscle cells

Hz	Hertz
ID	Integrin targeting peptide plasmid DNA
IL	Interleukin
iNOS	Inducible nitric oxide synthase
ISR	In-stent restenosis
IVIS	<i>In vivo</i> imaging system
Kip	Kinase inhibitor protein
KLF4	Krüppel-like factor 4
KO	Knock-out
L	Litres
LDL	Low-density lipoprotein
LID	Liposome integrin targeting peptide plasmid DNA
luc	Luciferase
LV	Lentiviral
µL	Microlitres
µm	Micrometres
M	mol/L
MACE	Major adverse clinical events
MAPK	Mitogen-activated protein kinases

mg	Milligrams
MI	Myocardial infarction
mins	Minutes
miRNA	Micro ribonucleic acid
MKK4	Mitogen activated protein kinase kinase 4
mL	Millilitres
MMP	Matrix metalloproteinase
mRNA	Messenger ribonucleic acid
ms	Milliseconds
m/z	Mass/charge
NAb	Neutralising antibody
NHS	N-hydroxysuccinimide
nm	Nanometres
nM	Nanomolar
NO	Nitric oxide
NOS	Nitric oxide synthase
ns	Non-significant
NTC	Non-treatment control
ODN	Oligonucleotide

OMT	Optimal medical therapy
OTC	Ornithine transcarbamylase
PAA	Polyallylamine
PABT	Polyallylamine bisphosphonate comprising latent thiol groups
PAH	Poly(allyl amine amino hydrochloride)
PBS	Phosphate Buffered Saline
PC	Phosphorylcholine
PCI	Percutaneous coronary intervention
PDGF	Platelet derived growth factor
PDT	Pyridyldithiol
PEI	Polyethyleneimine
PEM	Polyelectrolyte multilayer
PFA	Paraformaldehyde
PFU	Plaque forming unit
PKA	Protein kinase A
PLA	Poly(lactic acid)
pre-miRNA	Precursor-miRNA
pri-miRNA	Primary-miRNA
PSS	Poly(styrene sulfonate)

QCM	Quartz crystal microbalance
qRT-PCR	Quantitative real-time polymerase chain reaction
RISC	RNA-induced silencing complex
rlu	Relative light units
RNA	Ribonucleic acid
RPM	Revolutions per minute
RQ	Relative quantification
RT	Room temperature
RTN	Receptor targeting nanocomplex
RT-PCR	Reverse transcription polymerase chain reaction
S	Synthesis
S/C	Scramble control
SEM	Standard error of the mean
SERCA	Sarcoplasmic reticulum Ca ²⁺ -ATPase
SMC	Smooth muscle cells
SM-MHC	Smooth muscle-myosin heavy chain
SOS	Son of sevenless
SPDP	<i>N</i> -succinimidyl 1-3-(2-pyridyldithiol)-propionate
ss	Single-stranded

SS	Stainless steel
TCEP	(Tris-(2-carboxyethyl) phosphine)
TE	Trypsin-ethylene diamine tetra acetic acid
TGF- β	Transforming growth factor beta
TIMP	Tissue inhibitors of matrix metalloproteinases
TK	Tyrosine kinase
TRGP	Trans-activating response RNase binding protein
UTR	Untranslated region
UV	Ultraviolet light
v	Volume
VEGF	Vascular endothelial growth factor
VP	Virus particles
VSMC	Vascular smooth muscle cells
VSV	Vesicular stomatis virus
WHO	World Health Organisation
WT	Wild-type
wt	Weight

Summary

Cardiovascular disease (CVD) is the most common cause of death worldwide, accounting for 31% of the annual deaths per year. The term cardiovascular disease refers to many different disorders of the heart and blood vessels, the most prolific of which is coronary heart disease (CHD). The root cause of CHD is atherosclerosis, which is the build-up of plaque in the intima of the arteries, restricting the blood supply which reaches the heart.

If left untreated, the plaques lining the vessel can rupture and cause thrombosis and myocardial infarction (MI). Taking into account an individual's risk-benefit ratio, a suitable treatment is considered with the aim to prevent MI from occurring. The two main revascularisation strategies are coronary artery bypass graft (CABG) and percutaneous coronary intervention (PCI), the latter being the most frequently used; within the UK 80% of revascularisation is performed by PCI.

A PCI procedure is non-invasive and involves the deployment of an intravascular stent into the diseased vessel, which acts as a permanent scaffold that mechanically re-widens the vessel. However, despite the prolific use of intravascular stents within the clinic, there are significant problems associated with this revascularisation technique, such as in-stent restenosis (ISR) and late stent thrombosis (LST).

ISR is the re-narrowing of arteries after stent deployment, characterised by a neointima growth within the lumen of the vessel. ISR is a significant clinical problem, because it can lead to repeat revascularisation procedures and often patients present frequently with unstable symptoms, fulfilling the criteria for an MI diagnosis. ISR occurs as a complex wound healing response caused by the stent deployment. Denudation and tearing of the endothelium and the mechanical stress endured by the vascular smooth muscle cells (VSMC) is a stimulus for hyperplasia. VSMC de-differentiate from the contractile to synthetic states and proliferate and migrate into the lumen of the vessel, secreting ECM which forms the bulk of the neointima. The neointima growth will continue to form until the endothelium has re-established itself.

As a treatment to prevent ISR, drug-eluting stents (DES) were introduced which were coated with anti-proliferative drugs, to prevent ISR from occurring. DES proved to be very successful at preventing ISR; however elevated rates of LST were associated with these stents. This caused the initial gains in lower event rates, 6 months after DES deployment to be lost after higher event rates were reported when compared to BMS, after the 6 month time point (Lagerqvist *et al.*, 2007, Pfisterer *et al.*, 2006). This elevated event rate for DES by LST is thought to be caused as a result of delayed re-endothelialisation and by inflammatory reactions to the polymer used in the coating of DES (Virmani *et al.*, 2004, Joner *et al.*, 2006).

The aim of this study was consequently to investigate methods for delivery and coating of novel therapeutics, adenoviruses and miRNA onto stent surfaces. This would allow investigation into the prevention of ISR using these therapeutics, taking advantage of the localised stent setting. It was hoped that local delivery would provide significant advantages over systemic delivery by decreasing the dosage required, avoiding systemic side-effects and increasing delivery to the targeted area, thereby enhancing the therapeutic effect.

For the development of coating methods for adenovirus eluting stents, the majority of the work conducted was done using Ad5 as a model virus vector. Three different methods were investigated and evaluated *in vitro*; deposition onto polyelectrolyte multilayer (PEM) surfaces, by direct conjugation with a modified poly(lactic acid) (PLA) surface through covalent bond formation and collagen gel entrapment.

The development of coating methods for miRNA eluting stents focussed initially on collagen gel entrapment; however it was discovered that direct application onto a PLA surface provided a system whereby excellent delivery of the miRNA could be achieved. This methodology was extensively investigated and evaluated *in vitro* from stent material surfaces, and *in vivo* in both the porcine and murine stenting models.

The results presented here have extended current methodology for both miRNA and adenovirus eluting stents. To the best of our knowledge, this is the first time

that miRNA eluting stents have been used in these animal models and therefore contributes significantly to the field of miRNA-based therapeutics.

1 Introduction

1.1 Cardiovascular disease

Cardiovascular disease (CVD) is the leading cause of death globally; in 2012 the World Health Organisation (WHO) reported 31% of all deaths each year were caused by CVD (WHO, 2015). Within the UK, the British Heart Foundation (BHF) reported the number of deaths per year to be 160,000 which is roughly a quarter of the annual death toll. Therefore, CVD remains a serious medical issue both globally and locally (BHF, 2015).

The term CVD refers to a number of different disorders of the heart and blood vessels, the four main types are coronary heart disease (CHD), stroke, peripheral artery disease and aortic disease. The most prolific of these is CHD, which is a disease that affects the blood vessels supplying the heart. CHD is caused by a build-up of plaques (fatty deposits), which accumulate in the lumen of the coronary arteries, restricting the blood flow within these vessels. Since the coronary arteries supply the myocardium with blood, restriction of blood flow can cause angina (chest pain) or if the coronary arteries become completely blocked, myocardial infarction (MI) (NHS, 2015). CHD is the UK's single biggest killer and accounts for 73,000 deaths per year (BHF, 2015).

Atherosclerosis, which can be defined as the build-up of plaque in the intima of arteries, is the root cause of CHD. The term 'atherosclerosis' has Greek roots and stems from the terms 'atheroma', meaning a tumour which is composed of material that looks like gruel and 'sclerosis' meaning hardening, which comes from the Greek word skleros. Atherosclerosis is therefore a descriptive term which provides us with an image of what a diseased artery would look like. The plaques are formed from the accumulation of lipids and fibrous elements in large arteries. Atherosclerosis is a chronic inflammatory condition that can lead to an acute clinical event by plaque rupture and thrombosis (Lusis, 2000).

Figure 1-1 shows the anatomy of a healthy and a diseased artery. A normal artery has three distinct regions, the intima, media and adventitia. The intima, is predominantly composed of endothelial cells (EC), and is the innermost cellular region in the artery, directly in contact with the blood flow. Development of atherosclerotic plaques is initially characterised by changes to these intimal ECs, causing them to express adhesion molecules which promote

white blood cell (leukocyte) adhesion. This abnormal adhesion of leukocytes to the ECs is in response to inflammatory stimuli such as hypertension or dyslipidaemia (elevated levels of low-density lipoprotein (LDL)). The intima permits LDL entry and retention within the arterial wall, in parallel; the bound leukocytes migrate into the intima by chemoattractant mediators such as monocyte chemoattractant protein-1 (MCP-1) and lymphocyte chemokines, IFN-inducible protein 10 (IP-10), monokine induced by IFN-gamma (Mig) and IFN-inducible T-cell alpha chemoattractant (I-TAC) (Gu *et al.*, 1998, Boring *et al.*, 1998, Mach *et al.*, 1999). The predominant type of leukocyte which binds to the ECs are monocytes, which after recruitment to the intima, differentiate into tissue macrophages and work to engulf the LDL, forming foam cells (Libby *et al.*, 2011).

Resident smooth muscle cells (SMCs) within the intima and SMCs from the media are recruited into the intima through mediators, such as platelet derived growth factor (PDGF). These cells secrete extra-cellular matrix (ECM) over the macrophage derived foam cells, to form a fibrous cap, as a preventative measure to avoid plaque rupture (Libby *et al.*, 2011, Lusis, 2000). Unstable plaques however, can rupture, the clinical manifestation of this being thrombosis and MI, as shown in (Figure 1-1) (Robertson *et al.*, 2012). Prevention and treatment of CHD is discussed in the following section.

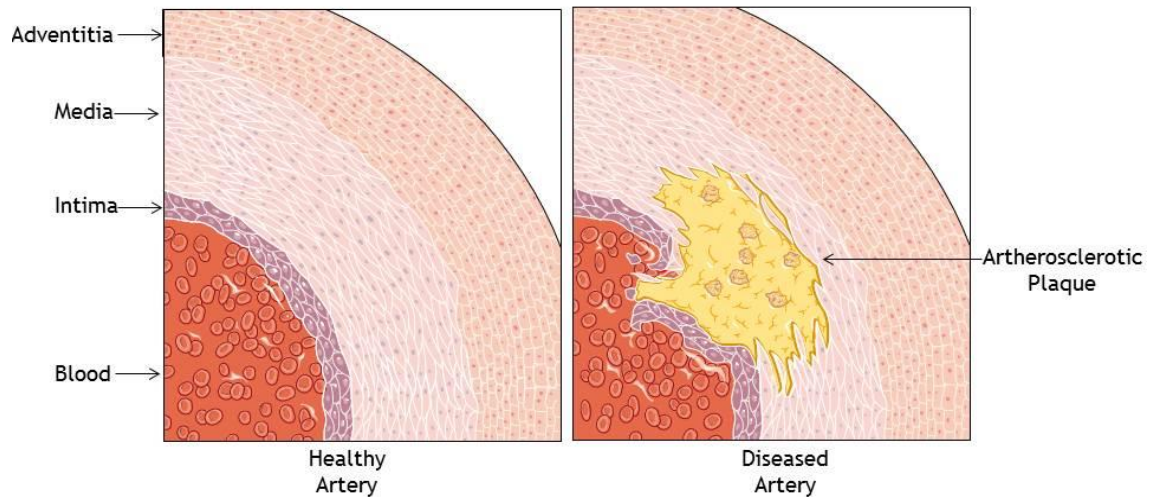


Figure 1-1 Structure of a healthy artery (left) and a diseased artery (right) showing a build-up of atherosclerotic plaque and plaque rupture.

Morphology of a large artery, showing the three distinct layers; intima, media and adventitia. The intima has an endothelial layer of cells which form a barrier between the blood flow and the artery, elastic fibre and internal elastic lamina layers. The medial layer is made up primarily of vascular smooth muscle cells, but also contains collagen and elastin. The adventitial layer is composed of mainly collagen and elastin and is separated from the media layer by the external elastic lamina.

1.2 Treatment of coronary heart disease

Atherosclerosis is an age related condition, with increasing age being identified as an independent risk factor for the disease (Wang and Bennett, 2012). It is thought it can start when damage is endured to the inner surface of the arteries which could be through smoking, high blood pressure, high amounts of fats or cholesterol in the blood, and high amounts of sugar in the bloodstream as a result of diabetes and insulin resistance (NIH, 2015).

Optimal Medical Therapy (OMT) is used to control and treat early stages of CHD, which involves the implementation of lifestyle changes and taking medication (Boden *et al.*, 2007). Healthy lifestyle changes include stopping smoking, healthy eating, losing and maintaining a healthy weight and undertaking regular exercise, all of which are factors contributing to atherosclerosis. Since the atherosclerotic lesions have the effect of narrowing the artery lumen and therefore increasing blood pressure, medications are prescribed to counteract this by reducing blood pressure and re-widening arteries. There are many different classes of medication that are used for this purpose, the main classes being Angiotensin-converting enzyme (ACE) inhibitors, calcium channel blockers, β -blockers (Chobanian *et al.*, 2003). More than two thirds of hypertensive patients' blood pressure cannot be controlled with a single drug, and therefore dual therapy is often required, whereby the patient receives drugs from different classes (Chobanian *et al.*, 2003).

If the symptoms cannot be controlled by OMT, interventional procedures will be considered to restore blood flow to the affected area. A coronary angiogram, which is the 'gold-standard' for diagnosing CHD is carried out to image and measure the blood flow through the vessels in the heart. For this, a catheter is inserted through an artery in the arm or groin and directed into the heart using X-rays to guide it. Once in the heart, a radiocontrast dye is pumped through the catheter and images of the vessels are taken using X-rays, these images will help to decide the treatment that the patient will receive.

The two main types of surgical intervention for the treatment of CHD are Percutaneous Coronary Intervention (PCI) and Coronary Artery Bypass Grafting (CABG). The decision for the best treatment to use is decided by taking into

account the risk-benefit ratios, weighting the risks of periprocedural death, MI, and stroke against improvements that could be gained in the quality of life, by prevention of future MI and further revascularisation (Windecker *et al.*, 2014). Different models are used to assess the various risks associated with the revascularisation strategies and aid the decision making depending on the particular situation, such as the SYNTAX (Mohr *et al.*, 2013) and EuroSCORE II systems (Nashef *et al.*, 2012).

The SYNTAX system was developed using the results from randomised clinical trials comparing the outcomes of patients with complex coronary artery disease receiving either CABG or PCI treatments with a first-generation paclitaxel-eluting stent. For the initial trial the end point was defined as death, MI, repeat revascularisation and stroke at 1 year post-operation. The findings from this trial enabled a scoring system to be developed to help predict the severity of the disease, the outcome of which is used to decide whether a patient would respond better to a CABG or PCI treatment (Serruys *et al.*, 2009). Under the current guidelines patients with an intermediate or high SYNTAX score are recommended for CABG, whereas patients with low SYNTAX scores or left main coronary disease are recommended for PCI (Mohr *et al.* 2013).

The EuroSCORE system was used to predict early mortality in cardiac surgery patients in Europe and used many patient-related factors (such as, age, chronic pulmonary disease, extracardiac arteriopathy, neurological dysfunction, previous cardiac surgery, serum creatinine >200 micromol/L) to generate a score which could be used to predict the risk of mortality caused by cardiac surgery (Nashef *et al.* 1999). This system has now recently been updated as it was thought that EuroSCORE over-estimated patient mortality, so consequently EuroSCORE II is now used (Mohr *et al.*, 2013). Often clinicians refer to both of these scores when determining an appropriate treatment for the patient, depending on the specific condition (Capodanno *et al.*, 2010).

Of the two revascularisation strategies, CABG is the older of the operative procedures and was first used in 1968 (Favaloro, 1968). The procedure for CABG surgery involves the grafting of a healthy artery or vein, (usually from chest, legs or arms) around the blocked coronary artery. This allows the blood to be

diverted around the obstructed region, which restores blood flow to the heart and provide relief from angina (Figure 1-2).

Percutaneous coronary intervention (PCI) was introduced in 1977, initially as a treatment for a single coronary artery with no involvement of side branches (Grüntzig, 1978, Grech, 2003). At this time, the operation involved inserting a balloon catheter percutaneously into the diseased vessel, inflating the balloon re-widened the occluded vessel mechanically (Figure 1-2). The equipment used to do this initial operation, did not benefit from the years of experience and research that modern-day PCI apparatus benefits from and this limited its application within the clinic; initially only 10% of cases would be suitable for this new type of revascularisation technique, it did however have the advantage of being a non-invasive procedure (Grech, 2003).

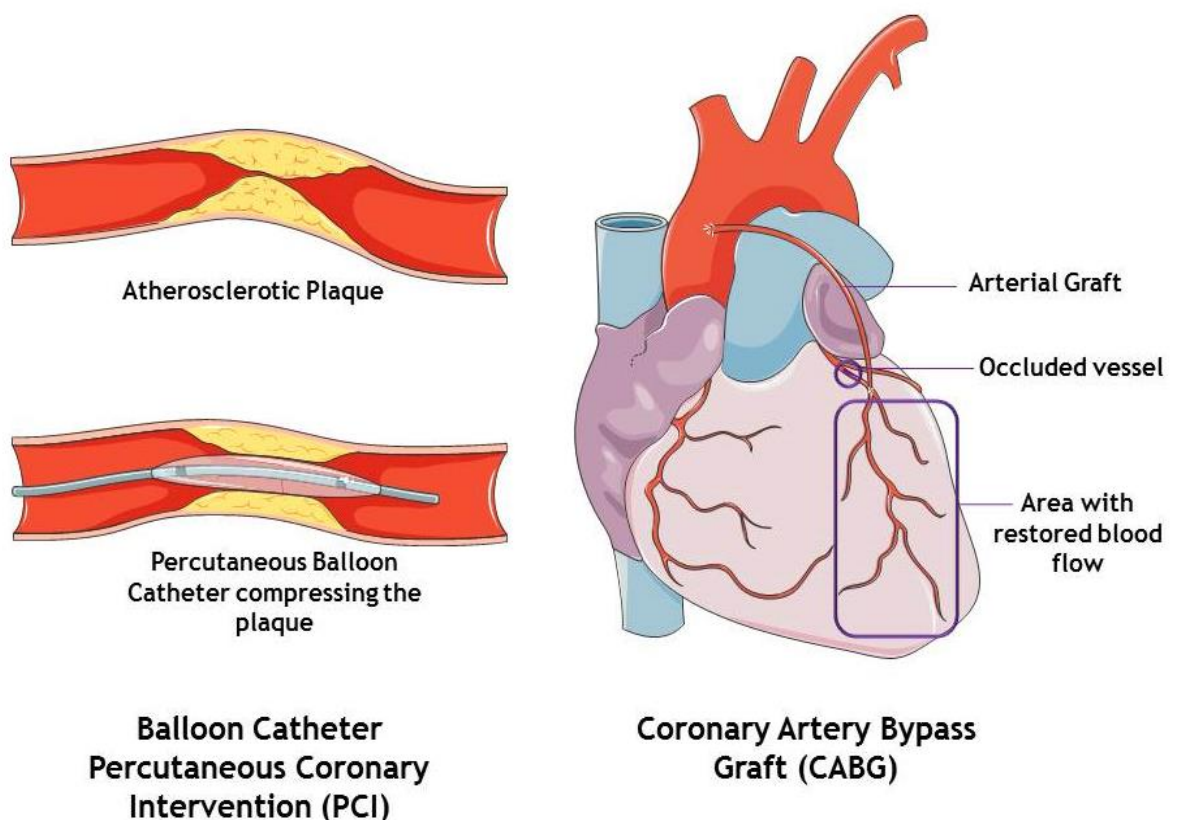


Figure 1-2 Revascularisation procedures, PCI and CABG.

As the technology advanced, the number of patients treated with PCI grew, the technology advanced as more complex lesions were able to be treated. Initially the guide catheters and balloons were large in comparison to today's standards

and guide wires and stents were not used (Grech, 2003). The main drawback for this new technology was restenosis, which is the re-narrowing of the artery lumen; it was found that the PCI procedure could trigger elastic recoil of the vessel and promote negative re-modelling (de Feyter *et al.*, 1994). Negative remodelling describes shrinkage in the external elastic membrane (EEM) area at the diseased site, which can be measured by IVUS (Schoenhagen *et al.*, 2001). Elastic recoil occurred as a result of the mechanical stress inflicted upon the elastic fibres within the vessel wall by the process of balloon inflation, which caused them to overstretch. Recoil occurred minutes after balloon deflation and was reported to cause up to 40% lumen loss (Kraitzer *et al.*, 2007). It was in this context that intravascular stents were introduced.

1.2.1 Stent Technology

The first time intravascular stents were deployed in humans was in 1986 (Sigwart *et al.*, 1987). The intravascular stent was made from a stainless steel (SS) mesh that was crimped around the balloon catheter. The balloon catheter was positioned so it traversed the narrowed region in the artery and then inflated; this would cause the stent to expand. The balloon was then deflated; however the stent was left in the artery as a permanent scaffold (Figure 1-3).

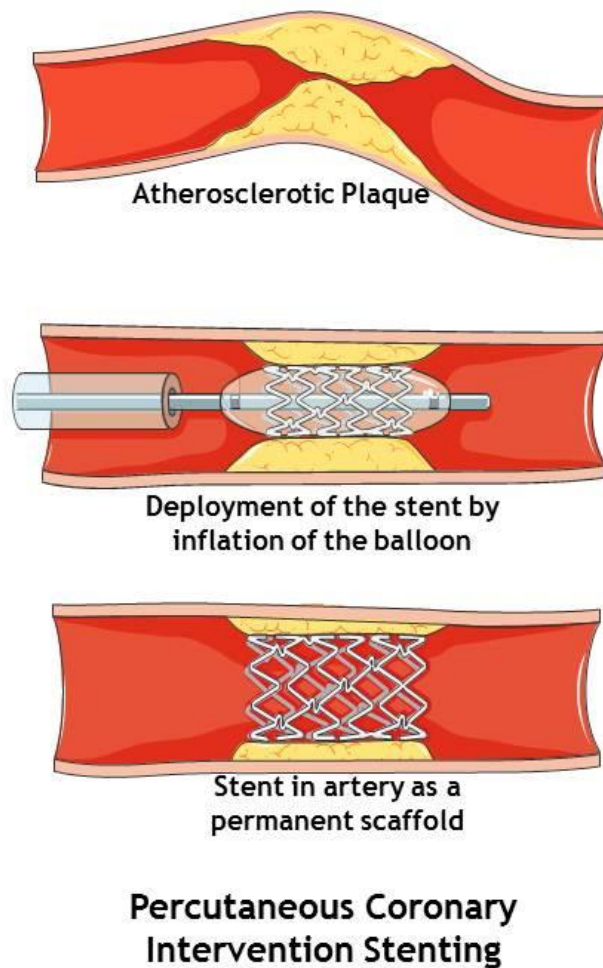


Figure 1-3 Revascularisation by deployment of a coronary stent.

The first randomised studies comparing PCI using the stent technology against traditional balloon angioplasty methods demonstrated a profound decrease in restenosis rates ~30%. This was caused by a decrease in elastic recoil and a gain in the initial lumen size after the stenting (Grech, 2003, Smith Jr *et al.*, 2001, Fischman *et al.*, 1994, Serruys *et al.*, 1994). It was as a result of the initial

comparative trials showing stenting to vastly improve the outcomes for restenosis when compared to balloon angioplasty PCI, which caused the rapid growth in the field and prolific use of the stents in the clinic. It took longer however, for the burden of the ISR to be realised and exposed as the Achilles heel to this treatment (Serruys *et al.*, 1994, Fischman *et al.*, 1994, Duckers *et al.*, 2007).

Since their introduction into the clinic in 1986, there has been an exponential growth in the number of stents deployed, as device technology and anti-thrombogenic drugs have advanced. Initially, they were thought of as a temporary solution to acute vessel occlusion; however, they proved to be more effective than balloon angioplasty, reducing the number of patients requiring repeat revascularisation and are now a key part of treatment for CHD (Serruys *et al.*, 2012, Moliterno, 2005, Sigwart *et al.*, 1987).

In 2012, the British Cardiovascular Intervention Society recorded that 80% of patients requiring treatment after the angiogram findings received PCI rather than CABG, which is in line with the NICE guidelines (NICE, 2003, Ludman *et al.*, 2014). Despite the intravascular stents' prolific use within the clinical setting, there are still significant problems associated with it such as in-stent restenosis (ISR) and late stent thrombosis, stenting therefore it is by no means the optimal treatment.

1.2.1.1 In-stent restenosis

ISR is the re-narrowing of arteries after stent deployment, characterised by the formation of a neointima in the lumen of the artery, formed as a response to the injury caused by the stent on the arterial wall. Neointima can be defined as simply the 'new' (neo) thickened arterial intima. Restenosis rates caused by deployment of bare metal stents (BMS) have been reported to be between ~16% and 44% (Farooq *et al.*, 2011). Initially, clinical presentation of ISR was thought to be benign and generally stable with acute presentation being treated satisfactorily with repeat revascularisation procedures (Alfonso, 2010). However, recently studies suggest that patients present frequently with unstable symptoms and exhibit markers fulfilling the criteria for an MI diagnosis (Alfonso *et al.*, 2014, Chen *et al.*, 2006).

There are multiple factors which govern ISR which result in neointima formation, giving a complex physiopathology to understand. ISR has proved difficult to study due to the scarcity of human tissues, and the animal models not being sophisticated enough to represent advanced atherosclerotic vessels (Geary and Clowes, 2007, Welt and Rogers, 2002). Nevertheless, much progress has been made in this field and there is now a good understanding of the process within the scientific community.

ISR is initiated during stent deployment, as a consequence of disruption and injury to the cells within the diseased vessel. It was Forrester and co-workers who proposed the paradigm for ISR the result of a complex wound healing response (Costa and Simon, 2005, Forrester *et al.*, 1991). Mechanical stress induced to the vascular smooth muscle cells (VSMCs) (Leung *et al.*, 1976, Clowes *et al.*, 1989) and denudation of the endothelium (Sanborn *et al.*, 1983) provides the stimuli for hyperplasia; this has been shown in many animal studies. The observation that intimal hyperplasia (abnormal increase in the number of cells within the intima), occurred in both atherosclerotic and normal segments after angioplasty, within humans, indicated that hyperplasia formation was not dependant on the presence of atherosclerosis; this therefore added weight to the animal studies, which observed the formation of hyperplasia as a vascular response to injury (Forrester *et al.*, 1991). Figure 1-4 depicts the process of in-stent restenosis from stent deployment to the neointima formation.

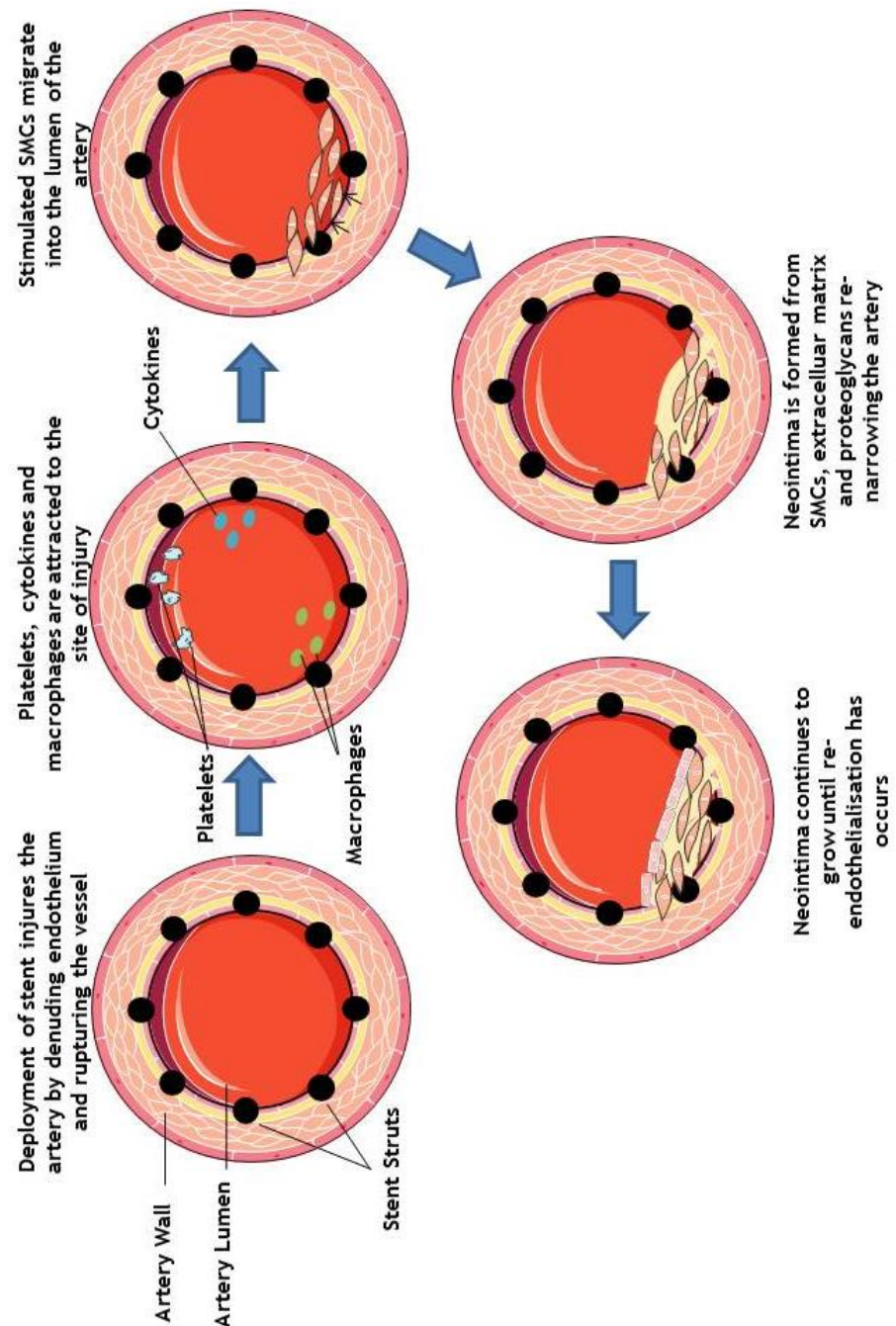


Figure 1-4 Cross-sectional representation of an artery undergoing in-stent restenosis.

The wound healing response triggering ISR can be thought of as three stages: inflammation, granulation & matrix formation. The inflammatory response is triggered instantly in response to the injury endured by stent implantation, which can denude endothelium. The inelasticity of the atheroma can also cause tears to develop as the pressure required to compress the plaque and deploy the stent can rupture and damage the cellular architecture (Forrester *et al.*, 1991). At the site of injury, platelets aggregate (Lobb, 1988) and release growth factors and other substances including an endoglycosidase, which are responsible for the cleavage of heparin proteoglycan from the surface of endothelial cells (ECs) and

smooth muscle cells (SMCs) making them receptive to action of the growth factors (Castellot Jr *et al.*, 1987, Campbell and Campbell, 1986, Forrester *et al.*, 1991).

The granulation phase occurs from days 3-5 after stent implantation and is characterised by SMC's phenotype switching from the contractile to the synthetic state; this causes them to proliferate and then migrate into the injured area and secrete ECM (Kocher *et al.*, 1991, Forrester *et al.*, 1991). Characterisation of phenotype switching of VSMCs from contractile to synthetic states following vascular injury can be monitored by viewing a change in cell morphology, with contractile phenotypes displaying a long-spindle like form whereas synthetic phenotypes exhibit a distinct epithelioid morphology (Walker *et al.* 1986). This change is also accompanied by decreased expression of proteins α -SMA and SM-MHC relative VSMC phenotype expression can be monitored by IHC staining methods (Kocher *et al.*, 1991, Kuro *et al.*, 1991). Early ECM is rich in fibronectin from the coagulated blood. Endothelial cells will also begin to migrate from the edges of the injury site in response to the growth factors release from the injury response and ECM (Forrester *et al.*, 1991, Folkman and Klagsbrun, 1987).

Once the cells have migrated into the site of injury, matrix formation begins to take place, converting the initial fibronectin matrix to a proteoglycan rich matrix, this process is regulated predominantly by transforming growth factor beta (TGF- β) (Bentley, 1967, Sprugel *et al.*, 1987). When the endothelial cells have covered the injured area they stop proliferating and synthesise and release heparin proteoglycan. SMCs bind to the proteoglycan with high affinity and this has the effect of making them unresponsive to the proliferative growth factor stimuli (Bassols and Massague, 1988). The SMCs then gradually revert back to their contractile state (Forrester *et al.*, 1991).

The degree of ISR has been directly correlated to the severity of the mechanical stretch and injury which the vessel receives. The formation of neointima hyperplasia is reliant on how quickly re-endothelialisation occurs, therefore when the injury is severe and the endothelium is severely denuded, neo-intima formation will be exaggerated (Forrester *et al.*, 1991).

1.2.1.2 Late stent thrombosis

Following the high incidence of restenosis with BMS and the discovery that ISR is not as benign as it was once thought and often requires repeat revascularisation procedures (Chen *et al.*, 2006, Alfonso *et al.*, 2014); much research has focused on stent design, materials and surface treatments to try and minimise ISR from occurring (O'Brien and Carroll, 2009).

In the early 2000's drug-eluting stents (DES) were at the forefront of cardiovascular research. DES's promised to reduce ISR by eluting therapeutic drugs which targeted cell proliferation and migration to eliminate the formation of the neointima. Early clinical results showed excellent results with respect to reduced ISR. Stone *et al.* conducted double-blind, multi-centred, randomised clinical trial which compared the safety and efficacy of paclitaxel-eluting stents to BMS. Paclitaxel induces cytostasis by stabilising microtubules which in turn inhibits VSMC division (Axel *et al.*, 1997). The site-specific delivery of paclitaxel from the DES demonstrated a marked decrease in restenosis rates from 26.6% to 7.9% at 9 months (Stone *et al.*, 2004). Similar findings were also shown with sirolimus eluting stents when directly compared to BMS at 9 months (Moses *et al.*, 2003). Sirolimus (rapamycin) was chosen as it was identified to induce VSMC cycle arrest by decreasing cell-cycle kinase activity at the G1/S and G2/M transitions (Marx *et al.*, 1995).

Shortly after these studies were conducted, a new problem emerged with the DES; late stent thrombosis, which often resulted in fatalities (Shedden *et al.*, 2009). It was found that the window for thrombotic risk was much longer for DES than for the BMS, and therefore the initial 9 month clinical trials did not detect the elevated rate of late stent thrombosis during the timescale of the trials. Studies comparing late stent thrombosis rates between BMS and both sirolimus and paclitaxel eluting stents showed an elevation in the incidence of late stent thrombosis with DES between 1-3 years, however no overall increase in cumulative rate of death was recorded between the BMS and DES groups (Stone *et al.*, 2007c). Although DES have been shown to be effective against limiting restenosis; late stent thrombosis presents a formidable clinical problem in terms of patient safety. The difference in the cumulative death rate between BMS and DES at 4 years is negligible; therefore an optimal treatment which will

demonstrate an improvement in the cumulative death rate is yet to be developed.

Late stent thrombosis is multifactorial and is thought to arise from a combination of incomplete endothelialisation of the stent struts, incompatibility with dual antiplatelet therapy and an inflammatory response caused by the polymer coating (Robertson *et al.*, 2012, Virmani *et al.*, 2004).

One of the main issues which has plagued the advances made with DES is the lack of specificity that the anti-proliferative drugs have. DES are unable to distinguish between the two main cell types involved in neointima formation; ECs and SMCs, preventing the proliferation of both and hence decreasing in stent restenosis. This suppression of cell proliferation, ultimately results in delayed re-endothelialisation which is thought to be an underlying cause of late stent thrombosis (Babapulle *et al.*, 2004, Shedden *et al.*, 2009). Histologic findings from human autopsies of patients who had died after receiving DES compared with patients that had received BMS revealed that there was a marked difference in arterial healing between the BMS and the DES (Joner *et al.*, 2006). The BMS showed near complete re-endothelialisation and an absence of fibrin around the struts, whereas for the DES, poor endothelialisation and peri-strut fibrin was observed. Incomplete re-endothelialisation of the stent struts therefore poses as a potent thrombogenic stimulus and could account for the observed trend in elevated late stent thrombosis rates associated with DES.

Despite the issue of late stent thrombosis which has limited the success of DES, the concept, of localised delivery from the stent surfaces, clearly works extremely well; as demonstrated by the marked decrease in restenosis (Stone *et al.*, 2004). Taking advantage of the site-specific delivery which can be achieved from stent surfaces is likely to feature in new stent technologies.

It is apparent that administering sirolimus and paclitaxel, which both inhibit cell proliferation, has a profound effect on the local SMC and EC populations surrounding the stent; although the overall lack of specificity of these drugs, has unfortunately led to an increased incidence of late stent thrombosis by delayed re-endothelialisation (Joner *et al.*, 2006). Understanding the mechanisms which underlie the process of ISR and designing an elegant treatment, which would

selectively target specific biological pathways could provide a treatment with a highly specific mode of action, more finely tuned to specific cell types. An optimal treatment would prevent ISR but not cause late stent thrombosis. The biological mechanisms for neointima hyperplasia and potential therapeutic targets which have been identified are discussed in the following section.

1.3 Mechanisms for neointima hyperplasia

The formation of neointima hyperplasia is a complex wound healing process, which stimulates multiple biological cascades to occur concurrently. A successful treatment for the prevention of ISR is likely to employ multiple approaches which target the different underlying molecular mechanisms that result in neointima formation. This is apparent from the implementation of DES, which aimed to prevent cell proliferation by administering a single anti-proliferative drug; this highlighted the complex nature of the disease pathology as the unwanted effect of late stent thrombosis emerged as a result of hindering re-endothelialisation (section 1.2.1.2). In order to design a suitable treatment which accounts for the complexity of the process, understanding the mechanisms which cause neointima formation will be integral to its success. The following section will give an overview of the disease process that underpins neointima hyperplasia.

During stent deployment (Figure 1-3), damage can be inflicted upon the vessel as a result of the mechanical force needed to inflate the stent. As the stented vessel will be atherosclerotic and therefore harder, the radial force required to expand the stents is often high; tearing of the endothelium can therefore easily occur. The resulting damage to the endothelium causes platelet aggregation and activation (McDonald *et al.*, 2012). Under normal circumstances platelets flowing within the blood stream do not interact with ECs, which inherently prevents thrombus from forming within the vessels. Upon disruption to the EC layer, exposure of the platelets to the sub-endothelial matrix stimulates them to aggregate together (Rumbaut and Thiagarajan, 2010). Fibrin is also deposited at the site of injury (Indolfi *et al.*, 2000). The activated platelets express adhesion molecules which can bind to leukocytes from the blood, the platelet-leukocyte complexes then begin to roll along the injured surface (Welt and Rogers, 2002).

Activated platelets will release many growth factors and cytokines, such as PDGF, TGF- β_1 , IL-1, IL-6, IL-8 and thrombin, which aids infiltration of the leukocytes into the vessel wall and begin to interact with the SMCs (McDonald *et al.*, 2012). Sustained release of adhesion molecules, growth factors, cytokines, and chemoattractants by the platelets, SMCs and leukocytes leads to further leukocyte recruitment and infiltration into the sub-endothelial layer (Mitra and

Agrawal, 2006b) and directs phenotypic modification of SMCs from their contractile to synthetic state (Indolfi *et al.*, 2003).

Adult VSMCs are usually quiescent and in the G₀ phase of the cell cycle. However, when they are injured they change from their usual non-proliferative state to G₁/S phase of the cell cycle. G₁ progression is regulated by cyclin-cyclin-dependent kinases (CDKs) which become active through binding with the regulatory protein, cyclin (Indolfi *et al.*, 2003). CDK inhibitors can therefore be used to prevent proliferation of VSMCs by blocking this pathway. The two main CDK inhibitor groups active within the cardiovascular system are the INK4 and Cip/Kip families (Nabel, 2002, Tanner *et al.*, 1998).

Another way in which proliferation of VSMCs is stimulated is through the activation of nuclear transcription factors. The main signalling cascade which has been identified that controls this is through the *ras-raf*-mitogen-activated protein kinases (MAPK). Growth factors, such as PDGF initially bind to the growth factor tyrosine kinase (TK), which is located in the cell membrane and begins the cascade by multiple phosphorylation of tyrosine. The phosphorylated tyrosine then connects to *ras* receptor upon activation by growth factor receptor bound 2 (GRB-2) and son of sevenless (SOS) molecules. This promotes binding of guanosine triphosphate (GTP) which activates *ras* which binds *raf*, which culminates in the activation of MAPK (Indolfi *et al.*, 2003).

In addition to these pathways, a hormone dependent route also contributes to the promotion of the VSMCs from contractile to synthetic state. Hormones bind to seven loop receptors within the VSMC cell membrane, which triggers the cyclin adenosine monophosphate (cAMP) pathway, through activation of the G-protein cascade. Upon hormone activation the α -subunit of trimeric G-protein complex is inactivated, this consequently drives the action of adenylate cyclase which catalyses the conversion of adenosine triphosphate (ATP) to cAMP. Activation of protein kinase A (PKA) through binding with cAMP, releases an active catalytic subunit C (C) that phosphorylates many substrates in the cytoplasm. A part of C also migrates into the nucleus and has the effect of activating transcription factors by phosphorylation, such as cAMP-responsive element binding protein (CREB). Activation of CREB has the effect of promoting

the transcription of cAMP regulated genes which ultimately act to promote cell proliferation (Indolfi *et al.*, 2003).

Once the VSMCs are in the synthetic state they release a collagen rich ECM, which forms the bulk of the neointima. A potent stimulator for this process is TGF- β_1 , which is synthesised and expressed by the VSMCs themselves as well as infiltrating macrophages expressing IL-1 (Chamberlain *et al.*, 2001).

Re-endothelialisation is an important process in neointima hyperplasia formation as it marks the end of the wound healing process. The rate at which an injured vessel is re-populated with ECs has been shown to be one of the governing factors which acts to determine the extent of the neointima growth (Mayr *et al.*, 2006). A recent study directed by Keith Channon, which used a mouse stenting model, revealed that ECs involved in the repopulation of the injured area come primarily from non-stented regions of the vessel and include endothelial progenitor cells (EPCs) (Douglas *et al.*, 2013). These findings therefore provide insight into another process which could be targeted in order to develop a therapeutic strategy to combat ISR.

1.4 Therapeutic strategies for prevention of in-stent restenosis

As described previously, (Section 1.3), the process of ISR is incredibly complicated and involves a plethora of molecular mechanisms that lead to the formation of the neointima. There are, therefore, a number of different approaches that can be taken to prevent ISR, employing the use of drugs, genes, RNA and cells for therapeutic gain. In the following section an overview of different treatment strategies is given; for clarity, ISR pathways have been grouped into the different stages of the process chronologically, with anti-inflammatory approaches first, followed by anti-proliferative approaches and then re-endothelialisation.

1.4.1.1 Anti-inflammatory approaches

The deployment of stents will inevitably cause an inflammatory response, in response to the placement of a foreign object into the vessel. In 1998, Kornowski and co-workers published a study which used the porcine stent restenosis model, and found a significant correlation between the extent of inflammation and the subsequent neointima formation (Kornowski *et al.*, 1998). These findings were mirrored in the human clinical setting exhibiting a strong correlation between stent associated inflammation and the degree of neointima formation (Farb *et al.*, 1999). Taken together, these results highlighted that using an anti-inflammatory approach could provide a useful prevention strategy for ISR.

TGF- β_1 , the inflammatory cytokine is one of the targets aimed to suppress this inflammatory response. Decorin and fibromodulin are both proteoglycans which act as antagonists for various isoforms of TGF- β_1 . Using an adenovirus-mediated gene transfer system, decorin and fibromodulin were delivered to human saphenous vein segments as a strategy to inhibit neointima formation through inhibiting TGF- β_1 's action. It was found that fibromodulin was a more potent inhibitor for the formation of neointima hyperplasia than decorin (Ranjad *et al.*, 2009).

The drug pioglitazone has also been reported to exhibit anti-inflammatory actions. In an atherosclerotic rabbit stenting study, pioglitazone was

administered orally and a 21% reduction of neointima formation was observed compared to the placebo control group. In addition, an 82% decrease in CCL2 was observed (Marx *et al.*, 2005). CCL-2 is a key chemokine that regulates the migration and infiltration of monocytes as part of the early inflammatory response; inhibition of its action could therefore account for the decrease in the decrease in neointima formation observed.

1.4.1.2 Suppression of VSMC proliferation

The phenotype-switching of the SMCs in response to the injury endured by the stent implantation can be inhibited to prevent and minimise neointima hyperplasia. The proliferation of SMCs can be targeted by expressing several anti-proliferative genes, such as thymidine kinase, and cytosine deaminase, these all work by inducing cell cycle arrest of SMCs in the S phase of the cell cycle, thereby providing a therapy which effectively prevents neointima hyperplasia in balloon injured vessels (Guzman *et al.*, 1994, Simari *et al.*, 1996, Yin and Agrawal, 2014).

Inhibition of the migration of the SMCs can be achieved by degrading the ECM, which is regulated by matrix metalloproteinases (MMPs) and tissue inhibitors of matrix metalloproteinases (TIMPs) (Yin and Agrawal, 2014, Osherov *et al.*, 2011). Inhibition of MMPs has been shown to have a profound effect on the prevention of neointima hyperplasia using marimastat, a broad spectrum MMP inhibitor. Neointima formation was reduced when marimastat was applied to human saphenous vein grafts, indicating it would be a good candidate as an anti-ISR drug candidate. Clinical trials of marimastat however, were halted at stage III due to high toxicity of the drug (Sparano *et al.*, 2004 Forough *et al.*, 1996).

Inhibition of MMPs using TIMPs was therefore an attractive venture for gene therapy, providing a more sophisticated solution to limit MMP activity. Baker *et al.* in demonstrated the versatility of this approach, using an adenoviral delivery system to overexpress TIMP 1, 2 & 3 in rat VSMCs, the findings showed that all three TIMPs effectively inhibited chemotaxis of the SMCs. TIMP-1 did not affect SMC proliferation, TIMP-2 exhibited a dose dependent inhibition of cell proliferation, and TIMP-3 induced DNA synthesis and promoted cell death by apoptosis (Baker *et al.*, 1998). The unique capabilities of the TIMP-3 expressing

virus were then explored to prevent neointima formation in a porcine stenting model at 28 days. This study indicated that the overexpressing TIMP-3 using an adenovirus vector provided a therapy which could effectively inhibit neointima formation, by promoting apoptosis and dysregulation of the MMPs (Johnson et al., 2005b).

In addition to delivering and targeting specific genes, RNA can also be used to provide a method for controlling neointima formation. One of the first examples of RNA based therapies within the context of prevention of neointima formation was demonstrated by directing the inhibition of SMC proliferation and migration has using an oligonucleotide (ODN) sequence that was complementary to the mRNA of the *c-myc* gene (Biro *et al.*, 1993). The *c-myc* gene had been previously implicated in encoding for a protein which modulates cell division. Using the RNA based therapy, the ODN sequence was delivered, which blocked the translation of the mRNA. This had the effect of downregulating the protein associated with cell proliferation, as well as a 50% decrease in VSMC proliferation and a >90% decrease in migration, when tested *in vitro*. A detailed overview of targeting mRNA using miRNA for the purpose of preventing ISR can be found in section 1.6.2.

Inhibition of VSMC proliferation is the main method for prevention of ISR used with DES, with rapamycin and sirolimus being two of the most prolifically used drugs to this effect. As discussed in section 1.2.1.2, using these anti-proliferative drugs yielded a profound decrease in restenosis rates when used in the clinic, however late stent thrombosis has hindered the progress of such therapies as these drugs delay the re-endothelialisation process, through their anti-proliferative modes of action. These findings have helped to define re-endothelialisation as a critical part of the wound healing process following stent implantation and deployment.

1.4.1.3 Promotion of re-endothelialisation

Several studies have focused on promoting re-endothelialisation as a strategy to prevent ISR. Injury sustained to the vessel by stent implantation causes significant damage to the endothelium as this is the first point of contact with

the stent. Encouraging re-endothelialisation using a variety of different techniques has therefore been extensively studied.

The vascular endothelial growth factors (VEGF) are a group of powerful endothelial mitogens which have been used as therapeutic agents for the prevention of ISR after injury. Expression of VEGF-D using an Adenovirus vector was used to decrease neointima growth by 50% following balloon denudation of rabbit aorta at 14 days (Rutanen *et al.*, 2005). Adenovirus mediated delivery of VEGF-C has also been shown to have a therapeutic effect on balloon injured rabbit aortas by reduction of a neointimal formation (Hiltunen *et al.*, 2000).

Another target for re-endothelialisation is nitric-oxide (NO), which is synthesised by nitric-oxide synthase (NOS). NO is a very important molecule for maintaining vessel homeostasis, it is a vasodilator and has been shown to promote re-endothelialisation, it inhibits platelet adhesion and aggregation as well as SMC proliferation and migration (Barbato and Tzeng, 2004). Using a lipopolyplex plasmid delivery system, endothelial NOS (eNOS) has been delivered from stent surfaces to rabbit arteries with the result of reduced neointima formation (Brito *et al.*, 2010). Due to NO's short half-life ~2.5 seconds, gene therapy in this instance is particularly attractive, as the short life span of NO can be circumvented by directing the synthesis of NOS. Localised delivery from the stent surface is also beneficial as it avoids systemic side-effects (Brito *et al.*, 2010).

As described in section 1.3, the discovery that the ECs which repopulate the injured area from stent implantation come from a combination of EPCs and ECs adjacent to the injured vessel and the relationship between an increased rate of re-endothelialisation brings a decrease in neointima formation (Douglas *et al.*, 2013) provides the grounds for EC based therapy. Technologies such as EPC seeded stents are being investigated as a means to kick-start the re-endothelialisation process and have been successful using *in vitro* models (Shirota *et al.*, 2003), however the real challenge lies in translation of these methods so that they are efficacious from *in vivo* settings.

1.5 Vectors for cardiovascular gene therapy

As our understanding of the biological mechanisms which underlie neointima formation and ISR advance (detailed in section 1.3); the therapeutic strategies used to prevent ISR have become increasingly more specialised as demonstrated by the use of gene and cell therapy for treatment of the disease (section 1.4). These therapies promise to offer a level of specificity which cannot be matched by traditional drug candidates. However, in order to employ gene therapy effectively as a therapeutic for the prevention of ISR, careful design and consideration is needed in the design of the gene delivery vector. An optimal gene delivery vector would possess the following characteristics; low toxicity and immunogenicity, efficient transduction of vascular cells with minimal transduction of non-target cells and appropriate longevity in order to achieve transgene expression to ensure a therapeutic effect (Baker, 2002). In 2011, it was reported that the most common method for delivery of genes into cells and tissues was by using virus vectors (68.8%), the second most reported method was naked/plasmid DNA (18.6%), non-viral chemical vectors accounted for 6.4%, and physical delivery methods (0.3%) were the least common (Su *et al.*, 2012). Each method has various advantages and disadvantages associated with it which are discussed in the following section.

1.5.1 Non-viral vectors

The main disadvantage of using non-viral vectors for delivery of genetic material is the fact that the transfection efficiency is low in comparison to using viral vector delivery systems. This is because viruses are the product of millions of years of evolution, specifically designed by nature to transport and express genetic material by infecting cells (Baker, 2002). On the other hand our immune systems have also benefitted from millions of years of evolution, to recognise the virus as a foreign body and prevent its action. Therefore using a non-viral delivery method should provide a method to circumvent a lot of the problems such as immunogenic responses and oncogenesis which plague the progress of virus vectors for their application in gene therapy on a practical level (Su *et al.*, 2012).

Perhaps the most promising of the non-viral vector strategies is the liposome, integrin targeting peptide, plasmid DNA, (LID) delivery system. Initially it did not contain the liposome component and was known as ID delivery system. The transfection efficiency of the ID delivery system was limited by endosomal degradation. The ID complex was shown to transfect many different cell types, however, this methodology was dependent on chloroquine to be present in the medium, which is an endosomal buffer (Hart *et al.*, 1997, Hart *et al.*, 1995). The incorporation of liposome, lipofectin, to form an LID delivery system was developed as a method to prevent endosomal degradation. Hart *et al.* demonstrated that including the liposome into the formulation of the non-viral vector, much higher transfection efficiency could be achieved when compared to the ID complexes. Transfection increased from 1-10% to over 50%, in three different cell lines (Hart *et al.*, 1998).

The scope of the LID delivery system was expanded by altering the integrin targeting peptide motif, to tune the properties of the LIDs so they selectively targeted certain cell types. Integrin receptors are membrane proteins, which are important for attachment of cells to ECM, cell-cell interaction and signal transduction. They are also the main route of entry for pathogenic viruses such as Ad, echovirus and the foot and mouth disease virus. Therefore inclusion of an integrin peptide motif in the self-assembling liposome delivery system was hoped to create a delivery vector which mimics viral methods of cell penetration.

The integrins on the VSMC and EC cell surface are $\alpha 5\beta 1$ and $\alpha v\beta 3$. Therefore Parkes *et al.* modified the LID vectors so they contained peptide binding motifs complementary to the VSMC and EC integrins to enhance transfection efficiency to these cell types making them suitable for cardiovascular gene therapy applications. Primary porcine VSMC and ECs were transfected with 40% and 35% transfection efficiency respectively. They demonstrated transfection using reporter genes GFP, luciferase and overexpression of TIMP-1, a potential therapeutic candidate for prevention of neointima hyperplasia (Parkes *et al.*, 2002).

Adapting the formulation of the LID system formulation furthermore by modifying the liposome composition, a wider family of receptor-targeted

nanocomplexes were developed (RTNs) and screened for their ability to transfect cultured vascular cells as well as rabbit aorta *ex-vivo* (Irvine *et al.*, 2008). Transfection of the rabbit aorta with the reporter gene peaked at 5 days, and was present up to day 14. This RTN composition was then used in the rabbit vein graft model to inhibit neointima hyperplasia. Using a therapeutic plasmid which encoded for inducible Nitric Oxide Synthase (iNOS), which was delivered adventitiously, a 50% reduction in neointima thickness and a 64% reduction in neointima area was measured at 28 days when compared to the surgery control groups (Meng *et al.*, 2013).

Sharif and co-workers reported the use of stent surfaces as a platform to deliver lipoplexes *in vivo* to rabbits to prevent neointima hyperplasia (Sharif *et al.*, 2012). The lipoplexes were less sophisticated than the liposomal delivery system reported by Meng *et al.* and contained plasmid DNA encoding for either a reporter gene (*LacZ*) or therapeutic gene eNOS and lipofectin. Importantly, they did not contain an integrin targeting peptide (Meng *et al.*, 2013). Previously, Sharif *et al.* had reported delivering Ad encoding eNOS from the stent delivery platform, and had observed a decrease in neointima hyperplasia and an increase in re-endothelialisation when compared to the surgery only control at 28 days (Sharif *et al.*, 2008). Therefore direct comparisons could be made with the lipoplex eluting stent, and the adenoviral eluting stent. At 28 days, an increase in the re-endothelialisation of the vessel was evident, however inhibition of neointima hyperplasia was not, compared to surgery only control.

Further investigation showed that the lipoplexes were targeting macrophages and not the SMCs, which was not the case with the Ads. It was hypothesised therefore, that the different targeting profiles of the Ad and the lipoplex could explain the different effects on the inhibition of neointima hyperplasia (Sharif *et al.*, 2012). Since the lipoplexes naturally targeted macrophages from the stent setting, a plasmid carrying anti-inflammatory genes could be carried to modulate the immune response post-stenting. It would also be interesting to see the inclusion of a targeting peptide for SMC integrins, using the RTN delivery system implemented by Meng, to see whether the effect of reducing neointima hyperplasia could be achieved with the non-viral vector as effectively as with the Ad vector from the stent setting (Meng *et al.*, 2013).

1.5.2 Adenoviral vectors

The adenovirus (Ad) is a non-enveloped DNA virus, which contains a linear double stranded 36 kb genome. They have an icosahedral capsid, made up of hexon, penton and fibre domains (Law and Davidson, 2005) (Figure 1-5). Different Ad serotypes are classified into different groups, A-G. This classification is dependent on the DNA sequence, the virus' ability to agglutinate erythrocytes and the serological profile of the virus (Russell, 2009, Bradshaw and Baker, 2013).

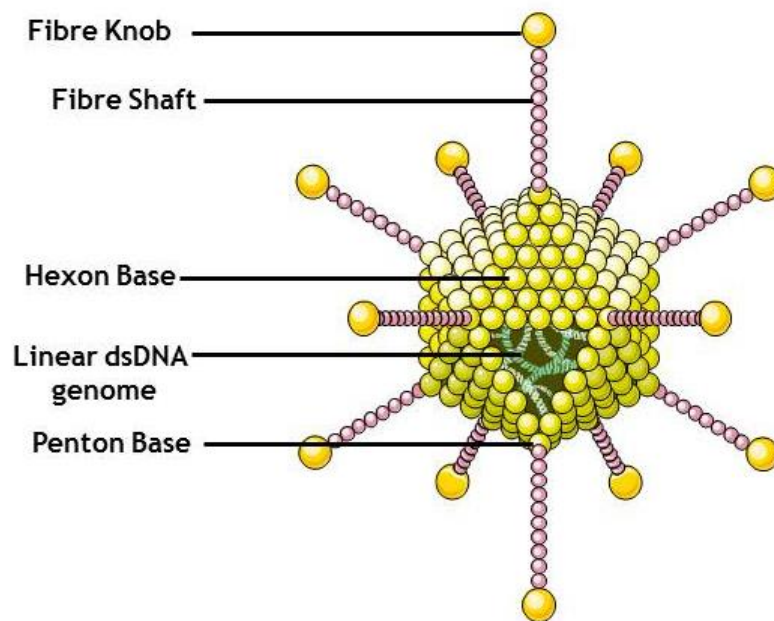


Figure 1-5 Structure of Adenovirus 5.

For use in the clinic, Ads have many properties which make them attractive candidates, for gene delivery vectors; they can be manipulated relatively easily, they can be made at high titres under GMP conditions, they do not insert their DNA into the host genome and can transduce a wide variety of quiescent and proliferating cell types. The most common serotype of Ad vector for use in clinical trials is replication deficient Ad5 (subgroup C), which has been extensively tested *in vitro* and in the *in vivo* setting (Bradshaw and Baker, 2013).

In 2003, a pilot safety study using the Ad5 vector for treatment of partial ornithine transcarbamylase (OTC) syndrome was halted after a patient on the

trial suffered an unexpected death. This was due to a systemic inflammatory response to the Ad5, which caused multiple organ failure (Raper *et al.*, 2003). The tragic death of Jesse Gelsinger in this trial highlighted the limitations in animal studies to predict human responses and reinforced how important it is to understand the complex interactions and responses of the Ad.

When Ad5 is administered systemically the interactions which can occur between the virus and the host are numerous, and should not be underestimated. These interactions need to be carefully considered when designing a study, to ensure a safe and therapeutic treatment. Ad5 infects respiratory epithelium and is therefore not a blood-borne virus, consequently it has not evolved strategies to stay within the circulatory system and is cleared rapidly; this presents many hurdles to overcome when using Ad5 vectors for gene therapy (Alemany *et al.*, 2000, Stone *et al.*, 2007a). One of the first observations when Ad5 was administered intravenously was that it was sequestered by the liver within 24 h in mice (Worgall *et al.*, 1997). Methods to minimise liver sequestration need to be taken therefore in order to create a vector suitable for cardiovascular gene therapy applications. Further detail on this sequestration mechanism was provided by Stone *et al.*, who reported that intravenous administration of Ad5 binds to circulating platelets which then directed uptake via the liver sinusoids with the result that the Ad5 particles are degraded by Kupffer cells (Stone *et al.*, 2007a).

If adenovirus vectors were judged on the criterion of their level of transduction for vascular cells they would not score highly, as innately they are targeted for the liver and spleen cells, they display limited abilities to transduce ECs, and are not efficient at transducing SMCs. This phenomenon can be explained by the adenoviral vectors receptor and the cells co-receptor on the cell surface. It is the case for most adenovirus serotypes in groups A, C, E and F that their primary target is the coxsackie and adenovirus receptor (CAR). In hepatocytes this receptor is expressed highly, to a lesser extent on endothelial cells and is virtually absent on SMCs, which therefore accounts for the Ads natural tropism (Bergelson *et al.*, 1997, Law and Davidson, 2005, Baker, 2002).

For the Ad5 serotype, there are a variety of mechanisms which the virus can use to gain entry to cells. The primary method is initiated by the virus docking to the

CAR receptor through the fibre knob domain (Law and Davidson, 2005, Bergelson *et al.*, 1997). Further interaction between an arginine-glycine-aspartic acid (RGD) motif on the penton base of the virus with $\alpha\text{v}\beta\text{3}/\alpha\text{v}\beta\text{5}$ integrins on the cell surface triggers endocytosis (Wickham *et al.*, 1993, Li *et al.*, 1998, Bradshaw and Baker, 2013). After systemic administration of Ad5, the primary target organ for Ad5 in rodents and non-primates is the liver (Alemany and Curiel, 2001, Martin *et al.*, 2003). However the method of entry for liver transduction requires a blood coagulation factor X (FX), to form a bridge between the hexon proteins of the Ad capsid to the heparin sulfate proteoglycans (HSPGs) on the cell surface (Bradshaw and Baker, 2013, Waddington *et al.*, 2008).

The high seroprevalance of Ad5 vectors is an important limitation to Ad5 vector based gene therapy. In 2011, a large international seroepidemiology was conducted which revealed that Ad5 neutralising antibody (NAb) titres were high within Sub-Saharan Africa and South-East Asia human populations. These findings could have consequences on Ad5 efficacy if delivered to these populations subsets as their action could be suppressed by the existing NAb's circulating in the blood (Sumida *et al.* 2005). Although this effect could be overcome by dosing with higher amount of the vector, this would not be an ideal solution due to the risk of triggering an increased innate immune response (Barouch *et al.*, 2011).

The surprising discovery that human erythrocytes have CAR and complement receptor (CR1), which is not the case with murine and rhesus macaque erythrocytes, was reported in 2009 (Carlisle *et al.*, 2009). The combination of CAR and CR1 on erythrocytes acts as a formidable defence for intravenous Ad5 particles. This finding furthermore highlights the limitations of using murine and other animal models to predict human clinical outcomes.

Finally, another issue with the Ad vector is their innate immunogenicity, causing the transduced cells to be cleared by T-cells, which results in a transient transgene expression profile (~4 weeks). Genetic modifications of the virus capsid can be performed to alter this and achieve longer-term gene expression *in vivo* (Baker, 2002, Oka *et al.*, 2001). For the purpose of preventing ISR from stent surfaces, this may not be an important issue as the therapeutic window for transgene expression would be from 0-30 days, during the inflammation and granulation phases of the disease.

1.5.2.1 Clinical Trials using Ad vectors for Cardiovascular Gene Therapy

Since the first human gene therapy clinical trial in 1990 (Rosenberg *et al.*, 1990), which used a retrovirus to treat advanced melanoma, many more trials have conducted. In 2012 it was estimated that over 2000 gene therapy clinical trials had taken place, or been approved worldwide, with the third most common application being cardiovascular diseases (~8.4%), after cancer (64.4%) and monogenic diseases (~8.7%) (Ginn *et al.*, 2013).

In 2003, a clinical trial was conducted using Ad mediated transfer of VEGF to prevent ISR by promoting re-endothelialisation following stent deployment. The Ad-VEGF therapy was delivered locally to the stented vessel, immediately after stent deployment using a perfusion-infusion catheter. This was a randomised, placebo-controlled, double-blind clinical trial, which aimed to compare the Ad-VEGF treatment against a non-viral delivery method using a VEGF plasmid liposome. The follow-up point of the trial was 6 months, with quantitative coronary angiographic analysis being used to judge whether the treatments were successful. At 6 months no significant improvement was observed between the groups (Hedman *et al.*, 2003). In addition to the initial trial, a follow-up study was also conducted 8 years after the initial trial, with the aim to establish whether intracoronary gene delivery of VEGF was associated with increased risks of major adverse clinical events (MACE), arrhythmias, cancer, diabetes and other diseases. No significant differences were recorded, leading to the conclusion that both therapies both viral and non-viral delivery of VEGF were safe and well tolerated in the short and long-term setting although both were ineffective for their purpose (Hedman *et al.*, 2009).

The AGENT clinical trial (Angiogenic GENE Therapy) used Ad5 as a delivery vector to enhance angiogenesis by expression of the FGF-4 gene, with the aim to treat angina. After the successful *in-vivo* results using a pig chronic induced stress ischemia model, which showed increased angiogenesis and left ventricular flow following administration of the Ad5-FGF4 vector. This provided promising data to validate proceeding with the clinical trial in humans (Gao *et al.*, 2004). The findings from the pooled data from AGENT-3 and 4 trials failed to show significant differences between the groups, judged by the different end points of the study, which were primarily done on the basis of exercise tolerance testing

(ETT). A significant difference in improved ETT measurements was observed when the data was analysed on the basis of gender, indicating an improvement in the female subset of patients receiving the Ad5-FGF4 treatment, although this has been attributed to a difference in the placebo effect between the groups (Henry *et al.*, 2007).

Although these trials have demonstrated no long term safety issues and side-effects which is a positive, the phase II and III randomised control experiments have, in general, failed to achieve the efficacy that was demonstrated so clearly in the earlier animal models and trials. Therefore, methods are needed to improve the efficacy of the vectors used so that the full potential of gene therapy can be unleashed and do justice to all the research and time taken to understand these diseases.

1.5.2.2 Novel Ad Vectors for Cardiovascular Gene Therapy

One method to increase transgene expression to the vasculature has been demonstrated by employing novel Ad serotypes which exhibits natural tropism for vascular cell types. Serotype D Ads show great variety with which receptors they use and their tropism; some use CAR, whereas others have been reported to use CD46 (Abbink *et al.*, 2007) and sialic acid (Arnberg *et al.*, 2000). Dakin *et al.* reported that using a novel Ad49 serotype (a species D Ad), they could transduce primary VSMCs, ECs and human CABG tissues, with remarkably higher efficiency compared to the Ad5 control (Dakin *et al.*, 2015). These findings warrant further pre-clinical testing using this novel vector. Further investigation into the identification of the primary receptor and mechanism for entry into the cells, could also provide new ways in which higher VSMC targeting could be achieved using Ad vectors.

1.5.2.3 Pseudotyping Ad vectors for Cardiovascular Gene Therapy

Success has also been made to enhance Ad5 transduction of human VSMCs by pseudotyping to make a chimeric virus with enhanced properties. This was demonstrated very effectively in the context of cardiovascular disease by Havenga *et al.* A library of Ad5 based vectors carrying fibres from different Ad serotypes were created and screened against cells and tissues from different species. It was found that the Ad5 vector carrying the fibre molecules from the

Ad16 serotype (a class B Ad) was far superior at infecting human and rhesus monkey VSMCs and ECs, this effect was even more heightened when the vessels were used in organ culture, with comparison to Ad5 transduction as a reference. Interestingly this result was not found for pig and rat models indicating the method for viral attachment to the cells is not conserved between species (Havenga *et al.*, 2001).

After the important discovery of CD46 being the receptor for most class B Ads, being made in 2003 (Gaggar *et al.*, 2003), Gaggar and co-workers designed a vector system which incorporated this receptor as a route of entry. This helped to create more chimeric Ad5 vectors which enabled enhanced gene expression in human SMCs. Since CD46 is highly expressed in hSMCs (60 to 100% cells stained positively for expression) whereas CAR is not (< 2% cells), Parker *et. al* rationalised that an Ad5 vector with Ad type B CD46 interacting structural components could enhance transduction efficiency to human vascular cells (Parker *et al.*, 2013). Using Ad35 as the type B virus, a chimeric Ad5-Ad35 hybrid was made with Ad5 capsid and Ad35 penton and fibre (Ad5/F35/P35). The resulting vector exhibited enhanced transduction efficiency for HVSMCs but not for HECs. This vector could be useful for use within cardiovascular gene therapy, but specifically for CABG procedures and stenting, where discrimination between the two main cell types could provide a unique and fine-tuned therapy.

1.5.3 Adeno-associated vectors

Adeno-associated viruses (AAVs) are part of the *paroviridae* family, which require helper viruses such as adenoviruses or herpes simplex viruses in order to facilitate infection and replication. They are smaller than Ads, with a diameter of 25 nm, and contain single-stranded DNA (ssDNA), 4.7 kb. In the absence of the helper viruses, they establish a latent infection by site-specific integration into the host genome (Wu *et al.*, 2006).

Adeno-associated viruses have the advantage of being a lot less immunogenic than the Ad vector. They also have the ability to express the target gene for the lifetime of the infected cell. This is because, unlike the Ad which is maintained episomally, the AAV vectors are able to integrate into the host genome. The natural tropism for AAV's is neurones, skeletal muscle cells and hepatocytes; transduction of SMCs and endothelial cells is very low, limiting their application for cardiovascular gene therapy without structural modification (Baker, 2002).

In order to increase the scope of the application of AAVs for cardiovascular gene therapy, different modifications and strategies have been employed to tune AAVs natural tropism, so they target cell types implicitly involved in cardiovascular diseases such as vascular endothelial and smooth muscle cells. Nicklin *et al.* genetically incorporated the EC targeting peptide SIGYPIP into an AAV capsid which enhanced the transduction efficiency to human ECs compared to the unmodified AAV wildtype vector (Nicklin *et al.*, 2001). The same method was used to design an AAV which can transduce SMCs efficiently by incorporating a SMC selective targeting peptide sequence into the capsid, which was identified by phage bio-panning (Work *et al.*, 2004).

Each AAV interacts with different receptors on the cell surfaces which is thought to account for the different tropism exhibited by each AAV (Summerford and Samulski, 1998). Another strategy for generating vascular-targeted AAV vectors therefore, is to screen different AAV serotypes and measure their transduction efficiency on different vascular cell targets. Chen *et al.* reported that AAV serotypes 1 and 5 in particular, exhibited a much higher transduction efficiency for rat and human aortic endothelial cells, compared to AAV 2, which is the most commonly used AAV for gene therapy applications. This tropism was thought to

be due to a sialic acid residue mediated mechanism for cellular uptake (Chen *et al.*, 2005).

Translation into the clinic of the AAV 1 vector in the cardiovascular setting has shown promising results in terms of efficacy and safety. The CUPID trial used an AAV 1 vector encoding for Sarcoplasmic reticulum Ca^{2+} -ATPase (SERCA) gene, which has been shown to be deficient in patients with heart failure. The virus was delivered to patients with advanced heart failure by an intracoronary infusion. Comparison against a placebo group enabled the conclusion that the overall condition of patients receiving the gene therapy treatment improved, indicated by a decrease in symptoms of heart failure and augmented heart functional status (Jessup *et al.*, 2011).

1.5.4 Lenti-viral vectors

Lenti-viral vectors are part of the retrovirus family which have an ssRNA genome with an 8 kb capacity. The most common vector for gene therapy is derived from HIV-1 serotype. These vectors are not inherently immunogenic which represents a significant advantage against other gene therapy vectors such as Ad5. Another advantage is that they are able to transduce quiescent cells making them suitable for cardiovascular gene delivery applications (Williams *et al.*, 2010).

Two major advances allowed for this vector to be considered as a possible gene therapy vector, firstly the U3 promotor region was inactivated, thereby reducing the chance of the generation of wildtype HIV-1 occurring (Miyoshi *et al.*, 1998). Secondly, the tropism for this virus was vastly improved by pseudotyping via the attachment of glycoprotein from a vesicular stomatitis virus (VSV-G) (Williams *et al.*, 2010). This modification made expanded its suitability for vascular gene therapy. Efficient human saphenous vein SMC and EC transduction was reported using third generation lenti-virus vectors. Furthermore, the construction a lenti-viral vector expressing TIMP-3 enabled comparisons to be made between Ad mediated gene transfer which showed that the lenti-viral vector performed to the same level as the Ad, inhibiting SMC migration and promoting apoptosis (Dishart *et al.*, 2003).

However, despite these advances on the bench level, there is still significant reluctance with regards to their safety which prevents the use of these vectors in the clinic. These concerns are well founded after 2 out of 10 patients receiving a gammaretrovirus therapy in a clinical trial developed T-cell leukaemia (Hacien-Bey-Abina, 2003).

1.6 miRNA

Vascular injury induced by stent implantation has many implications on the surrounding area, which leads to the formation of the neointima (Section 1.2.1.1). ECs and SMCs, which are the major cell types in arteries, are mainly affected; denudation of the ECs by stent placement and stimulation of the SMCs to proliferate and migrate, both contribute to the re-narrowing of the artery. In recent years much research has been focussed on the role of miRNAs in many different disease settings, as they have been shown to be key regulator molecules. One potential therapeutic strategy for controlling and preventing the neointima formation is therefore to administer key miRNAs known to be involved in the disease pathway of ISR.

1.6.1 Biogenesis of miRNAs

miRNAs are small non-coding RNA molecules, ~22 nucleotides in length, which can regulate gene expression post-transcriptionally by binding to complementary strands of messenger RNA (mRNA). This induces cleavage or repression of the mRNA (Brennecke *et al.*, 2005).

The biogenesis of miRNA begins in the nucleus with the transcription by enzyme RNA polymerase II, and occasionally RNA polymerase III, which produces primary (pri)-miRNA transcripts, which are often over 1 kb in length (Lee *et al.*, 2004, Borchert *et al.*, 2006, Brodersen and Voinnet, 2009). Endolytic cleavage of the pri-miRNA transcripts is catalysed by RNase III Drosha, to form several precursor (pre)-miRNA stem loop constructs which are ~65 base pair in length. (Kim, 2005, Yi *et al.*, 2003, Lee *et al.*, 2002). The pre-miRNAs are then transported out of the nucleus and into the cytoplasm by Exportin-5 (Yi *et al.*, 2003), where the pre-miRNAs are processed by RNase III Dicer, which cleaves off the loop of the hairpin to give the mature miRNA, ~22 nucleotides in length, which is paired to a complementary miRNA strand, known as the passenger or * strand (Lee *et al.*, 2002). Trans-activating response RNA-binding protein (TRBP) mediates binding of the miRNA duplex to the Argonaute II complex (Ago II), which is the catalytic component of RNA-induced silencing complex (RISC) (Chendrimada *et al.*, 2005). The duplex is unwound and the lead strand of the miRNA is stabilised, while the passenger strand is removed and normally degraded, although sometimes the

passenger strand has been shown to have biological activity as well (Meister, 2013, Bartel, 2009). The mechanism for unwinding of the duplex is still unclear, however there is some evidence to suggest that the Ago proteins within RISC might possess dissociation activity to aid this process (Meister, 2013, Wang *et al.*, 2009).

The mature miRNA guides the RISC to target mRNA, and binds through the seed sequence of the miRNA to complementary sequences on the 3' untranslated region (UTR) region of the mRNA through Watson-Crick base pairing. The seed sequence on miRNA is a sequence of 7 nucleotides in positions 2-8 from the 5' end (Flynt and Lai, 2008). The degree of complementarity between the seed sequence and the mRNA target 3'UTR region is thought to be important in determining the fate of the mRNA and the regulatory mechanism, which will either be degraded or translationally repressed (Carthew and Sontheimer, 2009). If the miRNA seed sequence has perfect complementarity with the mRNA 3'UTR region this usually results in cleavage and degradation of the mRNA (Rhoades *et al.*, 2002, Davis *et al.*, 2005). In animals, the majority of miRNA binding with mRNA is imperfect, with G:U interruptions and single nucleotide bulges, which instead of cleavage, usually directs repression of translation of the mRNA (Zeng *et al.*, 2003).

In animals a single miRNA can have 10's to 100's of mRNA targets. miRNAs which have the same seed sequences, and a high degree of sequence homology are grouped together into miRNA families which will target similar sets of mRNA (Friedman *et al.*, 2009, Baek *et al.*, 2008, Selbach *et al.*, 2008). The 3'UTR regions on mRNA are large enough to have multiple miRNA binding sites, it has been suggested that this could contribute to a cooperative effect between different miRNAs binding to the same 3'UTR region on the mRNA, adding complexity to the way in which miRNAs regulate mRNA translation (Davis *et al.*, 2008). A diagram of miRNA biogenesis is summarised in Figure 1-6.

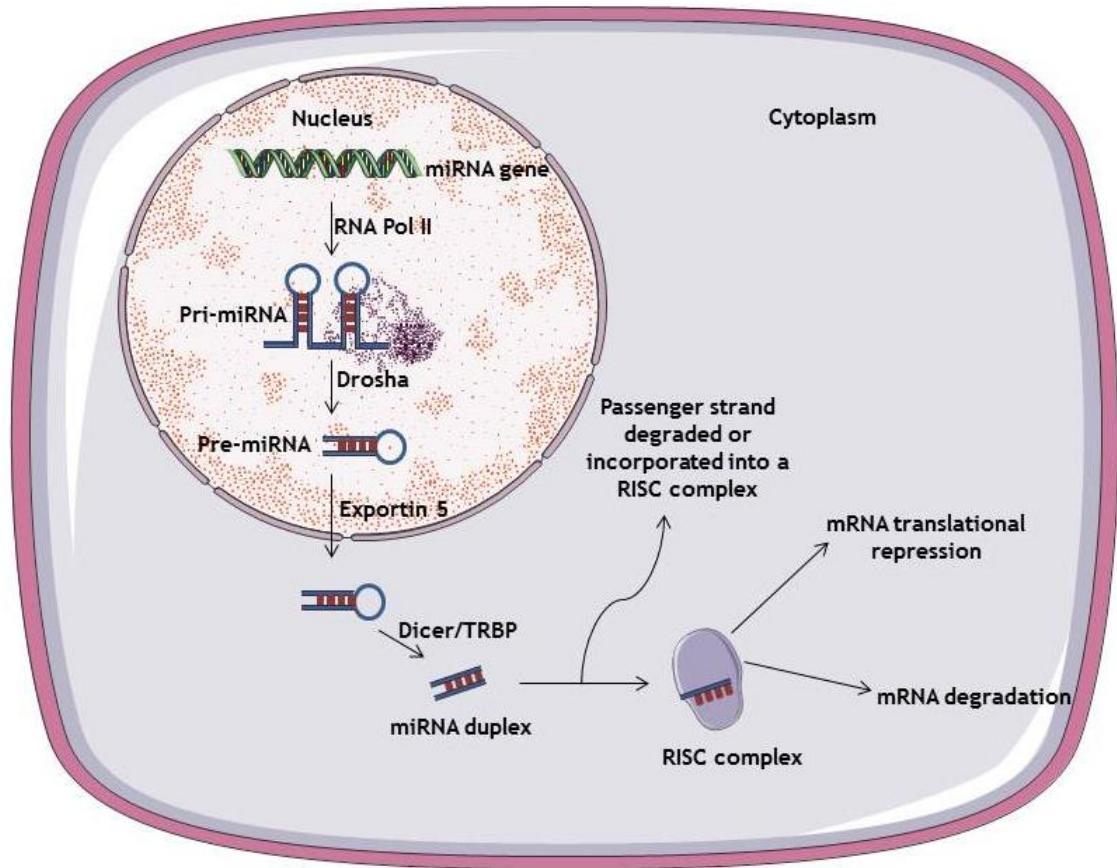


Figure 1-6 miRNA biogenesis pathway.

In the nucleus the pri-miRNA is transcribed by RNA polymerase II, which is then cleaved by Drosha to form preiRNA. The pre-miRNA strands are transported out of the nucleus by exportin5. The stem-loop is cleaved by dicer, to form the miRNA duplex. Association in the RISC complex unwinds the RNA and the passenger strand is either degraded or incorporated into another RISC complex. The lead strand is stabilised by the RISC complex and binds to target mRNA sequences through the seed sequence, which will either lead to mRNA translational repression or degradation depending on the complementarity of the interaction.

1.6.2 miRNAs involved in in-stent restenosis

A number of miRNAs have been identified to be involved in the process of in-stent restenosis and therefore modulating their expression could lead to a miRNA-based therapeutic to inhibit neointimal growth. A summary of these miRNAs is given in (Table 1).

References	RNA	After injury	Target Cell	Molecular Targets
(Ji et al., 2007b, McDonald et al., 2015)	miR-21	upregulated	VSMC	PTEN, PDCD4
(Cheng <i>et al.</i> , 2009b)	miR-145	downregulated	VSMC	ACE, KLF5
(Cordes <i>et al.</i> , 2009b)	miR-143	downregulated	VSMC	ELK1, FRA1
(Davis <i>et al.</i> , 2009)	miR-221	upregulation	VSMC	p27, C-KIT
(Iaconetti <i>et al.</i> , 2012)	miR-92a	upregulation	EC	KLF4, MKK4

Table 1 miRNAs associated with neointima formation which could be targets for treatment of ISR.

1.6.2.1 miRNA-21

miRNA-21 has been identified as a potential miRNA which could be used to modulate the wound healing process inflicted from stent deployment. A microarray was conducted on rat arteries before and after balloon injury, which indicated several miRNAs were aberrantly expressed before and after injury. miRNA-21 was one of the miRNAs which exhibited a dramatic change in expression resulting in a 5 fold increase at 7 days after injury. Therefore, knockdown of this miRNA was hypothesised as a strategy to inhibit neointima formation using antisense-miRNA-21. *In vitro* experiments confirmed a dose dependent response on antisense-miRNA-21 with decreased apoptosis and cell

proliferation, which was conformed *in vivo* using a ratballoon injury model, indicating that treatment of the vessel with antisense-miRNA-21 inhibited neointima formation (Ji et al., 2007b).

miRNA-21 has also been shown to be dysregulated after porcine vein grafting at 7 and 21 days, and has been identified as having a functional role in neointimal growth within this setting (McDonald *et al.*, 2013). Using miRNA-21 knock-out (KO) mice, miRNA-21s role in neointima formation after vein graft surgery was investigated, indicating that the absence of miRNA-21 had positive effects on preventing neointima formation. Due to the similar pathologies between neointima formation in vein graft surgery and in-stent restenosis, it was likely that miRNA-21 may play a similar role in vessels which have been injured through stenting.

In an *in-vivo* porcine study, both lead and passenger strands were shown to be upregulated 7 and 28 days after stenting, suggesting that this miRNA might play an important role in the post-stent injury response. A further investigation was conducted using miRNA-21 (KO) mice, which revealed that the neointima area, neointimal thickness and neointima/medial ratio was drastically decreased when compared to the WT controls, 28 days after stenting, giving support to the hypothesis that miRNA-21 could play a pivotal role in neointima formation. In order to investigate potential mechanisms which could help explain these observations, proliferation and migration assays were conducted with platelet derived growth factor (PDGF) as a stimulant on cultured miR-21 KO SMCs against wild type (WT) control cells. The miR-21 KO SMC showed attenuated proliferation and migration responses to this stimulus when compared to the KO control SMCs (McDonald *et al.*, 2015). These results suggest that downregulating miR-21 expression locally to stented vessels could provide a therapy which could suppress neointima formation and ISR.

1.6.2.2 miR-145 and miR-143

miR-145 is the most abundantly expressed miRNA in normal vascular walls and VSMCs which have been freshly isolated. However, expression of miR-145 is almost undetectable in ECs (Ji et al., 2007b, Cheng et al., 2009b). An interesting observation was made that the expression of miR-145 was suppressed in vessel

walls with neointimal growth (Ji et al., 2007b), leading to the hypothesis that miR-145 may have a regulatory role in modulating the SMC phenotype.

This theory was tested by monitoring the expression of miR-145 in PDGF stimulated VSMCs. PDGF is well-known to promote SMC proliferation and migration, by promoting a change in the SMC phenotype from contractile to synthetic states; this can be monitored by dedifferentiation markers such as SM α -actin, calponin and SM-MHC. It was observed that treatment of the cells with PDGF caused a decrease in miR-145 levels. Furthermore, overexpression of miR-145 was found to inhibit PDGF-induced VSMC dedifferentiation. Conversely, inhibition of miR-145 expression resulted in increasing levels of PDGF-induced VSMC dedifferentiation (Cheng *et al.*, 2009b).

The role of miR-145 on phenotype modulation of VSMCs was then investigated in the absence of PDGF stimulation, with VSMCs in the contractile state and interestingly it was shown that overexpression and inhibition of miR-145 levels resulted in decrease and increase in the synthetic phenotype VSMC markers respectively (Cheng *et al.*, 2009b). Inhibition of miR-145 immediately after stenting could therefore reduce neointima formation, by sequestering the VSMC response to injury and phenotype switching through the modulation of the miR-145 expression.

In the same year, other key findings were published with regards to the miR143/145 gene cluster role in SMC differentiation. Cordes *et al.* reported that myocardin upregulated miR-143 and 145 expression culminating in the induction of SMC marker gene expression and myofilament formation (Cordes *et al.*, 2009b). Boettger *et al.* demonstrated that, VSMCs from a miR-143/145 KO mouse exhibited VSMCs which did not express calponin, smoothelin, which are key contractile VSMC markers. The structure of the arteries also lacked myofilamentous cytoskeletal organisation, suggesting the key role that miR-143/145 gene cluster plays in the development of the vasculature and again highlighting its potential use as a therapeutic to regain vessel homeostasis after injury (Boettger *et al.*, 2009).

1.6.2.3 miR-221

miR-221 has also been implicated as a potential key regulator of VSMC phenotype, through action via the PDGF signalling pathway. PDGF is well known to promote neointima formation inducing SMC phenotype switching. In a study directed by Davis *et al.*, miR-221 was found to be transcriptionally induced by treatment of the VSMCs with PDGF, leading to downregulation of p27Kip1. The action of miR-221 on p27Kip1 was shown to be essential for PDGF induced VSMC proliferation (Davis *et al.*, 2009). These findings provide another example of how miRNAs play an important role in the maintenance of SMC behaviour, which leads to the development of them being used as potential therapeutics within the setting of stent deployment. In this case, if a miR-221 inhibitor was administered immediately after stenting, this could act as a suppressor for the PDGF pathway.

1.6.2.4 miR-92a

Tackling ISR by promoting re-endothelialisation could be achieved by the administration of a miR-92a inhibitor. This has been shown to be highly expressed in ECs but not in VSMCs and has been identified to promote EC proliferation when downregulated *in vitro*, using a BrdU assay. Delivery of antago-miR-92a has also been shown to be effective at preventing neointima formation *in vivo* after balloon injury of rat carotid arteries. The mode of action that miR-92a was having on EC function was investigated and it was found that key EC intracellular signalling molecules, c-Jun NH2-terminal kinase (JNK) and extracellular signal-regulated kinase (ERK) were increasingly phosphorylated upon inhibition of miR-92a. In addition, through loss of function assays, mitogen-activated protein kinase kinase 4 (MKK4) and Kruppel-like factor 4 (KLF4) were found to be mRNA targets for miR-92a (Iaconetti *et al.*, 2012).

1.7 Delivery of therapeutic vectors from stent surfaces

Despite a wealth of targets and mechanisms which have been identified to be involved in the process of ISR, and a multitude of different vectors tuned for cardiovascular delivery, the lack of an efficient localised delivery system hinders the progress within this field. In the following section delivery of viral vectors and miRNA from stent surfaces is discussed.

1.7.1 Local delivery of virus vectors from stent surfaces

Viral vector administration using catheters, whereby the virus is infused in the target vessel, was the first method of delivery used to treat ISR by gene therapy; however this has the disadvantages of suboptimal delivery and the possibility of distal spread of the virus which may cause many unwanted and potentially dangerous complications (Klugherz *et al.*, 2002b).

Therefore coating the stent with the virus vectors could provide a much improved system, which would achieve localised delivery to the stented vessel. Tethering viruses to stents was first reported by Klugherz; BMS were coated with a collagen matrix and then covalently linked to anti-adenoviral knob monoclonal antibodies. Covalent linkage was achieved by reacting collagen with *N*-succinimidyl 1-3-(2-pyridyldithiol)-propionate (SPDP), which enabled a covalent linkage to the antibody through the sulfhydryl moiety. This provided a surface upon which the adenovirus could be tethered to through antigen-antibody specific interactions. Using an Ad encoding green fluorescent protein (GFP), testing for localised delivery was achieved for rat arterial smooth muscle cells and porcine coronary arteries using fluorescent microscopy to detect the GFP transgene expression. GFP expression was monitored 7 days after deployment of the Ad5-GFP coated stents to the pig coronary arteries which revealed local transgene expression to the area around the stented region and additionally no distal expression of the transgene (Klugherz *et al.*, 2002b).

The concept of Adenoviral eluting stents was reported in 2002 using an Ad5-GFP reporter virus (Klugherz *et al.*, 2002b). This paved the way for developing stents that elute therapeutic viruses. In 2005, Johnson *et al.* reported the first therapeutic virus eluting stent as a treatment for ISR. In previous work they had

used an Ad vector expressing TIMP3 (AdTIMP3) to effectively prevent neointima formation in porcine saphenous vein grafts (Johnson *et al.*, 2005b). Due to the process of vein graft surgery, a window for treatment for the vein with therapeutic Ad is possible (after the vein has been excised but before it is sutured into the heart). For stenting however, this kind of delivery of the virus is not possible. Therefore they developed a method for coating the AdTIMP3 virus onto the stent surface to test whether this virus would be effective at transducing the stented vessel and importantly whether it would exhibit a therapeutic effect against ISR.

The method for coating relied on using electrostatic interactions between the Ad, which is inherently negatively charged, and the stent surface, which was coated in a positively charged phosphorylcholine (PC) material. This stent coating system had the advantage of being simpler than the method reported by Klugherz, as it utilised a commercial coating which already had safety records and FDA approval (Klugherz *et al.*, 2002b, Johnson *et al.*, 2005b). A disadvantage, however, is that relying solely on electrostatic interactions to bind the virus will result in a significantly weaker interaction than the antibody-virus attachment methodology. Nevertheless, the coating was robust enough to achieve localised delivery of the virus to the stented region of the vessel, and a therapeutic effect was observed. The AdTIMP3 PC coated stents were deployed into porcine vessels and after 28 days, a significant decrease in neointima area was recorded, compared to the AdlacZ PC coated control stents (Johnson *et al.*, 2005b).

Using the rabbit stenting model, whereby a stent is deployed into the right iliac artery, the PC adenoviral delivery system was also used to deliver Ad5-eNOS. At day 28, enhanced endothelialisation and a reduction in neointima formation was observed in the arteries treated with the Ad5-eNOS eluting stent when compared to the control stenting groups (Sharif *et al.*, 2008).

Fishbein *et al.* reported a methodology for virus linkage to stents, using polyallylamine bisphosphonate (PAA-BP). The bisphosphonate groups on the polymer backbone were able to co-ordinate to the metal oxide surface of the bare metal stents, whilst the amine groups could be reacted with succinimydyl 3-(2-pyridyldithio) propionate (SPDP), which allows covalent tethering of an

Anti-Ad antibody or recombinant Ad receptor protein, D1, through the formation of a disulfide bond. It was found that the D1 receptor protein allowed for a higher amount of virus vector to be bound to the surface and was therefore used in the *in vivo* model. Therapeutic efficacy was demonstrated with this system, by delivering Ad5 expressing iNOS (Ad-iNOS) to rat carotids from stent surfaces. At 16 days, the neointima areas were measured, and the treatment Ad-iNOS stent group demonstrated a decrease in the neointima/intima ratio by a half (Fishbein et al., 2006b).

This methodology was then expanded so that it did not rely on Ad binding to the receptor protein, and instead incorporated a direct covalent linkage between the Ad vector and the stent surface. The rationale being that this delivery system would be more robust, more versatile (not specific for a single virus species) and have higher affinity. The new delivery system used polyallylamine bisphosphonate comprising latent thiol groups (PABT), to coordinate to the stainless steel stent surface through the bisphosphonate moieties. The disulphide bonds were then activated using a reducing agent (tris-(2-carboxyethyl) phosphine) (TCEP), and then reacted with polyethyleneimine pyridyldithiol with PEI(PDT) to generate a higher density of thiol groups on the surface. A bi-functional cross-linking agent, HL, which has an amine functional group, that can be reacted with the lysine group on the Ad5 vector and a thiol functional group that can react with the activated stent surface, provides the bridge between the stent and the virus. In this way, the Ad was covalently anchored to the stent surface, however the HL crosslinking agent also has a labile ester group that enables vector release from the surface. This method of attachment and release was tested *in vitro* with rat SMC and *in vivo* by deploying stents into the carotid arteries of rats. When the stent was coated with Ad5-iNOS a significant reduction in ISR was observed indicating the potential for this type of coating (Fishbein *et al.*, 2008).

Further work by Fishbein *et al.* extended this methodology for covalent adenoviral attachment to stent surfaces, by using a library of different crosslinking agents, to tune the release profile of the Ads from the surface. Release of the Adenovirus from the surface depended on the hydrolysis kinetics of the ester groups within the crosslinker molecule, providing a route to fine-

tune the release and transduction of the Ad by modifying the linker chemistry (Fishbein *et al.*, 2014).

A summary of these studies reporting a variety of different methods for virus-eluting stents is detailed in Table 2. Having provided an overview from the initial concept using reporter viruses to deliver reporter genes from the stent surfaces, to efficacy studies, which demonstrated that the elution of viruses encoding therapeutic target genes can effectively be used to inhibit the process of ISR in this setting. It is clear that using the stent as a delivery platform not only provides an environment in which localised delivery can be achieved to the stented vessel, which will increase efficacy, it also limits safety problems as lower dosages of virus can be used and systemic interaction with the virus has been shown to be minimal. Identifying and using novel strategies for coating stents with viruses will be paramount for seeing the next generation of virus eluting stents which will hopefully result progress to the clinic. Current methods for generating virus eluting stents have required complicated surface chemistry providing bespoke stents which would be logistically very difficult to work with in the clinical setting. The quest for a simple, but effective virus delivery system from stent surfaces is therefore ongoing.

Reference	Model	Vector/ Gene	Method of Attachment	Outcome
(Klugherz et al., 2002b)	Porcine Arterial Stenting <i>in vivo</i>	Ad5-GFP	Collagen matrix covalently linked to anti-Ad antibodies	Detection of GFP localised to stented area after 7 days
(Johnson et al., 2005b)	Porcine Arterial Stenting <i>in vivo</i>	Ad5-TIMP3	Electrostatic interactions with positively charged phosphorylcholine coated stent	Significant decrease in neointima area was recorded after 28 days with the treatment group
(Fishbein et al., 2006b)	Rat Carotid Stenting <i>in vivo</i>	Ad5-iNOS	Bisphosphonate linker attached to D1 receptor protein	Significant decrease in neointima area was recorded after 14 days with the treatment group
(Fishbein et al., 2008)	Rat Carotid Stenting <i>in vivo</i>	Ad5-iNOS	Bisphosphonate linker covalently attached to Ad modified with labile ester linker	Significant decrease in restenosis after 14 days when treated with the Ad5-iNOS stent
(Sharif et al., 2008)	Rabbit Iliac Stenting <i>in vivo</i>	Ad5-eNOS	Electrostatic interactions with positively charged phosphorylcholine coated stent	Increased endothelialisation and decreased neointima formation at 28 days for treatment groups
(Fishbein et al., 2014)	Rat carotid stenting <i>in vivo</i>	Ad5-GFP	Bisphosphonate linker covalently attached to Ad modified with different labile ester linkers	Different release profiles of the Ad were achieved depending on how prone the ester linkages were to hydrolysis

Table 2 Summary of virus-eluting stents for prevention of in-stent restenosis studies.

1.7.2 Delivery of miRNA from stent surfaces

It is well recognised that the bottleneck to developing a successful miRNA therapy is in the development of a suitable delivery method that will reach the target tissue and cells *in vivo* (Zhang *et al.*, 2013). Delivering the miRNA from a stent surface therefore provides a unique platform for localised delivery for the prevention of ISR.

Up until very recently localised delivery of miRNA from stent surfaces had not previously been reported, and therefore represented a novel and innovative strategy to circumvent issues which plague other delivery systems of miRNA such as inefficient delivery, off-target effects, high dosage and the need for viral vectors.

To date the anti-miR-21 eluting stent reported by Wang *et al.* has been the only example of localised stent delivery (Wang *et al.*, 2015), which was demonstrated to have significant advantages over the systemic delivery methodology. It was documented that administering the anti-miR-21 intravenously in rats, caused significant off-target effects, lowering miR-21 levels in the kidney, liver and heart, which could cause unwanted biological effects and acute toxicity which would need to be addressed before intravenous delivery of miRNAs is translated to the clinic. However, when the anti-miR-21 was coated onto a stent surface, at the same concentration as used for intravenous delivery to rats (5 mg/kg), off-target effects were not detected in the kidney, liver and heart. However, inhibition of neointima formation was not compromised with the local stent delivery, indicating its potential for therapeutic stent delivery of miRNA.

The model used to investigate delivery of anti-miR-21 for the prevention of neointimal hyperplasia involved stenting human arteries coated with anti-miR-21 and transplanting into rats, arteries which were balloon injured but not stented were also transplanted. Repressing miR-21 levels had the effect of inhibiting neointimal growth, without affecting re-endothelialisation. This work builds upon previous work, described in Section 1.6.2.1., which identified miR-21 as being upregulated immediately after stent injury, and has been proven to modulate SMC proliferation when overexpressed.

The method for coating the stent with antimiR-21, was by direct application to a Translumina YUKON DES system, which is a microporous BMS, that allows for the adsorption of drugs onto the surface without the need for a polymer coating (Deuse et al., 2008, Wang *et al.*, 2015). This provided a successful method for local miRNA delivery to the vessel and paves the way for other miRNAs to be delivered in this manner, which ultimately brings us closer to seeing miRNA advancing to the clinic for the treatment of ISR, which could bring the next generation of stenting technology. Extending the methodology, so that delivery from other types of stent platform, such as biodegradable stents, could provide a novel delivery technology. Using a biodegradable material the stent would be a transient scaffold used to mechanically re-widening the vessel and neointima formation could be effectively prevented using localised miRNA therapy as discussed, and then over time the scaffold would dissolve.

1.8 Project aims

In-stent restenosis is a major clinical problem characterised by excessive VSMC proliferation and neointima formation in response to the injury endured and inflammatory response caused by stent deployment. A deeper understanding of the biological mechanisms which drive ISR have allowed gene and miRNA therapeutic strategies to be developed which could provide an elegant treatments for the prevention of ISR; however localised delivery methods are needed in order to take advantage of these specialised treatments and prevent unwanted systemic effects. Drug-eluting stents have proved to be efficacious at delivering anti-proliferative agents from stent surfaces *in vivo*, although issues with the specificity of drugs used, has caused higher incidences of late stent thrombosis to be recorded. This thesis aims to investigate different methods which allow for local delivery of virus' and miRNA from stent surfaces and evaluate the delivery methods *in vitro* and *in vivo*. The specific aims of the study are:

- To develop a method for localised delivery of Ad vectors from stent surfaces *in vitro*.
- To develop a method for localised delivery of miRNA from stent surfaces *in vitro*.
- To evaluate successful delivery methods *in vivo* using murine and porcine stenting models.

2 Materials and Methods

2.1 Materials

All chemicals were purchased from Sigma Aldrich (Poole, UK) and all cell culture reagents from Gibco (Paisley, UK) unless otherwise stated.

2.2 Cell culture techniques

Cells were maintained in a biological safety class II vertical laminar flow cabinet. Cells were grown as a monolayer in 25 cm², 75 cm², or 150 cm² cell culture flasks and incubated at 37 °C, 5% CO₂. The Human Embryonic Kidney (HEK) 293, rat A10 SMC and HeLa cell lines were grown in Dulbecco's Modified Essential Medium (DMEM) supplemented with L-glutamine (2 mM), penicillin-streptomycin (1% v/v), sodium pyruvate (1 mM) and foetal calf serum (10% v/v). Every 2-3 days the medium was replaced and cells were passaged when they reached 80% confluence to prevent overgrowth.

Prior to passaging, the cells were washed with PBS twice to remove any dead cells and debris. For the A10 and the HeLa cells a solution of Trypsin-Ethylene Diamine Tetra Acetic acid (TE) (0.02% w/v, 4 mL) was applied, and incubated at 37 °C until cells were detached. For HEK 293 cells a solution of 1x citric saline (2-3 mL) was applied and left at room temperature (RT) until detached. After the cells were dislodged the dissociation agent was quenched by adding an equal volume of cell media. Cells were then centrifuged (1500 RPM, 5 mins), the supernatant was discarded and the pellet re-suspended in an appropriate volume of medium for desired cell seeding density. For all experiments where cells needed to be plated at a precise seeding density, the re-suspended cells were counted using a haemocytometer and subsequently diluted to achieve the correct number of cells per well.

2.3 Production of adenoviral vectors

Serotype 5, replication defective recombinant adenovirus (Ad) containing the *lacZ* reporter gene (Ad5 CMV *lacZ*) was propagated in house as described by Nicklin *et al.* (Nicklin and Baker, 1999). Virus stock (50 µL, 5 x 10¹² VP/mL) was added to a bottle of supplemented DMEM (500 mL) identical to that used for cell culture. The medium was replaced on 24 flasks of 70-80% confluent HEK 293 cells

in 150 cm² cell culture flasks with Ad containing medium (23 mL) and left for a few days until a cytopathic effect was observed and the cells were peeling away from the bottom of the flask. At this point, the medium was harvested and centrifuged (2000 RPM, 10 mins); the cell pellet was re-suspended with PBS (6 mL). An equal volume of Arklone P (trichlorofluoroethane) (6 mL) was added to remove excess non-viral proteins; this was shaken and then centrifuged (3000 RPM, 10 mins). The top aqueous layer containing the crude Ad was removed and stored at -80 °C.

Replication deficient serotype Ad49 and Ad5 carrying luciferase marker genes (Ad49 luc, Ad5 luc) were obtained from Crucell (Leiden, Netherlands).

2.3.1 Adenovirus Purification

Adenovirus purification was achieved by ultracentrifugation of the crude Ad solution through CsCl gradients. Ultracentrifuge tubes were sterilised by rinsing with 70% EtOH and then PBS (14 x 95 mm, Beckman Coulter Ltd, High Wycombe, UK). A CsCl solution was added to the centrifuge tube (1.40 g/mL, 2.5 mL) then a second solution of CsCl was added on top of this (1.25 g/mL, 2.5 mL), finally the Ad solution was dripped on carefully and the rest of the tube was filled with PBS. The centrifuge tube was placed into a Beckman SW40Ti rotor and spun (35,000 RPM, 1.5 h, 16 °C) using a Beckman Optima L-80 ultracentrifuge. The white virus band was removed using a 5 mL syringe with a 23 Gauge needle. A second CsCl gradient was prepared using a new sterilised centrifuge tube with 5 mL, 1.34 g/mL CsCl, then Ad solution, and then PBS. The sample was spun overnight (35000 RPM, 16 °C) using the same rotor.

The virus layer was extracted again and injected into a Slide-a-lyzer dialysis cassette with 10000 Da molecular weight (wt) cut off (Thermo Scientific, Leicester, UK). A 10xTris-EDTA stock was prepared (10 mM Tris-HCL and 1 mM EDTA, pH 8) and diluted to 1xTris-EDTA with sterile dH₂O. The cassette was placed into 1xTris-EDTA buffer with stirring (2 L, 2 h, RT); this was then repeated for a further 2 h. Finally the cassette was placed in 1xTris-EDTA buffer with 10% v/v glycerol (2L, overnight, RT). The purified Ad solution was removed from the cassette and stored at -80 °C in 50 µL aliquots.

2.3.2 Virus Titration by End-Point Dilution Assay

The Plaque Forming Unit (PFU) titre of each Ad preparation was determined by an end-point dilution assay. 293 and HeLa cells were seeded in 96 well plates and grown to 60% confluence. 293 cells were used to assess the titre of the virus because they express the E1 section of the Ad genome enabling virus replication for replication defective Ads. The HeLa cell line however, does not contain this region of the Ad genome and was therefore used as a control to ensure replication deficiency in the Ads. A 10 fold serial dilution was made of the concentrated virus stock with DMEM, 100 μ L of each titration was added to each well as 10 replicates. Cells were maintained 37 $^{\circ}$ C, 5% CO₂. The medium was replaced every 2 days. The plates were examined under a 10x microscope and any wells exhibiting viral plaques were marked off. At 8 days the number of viral plaques was counted and the following calculation was made to determine the PFU titre:

$-X = \log_{ID_{50}}$ (infectivity dose) = log (dilution above 50% + proportionate distance x dilution factor)

Proportionate Distance = (%positive wells above 50% - 50%) / (%positive wells above 50% - %positive wells below 50%)

$$ID_{50} = 10^{-X}$$

$$TCID_{50} \text{ (Tissue Culture Infectivity Dose 50)} = 1 / 10^{-X}$$

$$TCID_{50} / 100 \mu\text{L} = 10^X$$

$$TCID_{50} / \text{mL} = 10^X \times \text{dilution factor (10)}$$

$$1 \text{ TCID}_{50} = 0.7 \text{ PFU}$$

$$\text{PFU/mL} = \text{TCID}_{50} / \text{mL} \times 0.7$$

2.3.3 Virus Particle Concentration Determination

Virus Particle (VP) titre was determined by performing a microBCA assay (Thermo Scientific) as per manufacturer's instructions. Briefly, a serial dilution of albumin standard in PBS were prepared (0.5, 1, 2.5, 5, 10, 20, 40 and 200 µg/mL), 150 µL of each solution was added in duplicate to a clear bottomed 96 well plate. In duplicate, 1 µL, 3 µL and 5 µL of virus stock was diluted with 150 µL PBS, 150 µL PBS was used as a blank control and added to the 96 well plate. Working reagent (150 µL) was added to each well and the plate was incubated at 37 °C, 2 h, in the dark. The absorbance at 570 nm was read using a Wallac Victor²™ Plate Reader (Wallac, Turku, Finland). A standard curve of the absorbance readings for the albumin standard was made and from this the relative amounts of protein was able to be determined for the virus samples. Using the relationship 1 µg protein = 1 x 10⁹ VP the concentration of the virus stock was determined (Von Seggern *et al.*, 1998).

2.3.4 Labelling adenovirus 5 with Alexa Fluor™ 555

Alexa Fluor™ 555 protein labelling kit was purchased from Life Technologies (Paisley, UK). The Alexa Fluor™ dye contains a succinimidyl ester which can react with primary amine residues on the virus capsid to form stable covalent bonds. The labelling procedure was carried out as outlined in the manufacturer's protocol. Briefly, a solution of sodium bicarbonate (1 M, 50 µL) was added to the adenovirus stock (2 mg of protein/mL, 500 µL). This was transferred to a vial containing the Alexa Fluor™ 555 dye and a magnetic stirrer bar and left to stir in the dark for 30 mins, RT. To remove any unreacted dye the reaction mixture was inserted into a Slide-a-lyzer dialysis cassette with 10000 Da molecular wt cut off (Thermo Scientific). The cassette was placed into a 1xTris-EDTA buffer and stirred (2L, 2 h, RT) the buffer solution was replaced twice with fresh 1xTris-EDTA after 2 h. If the labelled 555-Ad5 was not being used immediately the cassette was placed into 1xTris-EDTA buffer with 10% v/v glycerol (2L, overnight, RT). The 555-Ad5 solution was removed from the cassette and stored at -80 °C in 50 µL aliquots.

2.4 Formation of Polyelectrolyte Multilayers (PEMs)

For the (chi-ha)₈chi PEMs, chitosan was prepared 0.1% w/w, acetic acid 0.2% w/w in dH₂O as described by Meng *et al.* (2009b). The hyaluronan solution was prepared at a concentration of 1 mg/mL. After optimisation for viral transduction, 0.006% wt acetic acid was used instead of 0.2% w/w acetic acid.

The concentrations for the poly(allylaminohydrochloride) (PAH) and poly(styrenesulfonate) (PSS) solutions were prepared as follows: PAH (1mg/mL in 0.1 M NaOH), PSS (1 mg/mL).

To prepare the PEMs on glass microscope slides (Thermo Scientific), the slides were firstly cleaned by immersing in piranha solution for 15 mins (H₂SO₄ and H₂O₂ in a 3:1 ratio). The slides were then extensively washed with dH₂O. After cleaning, the slides were dipped into the polycationic solution for 1 min, rinsed with dH₂O and subsequently dipped into the polyanionic solution and then washed with dH₂O. This was repeated until the desired number of PEM layers was reached; the slide was then dried with N₂.

To prepare the PEMs on Stainless Steel (SS) surfaces, 316L SS discs were used as a model for the SS Bare Metal Stents (BMS) (Agar Scientific, Essex, UK). The SS disc was sterilised by soaking in 70% EtOH overnight prior to coating. The (chi-ha)₈chi PEM was prepared in the same way as described above for the glass microscope slides.

2.5 UV-visible light Spectroscopy to monitor build-up of PEMs

To monitor the sequential build-up of the PEM formation, UV-visible light spectroscopy was used. The PEMs were prepared on quartz microscope slides (H. Baumbach & co ltd, Ipswich, UK). The slides were prepared in exactly the same way as described above (section 2.4). The UV spectra were taken after each deposition of a polyanionic or polycationic solution. The spectra were recorded for the range of 200-500 nm using a UV-3101PC UV-VIS-NIR scanning spectrophotometer (Shimadzu, Kyoto, Japan). As the concentration of PEM deposited onto the quartz microscope slide increased, the absorbance increased

following the Beer-Lambert law: $A = \epsilon c l$ where A = absorbance, ϵ = molar absorption coefficient $L \text{ mol}^{-1} \text{ cm}^{-1}$, c = concentration mol L^{-1} l = pathlength cm.

2.6 Visualisation of fluorescently tagged adenovirus on polycationic monolayers

To enable the virus to be absorbed onto the PEM, the terminal layer must be polycationic. The polycationic solutions were chitosan and PAH prepared as described in section 2.4. For visualisation of the virus attached to the polycationic surface, fluorescently tagged Alexa Fluor™ 555-Ad5 was used (4.88×10^{10} VP/mL, 25 μL). Fluorescent tagging of the Ad5 virus with Alexa Fluor™ 555 was previously described in section 2.3.4. The virus solution was applied to the polycationic monolayer deposited on a glass microscope slide and left overnight, the PEM was rinsed thoroughly with PBS prior to visualisation under a Zeiss LSM 510 confocal microscope (Zeiss, Cambridge, UK) using a 60x immersion objective. A negative control of PEMs with unlabelled Ad5 was prepared and visualised in exactly the same way (4.88×10^{10} VP/mL, 25 μL).

2.7 Atomic Force Microscopy (AFM)

To visualise the topography of the surface after adsorption of Ad5 onto the polycationic monolayers (PAH or chi) and PEMs ((PAH-PSS)₈-PAH or (chi-ha)₈chi), atomic force microscopy was used. The surfaces were prepared on piranha cleaned glass microscope slides as described in section 2.4. Ad5 was applied to the PEM (2.44×10^{10} VP/mL, 50 μL), left overnight and then washed extensively with PBS. Once prepared micrographs were taken in non-contact mode, at a scan rate 1.01 Hz, dimensions of the images were either 5 μm x 5 μm , with a resolution of 256 x 256 pixels. Micrographs were recorded using a NTEGRA Spectra machine (NT-MDT, Moscow, Russia).

2.8 Adenovirus transduction *in vitro*

2.8.1 Transduction of A10 cells with Ad5 CMV lac Z

A10 cells were plated at a density of 2×10^4 cells/well in a 96 well plate and left overnight at 37 °C, 5% CO₂. Ad5 CMV lac Z was applied to the cells at concentrations 500, 1000, 2500 and 5000 VP/cell for 3 h, the medium was then

replaced and left for 72 h. Each concentration was performed in triplicate. The cells were then harvested and a β -gal assay was completed to allow for quantification of virus transduction (section 2.9.2).

2.8.2 Measuring the effect of polycationic solutions on adenoviral transduction

In a 96 well plate, A10 cells were plated at density of 2×10^4 cells/well and left overnight at 37 °C, 5% CO₂. Polycationic solutions, PAH and chi were prepared in the same way as described in section 2.4, but using DMEM as a diluent instead of dH₂O. Solutions were made at concentrations 1, 0.5, 0.25, 0.125, 0 mg/mL. Ad5 CMV lacZ(2500 VP/cell) was incubated with the polycationic solutions (PAH or chi, 50 μ L, 15 mins, RT) and then added to each well and left for 3 h, each condition was performed in triplicate with one extra well for staining. For the negative control group, A10 cells were replaced with medium which did not contain virus or polycationic solution. After 3 h the viral polycationic solutions were removed and fresh medium was added to the wells. The cells were left for 72 h at 37 °C, 5% CO₂. The cells were lysed and a β -gal assay was performed (section 2.9), for each condition one well was fixed with 2% (w/v) PFA, (100 μ L, 10 mins, RT) and stained with X-gal solution (sections 2.9.2, 2.11&2.12).

2.8.3 Measuring the effect of different concentrations of acetic acid on adenoviral transduction in a chitosan solution

In a 96 well plate, A10 cells were plated at density of 2×10^4 cells/well and left overnight at 37 °C, 5% CO₂. Chitosan solutions (0.1% w/w) were made up with MEM as a diluent, varying the concentration of acetic acid 0.2, 0.1, 0.05, 0.02, 0.01, 0.006, 0.002, 0% w/w. Ad5 CMV lac Z (1000 VP/cell) was incubated with the chitosan solutions (50 μ L) and applied to the A10 cells for 3 h, the medium was then replaced and the cells were left for 72 h, 37 °C, 5% CO₂. A non-treatment control of A10 cells which had not been treated with the adenovirus or chitosan solutions was used as a negative control. After 72 h the cells were lysed and a β -gal assay was performed (section 2.9.2). Three biological replicates were run per condition.

2.8.4 Measuring adenoviral transduction from SS surfaces coated with PEMs

SS discs were coated with a (chi-ha)₈-chi PEM, chi monolayer, or left uncoated, as described in section 2.4. Ad5 CMV lacZ (1.6 x 10¹² VP/mL, 30 µL) was added to the terminal layer of the PEM, chi monolayer or directly to the SS surface and left overnight at 4 °C. A non-treatment control was made by applying the uncoated SS disc to the cells without Ad5 CMV lac Z treatment. The PEMs were then washed thoroughly in PBS prior to being placed facedown onto the plated out cells.

A10 cells were plated in a 12 well plate at seeding density of 1 x 10⁵ cells/well and maintained at 37 °C, 5% CO₂ and left overnight. The next day the adenovirus coated surfaces were placed face down on the cells and left 72 h. The adenovirus coated surfaces were removed and the cells were washed thoroughly with PBS before harvesting and a β-galactosidase assay was performed on the cell lysates (section 2.9.2).

Initially, a concentration 0.2% w/w acetic acid for the chitosan solution was used as described by (Meng et al., 2009b). However after optimisation (section 2.8.3) 0.006% w/w acetic acid was used.

2.8.5 Measuring adenoviral transduction from adenovirus encapsulated in collagen gel from PLA and SS surfaces

In a 12 well plate, A10 cells were plated at a seeding density of 1 x 10⁵ cells/well and maintained 37 °C, 5% CO₂ and left overnight. The following day, Ad5 collagen gels were prepared as described in section 2.15.1 and coated onto PLA or SS discs (sections 2.14.1&2.4) at a concentration of 6.6 x 10⁹ VP/surface. PLA surfaces which were not coated with collagen but were coated with Ad5 were also prepared. The surfaces were washed thoroughly with PBS before being placed face down onto the cells and left for 72 h. The cells were then harvested and a β-galactosidase assay was performed on the cell lysates (section 2.9.2). A positive control of Ad5 in solution applied directly to the cells was used (6.6 x 10⁹ VP). Non-treated cells were maintained in medium throughout the experiment. Each condition was run as a biological triplicate.

For Ad49 luc the same protocol was followed. However a luciferase assay was used to determine the levels of virus transduction instead of a β -galactosidase assay (section 2.13).

For SS coated in PLA surfaces, PLA was dissolved in chloroform at concentrations 10%, 15%, 20% wt/wt and spread onto SS surfaces as described in section 2.16.1. The protocol for transduction as described above was used to determine viral transduction from SS coated with different concentrations of PLA.

2.9 Ex vivo transduction of Ad5

2.9.1 Ex vivo transduction of Ad5 from stent surfaces coated with (chi-ha)₈chi PEMs to rat aortas

Gazelle BMS were expanded and removed from the balloon before being coated with (chi-ha)₈-chi PEM, using the optimised concentration of acetic acid (section 2.4). Ad5 luc (1.6×10^{12} VP/mL, 30 μ L), was applied to the PEM coated stent and left overnight at 4 °C. Stents were then washed, crimped onto the balloon and deployed into rat aortas *ex vivo* and cultured for 72 h. Luciferase activity bioluminescence was quantified using an *in vivo* imaging system, (IVIS, Caliper Life Sciences, Massachusetts, USA) 25 mins after luciferin administration. Quantification of bioluminescence was recorded as an average radiance (photons/second/cm²/steradian).

2.9.2 Ex vivo delivery of Ad5 CMV lacZ to mouse aorta

2.9.2.1 Determining concentration for transduction of mouse aortas with Ad5 CMV lacZ *ex vivo*

Mouse aortas were dissected from MF1 mice and incubated with solutions of Ad5 (5×10^9 VP/mL, 5×10^{12} VP/mL, 5×10^{11} VP/mL in MEM) for 72 h, 37 °C, 5% CO₂. The aorta was then cut open and fixed in 2% PFA and then stained with X-gal for 4 h, 37 °C (as described in section 2.12).

2.9.2.2 Transduction of mouse aortas from PLA coated with collagen Ad5 gel

Mouse aorta was dissected from MF1 mice cut longitudinally and placed in a 12 well plate with the endothelial layer face up. An Ad5 CMV lacZcollagen gel was

applied to PLA squares using the method described in section 2.15.1, using a viral concentration of 5×10^{11} VP/mL. The squares were placed face down onto the endothelium. The aorta was left for 72 h in culture and fixed with 2% PFA for the Ad5 CMV lacZ-treated aortas they were stained with X-gal (section 2.12).

In order to model endothelium damage, a mini-trek balloon was expanded to 10 atm in the aorta prior to adenoviral delivery from PLA surfaces. For each group two aortas were balloon damaged prior to exposure to the virus, and two were uninjured, the groups were non-treatment control, Ad5 in solution (5×10^{11} VP/mL), and PLA-collagen-Ad5 gel (5×10^{11} VP/mL). After culture for 72 h, tissue was fixed and stained with X-gal (section 2.12).

2.9.3 *Ex vivo* delivery of Ad5 CMV lacZ from PLA coated stents to porcine coronary arteries

2.9.3.1 Preliminary testing of Ad5 CMV lacZ coated stents for transduction to porcine coronary arteries

Pig hearts (from large white pigs) were obtained fresh from Shotts abattoir (Scotland, UK). The coronary artery was dissected from the heart and stored in PBS at 4°C until stent deployment. The stents used were human bare metal Gazelle™ stents (3.0 x 18 mm, Biosensors International, Singapore). The stents were coated with 20% w/w PLA dissolved in chloroform and then in the collagen-Ad5 CMV lac Z gel, following same procedure as for *in vitro* testing (2.15.1) at a concentration of 1.25×10^{12} VP/mL. The stents were then deployed into the arteries and incubated for 72 h, they were then washed with PBS, cut longitudinally, fixed in 2% PFA (overnight, 4°C) and stained with X-gal (section 2.12) to confirm whether virus transduction had been achieved.

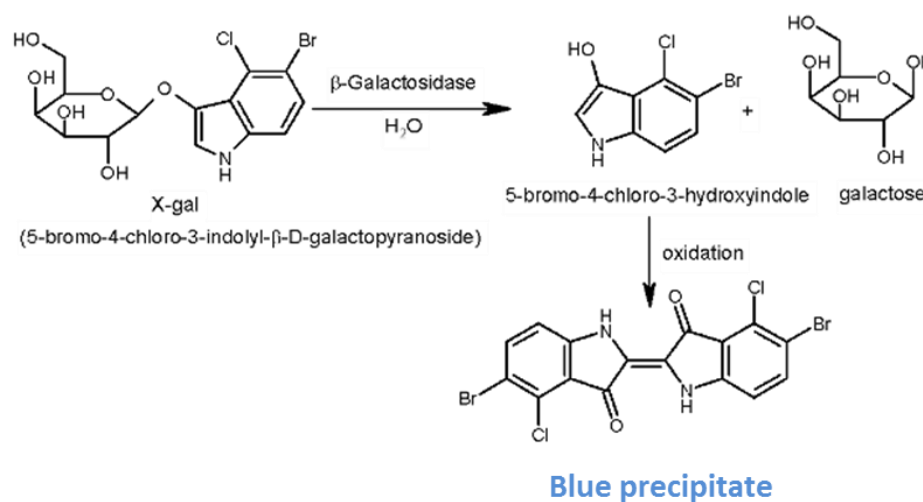
2.9.3.2 Effect of PLA concentration on efficacy of delivery of Ad5 CMV lacZ to porcine arteries *ex vivo*

PLA was dissolved in chloroform at concentrations (10%, 5%, 2.5%, w/w). The BMS were coated in the PLA solutions; they were then coated with Ad5 CMV lacZ collagen gel as described in section 2.15.1 at a concentration 1.25×10^{12} VP/mL. Once deployed, the stents were left in culture for 72 h and then fixed with 2% PFA and X-gal stained (section 2.12). The stents were then evaluated on three criteria for their suitability to be used for *in vivo* application; whether

they were able to fit through a guide catheter, whether they were able to be expanded with a balloon, and whether virus transduction was observed.

2.10 β -galactosidase transgene quantification

Ad5 CMV lac Z has been genetically modified so that it encodes for the enzyme β -galactosidase. Natively, this enzyme cleaves glycosidic bonds of β -galactosidases into monosaccharides in *E.coli*, however it can also be used to cleave the glycosidic bond of X-gal (5-bromo-4-chloro-3-indolyl- β -D-galactopyranoside). Cleavage of X-gal releases 5-bromo-4-chloro-3-hydroxyindole, which dimerises and precipitates to form a blue solid; it is in this manner that it can be used as a reporter for virus transduction (Scheme 2-1).



Scheme 2-1 Cleavage of X-gal glycosidic bond with β -galactosidase forms a blue precipitate which is used as a reporter for β -galactosidase expression.

A Tropix Galacto-Light Assay kit (Applied Biosystems, Foster City, USA) was used to determine the amount of β -galactosidase expressed. The assay was carried out as per manufacturer's instructions. After adenovirus transduction (sections 2.8), the cell medium was removed and the cells were washed with PBS, the cells were then lysed by adding lysis buffer (1 mL Triton X in 500 mL PBS) (100 μ L for a 96 well plate, 1 mL per well for a 12 well plate). Cells were scraped and then freeze thawed to aid lysis. The cell lysate from each well (10 μ L) was added to a black 96 well plate in triplicates. A 1:100 dilution of Tropix Galacton Plus: Galacto-light diluent mix was made and added to each well (100 μ L). The plate was protected from light and left for 1 h, RT. Tropix Accelerator II was

added to each well (100 μ L) and left for 2 mins. The luminescence was measured using a Wallac VICTOR²™ plate reader. Each sample was run as a technical triplicate. The luminescence readings were normalised to protein content of each of the samples giving values in relative light units/mg protein (rlu/mg). Protein content determination is described in the following section (section 2.11).

2.11 Protein concentration determination from cell lysates

To establish the concentration of the cell lysate samples, a Pierce™ BCA assay kit was used (Thermo Scientific). A 1:50 dilution of BCA reagent B:BCA reagent A was made and added to each well of a clear 96 well plate (100 μ L). The cell lysate (10 μ L) was added to each well and incubated (30 mins, 37 °C, in foil). The plate was cooled to room temperature and absorbances were read using a Wallac VICTOR²™ plate reader at 562 nm. Each sample was run in triplicate.

2.12 X-gal staining of cells and tissues

After incubating cells/tissue with Ad5 CMV lacZ for 72 h (sections 2.8& add in tissue bit) medium was removed from cells or tissue and washed with PBS. Cells and tissue were fixed with 2% (w/v) PFA, for cells (100 μ L, 10 mins, RT), for tissue (1 mL, overnight, 4 °C). The PFA was removed and cells/tissue washed with PBS and the X-gal stain (100 mM sodium phosphate pH 7.3, 1.3 mM magnesium chloride, 3 mM potassium ferricyanide, 3 mM potassium ferrocyanide, 1 mg/mL X-gal) was applied to the cells (100 μ L, 4 h, 37 °C) or to the tissue (1 mL, overnight, 37 °C). Cells and tissues were imaged using a Nikon Eclipse TS100 microscope, 40x magnification for cells, 4x for tissue.

2.13 Luciferase Assay

Luciferase Assay Kit was purchased from Promega (Southampton, UK). Cells were lysed by adding 1 x lysis reagent (500 μ L to each well of a 12 well plate). Lysis reagent solution is 25 mM Tris-Phosphate pH 7.8, 2 mM DTT, 2 mM 1,2-diaminocyclohexane-N,N,N',N' tetra acetic acid, 10% glycerol, 1% triton X-100. The plate was frozen at -80 °C for 1 h. The plate was thawed, and cell lysate from each well (10 μ L) was added to a white 96 well plate, with the luciferase

assay reagent (100 μL). The light emitted was measured immediately using a luminometer plate reader. The protein concentrations of each cell lysate (10 μL) were determined by performing a BCA assay (section 2.11). The luminescence readings were normalised to protein content of each of the samples giving values in relative light units/ mg protein (rlu/mg).

2.14 Modification of PLA surface chemistry

2.14.1 3D printing PLA squares

PLA filament and 3D TouchTM printer was supplied by Bits from Bytes (Clevedon, UK). PLA Squares were designed using Autodesk software. The squares were printed using a layer deposition method and had the dimensions of 1.5 cm² by 2 mm.

2.14.2 Measuring extent of hydrolysis of PLA by percentage weight loss

3D printed PLA squares were prepared as described above (section 2.14.1). PLA squares were weighed and placed into NaOH_(aq) (1 M, 1 mL, RT). The squares were left in the NaOH solution and removed at timepoints 5 mins, 30 mins and 24 h. After removal they were dried under vacuum and weighed again. This enabled the %wt loss of PLA to be determined. A control PLA square was placed in dH₂O for 24 h to control for water hydrolysis.

2.14.3 Binding of hexamethyldiamine (HMD) to a PLA surface by EDC/NHS activation

3D printed PLA squares (section (2.14.1)) were washed in ethanolic aqueous solution (1:1, v/v), and then washed with dH₂O (10 mins). Activation of the PLA was performed by immersing the PLA in NaOH_(aq) (1 M, 5 mL, 5 mins). The PLA squares were immersed in an aqueous solution of 1-ethyl-3(3-dimethylaminopropyl)carbodiimide hydrochloride (EDC, 0.1 M) and N-Hydroxysuccinimide (NHS, 0.2M) for 30 mins (2 mL). Activated PLA was then immersed in a solution of HMD dissolved in iPrOH (0.04 g/mL, 30 mins, 4 °C) then (20 h, RT). Before testing the PLA surface for primary amine functionality

(section 2.14.5), the PLA squares were washed with EtOH (3 x 10 min, 5 mL, 37 °C).

2.14.4 Binding of HMD to PLA surface by direct aminolysis

PLA squares were washed in ethanolic aqueous solution (1:1 v/v) for 1 h, and then washed in 10 mL dH₂O for 10 mins. PLA was immersed in a solution of hexamethyldiamine (HMD) (0.04 g/mL, 30 mins, 50 °C) in 2.5mL iPrOH. The squares were then washed with EtOH (3 x 10 min, 5 mL) and tested for primary amine functionality by ninhydrin assay (section 2.14.5).

2.14.5 Ninhydrin assay to test for functionalisation of PLA with primary amine groups

The two different methods for amine functionalisation of the PLA (after EDC/NHS activation (section 2.14.3) and by direct aminolysis (section 2.14.4)), were tested for the presence of primary amines on the surface by performing a ninhydrin assay. Briefly, a ninhydrin stock solution was prepared (0.35 g dissolved in 100 mL EtOH), 1 mL was added to each PLA square (stirred, 95 °C, 15 mins). A deep purple colour on the PLA surface indicated a positive result for primary amines. Non-treated PLA was used as a negative control.

2.14.6 Derivatisation of PLA with benzaldehyde

Aminolysed PLA was prepared using the two methods described in sections 2.14.3 and 2.14.4. Untreated PLA and hydrolysed PLA were also prepared. All pieces were immersed in a solution of benzaldehyde in MeOH and stirred (10 mM, 5 mL, 2.5 h). The pieces were washed in MeOH (10 mL, 12 h, 37°C) and then dH₂O (3 x 10 mL, 30 mins, 37 °C). Finally, HCl (1 M, 10 mL) was added to the PLA overnight to remove the benzaldehyde. Absorbances at 220 nm were taken of the HCl solutions for detection of benzaldehyde using a UV-vis spectrometer.

2.14.7 Deprotection and detection of Fmoc from Fmoc lysine

Fmoc-lys-OH HCl (10 mg) was dissolved in MeOH (800 µL). Piperidine (5% wt in EtOH, 200 µL) was added and left to react for 40 mins. Samples before and after

deprotection were run on the electrospray ionisation mass spectrometer (ESI-MS), see section 2.14.8.

2.14.8 ESI-MS

Excess solvent was removed by evaporation and samples were then dissolved in MeOH. Mass Spectrometry data was collected using MicroTOF-Q MS instrument with an electrospray ionisation source (ESI), (Bruker Daltonics Ltd, Coventry, UK) spectra were recorded in positive ion mode.

2.14.9 Derivatisation of PLA with Fmoc-lysine-OH

PLA was washed in ethanolic aqueous solution (1/1 v/v) for 1 h then dH₂O. For the EDC/NHS activated surface the PLA was then placed in NaOH (1M, 5mL, 5 mins) then washed in dH₂O. The PLA was then immersed in a solution of EDC (0.1M, 0.038 g) and NHS (0.2 M 0.046 g) in 2mL dH₂O for 1 h on ice and then rinsed with dH₂O. Both EDC/NHS activated and PLA which was to undergo direct aminolysis with Fmoc-lys-OH HCl were placed in a solution of Fmoc-lys-OH HCl (0.04 g/mL) in 2.5 mL EtOH. For the EDC/NHS activated PLA the solution was stirred for 30 mins on ice and then 30 mins at RT. For the aminolysis PLA the solution was stirred at 50°C for 1 h. The PLA was then washed in EtOH (3 x 5mL, 10 mins, 37 °C) and samples collected for UV-vis measurement. The PLA was then immersed in 5% piperidine in EtOH (5mL, 40 mins, RT). UV-vis measurements were taken for piperidine measurements. The samples were then rotary evaporated and then redissolved in MeOH and ESI-MS spectra were taken.

2.15 Methods for collagen adenovirus gel formation and coating onto stent surfaces

2.15.1 Entrapping adenovirus into a collagen gel and coating onto PLA surfaces

Bovine Type I collagen (5 mg/mL, Gibco, Life Technologies) was diluted with 1M NaOH and PBS to a concentration of 3 mg/mL as described in the manufacturer's gelling protocol. To prepare the adenovirus collagen coated PLA squares, Ad5 CMV *lacZ* (2.45 x 10¹² VP/mL, 2.7 µL, 6.6 x 10⁹ VP/surface) was mixed with the collagen solution (25 µL, 3 mg/mL), and spread onto the PLA square. The PLA

square was incubated at 37 °C for 1 h followed by 1 h RT. The PLA was then washed thoroughly with PBS before transduction with cells.

2.15.2 555-Ad5 collagen gel on PLA preparation and visualisation

Ad 5 was fluorescently tagged with Alexa Fluor™ 555 dye as described in section 2.3.4. To prepare a fluorescent virus collagen gel, 555-Ad5 was used at same concentration and prepared as described previously (section 2.15). A negative control was prepared by coating PLA + collagen gel without 555-Ad5. In order to compare the collagen virus gel PLA surfaces with PLA surfaces without collagen, 555-Ad5 was applied directly to the PLA. Images of the PLA squares were taken using a fluorescent microscope. Images were taken at 4x magnification, 1000 ms exposure time, 572 nm excitation.

2.15.3 Quantification of amount of virus on surface

2.15.3.1 Quantification by MicroBCA

A serial 10 fold dilution of Ad5 CMV lac Z in PBS was made to make 10 solutions ranging from 5.0×10^{10} VP/mL to 50 VP/mL. A microBCA assay was performed on these solutions using the instructions provided by the supplier as explained in section 2.3.3 (MicroBCA Protein Assay Kit, Thermo Scientific).

2.15.3.2 Quantification by quantitative reverse transcription polymerase reaction (qRT-PCR)

DNA was extracted from the virus solutions prepared at concentrations 5.0×10^{10} VP/mL to 50 VP/mL (1000 μ L) using the QIAamp UltraSens Virus Kit following the manufacturer's instructions (Qiagen, Limburg, Netherlands). Briefly, each virus solution was added to a 2 mL microcentrifuge tube and 800 μ L of buffer AC was added as well as carrier RNA solution (5.6 μ L, 1 μ g/ μ L), the tube was inverted 3 times and then vortexed for 10 seconds, the tube was then left for 10 mins, RT. Buffer AC contains a compound which can complex with DNA allowing sedimentation by low g force centrifugation to form a cell pellet. The tube was centrifuged at 1200 x g for 3 mins. The supernatant was discarded and the pellet re-suspended in Buffer AR, pre-heated to 60 °C and proteinase K (20 μ L). The tube was vortexed until the pellet was completely re-suspended. The tube was

then incubated in a water bath for 10 mins, 40 °C. Buffer AB (300 µL) was added and mixed thoroughly by vortexing. The solution was then applied to a Qiamp spin column and centrifuged (4000 x g, 1 min). The spin column was then placed into a new collection tube, AW1 was added to the column (500 µL) and centrifuged for (6000 x g, 1 min). The spin column was then placed into another spin column and buffer AW2 (500 µL) was added and centrifuged for 3 mins, 16000 x g. The spin column was finally placed into a 1.5 mL microcentrifuge tube and buffer AVE was applied to the column (30 µL). The tube was centrifuged for 6000 x g, 1 min. AVE buffer was added again to the spin column (30 µL) and centrifuged for 6000 x g, 1 min. The extracted DNA was stored at -20 °C.

For the qRT-PCR, each reaction contained Power SYBR® green PCR Master Mix 2x (6.25 µL), Forward Primer (0.05 µL), Reverse Primer (0.05 µL), H₂O (5.15 µL), and extracted DNA (1 µL), triplicates of each sample were run in a 384 well plate, using ABI 7000 qRT-PCR machine (Applied Biosystems). A standard curve was plotted cycle threshold (Ct) value vs concentration VP/mL of the known virus concentrations; this enabled unknown virus concentrations to be determined. To measure the amount of virus washed off from the surfaces, the surfaces were washed with PBS (1 mL), the viral DNA was then extracted and quantified by qRT-PCR as described above.

2.16 PLA coating onto SS methodology

2.16.1 Preparation of PLA coated onto SS discs

PLA filament was dissolved in chloroform at 10%, 15%, 20% wt/wt, stirring vigorously. Stainless steel discs (Agar Scientific) were then dipped into the PLA chloroform solution, removed and then left to dry at room temperature overnight. For *in vitro* testing, transduction of adenovirus from PLA coated SS was performed by coating collagen-Ad5 gels as described in section 2.8.5.

2.16.2 Coating PLA onto mouse stents

For *in vivo* experiment, mouse stents (2.5 x 0.6 mm, Cambus medical, Galway, Ireland) were threaded onto a western loading tip and coated with PLA dissolved in chloroform (10% wt/wt) and left to air-dry. Dichloromethane was heated to

65°C in a lidded beaker, the stent was placed into the vapour for 10 seconds and then removed to smooth the PLA.

2.16.3 Coating PLA onto pig stents

For *in vivo* work, the stents were removed from the balloon and the exterior surface of bare metal Gazelle™ stents was coated manually with 2.5% PLA in chloroform wt/wt and left overnight to dry in sterile conditions. Stents were placed over a pipette tip to aid the coating process. After the stents were coated with PLA, the stent was smoothed by vaporisation with DCM (as described above, section 2.16.2). The stents were then crimped onto the balloon catheter.

2.17 Transfection of miRNA *in vitro*

2.17.1 Transfection of rat A10 cells with cel-miR-39-3p at different concentrations

In order to modulate miRNA delivery from stent surfaces initially a *miRVana*™ miRNA mimic was used. The miRNA mimic is a double stranded miRNA molecule that has been chemically modified so that it acts like a mature miRNA strand. A miRNA mimic from *Caenorhabditis elegans* (cel-miR-39-3p, Life Technologies) was chosen initially to investigate whether it was possible to deliver the miRNA to mammalian cells and tissues due to this miRNA not being expressed in mammals. Rat SMCs (A10s) were plated at a seeding density of 100,000 cells/well in a 12 well plate and maintained at 37 °C, 5% CO₂ for 24 h. siPORT™ Neo FX™, (Thermo Scientific) was used as a transfection agent. siPORT™ (3 µL) was added to cel-miR-39-3p (0.15, 1.5, 15 µL, 20 µM, 10 mins). MEM was replaced on the cells with the SiPORT™ cel-miR-3p solutions, so that a final concentration of 3, 30, 300 nM was obtained and left for 48 h, 37 °C, 5% CO₂. After 48 h, RNA was extracted and quantified as described in sections 2.19&2.20.

2.17.2 Transfection of rat A10 cells with cel-miR-39-3p from PLA and SS surfaces ± collagen

Rat SMCs (A10s) were plated at a seeding density of 100,000 cells/well in a 12 well plate and maintained at 37 °C, 5% CO₂ for 24 h. siPORT™ Neo FX™, (Thermo

Scientific) was used as a transfection agent. siPORT™ (3 µL) was added to cel-miR-39-3p (1.5 µL, 20 µM, 10 mins). A collagen solution was prepared by adding bovine type I collagen (5 mg/mL, 15 µL) with NaOH_(aq) (1 M, 10 µL). The siPORT-miR-39 mix was then added to collagen solution and spread onto PLA surface (as prepared in section 2.14.1) or SS surface (Agar Scientific). The collagen coated PLA and SS surfaces were left in the incubator (37 °C, 1 h) and then removed from the incubator (RT, 1 h). For the SS and PLA surfaces without collagen, the miRNA-siPORT solution was simply applied directly to the surfaces and the same procedure was followed as described above. The surfaces were washed thoroughly with PBS (3 x 1 mL) before being placed face down onto the cells and left for 48 h. A mock control was prepared by having siPORT (3 µL) and PBS (1.5 µL) instead of cel-miR-39-3p. The in solution control was prepared by adding the same amount of cel-miR-39-3p-siPORT mix directly to the cells, a non-treatment control was made simply by replacing the medium at the point of transfection to the other wells. After 48 h, RNA was extracted and quantified as described in sections 2.19&2.20.

2.17.3 Transfection of rat A10 cells with miR-145-5p and miR-145-inhibitor

Rat SMCs (A10s) were plated at a seeding density of 100,000 cells/well in a 12 well plate and maintained at 37 °C, 5% CO₂ for 24 h. siPORT™ Neo FX™, (Thermo Scientific) was used as a transfection agent. siPORT™ (3 µL) was added to miR-145-5p (1.5 µL, 20 µM, 10 mins) or miR-145-5p inhibitor (1.5 µL, 20 µM, 10 mins). The siPORT-miR-145/miR-145-5p inhibitor mix was then spread onto PLA surface (as prepared in section 2.14.1). The surfaces were washed thoroughly with PBS (3 x 1 mL) before being placed face down onto the cells and left for 48 h. The in solution control was prepared by adding miR-145-5p/miR-145-5p inhibitor-siPORT mix directly to the cells, a non-treatment control was made simply by replacing the medium at the point of transfection to the other wells, a control mimic control was made by using pre-miR™ precursor negative control and mixing with siPORT™. After 48 h, RNA was extracted and quantified as described in sections 2.19&2.20.

2.18 Transfection of miRNA ex vivo

2.18.1 miRNA transfection from PLA squares:

Mouse aortas were dissected from MF1 mice and cut longitudinally. miRNA mimic from *Caenorhabditis elegans* (cel-miR-39-3p), (20 μ M, 1.5 μ L) was incubated with siPORT™ Neo FX (3 μ L) for 10 mins. The cel-miR-39-3p-siPORT mix was applied onto the PLA square, or for the mimic in solution control, added directly to the aorta. Mock PLA squares were prepared by adding siPORT™ Neo FX™ transfection reagent (3 μ L) to the PLA squares but not miRNA. Non-treated aortas were also used as a negative control. The PLA squares were placed directly onto the inner arterial surfaces in a 12 well plate, and aortas were kept in MEM (1 mL, 37 °C, 5% CO₂, 48 h). The PLA squares were removed from the plates and the aortas were washed thoroughly with PBS. RNA extraction was then performed on the tissue and quantification of transfected miRNA was determined by qRT-PCR as described in sections 2.19.2, 2.19.4&2.21.

2.18.2 miRNA transfection from stents coated with PLA

Custom-made SS murine stents (2.5 x 0.6 mm, Cambus medical) were coated with 10% and 15% wt/wt PLA dissolved in chloroform and left to air-dry, which were then smoothed by DCM vapourisation. They were then hand crimped onto a coronary dilation catheter (Abbott laboratories). The cel-miR-39-3p-siPORT mix was made up as described above and applied directly onto the stent or onto the aorta. A non-treatment control was used, as well as an aorta which had siPORT™ Neo FX™, but not the miR, which was used as a mock control. After coating the stent with miRNA, it was left to air-dry for 5 mins and then it was washed with PBS before deploying into the aorta of the mouse *ex vivo*, details of this procedure can be found in section 2.24.1. Aortas were cultured in MEM for 48 h before the stent was removed, the vessel washed and then miRNA expression was quantified by following the RNA extraction and qRT-PCR protocols (sections 2.19, 2.20&2.21).

2.19 Extraction of RNA from cells and tissues

2.19.1 RNA sample preparation from cells:

Cell medium was removed and the cells were washed twice with PBS. QIAzol lysis reagent™ (700 µL, Qiagen) was added to each well. Homogenisation of the cells was achieved by pipetting the cells prior to storage in 1.5 mL microcentrifuge tubes at -80 °C.

2.19.2 RNA sample preparation from mouse aorta

After transfection with miRNA, the aortas were washed with PBS. The aortas were then stored in RNAlater®-ICE (Life Technologies) (500 µL, -80 °C) until ready for extraction. The frozen aortas were dried and each placed into 2 mL eppendorfs with two 5 mm stainless steel balls and QIAzol lysis reagent™ (700 µL). The tubes were placed into a QIAgen TissueLyser II machine, and shaken at 25 Hz for 2 x 30 seconds pausing in between shakes. The tubes were then placed on ice for 1 min, the shaking procedure was repeated twice more. After lysing, the aortas were sufficiently broken up to enable efficient RNA extraction as described in section 2.19.4.

2.19.3 RNA sample preparation from pig coronary arteries

Vessels were removed from -80 °C storage and placed on dry ice. No more than four vessels were RNA extracted at the same time. All surfaces and instruments were treated with RNaseZap® RNase decontamination solution (Life Technologies). If the vessel had been stented, the vessel was cut longitudinally and the stent was removed. The vessel was placed into a ceramic mortar that was cooled on dry ice. Using a sterile scalpel blade, the vessel was cut into small pieces. Liquid N₂ was then poured into the mortar and the pieces of vessel were ground with the pestle. This was repeated twice. The ground vessel was then transferred into a pre-cooled bijoux containing QIAzol (1400 µL). A polytron was then used to homogenize the tissue further; samples were placed on ice after 30 seconds of homogenisation to prevent degradation of the RNA through heating. Once the samples were sufficiently homogenised they were transferred to a 2mL eppendorf and chloroform was added (280 µL) and vortexed. The RNA procedure (described below, section 2.19.4) was then followed.

2.19.4 General RNA extraction procedure

RNA was extracted from the homogenised samples (as prepared in sections 2.19.1, 2.19.2&2.19.3) using a miRNeasy mini kit (Qiagen). The samples were left at RT for 5 mins this aids dissociation of nucleoprotein complexes. Chloroform (140 μ L) was then added to each tube and vortexed for 15 seconds and left to settle at RT for 2 mins. The tubes were then centrifuged (12000 x g, 15 mins, 4 $^{\circ}$ C). This allowed phase separation to occur, between the organic (containing proteins), intermediate (containing DNA) and aqueous layers (containing RNA). The upper aqueous layer containing the RNA was then removed and put into a new 1.5 mL RNase free eppendorf. 100% Ethanol was added to each tube (525 μ L) and mixed by pipetting up and down. Each sample was then placed into an RNeasy mini spin column and centrifuged at 8000 x g, 2 mins. The RNA binds to the column membrane whereas the other contaminants such as phenol wash through and are discarded. The columns are then washed with buffer RWT (350 μ L) and centrifuged (8000 x g, 15 s, RT).

An on column DNase digestion is done to remove contaminating genomic DNA using an RNase free DNase set (Qiagen). DNase is diluted according to manufacturer's instructions and then diluted 1:8 v/v with buffer RDD. This solution is then applied directly to each column (80 μ L) and left for 15 mins, RT. Buffer RWT (350 μ L, 8000 x g, 15 s) was then washed through the column, followed by buffer RPE (500 μ L, 8000 x g, 15 s), buffer RPE (500 μ L, 8000 x g, 2 mins). The column was then placed into a new collection tube and spun at 16000 x g, 1 min). Finally the column was placed into a 1.5 mL RNase free tube, RNase free water was applied to the column (50 μ L) and then the column was centrifuged (8000 x g, 1 min) to elute the RNA through the column and into the tube. The RNA solution was run through the column again to increase the RNA yield.

The concentration of RNA was determined using a NanoDrop 1000 spectrophotometer (Thermo Scientific), by measuring the samples absorbance at 260 nm. This purity of the RNA was also assessed by measuring the ratio of absorbance 260:280 nm for a pure sample of RNA without contaminants the 260:280 nm ratios was ~2.

2.20 Reverse-transcription polymerase chain reaction (RT-PCR)

The extracted RNA samples underwent reverse transcription to form complementary DNA sequences (cDNA) using Taqman® miRNA Reverse Transcription Kit (Applied Biosystems). The RNA was firstly diluted with RNase free water to 2 ng/μL. The PCR reactions were done in a 96 well PCR plate. Each well contained dNTPS (0.075 μL), multiscribe (0.5 μL), 10 x RT buffer (0.75 μL), RNA inhibitor (0.095 μL), RNase free water (2.08 μL), 5 x RT primer (1.5 μL) and extracted RNA (2.5 μL, 2 ng/μL). The Taqman® miRNA Reverse Transcription primers contained the sequence for the mature form of the miRNA of interest (listed below). Reverse transcription was also performed on an endogenous control housekeeping genes U87, hsa-miR-103 and U6, and RNU48b for murine, porcine and human samples respectively in order to be able to normalise any anomalies in miRNA expression.

miRNA	sequence	species
cel-miR-39-3p	5'UCACCGGGUGUAAAUCAGCUUG3'	<i>caenorhabditis elegans</i>
hsa-miR-145-5p	5'GUCCAGUUUCCCCAGGAAUCCCU3'	human, mouse, rat
hsa-miR-145-3p	5'GGAUUCUGGAAAUACUGUUCU3'	human, mouse, rat
hsa-miR-let7e-5p	5'UGAGGUAGGAGGUUGUAUAGUU3'	human
hsa-miR-99b-5p	5'CACCCGUAGAACCGACCUUGCG3'	human
hsa-miR-125a-5p	5'UCCCUGAGACCCUUUAACCUUGUGA3'	human
hsa-miR-let7e-3p	5'CUAUACGGCCUCCUAGCUUUC3'	human
hsa-miR-99b-3p	5'CAAGCUCGUGUCUGUGGGUCCG3'	human
hsa-miR-125a-3p	5'ACAGGUGAGGUUCUUGGGAGCC3'	human

PCR cycling conditions were 16 °C for 30 mins, to enable the RT primer to bind to the RNA, 42 °C for 30 mins, to enable reverse transcription to occur and finally 85 °C for 5 mins, to inactivate the reverse transcriptase, the plate was then kept at 4 °C.

A non-template control was run where RNase free water was used in place of RNA. The plates containing the cDNA were stored at 4 °C for short term or -20 °C for longer term storage, until qRT-PCR was run on the samples section 2.21.

2.21 Taqman quantitative real time PCR (qRT-PCR)

qRT-PCR is a technique which enables the amount of cDNA to be quantified by measuring the amount of fluorescence detected during each PCR cycle. Taqman probes are used which are complementary oligonucleotide sequences to the target cDNA which have a fluorescent tag at 5' end and a quencher at the 3' end. In this format, when the fluorophore is excited by a light source any fluorescence is quenched by fluorescence energy resonance transfer (FRET) due to the quenchers close proximity to the fluorophore. When the taqman probe binds to the target cDNA sequence it is cleaved by Taq polymerase which releases the fluorophore so it is no longer in close proximity to the quencher, this emission of fluorescence is proportional to the amount of target sequence present in the sample. The number of cycles a product takes to reach a fixed threshold is known as the cycle threshold (C_t). The lower the C_t value the higher the amount of product. An endogenous control which is stably and uniformly expressed in the cell line or tissue was used to normalise the target RNA expression values. To measure fold changes in RNA expression, the calculation $2^{-\Delta\Delta C_t}$ was taken, as described (Schmittgen and Livak, 2008).

The reverse transcription product for each sample were then run in triplicate on a 384 well plate, with each well containing 2 x Taqman mastermix (5 μ L), 20 x miR probe, H₂O (3.8 μ L) and reverse transcription product (0.7 μ L). The thermocycling conditions were 95 °C for 15 mins, followed by 40 cycles of 95 °C for 15 secs and 60 °C for 1 min, using an ABI 7900 qRT-PCR machine (Applied Biosystems).

2.22 Cell Proliferation EdU Assay

Cell proliferation was assessed using a Click-iT® EdU Alexa Fluor® 488 Flow Cytometry Assay Kit (Life Technologies). This assay works by using EdU (5-ethynyl-2'-deoxyuridine) which is an alkyne tagged thymidine analogue that is incorporated into newly synthesised DNA. Detection of EdU takes place by reacting with an Alexa Fluor® 488 dye which has an azide tag by a copper catalysed click reaction. Fluorescence-activated Cell Sorting (FACS) is then used to determine the population of proliferating cells.

HVSMC were plated at 3.5×10^4 cells/well in a 12 well plate and transfected with miRNA mimics, has-let-7e 3p and 5p strands, hsa-99b 3p and 5p strands, hsa-125a 3p and 5p strands, and Pre-miR scramble control at the same time as plating. This was done by adding siPORT™ Neo FX™ (3 μ L) to optiMEM (47 μ L) and miRNA mimics/scramble control (5 μ M stock, 0.6 μ L) to optiMEM (47 μ L) for 10 mins. 15% FCS SMC medium was then added to each well (900 μ L). The siPORT™ Neo FX™ and miRNA solutions were then added together and left for 10 mins and then applied to each well (100 μ L).

Virus transductions were done 24 h after plating the cells. Lenti-virus cluster (LV-cluster) and control Lentivirus-GFP (LV-GFP) were added incubating with polybrene (1 μ L, 37 °C, 30 mins) and then adding to wells at a concentration of 20 MOI.

The cells were then left for 24 h (37 °C, 5% CO₂). The cells were then arrested by replacing medium with 0.5% FCS MEM (1 mL). The cells were then left for 48 h, the medium was replaced with 15% FCS DMEM, and EdU was added to each well (10 mM stock, 10 μ L), the cells were left for another 48 h and then harvested by adding trypsin to each well (200 μ L, 5 mins, 37 °C), and then SMC medium (800 μ L). The cells were then put into 1.5 mL eppendorfs and centrifuged (600 x g, 6 mins, RT), the supernatant was then discarded and then the cells were resuspended in PBS (100 μ L) and then fixed by adding 70% EtOH (900 μ L, overnight), light vortexing helped cells not clumping together. The cells were then centrifuged (600 x g, 5 mins, RT) and the supernatant was discarded. A solution of 0.2% Triton X-100 was applied (750 μ L) to re-suspend the pellet, the samples were then left for 30 mins, RT. PBS + 1% BSA w/v (750 μ L) was added to

each tube, left for 1 min and then centrifuged at (600 x g, 5 mins, RT). The supernatant was discarded and the pellet was re-suspended in click it reagent (0.5 mL per tube, 60 mins, dark, RT). The Click-iT® reagent was prepared by adding PBS (438 µL), CuSO_{4(aq)} (100 mM stock, 10 µL), Alexa Fluor® 488 azide (18 ng/µL, 0.8 µL), 1 x Click-iT® EdU reaction buffer additive (50 µL). After 1 h PBS + 1% BSA w/v was added to each tube (750 µL) and the cells were centrifuged (600 x g, 5 mins, RT) and the supernatant discarded. The cells were re-suspended in PBS + 1% BSA (350 µL) and transferred to FACS tubes and cell counted as described in section 2.23. Each group had 2 biological replicates and also 2 samples were taken for RNA extraction and q-RT-PCR to verify overexpression of the miRNA either from viral transduction or miRNA transfection as described in sections 2.19, 2.20&2.21.

2.23 Flow assisted cell sorting

For the FACS, control tubes were prepared and run first, these were: positive control for proliferation (cells stimulated 15% FCS, + EdU, + Alexa Fluor), negative control for proliferation (cells not stimulated kept in 0.5% FCS, + EdU, +Alexa Fluor™), negative control for EdU (cells stimulated with 15% FCS, -EdU, + Alexa Fluor™), background cells (cells stimulated 15% FCS, -EdU, - Alexa Fluor™). Samples were processed using a BD Biosciences FACS Canto II with a two laser setup (Red and Blue lasers). Analysis of the data was performed using FlowJo software (TreeStar, Ashland, USA).

2.24 *In vivo* models

2.24.1 Mouse stenting model

In vivo experiments were done in accordance with the United Kingdom Home Office Guidance and the Animals Scientific Procedures Act of 1986. Male 30 g + MF1 mice were purchased from Harlan laboratories (Derby, UK), the mice were housed and procedures were performed at the Central Research Facility at the University of Glasgow. Mice were fed on normal chow diet and had free access to food and water and were kept on a 12 h light/dark cycle.

The mouse stenting model used was first described by Ali *et al.*, which requires the use a donor and a recipient mouse per operation (Ali *et al.*, 2007). Custom

made mouse stents as used for the *ex vivo* testing (section 2.18.2), were crimped onto the coronary dilation catheter. Stents were sterilised by submerging into Actril® cold sterilant (Guardline technologies ltd, Norfolk, UK), prior to deployment.

The donor mouse was euthanised by an intraperitoneal (IP) injection of sodium pentobarbitol (150 mg/kg). The abdomen and ribcage were opened so that an incision can be made in the right atrium followed by perfusion of heparin saline (100 IU/mL) via an injection in the left ventricle. The thoracic aorta was isolated, removing any excess fat lining the vessel and a small incision was made to the distal end of the aorta so that the coronary dilation catheter could be inserted into the vessel. The stent was expanded by applying a pressure of 10 atm for 30 secs; the catheter was then removed leaving the stent in place. The stent was excised by cauterisation of the vessel and was left in PBS whilst the recipient mouse was prepared.

Recipient mice were anaesthetised using vapourised isoflurane (1-3%, Abbott), the common carotid was isolated and ligated using two 7-0 sutures (Ethicon, Edinburgh, UK) distal to bifurcation. The carotid was then dissected between the sutures and each end of the carotid was passed through a 0.65 mm cuff (Smiths medical, Kent, UK) and secured with a microhemostatic clamp. The sutures were then removed and the free end of the carotid was everted over the cuff and sutured in place using 8-0 silk sutures (Ethicon). The donor aorta was then sleeved over the everted ends and sutured in place. The microhemostatic clamps were removed, and blood flow was restored to the vessel. The skin was closed using 5-0 sutures (Ethicon). Following the surgery the mice were transferred to a 37 °C chamber for recovery.

Prior to surgery recipient mice received a 7 day course of aspirin (10 mg/kg), and for each day afterwards until they were euthanised. Euthanasia was performed at 48 h post-surgery by administration of a lethal amount of anaesthetic, followed by an excision to the heart.

For the 48 h mouse stenting study, murine stents were coated with PLA dissolved in chloroform (10% wt/wt) and miR-39-3p (1.5 µL, 20 µM) as described in section 2.18.2. Stents were also prepared in this manner for the PLA BMS group but were

not coated with miR-39-3p. Untreated aorta was kept during the procedure and used as a non-treatment control. After 48 h of being deployed the stented segment were excised from the mouse, the stent was removed and the vessel bathed in PBS, prior to RNA extraction and quantification of the miRNA by qRT-PCR as described in sections 2.19.2, 2.19.4, 2.20&2.21.

2.24.2 Pig stenting model

Male Large White/Landrace Pigs were purchased from SAC commercial ltd (Edinburgh, UK) (12 weeks old, 30-35 kg). Pigs were housed and procedures were performed in the Biological Procedures Unit at the University of Strathclyde. In line with the local animal guidelines, the animals had a period of at least 7 days acclimatisation prior to any procedures being performed. Pigs were kept in controlled conditions on a 12 h light/dark cycle with free access to water and were fed twice a day.

All operations were done in a designated operating theatre under sterile conditions. During the operation, the electrical activity of the pigs heart was monitored by continuous single lead ECG which was connected subcutaneously, the blood pressure, heart rate and %O₂ saturation of the blood were also monitored. The temperature of the pig was monitored by a rectal probe. A monophasic direct current defibrillator was also present in the operating room to be used in the case of a cardiac arrest.

2.24.2.1 Periprocedural pharmacotherapy

A day prior to surgery, the pigs were dosed orally with aspirin (150 mg, Teeva, Leeds, UK) and clopidogrel (150 mg, Sanofi-Aventis, Guildford, UK). On the day of surgery the pigs were dosed with a further 75 mg of both aspirin and clopidogrel this was continued every second day until sacrifice. Once stable anaesthesia had been reached the pigs were dosed intravenously with an anti-arrhythmic cocktail of drugs, amiodarone (75 mg, Sanofi-Aventis) and lidocaine hydrochloride (50 mg, Taro Pharmaceuticals, Ireland) via a 20G canula in the large ear vein. Anticoagulant was also administered intravenously following the insertion of the arterial sheath (3000 units heparin,). After anaesthesia the pigs were given 0.15

mg, buprenorphine as a painkiller and 300 mg ampicillin as an antibiotic which were administered by an intramuscular injection.

2.24.2.2 Anaesthesia

All procedures were performed with the pig being under anaesthesia. Initially the pigs were sedated by an intramuscular injection of tiletamine/zolazepam (100 mg Zoletil, Virbac, Suffolk, UK) this enabled the pig to be transported from the animal enclosure to the operating table. Using a snout mask the pigs anaesthesia was further induced through inhalation of 4% isoflurane (Abbott laboratories ltd, Maidenhead, UK) in O₂ (7 L/min) and NO (2 L/min). The pigs were moved into a supine position and intubated by insertion of a lubricated 6F endotracheal tube through the vocal cords by direct vision. To aid the intubation procedure propofol was administered intravenously (30 mg, Rapinovet, Schering-Plough, Welwyn Garden City, UK). Anaesthesia was maintained with 2% isoflurane in nitrous as described above. Saline was injected intravenously to maintain hydration.

2.24.2.3 Arterial Access

Arterial access was secured via the left femoral artery. The groin area was wiped down with a povidone-iodine solution and surgical drapes were placed around the area where the incision was to be. The left femoral artery was dissected and freed from peripheral fascia using a cut-down approach. The artery was sutured proximally and distally. Using a modified Seldinger technique to obtain safe access into the vessel, the artery was punctured using a sharp hollow needle from a human transradial artery access kit (Arrow® International UK ltd, Middlesex). A soft tipped guidewire (0.0025 in) was threaded through the needle and into the lumen of the artery, the needle was then removed and a 6F radial sheath was placed over the guidewire, the wire was removed and the sheath was sutured to the skin.

2.24.2.4 Coronary Catheterisation and Stenting Procedure

A human 6F guide catheter and 0.035 inch guidewire was inserted through the descending aorta, around the aortic arch and into the coronary ostia using angiography by injecting radiographic contrast agent (Ominipaque 140, GE

healthcare, Buckinghamshire, UK). Once the catheter was in the correct position for stenting the coronary artery, the guidewire was removed and the Gazelle™ bare metal stents which was mounted onto a balloon delivery catheter was inserted through the guide catheter. The balloon delivery catheter had two radiopaque markers which marked the ends of the stent; angiography confirmed that the stent was in the correct position. The balloon was inflated using a inflator (Boston Scientific, MA, USA) up to 12 atm, then deflated and removed, leaving the stent deployed in the artery. Two stents were deployed per pig into the left anterior descending artery and the right coronary artery or left circumflex.

2.24.2.5 Closure

To close the wound, the guide catheter was removed and the proximal suture was tightened to allow removal of the sheath. The artery was then ligated and the wound was closed using absorbable sutures (Dexon™, Covidien, Dublin, Ireland).

2.24.2.6 Recovery

Animals were extubated and left to recover from anaesthesia under supervision, once the animals were awake they were taken back to the enclosure and fed a normal chow diet. The animals were given a course of antiplatelets post-procedure.

2.24.2.7 Animal Sacrifice

After 48 h, animals were given an intramuscular injection of tiletamine /zolazepam (100 mg Zoletil, Virbac), to sedate them and allow transport to the operating theatre. Following cannulation of the large ear vein a lethal injection of pentobarbital (100 mg/kg, Merial, Harlow, UK) was given. Bone cutters and rib retractors were used to access the thoracic cavity. The heart was mobilised by stripping back the visceral and parietal pericardium. The great vessels were cut and the heart was then removed from the thoracic cavity. The coronary arteries were then quickly dissected out of the heart. If the artery was to be used for and RNA extraction, it was immediately stored in RNAlater®-ICE (2 mL

per vessel) at -80 °C. RNA extraction from pig coronaries is described in section 2.19.3.

2.24.2.8 Stent based delivery of miRNA

Gazelle™ stents were coated with PLA as described in section 2.16.3. Prior to surgery the stents were then coated with miRNA/siPort mix. siPort™ (9 µL) was added to miRNA (20 µM, 4.5 µL) and left for 10 mins, this solution was then applied to the stent, air-dried and then deployed as described in section 2.24.2.4. For the miR-39-3p coated stents, 6 stents were coated and deployed, with 6 BMS and 6 PLA BMS for the control groups. 2 stents were deployed per pig, ensuring that the same group were not deployed in the same pig. For the miR-145-5p coated stents, 4 stents were coated and deployed. For the antimiR-21 coated stents, 3 stents were deployed and 2 stents were coated with antimiR-21 scramble control.

3 Development of methods for coating adenovirus particles to stent materials and surfaces

3.1 Introduction

Adenovirus vectors are the most commonly used vector for gene therapy (Wiley, 2015). They are particularly suitable for this application because they can be relatively easily manipulated, they can be made under GMP conditions to produce high-titre stocks and they transduce many different cell types, including quiescent and proliferating cells, without integrating into the host genome (Bradshaw and Baker, 2013).

The virus serotype most commonly used for gene therapy is adenovirus 5 (Ad5). However, despite Ad5 being a popular choice for gene therapy, there are a number of limitations associated with it. High seroprevalence in the human population and consequent neutralisation by anti-Ad5 Ab can decrease the overall transduction of target tissues (Bradshaw and Baker, 2013, Barouch *et al.*, 2011). The Ad5 vector has also been shown to trigger an innate immune response following intravascular delivery, resulting in the virus being removed from circulation (Bradshaw and Baker, 2013, Schoggins and Falck-Pedersen, 2006, Muruve *et al.*, 2008, Di Paolo *et al.*, 2009). Despite these drawbacks, it was chosen to develop stent coating methods, due to its efficient vascular uptake and it being one of the most well-characterised gene therapy vectors. Coating methods developed have also been tested for compatibility with other more novel virus vectors that have been assessed specifically for delivery to the vasculature, such as Ad49 (Lemckert *et al.*, 2006).

In stent restenosis occurs as a result of acute vessel wall injury endured during deployment of the stent. This stimulates platelet aggregation, which in turn causes smooth muscle cell proliferation and migration into the intima (Mitra and Agrawal, 2006a). Targeting the cell proliferation pathway by coating the stent in anti-proliferative drugs has been extensively investigated, to provide localised delivery to the vasculature. These drug eluting stents (DES) have been shown to have a drastic effect on SMC proliferation; however they have been associated with late stent thrombosis, which is often fatal (Bradshaw and Baker, 2013, Stone *et al.*, 2007b, Yeh *et al.*, 2011). DES are also costly and require patients to take long-term anti-thrombogenic medication. Furthermore, the drugs that are coated onto the stent often do not discriminate between proliferating VSMC and EC which can therefore delay re-endothelialisation (Santulli *et al.*, 2014).

There is therefore a window of opportunity for a novel, more SMC specific and sophisticated treatment to be applied to the stent surface which would target the in stent restenosis pathway, to prevent SMC proliferation and not hinder re-endothelialisation. It has been envisaged that coating the stent in therapeutic virus vectors could provide a powerful way to maximise the potential for viruses to deliver therapeutic genes for treatment of ISR, by enhancing transduction of the virus by local delivery and avoiding distal spread of the virus. Therefore, methods for attaching Ad5 vectors to stent surfaces were investigated.

To date there have been a number of studies which have investigated the delivery of virus vectors from stent surfaces. A successful way to enable virus delivery has involved coating the stent with adenovirus antibodies which act as a surface for virus capture and release. Levy and co-workers used a stainless steel stent coated in collagen with anti-adenoviral monoclonal antibodies covalently bound to the collagen surface; this provided a surface upon which the Ad5 GFP vector could be selectively tethered via antigen-antibody specific interactions. This method proved successful *in vitro* and *in vivo*, with a transduction efficiency of 5.9% of porcine arterial smooth muscle cells and 17% of cells in the neointima of pig coronaries showing expression of GFP after stent deployment for 7 days (Klugherz *et al.*, 2002a). Fishbein *et al.* bound an anti-Ad antibody to a bare metal stent surface using polyallylamine bisphosphonate as a linker molecule; the phosphonate groups coordinated with the metal surface and the amine group was then reacted with crosslinker SPDP, leaving a thiol group, which could then bind to the anti-ad antibody by formation of a disulfide bond (Fishbein *et al.*, 2006a).

Another method for adenoviral attachment to the stent surfaces exploited the adenoviruses net negative charge, and used electrostatic interactions to bind to a positively charged phosphorylcholine coating on BiodivYsio stents (Sharif *et al.*, 2006, Johnson *et al.*, 2005a). This concept of using surface charge to attach the adenovirus vector has provided some inspiration for the work carried out here, by using poly(electrolyte) multilayers as a charged base to attach the adenovirus to. This chapter aims to describe and evaluate different methods for coating of Ad5 to stent surface materials both *in vitro* and *ex vivo*, with the objective of discovering a delivery system which would function *in vivo* to deliver a therapeutic Ad from stent surfaces to treat ISR locally at the point of injury.

3.1.1 Aims

- To develop a method for coating of Ad5 onto stent surfaces that enables localised delivery to arteries from mice and pig stents
- Quantify the amount of virus deposited onto the stent surface

3.2 Results

3.2.1 Poly electrolyte multilayers

Polyelectrolyte multilayers (PEMs) were investigated as a method for the attachment and delivery of adenoviral particles from stent surfaces. PEMs were formed by depositing oppositely charged polymers onto surfaces in a layer by layer fashion to form a polymer film on the surface (Figure 3-1).

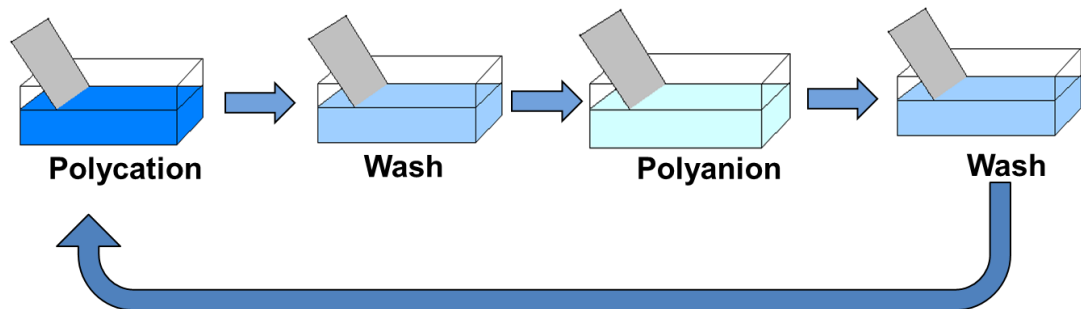


Figure 3-1 Diagram of method for poly(electrolyte) multilayer formation.

In order to form a poly electrolyte multilayer on a surface, the surface is first immersed into a polycationic solution for 1 min, they are then washed in dH₂O and then immersed into a polyanionic solution for 1 min, and washed in dH₂O. This process is repeated until the desired number of layers have been deposited onto the surface.

It was hypothesised that because adenovirus particles carry a net negative charge, if they were deposited onto a cationic polyelectrolyte layer they would be adsorbed and held onto the surface through electrostatic interactions. This principle has been used to successfully deliver DNA from stent surfaces coated with a PEM (Saurer *et al.*, 2013). PEMs have previously been shown to be able to be deposited uniformly onto a stent surface, which is important since stents have a complex geometry and are therefore often difficult to coat (Dimitrova *et al.*, 2007). Two different PEM systems were tested; chitosan-hyaluronan (chi-ha) which are both biopolymers, and poly(allyl amino hydrochloride)-poly(styrene sulfonate) (PAH-PSS) which are synthetic polymers. These systems were chosen because they are well characterised and have been studied previously for adenoviral delivery (Dimitrova *et al.*, 2007).

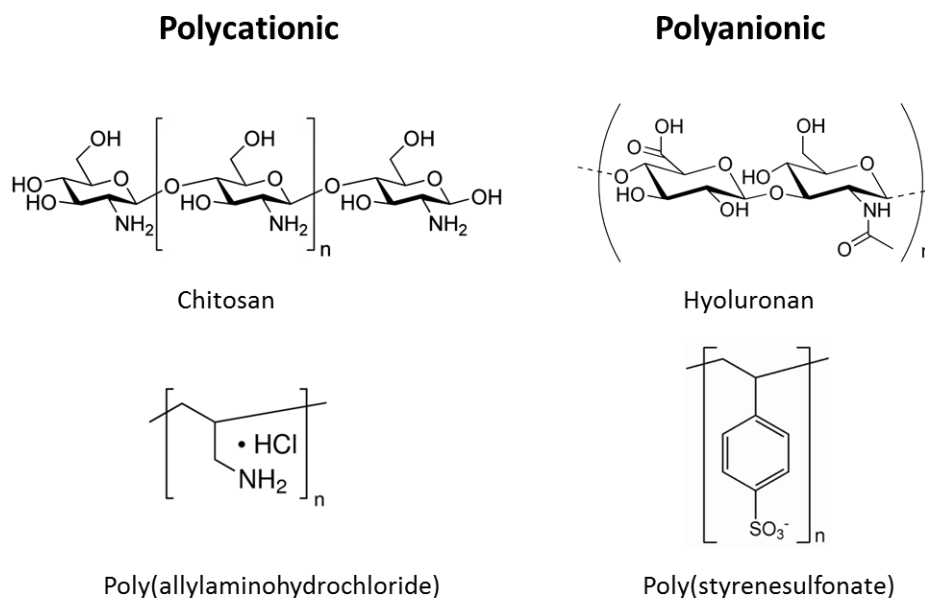


Figure 3-2 Chemical structures of polycationic and polyanionic species used for the formation of PEMs.

The polycationic group species, chitosan and poly(allylaminohydrochloride) both exhibit amine groups which when protonated will become catatonically charged. The polyanionic species poly(styrenesulfonate) contains a sulfonate group which will be anionically charged and hyaluronan which has carboxyl groups which when deprotonated will become anionically charged.

In order to monitor the formation of the PEMs, they were initially deposited onto quartz slides which have a low absorbance range. Before deposition the slide was washed in piranha solution to clean the surface, the slide was then submerged into the polycationic solution, washed with dH_2O followed by the polyanionic solution, this procedure was then repeated 8 times to form a PEM. In order to confirm that the PEM was forming on the quartz, a UV-visible spectrum was taken after each deposition (Figure 3-3). The PEM formation procedure is detailed in section 2.4.

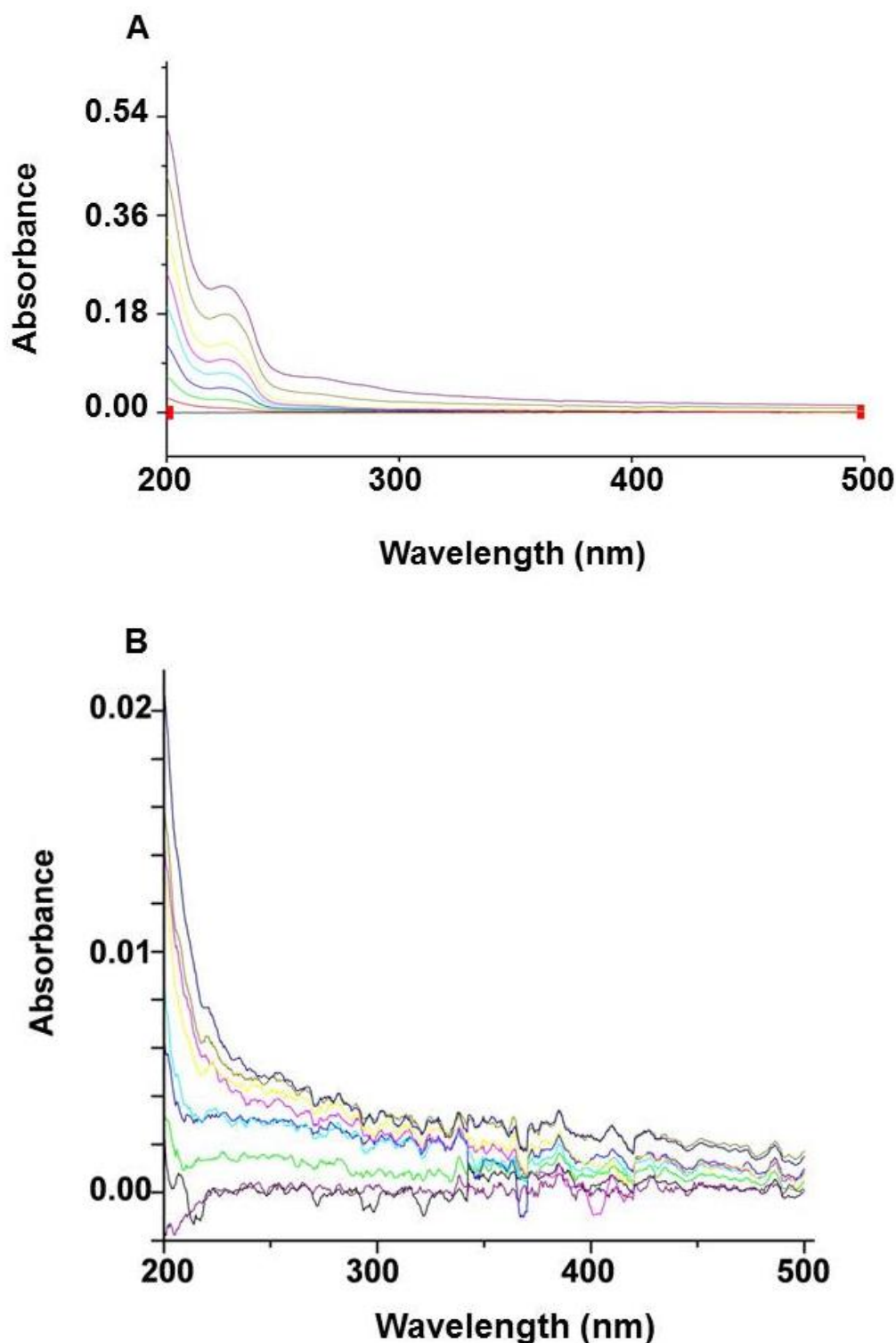


Figure 3-3 UV-vis spectra of PAH-PSS and chi-ha PEMs forming on quartz slides.

Quartz slides were submerged into polycationic solution for 1 min, washed with dH₂O and dried with N₂, they were then submerged into the polyanionic solution for 1 min, this was repeated 8 times to form a PEM. UV-vis spectra were recorded after each layer of polycation-polyanion was deposited. A) The UV-vis spectra for PAH-PSS PEM formation: black (baseline), red (after PEM 1), green (after PEM 2), dark blue (after PEM 3), light blue (after PEM 4), pink (after PEM 5), yellow (after PEM 6), olive green (after PEM 7), purple (after PEM 8) B) The UV-vis spectra for the chi-ha PEM formation: maroon (baseline), black (after PEM 1), green (after PEM 2), dark blue (after PEM 3), light blue (after PEM 4), pink (after PEM 5), yellow (after PEM 6), olive green (after PEM 7), purple (after PEM 8). Representative graphs of three independent experiments.

The layer by layer deposition of both the PAH-PSS and the chi-ha PEMs was clearly observed by UV-vis spectroscopy, as each layer added corresponds to an increase of the absorbance. For the PAH-PSS PEM the sequential increase in absorbance at 230 nm was more pronounced which was due to the presence of the phenyl rings on the poly styrene sulfonate which exhibits a high absorbance at this wavelength. This can be seen clearly in the absorbance spectra for PAH-PSS PEM. It is not present in the CHI-HA PEM as neither of these poly(electrolytes) have groups which absorb UV and visible light strongly. Despite this, an increase in absorbance can be viewed for both PEMs as sequential layers are deposited.

As it was clear that this methodology was successful at forming the two different PEMs, the next objective was to see if it was possible for adenovirus particles to adsorb onto the terminal polycationic layer of the PEMs. This was evaluated, using a virus which was fluorescently tagged with a dye molecule (Alexa Fluor 555). The PEMs were prepared in the same way as described above, after which the fluorescent virus (Ad-555) or unlabelled virus (Ad5) at a concentration of (1.22×10^9 VP/surface) was deposited onto the PEM and left overnight, the surfaces were then washed with PBS, prior to visualisation of the fluorescence by confocal microscopy (Figure 3-4). Unlabelled Ad5 was used as a negative control, to confirm that the fluorescence observed from the surfaces could be attributed to the presence of the fluorescent virus and not materials or the virus itself.

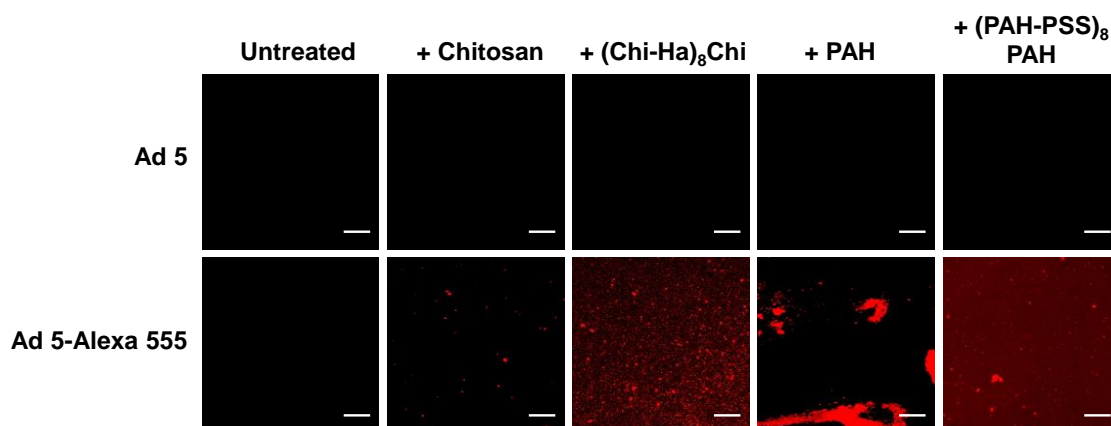


Figure 3-4 Confocal micrographs of PEMs chi-ha and PAH-PSS incubated with fluorescently tagged adenovirus.

The top row shows the surfaces which have been incubated with the unlabeled Ad5 control virus (1.22×10^9 VP/surface). The bottom row shows the surfaces which have been incubated with Ad5-Alexa Fluor™ 555 (1.22×10^9 VP/surface). Untreated samples were the slide prior to PEM deposition, +chitosan and +PAH indicates a monolayer of the corresponding polycations. +(chi-ha)₈chi and +(PAH-PSS)₈-PAH indicates an 8 layer PEM with an additional terminal layer of polycation. Images were taken at 60 x magnification, scale bar = 50 μ m, 1000 ms exposure, 572 nm excitation wavelength. Representative images from two independent experiments.

As no fluorescence was observed for the surfaces which had unlabelled Ad5 deposited onto it, we attributed any fluorescence observed as a result of the fluorescently tagged virus being adsorbed onto the surface. Both the PEMs showed that the virus had been effectively absorbed onto the surface after washing extensively with PBS. Quantitatively, there were higher levels of fluorescence observed for the PAH-PSS PEM; this may be because the virus had a higher binding affinity to this surface. When one layer of PAH was deposited, large swathes of fluorescence were observed (Figure 3.4), which indicates that the virus was not spread evenly on the surface. It is possible that this is due to an uneven distribution of PAH after one layer, as this effect is not observed for the (PAH-PSS)₈PAH multilayer. This indicates that using the multilayer approach allows for a more even coverage of the poly(electrolyte) and therefore the virus, which is demonstrated by both the PAH-PSS and chi-ha PEMs.

The topography of these surfaces was also recorded using atomic force microscopy (AFM) (Figure 3-5). AFM works by scanning a sharp tip across a surface whilst maintaining a constant force between the tip and the surface. As the tip scans along the surface and the surface topography changes, the tip will move up and down, in order to maintain a constant force between the surface and the tip. This movement will mirror the surface contours. In order to amplify

this movement, a laser is directed onto the tip which is then reflected to a sensor. This information can be used to create an atomic force micrograph which is representative of the surface topography.

Adenovirus particles are icosahedral in shape and have been reported to have a diameter of 60-90 nm (Volpers and Kochanek, 2004). The AFM images showed distinct particles on the monolayer and PEM surfaces close to this size range which, therefore, suggests that the ad particles had been efficiently deposited onto the surfaces. When comparing the monolayer + Ad5 group for the chitosan and PAH surfaces, there was a distinct difference in the size of the particles measured on the surface. The particles on the chitosan surface exhibited a height of approximately 30 nm, however for the PAH surface the particles a height of 60 nm was recorded. These differences may suggest that the virus particles on the chitosan surface were more submerged into the polymer layer.

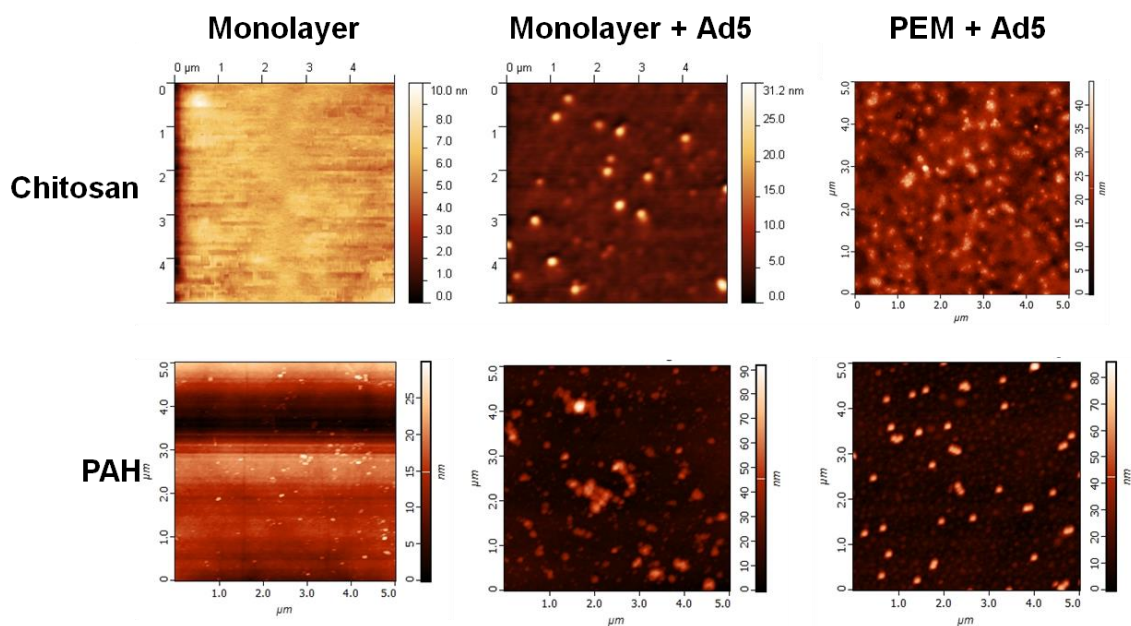


Figure 3-5 Atomic force height images of the microscope slides coated with PEMs.

(chi-ha)₈chi and (PAH-PSS)₈PAH and chitosan and PAH monolayers were prepared on glass microscope slides and incubated with Ad5 (1.22×10^9 VP/surface). Control surfaces of PAH and chitosan without virus incubation were also prepared, the surfaces were washed with dH₂O and dried with N₂ prior to AFM. AFM images were taken using non-contact mode, at a scan rate of 1.01 Hz. Differences in scales are used to allow for definition of the individual surfaces. Representative images from three independent experiments.

As both the AFM and confocal microscopy results indicated that virus particles can adhere to surfaces by incubating on the two PEMs, it was important to evaluate whether the virus was able to elute from the surface and after doing so if it was still biologically active. Ad5 CMV lac Z was used in order to investigate

this which has been genetically modified so that it expresses β -galactosidase which can be used as a reporter for virus transduction (section 2.10). The Ad5 serotype was chosen to model the stent delivery system because it is the most commonly used virus vector for gene therapy, it has been reported to transduce vascular cells with high efficiency *in vivo* and high titre stocks can easily be prepared (French *et al.*, 1994, Sharif *et al.*, 2006).

To verify expression of β -galactosidase from the Ad5 CMV lac Z vector, rat A10 SMC were plated and a serial dilution of virus was made and applied to the A10 cells in the range of 500-5000 VP/cell (Figure 3-6). The virus was left on the cells for 3 h and then the medium was replaced and left for 72 h before harvesting the cells. Quantification of β -galactosidase expression was performed by doing a β -gal assay. For all the concentrations used, a significant expression of the transgene in comparison to the untreated control cells was observed.

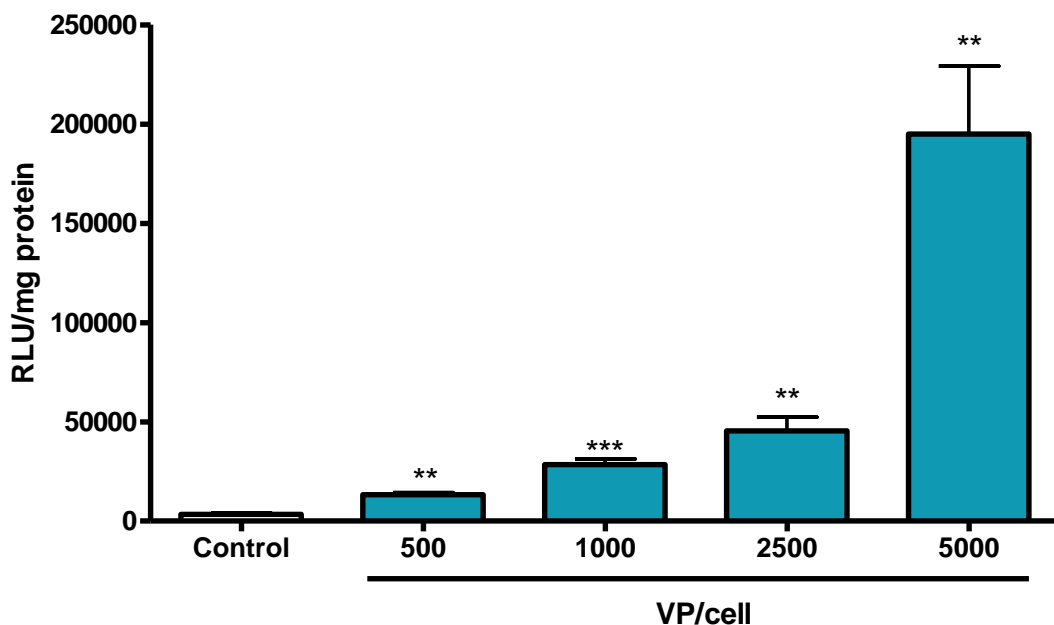


Figure 3-6 Transduction of A10 cells with Ad5 CMV lac Z.

A10 cells were treated with medium (control) or Ad5 CMV lac Z at concentrations of 500, 1000, 2500, 5000 VP/cell for 3 h, the virus was then removed and replaced with fresh medium and left for 72 h. A β -galactosidase assay was used to determine the β -gal expression by measuring the relative light units (rlu) normalised to the protein concentration (mg). Results are displayed as mean \pm SEM, statistical analysis was performed using an unpaired student's t test, ** p <0.01, *** p <0.001 vs control, representative graph from three independent experiments, each with three technical triplicates per condition.

The effect of the polycations on Ad5 CMV lac Z transduction of A10 cells was investigated by incubating the virus (2500 VP/cell) with the polycation solutions (chitosan and PAH) at concentrations in the range of 0.125-1 mg/mL for 3 h, the

virus polycation solutions were removed and replaced with fresh medium. Transgene expression was measured using a β -gal reporter assay. Non-treated cells were used as a negative control and were maintained in medium throughout the experiment (section 2.8.2). In order to see the effect that the polycations had on virus transduction, cells treated with virus but not with a polycation solution were used as a positive control (Figure 3-7).

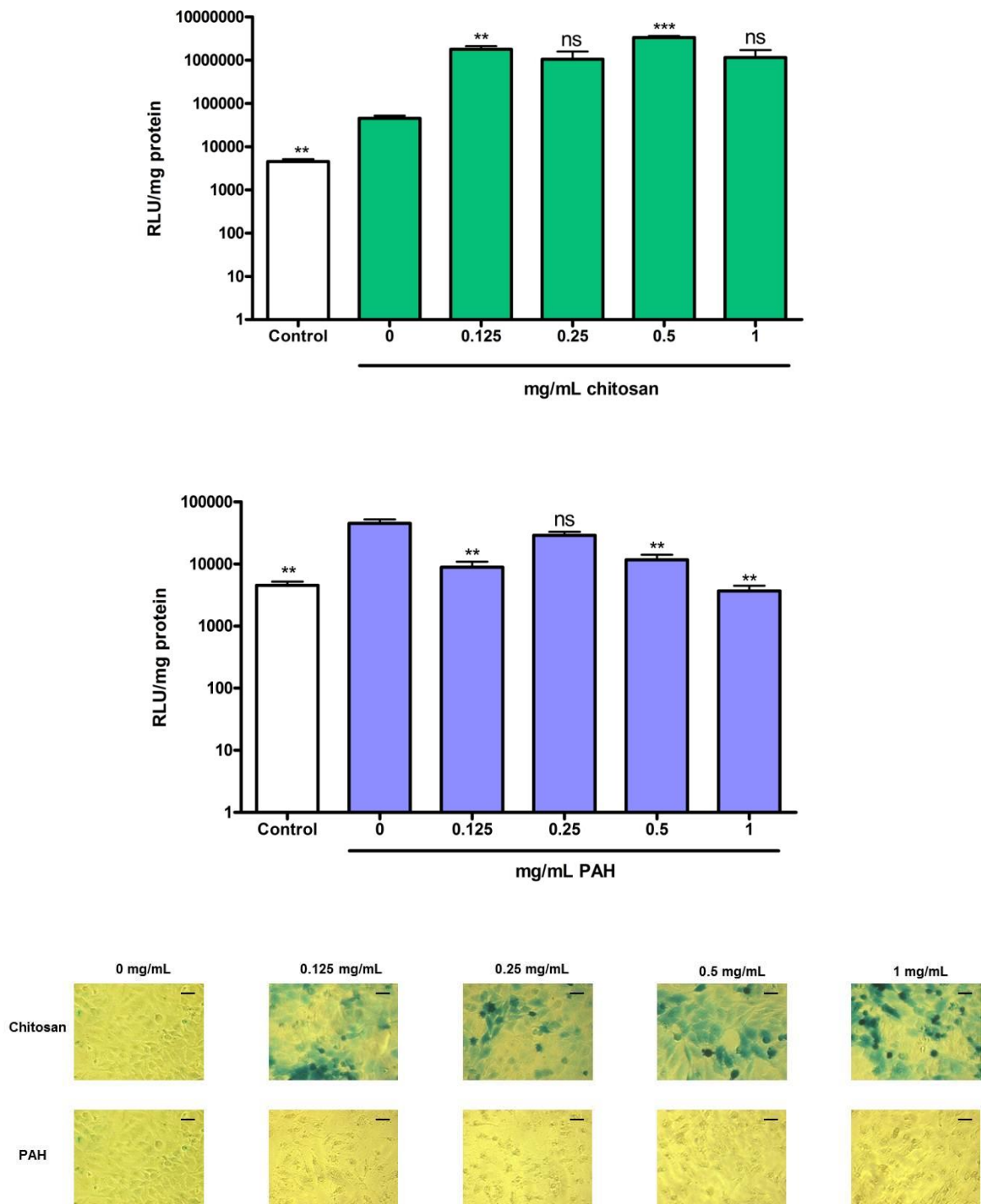


Figure 3-7 Transduction of A10 cells with Ad5 CMV lac Z treated with polycations, chitosan and PAH.

A10 cells were treated with medium (control) or Ad5 CMV lac Z (2500 VP/cell) with polycationic solutions PAH and Chitosan at concentrations of 0, 0.125, 0.25, 0.5 and 1 mg/mL for 3 h, the virus was then removed and replaced with fresh medium and left for 72 h. A β -galactosidase assay was used to determine the β -gal expression by measuring the relative light units (rlu) normalised to the protein concentration (mg). Results are displayed as mean \pm SEM, statistical analysis was performed using an unpaired student's t test, *** $p < 0.001$, ** $p < 0.01$, ns=non-significant vs 0 mg/mL control, $n=3$. Bottom displays representative images of x-gal stained A10 cells after incubation with Ad5 CMV lac Z in different cationic polymer conditions, 10x magnification, scale bar = 100 μ m. Three technical triplicates per condition.

It was observed that incubating the virus with chitosan solutions caused an increase in β -gal expression for all the concentrations used. The highest level of

transduction was at 0.5 mg/mL chitosan where the increase was 74 fold compared to 0 mg/mL chitosan control. This enhancement in viral transduction has been previously documented and is due to the cationic polymer facilitating entry of the adenovirus into the cells via a CAR independent pathway. This is driven by the attraction between the polymer and the net negative charge on cell surface membranes (Zhong *et al.*, 2011, Kawamata *et al.*, 2002). For the PAH polymer, a decrease in virus transduction was observed when compared to the adenovirus only positive control. The biggest decrease in viral transduction was at the highest concentration of PAH used (1 mg/mL) which showed a 12 fold reduction which was of a similar level to the non-treatment negative control cells. For these reasons, no further work was carried out using PAH as a platform for virus delivery. On the other hand, further *in vitro* testing was explored with the (chi-ha)₈chi PEM as this augmentation of viral transduction could provide a very effective method for adenoviral delivery from chitosan coated surfaces. For both PAH and chitosan, a dose dependent response on β -gal expression wasn't observed when the concentration of the polycations was increased, this variation could be due to the solubility of the polycations in solution, as increasing concentration could lead to saturation.

Since the overall objective was to provide a system for coating a stent surface, an *in vitro* model was designed to emulate this by using 316L surgical grade stainless steel discs as a substitute for bare metal stent surfaces. The discs were coated with (chi-ha)₈chi PEM using the layer by layer deposition techniques developed previously and then incubated with Ad5 CMV lac Z. Uncoated SS and SS-chi monolayer with Ad5 CMV lac Z were also used to enable a comparison to be made to the PEM, non-treated A10 cells were used as a negative control. Once the discs were coated they were washed with PBS and were placed face down onto A10 cells that had been plated for 24 h prior. This was to mimic the contact between the stent surface and the vessel wall which would occur in an *in vivo* setting. The discs were left for 72 h before the cells were harvested and the amount of virus transduction was quantified by performing a β -gal assay (Figure 3-8) (section 2.8.4).

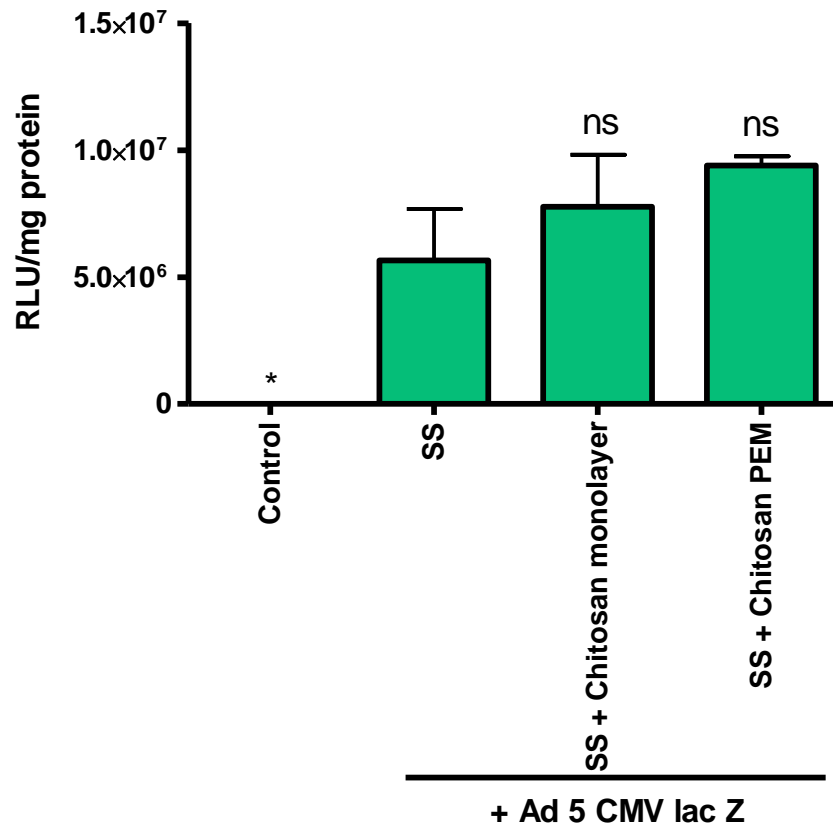


Figure 3-8 Transduction of A10 cells with Ad5 CMV lac Z from Stainless Steel surfaces
 A10 cells were treated with medium (control) or Ad5 CMV lac Z (4.8×10^{10} VP/disc) incubated on SS discs, SS + chitosan disc, or SS (chi-ha)₈chi PEM discs and left for 72 h. A β -galactosidase assay was used to determine the β -gal expression by measuring the relative light units (rlu) normalised to the protein concentration (mg). Results are displayed as mean \pm SEM, statistical analysis was performed using an unpaired student's t test, * $p < 0.05$, ns=non-significant vs SS control. Representative graph from three independent experiments.

From each of the SS surfaces virus transduction was observed. Using the SS (chi-ha)₈chi PEM as a method for depositing the virus onto the SS surface yielded a 1.7 fold increase, compared to the SS control, however this did not reach significance. The chitosan monolayer deposited onto the SS yielded a 0.7 fold increase in virus transduction.

In order for chitosan to act as a polyelectrolyte it was dissolved in acetic acid solution, to protonate the amine groups (Rinaudo *et al.*, 1999). To work out the optimal conditions for viral transduction the %weight (wt) acetic acid was probed. Different %wts of acetic acid were used to modify the pH of the chitosan solution the virus was incubated in and then were applied to the A10 cells for 3 h. The virus chitosan solution was then removed and then medium was replaced and the cells left for 72 h in culture. Virus Transduction was monitored by performing a β -gal assay (Figure 3-9) (section 2.8.3).

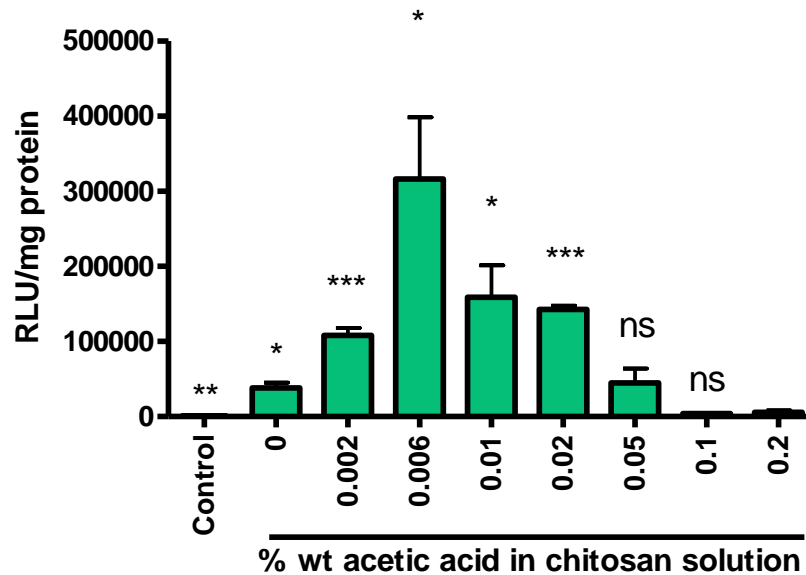


Figure 3-9 Transduction of A10 cells with Ad5 CMV lac Z in chitosan solution with different concentrations of acetic acid.

A10 cells were treated with medium (control) or Ad5 CMV lac Z (1000 VP/cell) with polycationic chitosan (0.1% wt) dissolved in acetic acid at concentrations 0, 0.002, 0.006, 0.01, 0.02, 0.05, 0.1, 0.2% wt, for 3 h, the virus was then removed and replaced with fresh medium and left for 72 h. A β -galactosidase assay was used to determine the β -gal expression by measuring the relative light units (rlu) normalised to the protein concentration (mg). Results are displayed as mean \pm SEM, statistical analysis was performed using an unpaired student's t test, *** p <0.001 ** p <0.01, * p <0.05 ns=non-significant vs 0 mg/mL control. Three biological triplicates were performed per condition.

Prior to this experiment the chitosan (0.1% wt) and acetic acid (0.2% wt) concentrations were used as described in the literature (Meng et al., 2009a). The %wt acetic acid was varied from 0.2% to 0% and comparisons were made to the original concentration of 0.2%, the concentration of chitosan was kept constant at 0.1% wt. An optimal concentration of 0.006% wt acetic acid was found which increased virus transduction by 58 fold. Increasing the % of acetic acid in chitosan solution and therefore lowering the pH of the solution has an initial beneficial effect on virus transduction, however at higher concentrations of acetic acid the low pH is likely to disrupt the structure of the adenovirus, which will prevent viral transduction.

Using this optimised concentration of acetic acid for virus transduction, PEMs were deposited onto a SS disc and the virus was incubated onto the surface. The discs were placed face down onto pre-plated A10 cells and left for 72 h. Virus transduction was measured using a β -gal assay (Figure 3-10).

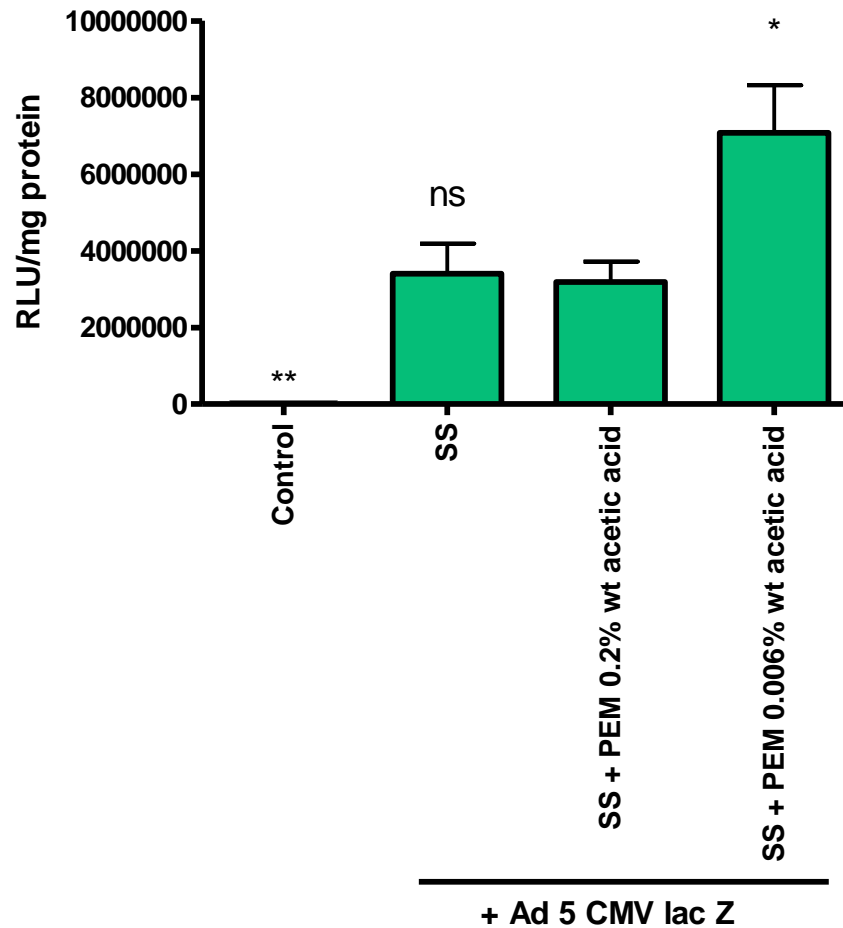


Figure 3-10 Transduction of A10 cells with Ad5 CMV lac Z deposited on (chi-ha)₈chi PEM coated SS disc.

A10 cells were treated with medium (control) or Ad5 CMV lac Z (4.8×10^{10} VP/disc) incubated onto an uncoated SS disc or on a SS disc coated with (chi-ha)₈-chi PEM. The chitosan solutions in the PEM were prepared; (0.1% wt) dissolved in the original and optimised concentrations of acetic acid (0.2% and 0.006% wt). The discs were left for 72 h. A β -galactosidase assay was used to determine the β -gal expression by measuring the relative light units (rlu) normalised to the protein concentration (mg). Results are displayed as mean \pm SEM, statistical analysis was performed using an unpaired student's t test, ** $p < 0.01$, ns = non-significant vs 0.2% wt acetic acid PEM control. Representative graph from three independent experiments; each with three biological replicates per condition.

Using the optimised concentration of acetic acid (0.006% wt) for virus transduction an increase of 2.2 fold was recorded when the virus was delivered to the cells by a chi-ha PEM coated SS disc compared to when 0.2% wt acetic acid was used. This indicated that by changing this parameter a better delivery system for the virus was obtained.

The next step was to see whether delivery could be achieved from a SS bare metal stent (BMS) as a platform instead of a SS disc in an *ex vivo* setting. Gazelle BMS were coated with (chi-ha)₈chi PEM and Ad5 luciferase, using the methods developed (section 2.8.4), the stents were deployed into rat carotid arteries *ex*

vivo. No virus transduction was observed using this system; this could have been because the electrostatic interactions that the virus was attached to the stent surface with were not strong enough to withstand stent deployment. Therefore, methods for covalently bonding the virus directly to the surface were investigated.

3.2.2 Covalent attachment of virus to PLA surfaces

3.2.2.1 Hydrolysis of PLA

To enable a covalent bond to form between the stent surface and the virus capsid, a suitable material needed to be carefully chosen which would allow chemical modification of the stent material. Poly lactic acid (PLA) was chosen for this role because it is the most commonly used material for biodegradable stents and is an organic polymer, therefore, chemical modification of the surface was considerably more straightforward than for BMS (Wiebe *et al.*, 2014).

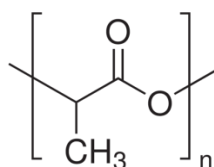
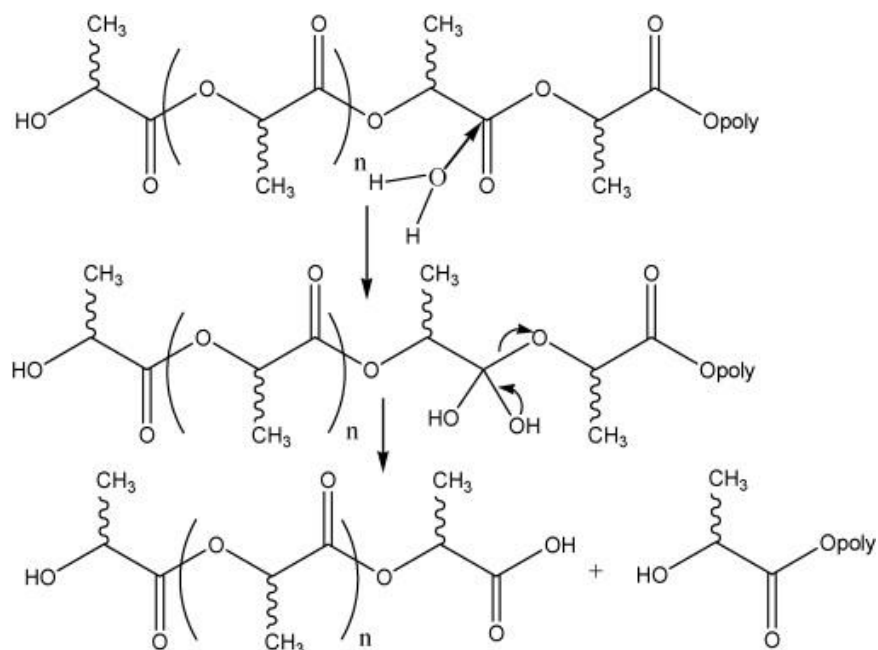


Figure 3-11 Chemical structure of PLA.

PLA does not have any reactive side chains so introduction of reactive groups was needed if a covalent bond was to be formed between the virus and the PLA surface. One method of doing this is by alkaline hydrolysis of the polymer to form hydroxyl and carboxyl groups. These groups could then be used to react with other chemical species (Yang *et al.*, 2003).



Scheme 3-1 Mechanism for hydrolysis of PLA (Maharana *et al.*, 2009).

In order to investigate the extent of hydrolysis occurring on the PLA surface after exposure to 1 M NaOH solution, the %wt loss of the PLA squares were measured as a function of time. A higher %wt loss of the PLA indicated a greater degree of hydrolysis (Figure 3-12).

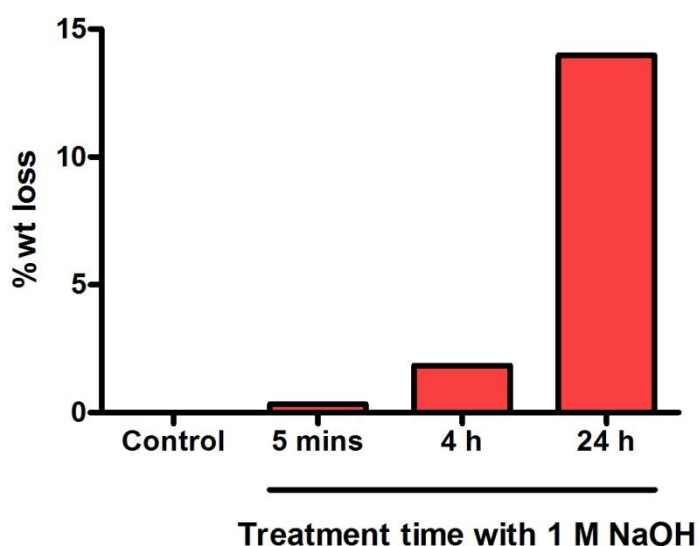


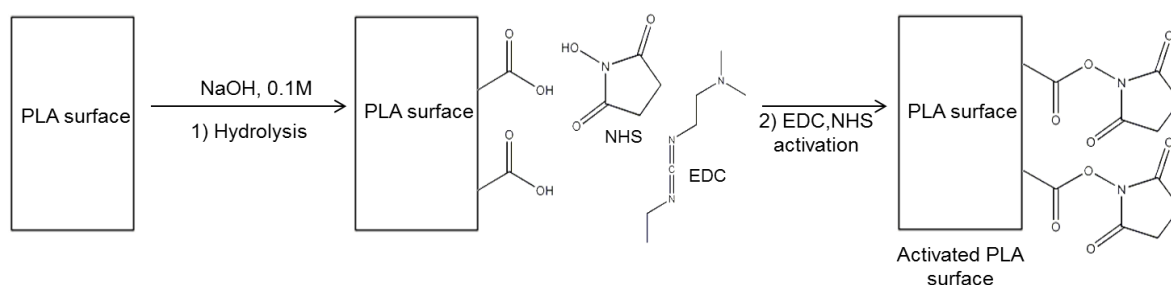
Figure 3-12 %wt loss of PLA after exposure to 1 M NaOH solution at different time points. PLA squares were weighed prior to exposure of 1 M NaOH solution and after exposure for 5 mins, 4 h and 24 h. The control PLA was exposed to dH₂O for 24 h. Representative graph from three independent experiments, n=1 per condition.

It was observed that increasing the length of treatment of the PLA in the 1 M NaOH solution increased the %wt loss of PLA indicating that hydrolysis had

occurred. As the proposed function of the PLA is for a cardiovascular stent it was important to maintain the structural properties of the polymer and achieve a balance between surface functionality and structure. Therefore, for future experiments it was decided that exposing the PLA to 1M NaOH for 5 mins would be adequate to ensure the generation of carboxyl groups but not cause bulk degradation of the PLA. As increasing the time of exposure of biodegradable polymers to degrading solutions increases the amount of bulk degradation occurring in the polymer structure (von Burkersroda *et al.*, 2002)

3.2.2.2 Activation of carboxyl groups on PLA surfaces by treatment with EDC/NHS

After the hydrolysis of the PLA surface, activation of the carboxyl groups was needed in order to create a surface that would covalently bind viruses or other biological materials to the stent surface. A proposed route of carboxyl activation using 1-Ethyl-3-(3-dimethylaminopropyl)carbodiimide hydrochloride (EDC) and N-hydroxysuccinimide (NHS) was envisaged to yield NHS esters as reactive intermediates (Scheme 3-2). NHS esters can readily undergo condensation reactions with primary amines to form a covalent bond. Since the virus capsid has lysine residues, which have a primary amine functional group, it could therefore be possible to link the virus to the PLA surface using this route.



Scheme 3-2 EDC/NHS activation of PLA surface.

To test this reaction pathway for surface activation, the PLA was hydrolysed, treated with EDC/NHS and then reacted with hexamethyldiamine (HMD). A ninhydrin test was then performed to test for the presence of amines on the surface.

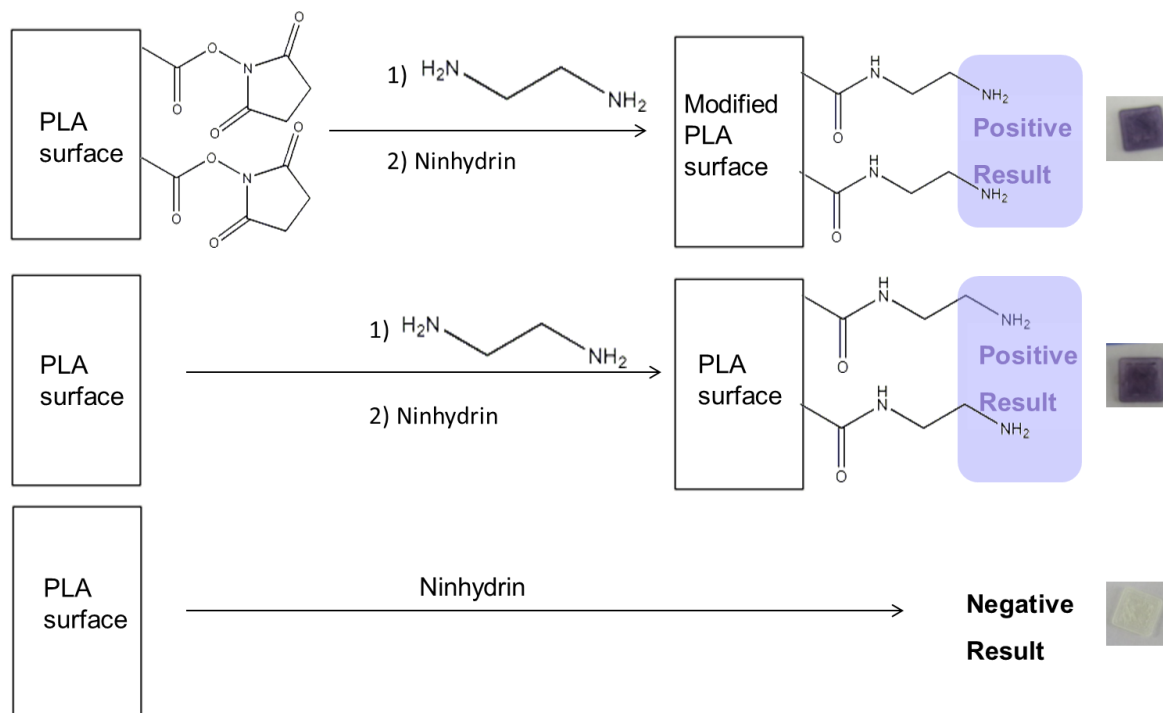
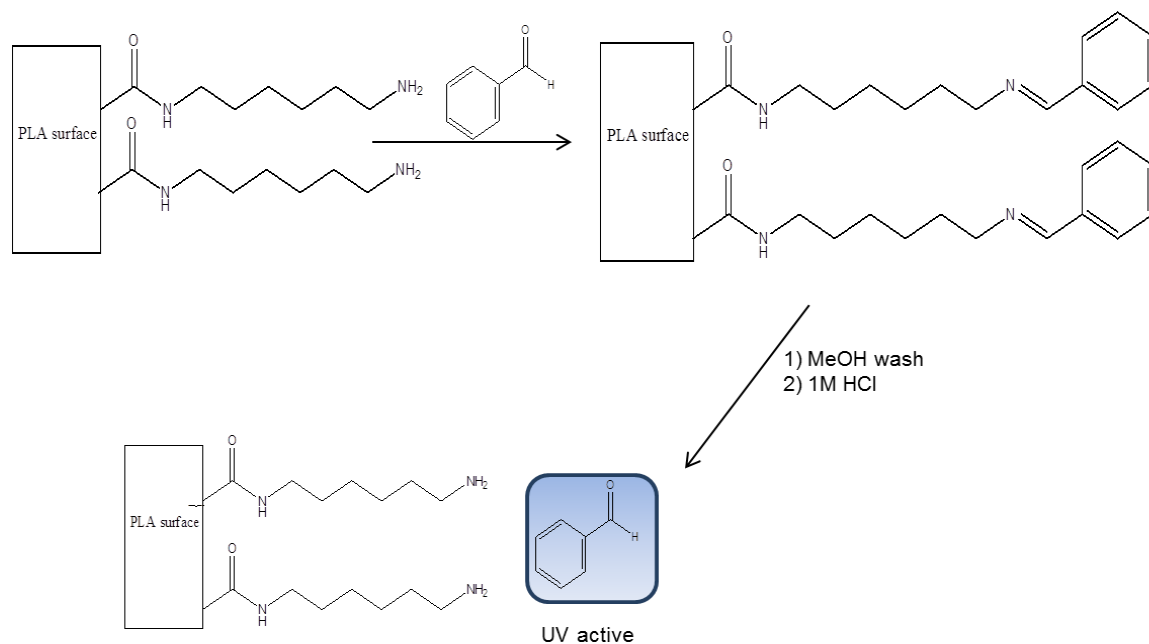


Figure 3-13 Treatment of PLA with ninhydrin to test for primary amines on the PLA surface.

It was observed that the PLA control tested negative for amines whereas the NHS/EDC modified PLA was positive (section 2.14.3), exhibiting a purple PLA surface. Interestingly, it was observed that direct aminolysis could occur between the PLA surface and the HMD bypassing the need for EDC/NHS activation (Figure 3-13) (section 2.14.5). Quantification of the amount of aminolysis occurring was attempted by dissolving the PLA in solvent and then measuring the UV-absorbance, however the process of exposing the PLA to the solvent caused the purple compound to degrade.

Since an established route to yield a PLA surface modified with primary amine groups was achieved. We wanted to test whether it would be possible to get a controlled binding and elution from the PLA surface of benzaldehyde by imine formation. Benzaldehyde was chosen because it can readily react with amine groups to form imines and is UV active so it could be detected by UV-vis spectroscopy (Scheme 3-3).



Scheme 3-3 Reaction of aminolysed PLA with benzaldehyde to show controlled elution.

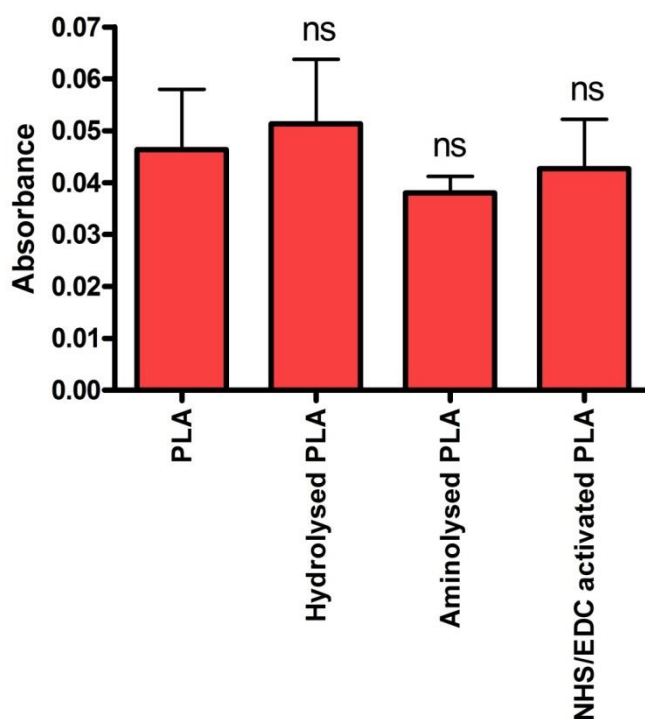


Figure 3-14 UV absorbance at 220 nm of 1 M HCl solutions after exposure to PLA surface following benzaldehyde conjugation.

PLA squares were aminolysed using the two methods detailed in Figure 3-13 and reacted with benzaldehyde, the squares were washed with dH₂O and then treated with 1 M HCl solution. The absorbance at 220 nm was measured of the HCl solutions to test for benzaldehyde elution from the surface. Results are displayed as mean absorbance at 220 nm ± SEM, statistical analysis was performed using an unpaired student's t test, ns=non-significant vs PLA non-treatment control. Representative graph from three independent experiments; each with three replicates per condition.

After treatment of the PLA with benzaldehyde, the PLA was washed with dH₂O to ensure any residual unbound benzaldehyde was rinsed away. To remove and detect the benzaldehyde, that had bound to the PLA, the surface was treated with 1 M HCl. UV-vis spectroscopy was used to monitor the HCl solutions to test for the presence of benzaldehyde; however a change in the absorbance at 220 nm was not observed (Figure 3-14). This could have been due to imine formation being a reversible process and susceptible to hydrolysis by dH₂O in the washing steps. Due to the instability of the imine bond, a different method was needed which yielded a bond which was not susceptible to water hydrolysis. Protecting group Fmoc-lysine was proposed; as the lysine group would be a good 'model' for the virus capsid (which would also react through the lysine amino acid residue). The Fmoc group could be cleaved and detected by UV-vis spectroscopy and ESI-MS, enabling verification of the success for this PLA surface modification procedure by controlled binding and elution (Figure 3-15).

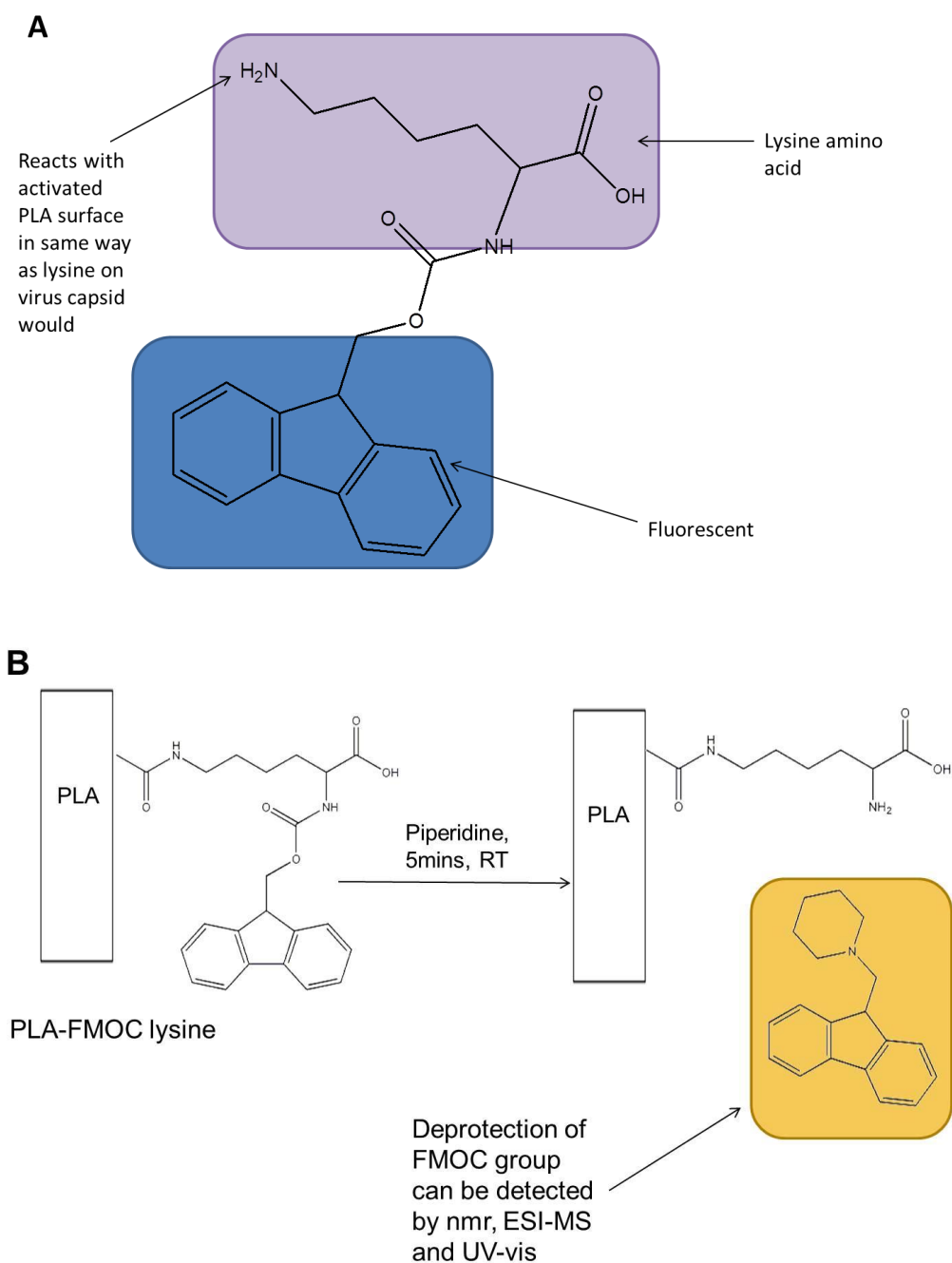


Figure 3-15 A) Chemical structure of Fmoc-lysine, B) Deprotection of PLA-Fmoc-lysine using piperidine.

In order to follow the deprotection of the Fmoc-lysine, electrospray ionisation mass spectra were taken before and after deprotection (Figure 3-16) (section 2.14.7).

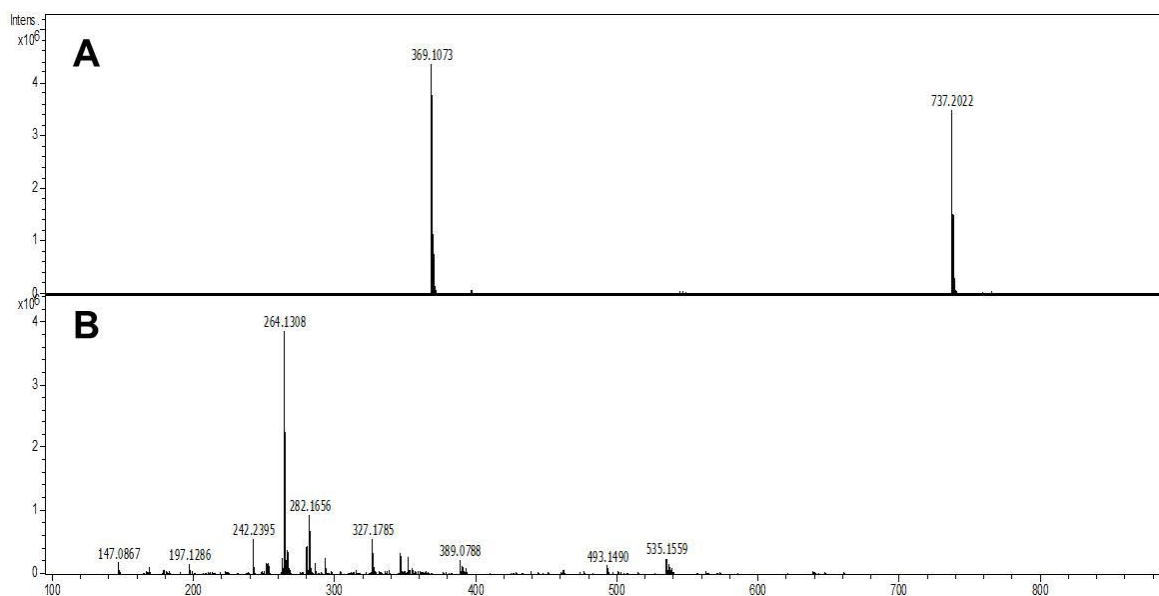


Figure 3-16 ESI-MS of Fmoc lysine deprotection in solution after treatment with piperidine.

A) Fmoc lysine before piperidine deprotection B) Fmoc lysine after piperidine deprotection.

As characteristic spectra of the protected and deprotected Fmoc-lysine were obtained, using ESI-MS. Testing to see whether Fmoc-lysine could be deposited on the PLA surface and then Fmoc cleavage could be monitored to verify that attachment of the Fmoc-lysine to the surface had been successful.

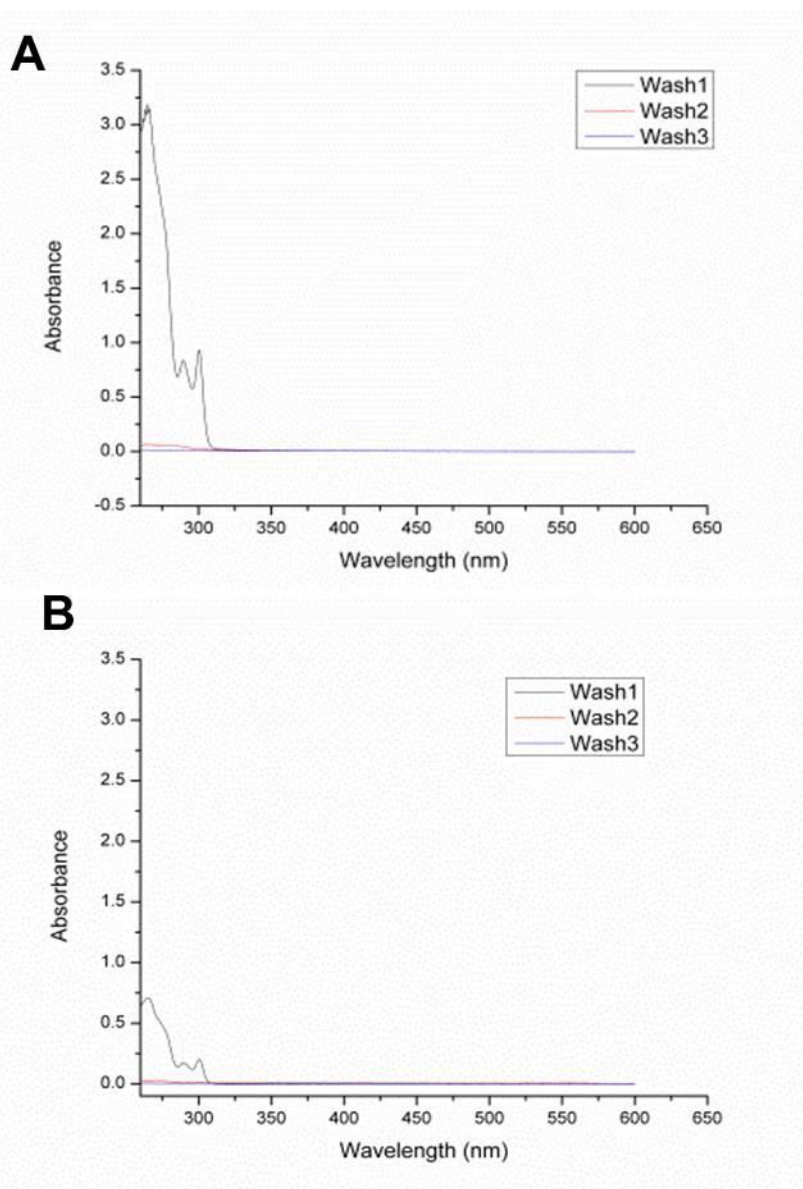


Figure 3-17 UV-vis of washes with EtOH of PLA surface after Fmoc functionalisation. A) Aminolysis and B) EDC/NHS activated PLA surface.

Two different methods were tested for Fmoc-lysine functionalisation of the PLA; direct aminolysis of the amine group on Fmoc-lysine reacting with PLA surface and via hydrolysis followed by EDC/NHS activation of carboxyl groups, with the resulting NHS-ester reacting with the amine group from Fmoc-lysine. After Fmoc-lysine was left to react with the surface, it is important to wash the surface thoroughly to ensure any unbound Fmoc lysine was washed off. This was monitored by UV-vis spectroscopy (Figure 3-17).

As demonstrated by the UV-vis traces in Figure 3-17, we can see that all the non-bound Fmoc-lysine was efficiently removed from the surface as the UV signal of the EtOH washes drops to zero with successive washing.

In order to test for the presence of Fmoc-lysine to see whether the conjugation to the PLA had been successful, piperidine was then added to the PLA surface, which would release the fluorenyl group that could be detected by and UV spectra and ESI-MS (Figure 3-18&Figure 3-19).

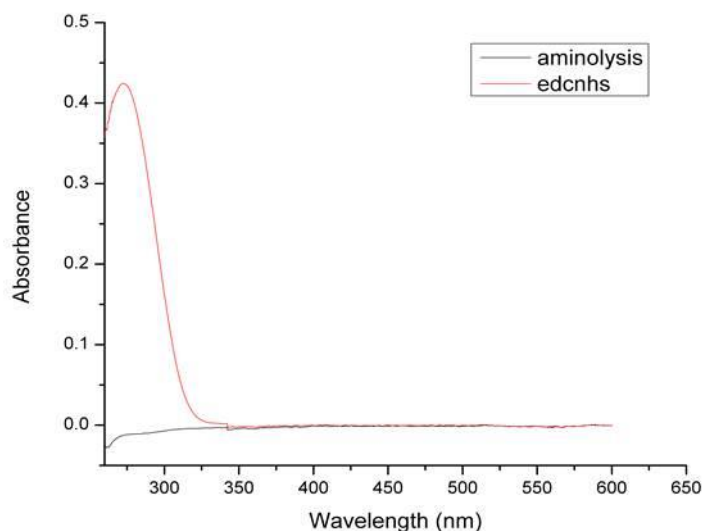


Figure 3-18 UV-vis spectra of piperidine solutions after removal of Fmoc group. Black) aminolysis PLA, red) EDC/NHS activated PLA.

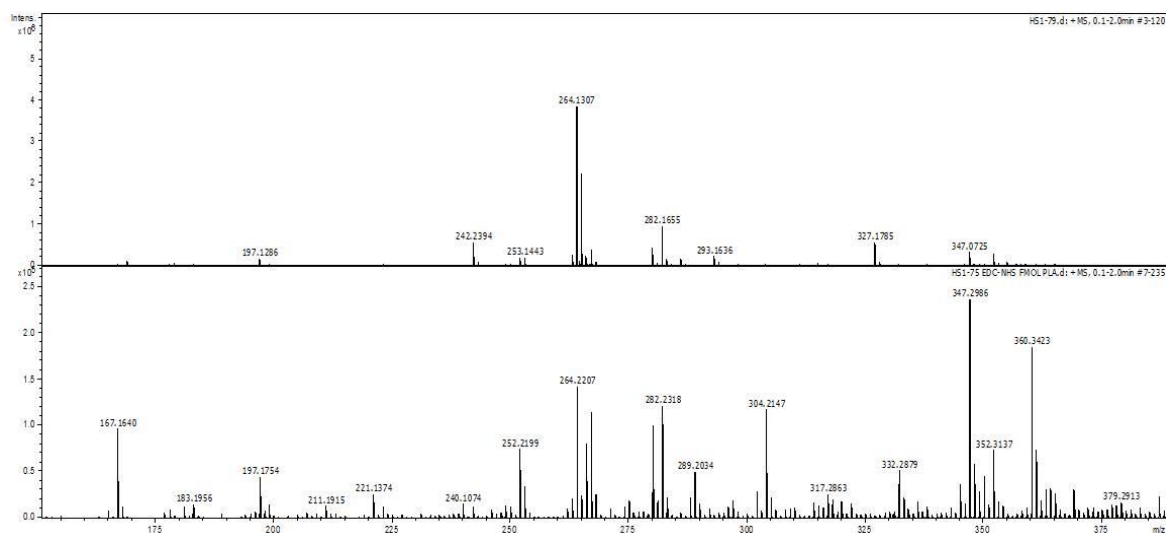


Figure 3-19 ESI-MS of PLA after Fmoc deprotection.

Above) Deprotected Fmoc/lysine in solution Below) Deprotected solution from EDC/NHS activated PLA.

By comparison with the spectrum of the deprotected Fmoc-lysine (Figure 3-19) it was observed that, the peak at 264 m/z, which corresponds to the fluorenyl-piperidine adduct appears in both spectra, confirming that the Fmoc-lysine was

successfully attached and eluted off from the PLA surface. A spectrum from the direct aminolysis PLA was also taken but no corresponding peaks were found, which was consistent with the UV-vis data (Figure 3-18).

As a successful method for attachment and elution of FMOC-lysine to the PLA surface was found, it was important to repeat the methodology, to make sure that the method was robust before moving on to viral attachment and elution. However, disappointingly this method did not always work reliably; therefore other methods for attaching the adenovirus to the surface were investigated.

3.2.3 Collagen Entrapment of Virus onto PLA surfaces

A different method for coating stent materials with virus was investigated by entrapping the virus into a collagen gel, which was set onto the stent material. Atthoff *et al.* had previously reported the observation that collagen could be directly deposited onto PLA surfaces, and that modification of the PLA by hydrolysis prior to collagen deposition did not enhance that amount of collagen deposited, however the absorption kinetics did vary when monitored by a quartz crystal microbalance (QCM) (Atthoff and Hilborn, 2007). Therefore it was hypothesised that PLA would be a promising material to use for collagen deposition; firstly entrapment of the adenovirus into the collagen gel would be achieved by mixing the two components together, this could then be spread onto a PLA surface and heated to 37 °C in order to form a collagen-adenovirus gel.

3.2.3.1 Visualisation of Ad-555 in collagen gel set onto PLA surfaces

Initially, we wanted to test whether it would be possible to encapsulate the virus into a collagen gel, and set onto a PLA disc. In order to visualise whether encapsulation of the virus had been successful, Ad5 labelled with Alexa Fluor™ 555 was used so that, after washing the PLA, we could see if the virus was still retained on the PLA surface within the collagen gel. Figure 3-20 shows that the Ad5 can be successfully retained onto the PLA surface by entrapment within the collagen gel. This method could therefore provide a route for attachment onto a PLA stent, providing the virus is able to be released from the collagen gel and is still biologically active.



Figure 3-20 Fluorescent micrographs of PLA surfaces with fluorescently tagged Ad5. PLA + collagen and PLA surface + Ad555 were used as controls. PLA collagen Ad555 as test for collagen entrapment of virus and retention on the PLA surface. Scale bar = 100 μm . Images taken at 40 x magnification.

3.2.3.2 In vitro transduction of adenovirus from collagen coated PLA and SS surfaces

Since we could visualise the adenovirus successfully encapsulated and secured onto the PLA surface within the collagen gel, it was important to find out whether the virus maintained its biological viability and whether it would be able to be released from the collagen gel and transduce cells.

This was tested *in vitro* by coating PLA surface with Ad 5 either encapsulated within the collagen gel or directly onto the PLA surface. A positive control for Ad5 transduction was used to ensure the reporter assay was working and a negative control of non-treated rat SMC was used to gauge background levels of absorbance. Once the surfaces were prepared they were washed thoroughly with PBS before being placed face down onto the rat SMC. These washing processes were to test the robustness of the collagen gel because if this was applied *in vivo*, blood flow would cause a similar obstacle. A β -galactosidase assay was performed after 72 h of incubation of the surfaces with the cells (Figure 3-21).

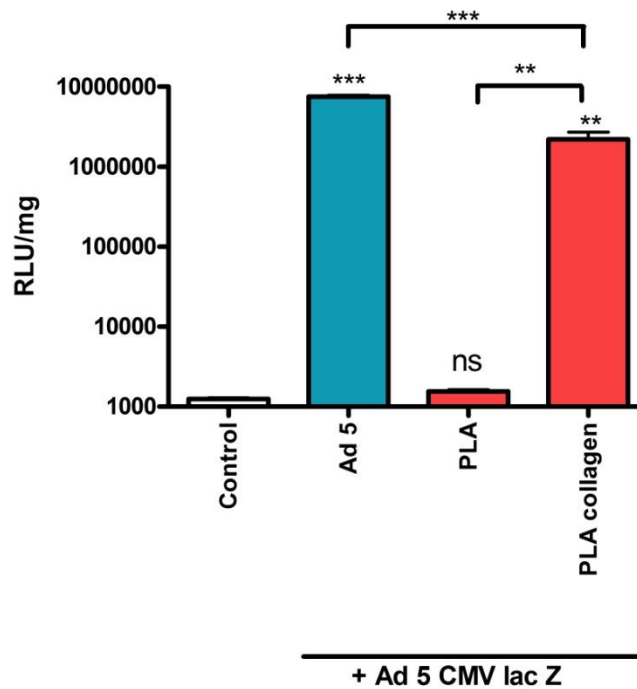


Figure 3-21 Transduction of A10 cells with Ad5 CMV lac Z encapsulated in collagen and deposited on PLA surfaces.

A10 cells were treated with medium (white), or Ad5 CMV lac Z (blue), Ad5 CMV lac Z directly onto PLA (red), PLA + collagen + Ad5 CMV lac Z (red), the virus concentration was (6.6×10^9 VP/disc). The discs were placed onto the A10 cells and left for 72 h, they were then removed, the cells were washed and a β -galactosidase assay was used to determine the β -gal expression by measuring the relative light units (rlu) normalised to the protein concentration (mg). Results are displayed as mean \pm SEM, statistical analysis was performed using an unpaired student's t test, *** $p < 0.001$, ** $p < 0.01$, vs non-treated cell control, representative graph from three independent experiments with three biological replicates for each condition.

It was observed that the virus maintains its biological activity when encapsulated into the collagen gel and is released from the collagen gel within the 72 h timeframe. High levels of β -galactosidase expression are observed from the PLA + collagen and give levels of transduction, which are significantly higher than when the virus is coated onto the PLA directly without the collagen. When β -galactosidase expression of the PLA collagen is compared to the Ad5 in solution control, at 72 h are significantly higher for the Ad5 in solution. This could be due to some virus particles being washed off during the preparation procedure, similarly it could also indicate that residual virus is still trapped in the collagen gel. Further testing at different timepoints would be required to give more information on the elution profile of the virus from the collagen gel.

Although PLA stents can be purchased, currently commercial PLA stents have an everolimus coating on them and would interfere with SMC proliferation (Khamis *et al.*, 2014, Abbott, 2015). Therefore in order to test the efficacy of virus transduction from stent surfaces, it was important to develop a delivery system

from 316 L stainless steel which is the material that most bare metal stents are made from. As BMS are a longer established cardiovascular technology there is a broader range of different stent sizes for animal models such as pigs and mice and can be obtained without anti-proliferative drugs coated on them. It would be advantageous if we could translate the collagen-virus encapsulation onto SS surfaces.

In order to compare collagen encapsulation of the virus on PLA and SS surfaces, a β -galactosidase assay was carried out comparing the two surfaces with Ad5 in solution as a positive control and non-treated rat SMC cells as a negative control.

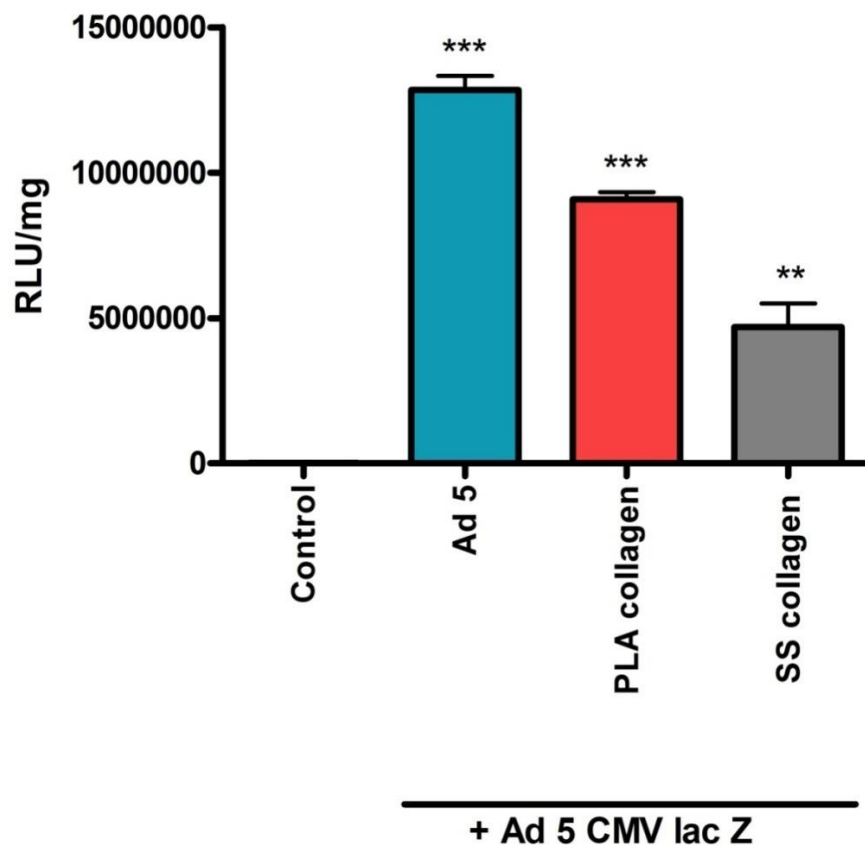


Figure 3-22 Transduction of A10 cells with Ad5 CMV lac Z encapsulated in collagen and deposited on PLA and SS surfaces.

A10 cells were treated with medium (white), or Ad5 CMV lac Z (blue), Ad5 CMV lac Z onto PLA + collagen (red), and SS + collagen (grey), virus concentration was (6.6×10^9 VP/disc/well). The discs were placed onto the A10 cells and left for 72 h, they were then removed, the cells were washed and a β -galactosidase assay was used to determine the β -gal expression by measuring the relative light units (rlu) normalised to the protein concentration (mg). Results are displayed as mean \pm SEM, statistical analysis was performed using an unpaired student's t test *** $p < 0.001$, ** $p < 0.01$, vs non-treated cell control, representative graph from three independent experiments with three biological replicates for each condition.

After 72 h, cells were harvested and the amount of transgene expressed was quantified (Figure 3-22). It was observed that the PLA surface is a more efficient

platform for the collagen virus encapsulation, with 2 fold increase in transgene expression from the PLA collagen compared to the SS surface. This could be due to improved adherence of the collagen gel onto the PLA surface and therefore more of the collagen virus gel could have been removed during the washing steps from the SS surface.

3.2.3.3 Quantification of virus deposited on PLA and SS surfaces

In order to gain more insight into the amount of virus on the surface, a method for quantification needed to be developed. Two different methods were investigated microBCA and qRT-PCR. The microBCA assay works by quantifying the amount of protein present from the viral capsid whereas qRT-PCR measures the amount of viral DNA. A ten-fold dilution of the stock virus solution was made to obtain concentrations from 5×10^{10} - 5×10^1 VP/mL. These solutions were tested for protein concentration by performing a microBCA assay or for viral DNA concentration by qRT-PCR.

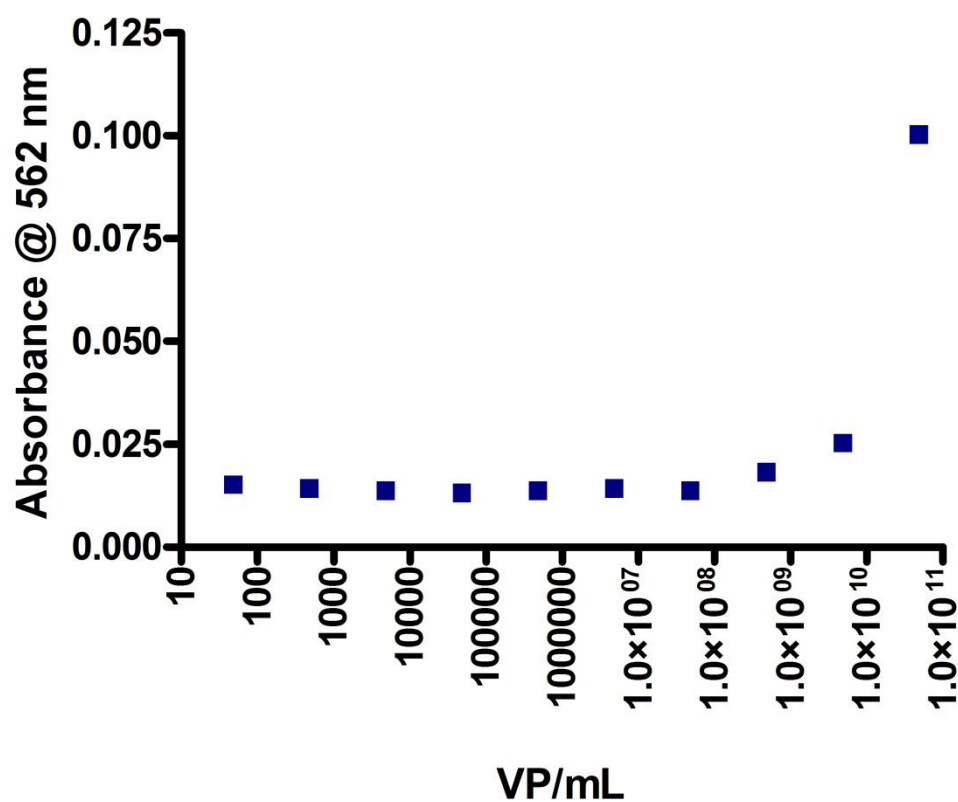


Figure 3-23 microBCA assay of serial dilution of Ad5 CMV lac Z

A 10 fold serial dilution of Ad5 CMV lac Z was made to make concentrations 5×10^{10} – 5×10^1 VP/mL range and microBCA assay was run for these solutions to measure the protein content.

Figure 3-23 shows the results for the microBCA assay performed on the viral dilutions. It was clear that this method is only effective at relatively high concentration of adenovirus (1×10^9 - 1×10^{11} VP/mL), so would not be sensitive enough to detect the amount of virus deposited on the surfaces. In addition, the method used for binding the virus to the surface uses encapsulation in a collagen gel, which is also a protein, this would cause background levels of absorbance and may saturate the signal caused by virus deposition.

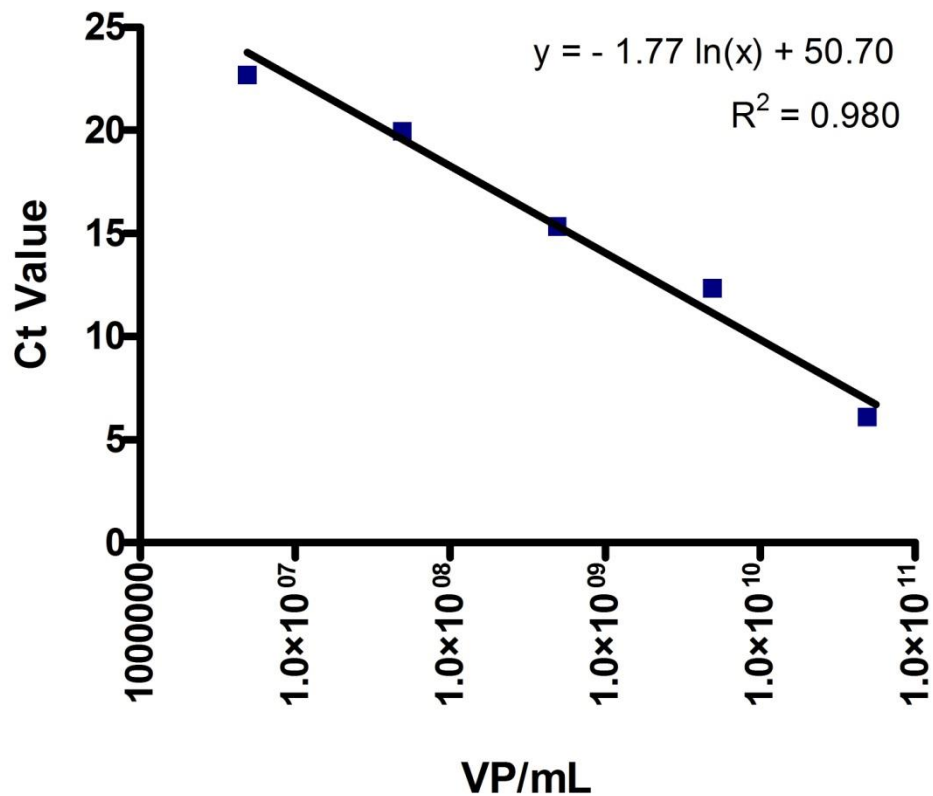


Figure 3-24 qRT-PCR from a serial dilution of Ad5 CMV lac Z.

A 10 fold serial dilution of Ad5 CMV lac Z was made to make concentrations 5×10^6 – 5×10^{10} VP/mL range, quantification of the DNA was done by performing DNA extraction on all the samples followed by reverse transcription and qRT-PCR.

Using the qRT-PCR method would give access to greater sensitivity ranging from 1×10^9 - 1×10^5 VP. Although this method was more time consuming, it offers a higher sensitivity which would be suitable for monitoring the amount of virus on a surface.

The general approach for measuring the amount of virus on a surface was reported (Johnson *et al.*, 2005a), whereby the amount of virus attached to the surface, is estimated to be equal to the total amount of virus added, minus the

virus removed in the washing steps. DNA extraction and qRT-PCR was used to determine the virus concentrations before being applied to the surface and using the PBS wash solution (to infer how much virus was retained on the surface within the collagen gel) (Figure 3-25).

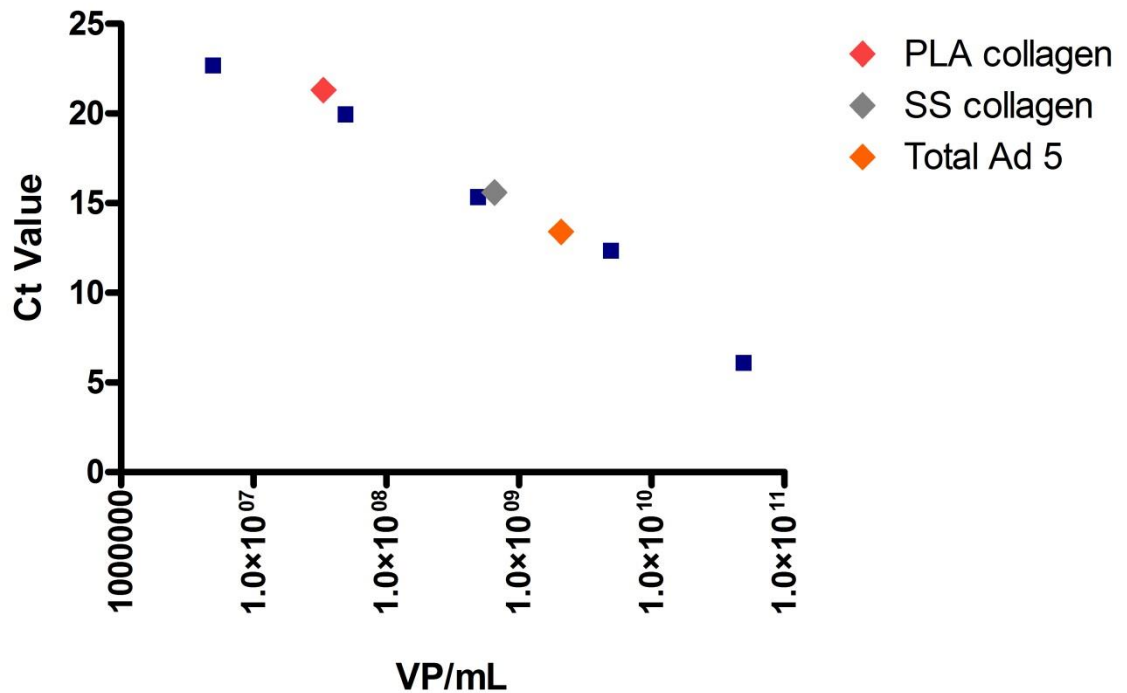


Figure 3-25 qRT-PCR of serial dilution of Ad5 CMV lac Z and of washings from collagen coated PLA surfaces.

A 10 fold serial dilution of Ad5 CMV lac Z was made to make concentrations $5 \times 10^{10} - 5 \times 10^1$ VP/mL range (blue), samples were also made using the total amount of virus deposited onto the surfaces (orange), washings after collagen gel virus deposition on SS surface (grey) and from PLA surface (red). Quantification of the DNA was done by performing DNA extractions on all the samples followed by qRT-PCR.

In agreement with the observations made previously (Figure 3-22), more virus was retained on the PLA collagen surface compared to the SS surface. An estimate for the amount of virus left on the PLA collagen surface was 1.20×10^9 VP/mL, and for the SS collagen it was 1.01×10^9 VP/mL.

Having identified that PLA retains more virus particles on the surface using the collagen entrapment of the adenovirus method than the SS. PLA surfaces were used in the next experiments. For all the experiments up to this point adenovirus 5 was chosen as a model virus vector for attachment to the stent surfaces. This was because it can be produced in high titre stocks, it has a high levels of transduction in a broad range of cell types, and insertational mutagenesis is uncommon, and is the most commonly used viral vector for gene

therapy (Bradshaw and Baker, 2013). However, one of the disadvantages with Ad5 is the existing level of anti-Ad5 antibodies within the human population, it is therefore important to develop rare or non-human serotypes of virus for gene therapy. Ad 49, is a promising novel vector for gene therapy because it does not cross react with Ad5 neutralising activity (Lemckert *et al.*, 2006). Ad 49 was therefore chosen to see whether it could be incorporated into the collagen coating and maintain its biological activity (Figure 3-26). However as shown in Figure 3.26, incorporation of Ad 49 into the collagen gel was not successful, indicating that this technique may be sensitive to different adenoviral serotypes.

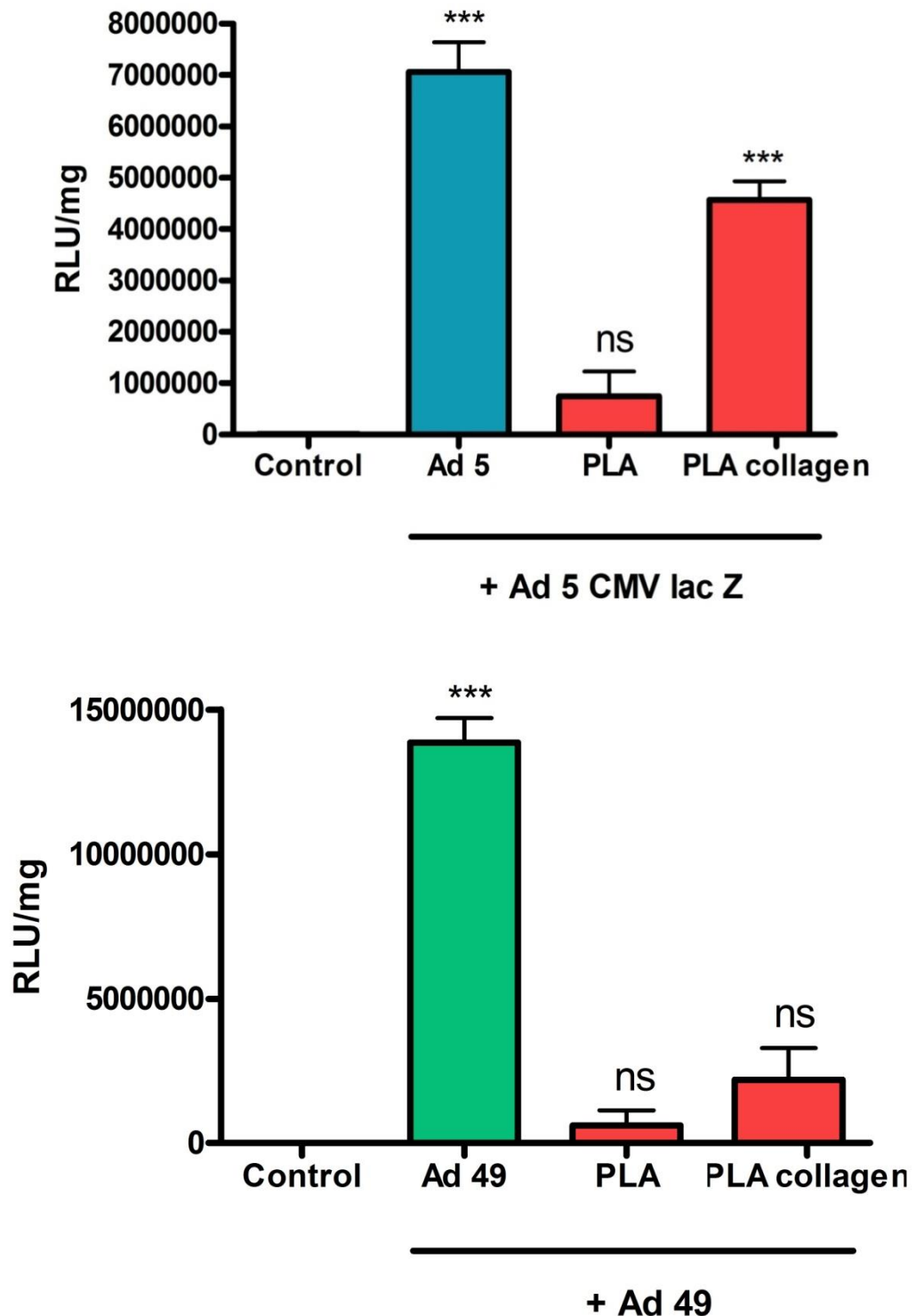


Figure 3-26 Transduction of Ad5 CMV lacZ and Ad49 from collagen coated PLA surfaces. Above) Ad5 β -galactosidase activity in lysates of A10 rat SMCs, for PLA+ collagen+Ad5 (red), PLA surfaces – collagen + Ad5 (red) and Ad5 in solution (blue). Below) lysates of A10 SMCs tested for luciferase activity after culture with PLA + collagen+Ad49luc (red), PLA surfaces – collagen + Ad49 luc (red) and Ad49luc in solution (green). Error bars are shown as mean \pm SEM, significance was determined by student's t-test compared to control, ns= non-significant, *** p <0.001. Each group was run as a biological triplicate.

PLA stents are not currently manufactured for mice, and human PLA stents are coated with anti-proliferative drug everolimus (Abbott, 2015). Therefore, in order to move from *in vitro* testing of the delivery system to *ex vivo* and *in vivo*

testing, a method for coating PLA onto SS was needed to be developed. This would allow BMS coated with PLA to be used as a platform for collagen Ad5 gel to be applied to. A method for doing this was investigated by dissolving the PLA in chloroform and then applying onto the SS surface and leaving it to dry. This method worked well and the PLA coating adhered well to the SS surface and did not get removed after extensive washing. Using this method, the PLA coated onto the surface was not very uniform, so methods for smoothing the PLA layer was achieved by exposing the PLA to vapourised dichloromethane.

To test the effect of PLA concentration (%wt/wt) applied to the SS on Ad5 transduction from the collagen gel, SS discs were coated with 10% wt/wt, 15% wt/wt and 20% wt/wt PLA in chloroform and then collagen-Ad5 gel and applied to the surfaces. PLA discs with collagen Ad5 gel, and Ad5 in solution were used as positive controls and to provide a point of comparison for the SS surfaces. Non-treated cells were used as a negative control. The discs were on the cells for 72 h, before being removed and a β -galactosidase assay was used to evaluate the amount of transgene expressed.

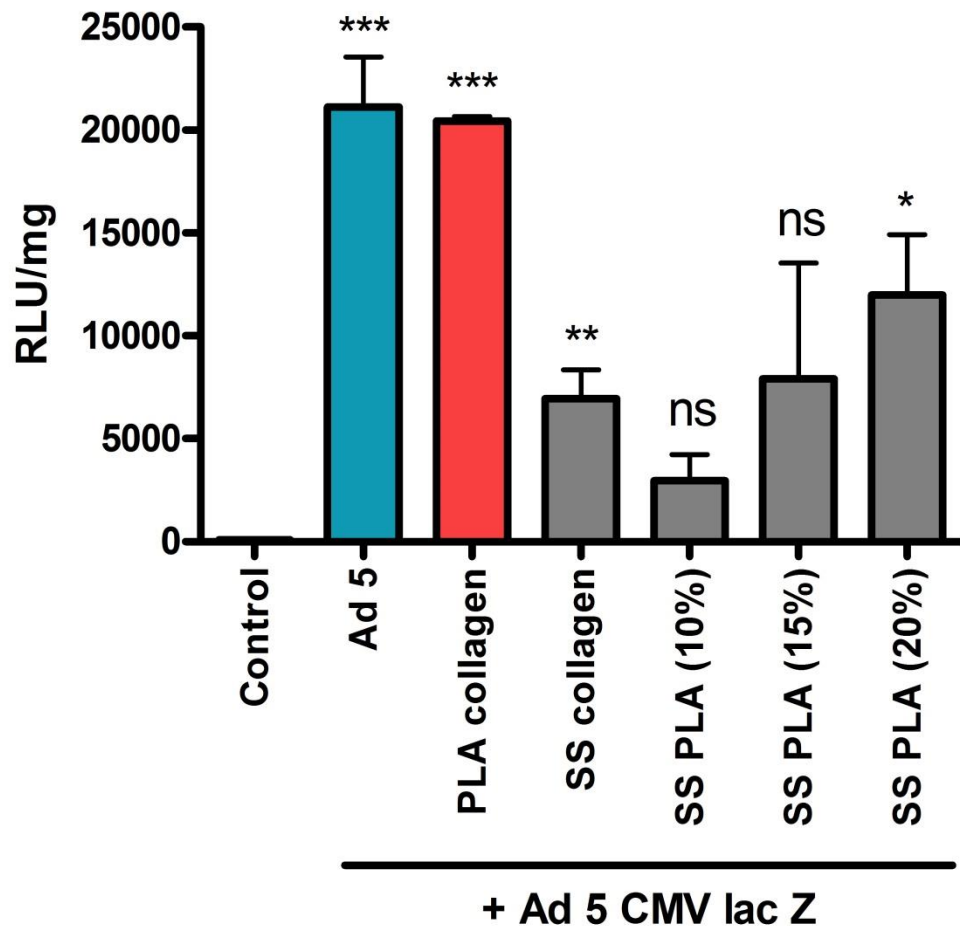


Figure 3-27 Transduction of A10 cells with Ad5 CMV lacZ encapsulated in collagen and deposited on PLA and SS and SS coated in PLA surfaces.

β -galactosidase activity in lysates of A10 rat SMCs after culture with PLA and SS surfaces coated with collagen virus gel for 72 h. NTC (white), Ad5 in solution (6.6×10^9 VP) (blue), PLA coated with collagen Ad5 gel (red), SS coated with collagen Ad5 gel (grey), SS coated with different %PLA dissolved in chloroform wt/wt then coated in collagen virus gel (grey). Error bars are shown as SEM, significance determined by students t test compared to non-treatment control, ns= non-significant, * $p < 0.05$, ** $p < 0.01$, *** $p < 0.001$.

When SS was coated with 20% PLA we observed a significant difference in β -galactosidase expression when compared to control cells. However, using a 20% of PLA on the metal surface is likely to cause logistical problems for the stent as it may be too thick to fit into the guide catheter. The coating may also fill the space in between the stent struts and could alter and prevent inflation of the stent when it is expanded by the balloon.

To move forward with *ex vivo* testing of the coatings, a suitable concentration of virus was needed to be identified. This was determined by bathing mouse aorta in different concentrations of Ad5 CMV lac Z, leaving in medium for 72 h then staining with X-gal to visualise β -galactosidase expression. Mouse aortas were exposed to Ad5 at concentrations varying from 5×10^9 VP/mL to 5×10^{11} VP/mL.

Blue cells were visible for the 5×10^{10} VP/mL and 5×10^{11} VP/mL so therefore the amount of virus put into the coatings will need to be within this range (Figure 3-28).

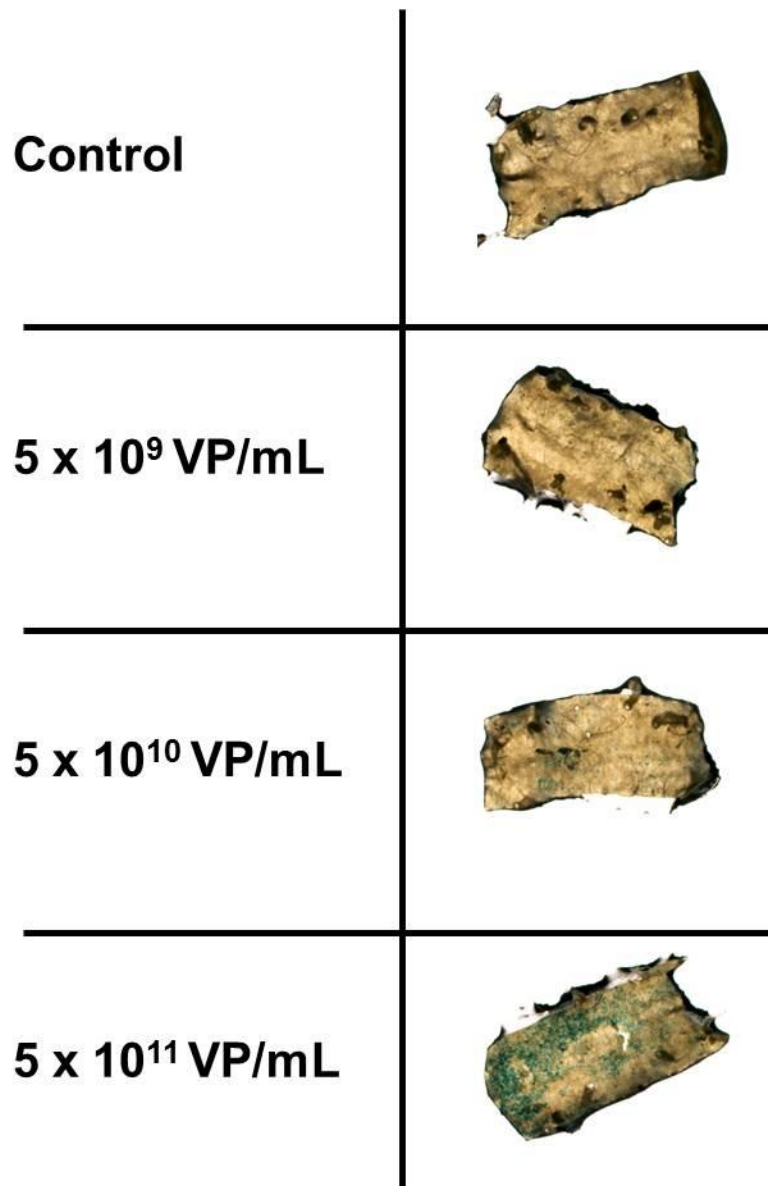


Figure 3-28 X-gal stained mouse aorta after incubation with Ad5 CMV lac Z for 72 h. Microscope images were taken at 4 x magnification after incubation with Ad5 for 72 h and then fixed with PFA and X-gal stained. Control was not treated with Ad5, the other aortas were exposed to Ad5 at concentrations 5×10^9 VP/mL Ad5, 5×10^{10} VP/mL, and 5×10^{11} VP/mL.

Since a concentration of Ad5 CMV lac Z had been determined which achieve transduction of mouse aortas *ex vivo*, testing to see whether transduction could now be achieved from PLA surfaces coated with the Ad5 collagen gel was undertaken (Figure 3-29). PLA surfaces were coated with Ad5 CMV lacZ collagen gel at concentration 5×10^{11} VP/mL.

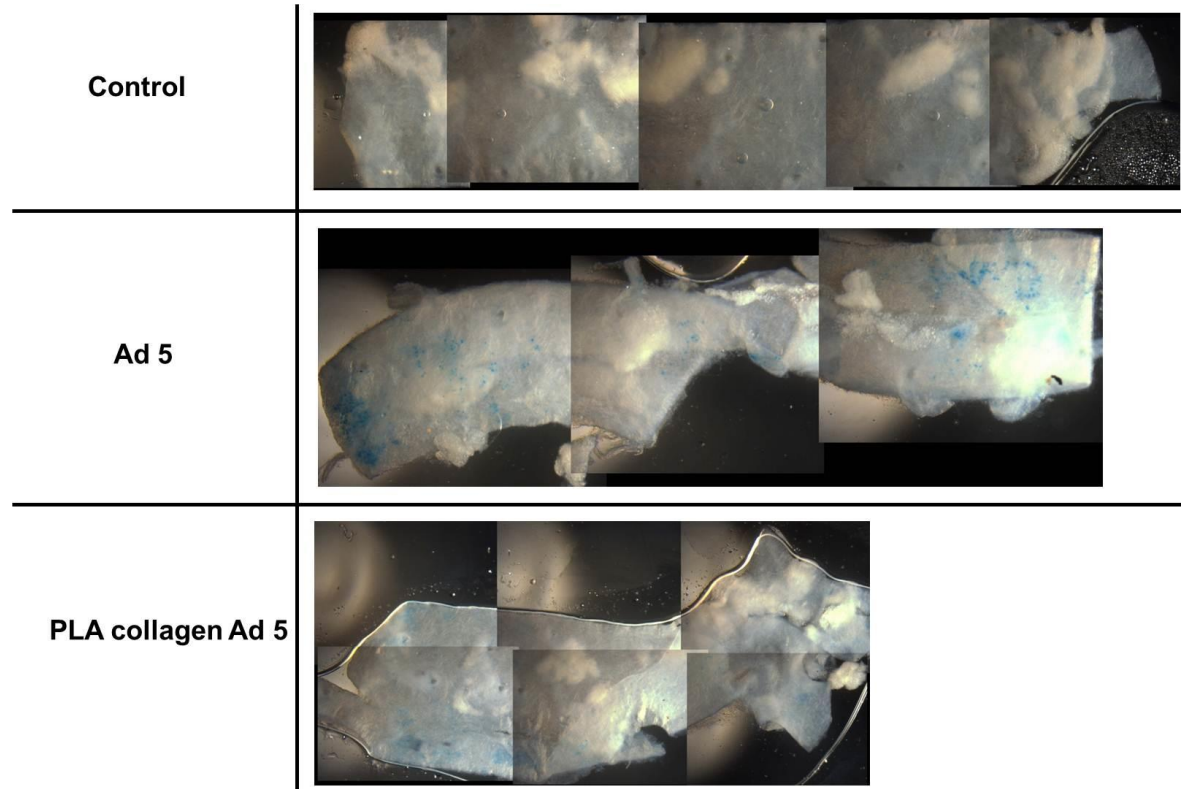


Figure 3-29 X-gal stained mouse aorta after incubation with Ad5 CMV lacZ collagen gel coated onto PLA for 72 h.

Microscope images were taken at 4x magnification after incubation with Ad5 for 72 h and then fixed with PFA and X-gal stained. Control was not treated with Ad5, Ad5 positive control was exposed to Ad5 CMV lac Z solution at 5×10^{11} VP/mL, and the PLA collagen Ad5 was PLA coated with collagen Ad5 gel at the same concentration of 5×10^{11} VP/mL.

Since transduction of Ad5 CMV lac Z was observed from the PLA Ad5 collagen gel (Figure 3-29), we now wanted to simulate stent deployment to see whether damaging the vessel would alter and enhance Ad5 delivery to the aorta. To test this, aortas were damaged by inflating a balloon that would usually be used for stent deployment, the balloon was removed and the aortas were cut longitudinally. Ad5 collagen coated PLA were placed onto the aorta and left in culture medium for 72 h and were then stained with X-gal to visualise transgene expression (Figure 3-30).

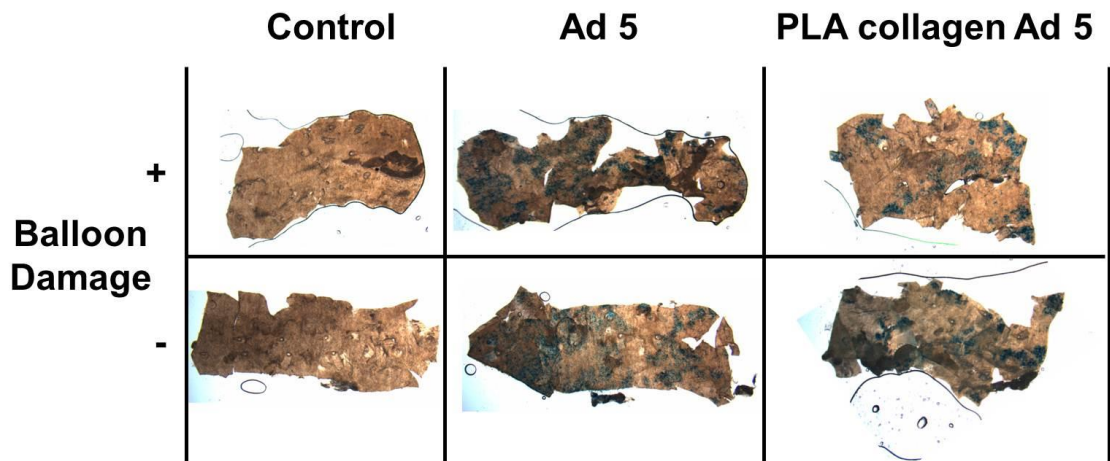


Figure 3-30 X-gal stained mouse aorta \pm balloon damage after incubation with Ad5 CMV lac Z collagen gel coated onto PLA for 72 h.

Microscope images were taken at 4 x magnification after incubation with Ad5 for 72 h and then fixed with PFA and X-gal stained. Control was not treated with Ad5, Ad5 positive control was exposed to Ad5 CMV lac Z solution at 5×10^{11} VP/mL, and the PLA collagen Ad5 was PLA coated with collagen Ad5 gel at the same concentration of 5×10^{11} VP/mL. Aortas in the + balloon damage group were damaged by inflating a coronary balloon for 10 seconds placement of the PLA surfaces onto the vessels.

From the resulting images of the vessels (Figure 3-30), we did not observe any difference in the amount of Ad5 transduction when the vessel is injured with the balloon. The next step for was to translate this delivery system, which works very effectively on the PLA surfaces, to work from murine stents. This was tested by coating the murine stents with 10% wt/wt PLA and then applying the collagen-Ad5 gel onto the PLA coated stent and deploying into mouse aortas *ex vivo*. However, after leaving for 72 h and staining with X-gal, no virus transduction was observed from the stents. 10% wt/wt PLA was the highest concentration of PLA that allowed full expansion of the mice stents. However, if we look at previous *in vitro* results using this concentration of PLA applied on SS discs, very low levels of Ad5 transduction are observed (Figure 3-27), which may explain why this concentration of PLA did not enable Ad5 transduction *ex vivo*.

In order to develop a stent which could be used in the porcine model, human Gazelle BMS stents were coated with higher concentrations of PLA. It was hypothesised that due to the human stents inherent greater mechanical strength they would still allow for stent expansion by the balloon despite the concentration of PLA being greater than for the murine stents. The stents were therefore coated with 20% wt/wt PLA. To test whether Ad5 delivery from the BMS coated with PLA was possible, Ad5 collagen gel was applied to the BMS PLA and then deployed into a pig coronary *ex vivo* (Figure 3-31).



Figure 3-31 X-gal stained pig coronary arteries after Ad5 CMV lac Z collagen gel was coated onto PLA 20% wt/wt BMS for 72 h.

Images were taken after incubation with Ad5 for 72 h and then fixed with PFA and X-gal stained. A) Control was not treated with Ad5, b) Ad5 positive control was exposed to Ad5 CMV lac Z solution at 1.25×10^{12} VP, and c) the PLA collagen Ad5 was PLA coated with collagen Ad5 gel at the same concentration of 1.25×10^{12} VP/mL.

The images in Figure 3-31, show that Ad5 transduction can be achieved from BMS surfaces, after coating with PLA (20% wt/wt) followed by the Ad5-collagen gel. However the same problem occurred as with the mice stents, the stent was unable to inflate properly due to the PLA coating restricting the stents flexibility. Further testing was done to try and find a concentration of PLA that would allow full inflation of the stent, but also ensure adherence of the Ad by a sufficient coating of PLA.

In order to do this, three different concentrations of PLA were tested, 10%, 5% and 2.5% wt/wt PLA dissolved in chloroform. The stents were coated in collagen-Ad5 gel and then inflated and deployed into pig coronary arteries. Transduction of the virus was measured, the results of which are shown in (Table 3).

%PLA wt/wt	Can the stent inflate?	Virus transduction observed?
10	No	Yes
5	Yes	No
2.5	Yes	No

Table 3 Results on %wt/wt PLA coating on BMS ability to be inflated and whether virus transduction was observed after the PLA coated BMS were then coated with Ad5 CMV lacZ collagen gel.

Stents were coated with 10% wt/wt, 5% wt/wt, and 2.5% wt/wt PLA in chloroform. The stents were deployed into pig coronary arteries *ex vivo* and left for 72 h, the stents were then removed and virus transduction was visualised by fixing and staining the tissue with X-gal.

These results indicate that when the stent is coated with 10% wt/wt PLA dissolved in chloroform, virus transduction can be achieved; however the stent

was not able to fully inflate due to the thickness of the coating. This would prevent it being used to deliver virus *in vivo*. However, when lower concentrations of PLA were used no virus transduction was observed, suggesting that adherence of the Ad5- collagen gel to the lower concentrations of PLA was not effective, although at these lower concentrations the stent could be deployed properly.

3.3 Discussion

In this chapter three different methods for virus attachment to stent surfaces were investigated and evaluated using *in vitro* and *ex vivo* models. Due to the Ad5 virus's net negative charge, it was thought that electrostatic interactions could provide the basis for adsorption onto stent materials which were coated with oppositely charged PEMs. Two different PEM systems were investigated, chi-ha and PAH-PSS, both of these systems demonstrated that the virus could be held onto SS surfaces coated with the PEM systems after extensive washing procedures as monitored by confocal microscopy; visualisation of the virus was enabled by using a fluorescently tagged virus, and by AFM.

After confirmation that we could create a SS surface coated with Ad5 particles superficially, biological testing of Ad5 was completed in order to see if exposure of Ad5 to the polycationic solutions had an effect on viral transduction. A striking difference in activity was observed between the two polycations, chitosan and PAH. When Ad5 was incubated with a solution of chitosan, a 73 fold increase in β -galactosidase expression was observed when compared to the Ad5 without the polycation, this increase in transduction could be attributed to increased viral uptake through a CAR independent pathway, via interaction of the negatively charged cell surface and the positively charged polycationic coating on the viral capsid (Zhong *et al.*, 2011, Kawamata *et al.*, 2002). It has also been suggested that electrostatic interactions alone cannot solely be attributed for the enhanced viral transduction with chitosan, and in addition we should consider the effect that chitosan has on decreasing the elasticity of cell membranes; a decrease in cell membrane elasticity has been linked to higher levels of virus transduction (Pavinatto *et al.*, 2009). As PAH and CHI are both polycationic amine based polymers, it would be expected that they would behave in a similar way and increase virus transduction as a result of their electrostatic interactions through the charged amine groups. In a study by Pavinatto *et al.*, a comparison between PAH and Chi was made on phospholipid membranes, in which chitosan was shown to decrease the elasticity of the membrane whereas PAH did not exhibit the same effect (Pavinatto *et al.*, 2009). This could therefore explain the observation that exposure of the Ad5 to the PAH polycation, did not cause the same augmentation in viral transduction that was present when the virus was exposed to the chitosan solutions.

The (chi-ha)₈chi PEM was therefore taken forward for further *in vitro* testing from SS discs and the composition was optimised to get enhanced virus transduction. Whilst this PEM did show positive results as a surface for virus retention and delivery, it did not perform well in the *ex vivo* testing and therefore did not warrant *in vivo* testing. PEMs were chosen as a potential method for delivery of virus' from stent surfaces because they are suitable for delivery of biomacromolecules unlike more traditional methods for delivery of smaller drug molecules, which rely on mixing polymers with the drug molecule and then coating onto the stent surface; the drug molecules then diffuse out of the polymer over time providing localised temporal delivery (Saurer *et al.*, 2011). There are a few studies which have demonstrated virus incorporation and delivery from PEMs using various *in vitro* set ups (Dimitrova *et al.*, 2007, Yoo *et al.*, 2008); however despite in depth characterisation of the PEMs, translation of the PEMs as a material for delivery *ex vivo* and *in vivo* has not been reported. This could be due to a number of reasons, however in the context of PEMs on stent surfaces, the most likely explanation is that they are not stable enough as there are no covalent bonds formed between the PEM and the SS surface, therefore they could detach from the surface during the involved stenting procedure.

The following approach to create a surface for viral attachment to stent surfaces consequently involved devising a method in which the virus was bound to the surface by covalent interactions, thereby providing a robust link between the virus and the stent surface that would be able to withstand stent deployment procedures. SS has been used for medical implants since 1930, and is still widely used today (Niinomi, 2002). The reason for its suitability for this role is that it has structural strength needed for applications such as intravascular stents, but also it is inert and unreactive and does not react adversely with the body. It is also for this reason that surface modification of SS is extremely limited due to the inherent inert behaviour. Therefore other stent materials were considered as starting points to develop a covalent link between the stent surface and the virus.

Recently we have observed the emergence of bioresorbable stents onto the market, which are made from materials which biodegrade over time such as PLA; therefore the implanted stent is a transient scaffold unlike previous bare metal

and drug eluting stents. This ability to biodegrade is thought to reduce the risk of late stent thrombosis, neoatherosclerosis and local inflammation because there will be no residual stent/polymer left in the artery. It would also decrease the need for long-term dual-anti platelet therapy, thereby reducing side effects such as bleeding. They could also avoid problems associated with permanent scaffolds such as the blockage of side branches and is compatible with IVUS imaging (Serruys *et al.*, 2012, Bourantas *et al.*, 2012).

Although PLA itself does not contain reactive groups on its surface which could be used to covalently link the virus to the surface, there are several methods available which can generate reactive sites by wet chemistry methods; one way to introduce reactive groups on to the surface is by alkaline hydrolysis, generating hydroxyl and carboxyl groups which will then be able to react with other chemical species (Yang *et al.*, 2003). Another method is by direct aminolysis by reacting PLA with 1,6-hexanediamine this method generates amine groups on the surface of the PLA which can then be conjugated with other molecules such as caffeic acid (Chuysinuan *et al.*, 2012). Both these routes of hydrolysis and aminolysis were successful in generating reactive groups on the surface of PLA as demonstrated by %wt loss and using the ninhydrin assay for amines.

Instead of using the virus directly to bind to the surface, using small molecules such as benzaldehyde and Fmoc-lysine as a 'model virus' would enable a simple readout to see if the chemistry modification of the PLA surface was successful. Benzaldehyde was used initially as this can readily form imines with primary amine groups, and can be removed using HCl. Benzaldehyde is also UV active, thus detection of benzaldehyde is straightforward, however due to the reversible nature of the imine bond formation, and the necessity of the dH₂O washing steps, detection of benzaldehyde was not observed.

Fmoc-lysine was then chosen as a compound to react with the derivatised PLA surface. Fmoc-lysine, provided a more relevant model as a virus, because the lysine moiety on adenovirus particles would have the same reactivity as the Fmoc lysine group through the primary amine group. In order to react the carboxyl groups on the PLA surface with the amine group from Fmoc-lysine, EDC/NHS activation was employed. Fmoc-lysine has a protecting group on the

amine group that would usually react with carboxylic acid groups of adjacent amino acids to form peptide chains, it was envisaged therefore that after reacting Fmoc-lysine with the PLA surface, the Fmoc protecting group could then be deprotected with piperidine, releasing fluorenyl-piperidine, which could be detected by ESI-MS, as well as UV-vis spectroscopy. This proved to be successful; however using this methodology Fmoc-lysine did not reliably bind to the surface. In order to progress to a workable virus covalently bound stent surface, whereby the virus could elute off, further investigation and development of the polymer would be needed in order to introduce a labile site to enable the virus to detach and enter the surrounding cells. Different approaches were therefore investigated which would provide an intermediate between the robustness and permanency of covalent bonding and the instability of the PEMs for this application.

The next approach that was investigated involved mixing the virus with collagen and then setting onto SS and PLA surfaces. Using collagen as a method for adenovirus attachment had previously been documented by Levy and co-workers, however they also employed anti-adenoviral monoclonal antibodies which were covalently bound to the collagen surface; this provided a surface upon which the adenovirus could be selectively tethered. This method proved successful *in vivo*, with a transduction efficiency of 5.9% of porcine arterial smooth muscle cells (Klugherz *et al.*, 2002a). In the present study a comparison of SS and PLA surfaces for deposition of the collagen virus gel and subsequent transduction of A10 cells, revealed that twice the amount of transduction was monitored from the collagen virus gel on the PLA surface than the SS surface. This differed in the approach as documented by Levy and co-workers as the virus was encapsulated within the collagen gel and antibodies were not used to aid tethering, allowing for a more simplified method of attachment (Klugherz *et al.*, 2002a). To confirm that this was due to more virus retained on the PLA surface, qRT-PCR was used to quantify how much virus was washed off the surface prior to incubation of the surfaces with A10 cells. This confirmed that more virus was washed off from the SS surfaces compared to the PLA surface, indicating that PLA was the optimal material for further development of the collagen encapsulation technique. Further *in vitro* testing revealed that higher concentrations of PLA deposited onto SS surfaces exhibited higher transduction

levels of the adenovirus, in line with observation that PLA was an effective material for collagen deposition.

Moving from *in vitro* to *ex vivo* models, the concentration for adenoviral transduction was found to be much higher in order to observe mouse aorta transduction of Ad5 than it was for the rat A10 cells, this could be due to the endothelial cells presenting a barrier for Ad5 transduction. After determining the concentration for viral transduction, a collagen-virus gel was incubated on PLA squares and placed onto mouse aortas, after 72 h transduction of the Ad5 CMV lacZ was observed through expression of the reporter gene. This was also tested on porcine coronary arteries and expression of the virus was observed using this model as well.

Progressing from virus delivery from PLA squares to stent surfaces, a method needed to be developed that would enable coating of the BMS with PLA. This was done by dissolving PLA in different wt/wt ratios of chloroform and the spreading a thin layer over the stent surface. Smoothing of the surface was then done by solvent vapour evaporation of CH₂Cl₂. When testing the stents to see whether the PLA coating had affected their ability for stent balloon expansion, we observed that at the highest %PLA (10% wt/wt), the stent was not able to fully expand due to the PLA coating, however at the lower PLA concentrations of PLA (5 and 2.5% wt/wt), inflation of the stent was possible, however, when coating the stent in the collagen-virus gel we only observed transduction at the highest PLA concentration, therefore prohibiting further *in vivo* testing, due to incomplete stent expansion.

Taken together these data demonstrate the potentials and pitfalls of different methods for coating adenovirus onto stent surfaces. Using a pure biodegradable PLA stent and coating with collagen virus gel could provide the answer to the logistical problems faced with the coating BMS with PLA manually. However, currently PLA commercial stents are not available without antithrombotic drugs already coated on them, so obtaining a pure PLA stent would be optimal for future development of the collagen/virus delivery system.

4 Development of methods for coating miRNA onto stent materials and stent surfaces

4.1 Introduction

In stent restenosis (ISR) is defined as >75% narrowing of the cross-sectional luminal stented area by neointimal tissue (Chaabane *et al.*, 2013), it occurs as a healing response to the injury of the vessel caused by the process of stent implantation during percutaneous coronary intervention (PCI). Stenting can damage the vessel in a number of ways (as described in section 2); de-endothelialisation, whereby the endothelium can be denuded, crushed or torn as a result of stent implantation which can trigger a wound healing cascade (Costa and Simon, 2005, Sanborn *et al.*, 1983). In addition to this, the process by which the stent is deployed, by inflating a balloon, exerts a considerable amount of mechanical pressure on the VSMCs. Furthermore, potential for the VSMCs to come into contact directly with the blood flow can also expose them to shear stress. The mechanical trauma endured by the VSMCs has been attributed as a key factor governing neointima formation as it modulates a phenotypic switch for the VSMCs from contractile to the synthetic state, this ultimately promotes the migration from the media to the intima (Clowes *et al.*, 1989).

The cellular cascade caused by damage to both ECs and VSMCs induces platelet aggregation, thrombus formation as well as inflammatory reactions at the site of injury (Welt and Rogers, 2002). Both platelets and macrophages play a leading role by the secretion of cytokines and growth factors which trigger phenotypic switching of VSMCs and secretion of extracellular matrix which ultimately forms the scaffold for the neointima to form (McDonald *et al.*, 2012). As VSMCs proliferate and migrate into the intima, the lumen will continue to narrow until a new layer of endothelial cells has re-established itself on the inner arterial surface (Douglas *et al.*, 2013).

MiRNAs are an endogenous class of small non-coding RNA molecules (approx. 22 nucleotides), which can regulate genes and proteins, operating primarily through promoting the degradation or suppression of the translation of mRNA molecules. Using miRNAs as a therapeutic to help suppress neointima formation and restore vessel homeostasis induced by stent implantation was at the time this work was carried out an unexplored area of research. However, the first paper detailing a therapeutic miRNA eluting stent was published in July of this year, highlighting

the potential for miRNA based therapy for ISR prevention, which successfully delivered antimiR-21 (Wang *et al.*, 2015).

Several miRNAs and miRNA clusters have been identified as therapeutic targets in the vasculature setting. miR-145 is the most abundant miRNA present in vascular walls, and has been identified as a marker and a modulator for neointimal formation (Ji *et al.*, 2007a, Cheng *et al.*, 2009a). It was observed that miR-145 levels changed upon differentiation of the VSMC phenotype, with high levels of miR-145 characteristic of the contractile phenotype. Upon stimulation of PDGF, miR-145 levels dropped in conjunction with the phenotype switching to the synthetic state. It was found that inhibition of miR-145 had the effect of suppressing the action of PDGF, maintaining the VSMCs in their contractile phenotype, this suggested that miR-145 had a regulatory effect on SMC phenotype. Further investigation identified Krüppel-like factor 5 (KLF5) as a target gene for miR-145, which could explain these miR-145 mediated effects on VSMC phenotype modulation (Cheng *et al.*, 2009a).

miR-145 is just one example of the many different miRNA gene regulator targets which could be used to prevent neointimal growth following stent implantation. Other examples include miR-21, miR-143 and miR-221, which are discussed in detail in section 1.6.2 However, delivery of these novel therapeutics remains a barrier, particularly in the *in vivo* setting.

Drug eluting stents (DES) have evolved from BMS, as it was realised that as well as fulfilling the structural role of re-widening the artery, they could also be coated in anti-proliferative drugs and therefore act as a delivery medium to the stented region. It is in this context that we wish to develop a delivery system for the miRNAs that would be able to coat a BMS surface to achieve this localised delivery to the target region.

miR-39-3p was chosen as the miRNA mimic to deliver from stent materials *in vitro*, because it originates from a nematode, *caenorhabditis elegans* (*c.elegans*) and, therefore, background levels of this miRNA are not present in mammalian cells. It was thought that detection of the miR-39-3p would therefore be facile, and probing different materials for their suitability for miRNA delivery would be easy to interpret.

4.1.1 Aims

The aims of this chapter were:

- To develop a delivery platform for miRNA from stent materials *in vitro* using *c.elegans* as a model miRNA that would be suitable for *in vivo* setting.
- To extend the delivery platform capabilities to test for delivery of therapeutic target miRNAs for the prevention of ISR *in vitro*.
- To examine therapeutic target miRNAs effects on proliferation and target gene regulation.

4.2 Results

4.2.1 Transfection of miRNAs *in vitro*

Initially, A10 cells were transfected at three different concentrations of miR-39-3p, (3 nM, 30 nM and 300 nM), this range of concentrations of the miR-39-3p was chosen because the manufacturers' protocol suggested that the miRNA mimics could be detected as low as 1 nM but often required higher levels of miRNA in the region of 50 nM. miRNA mimics are small chemically modified double stranded miRNA molecules which mimic the function of endogenous miRNAs. Transfection was carried out as described using the guidelines provided by the manufacturer.

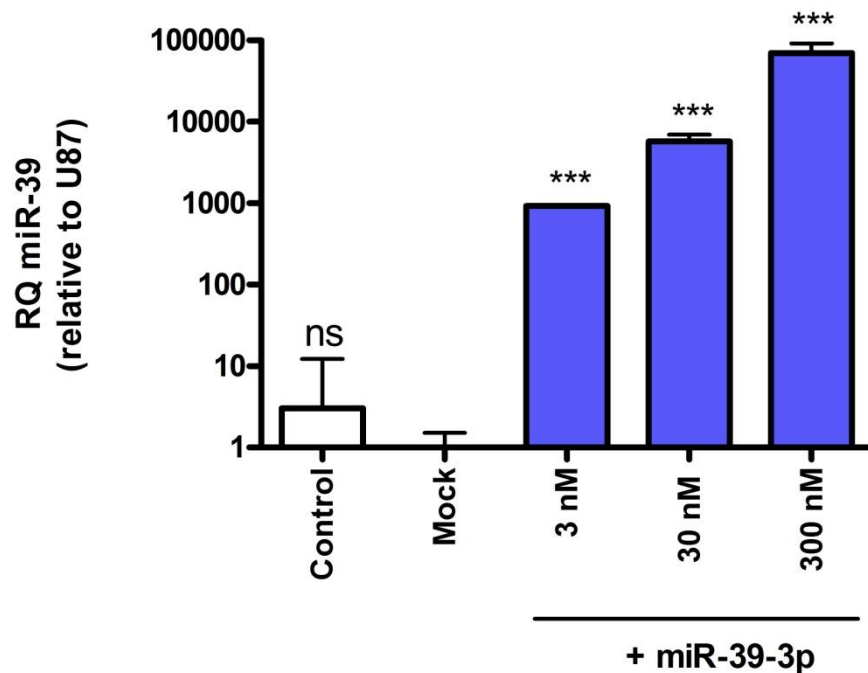


Figure 4-1 miR-39-3p expression in A10 cells transfected with miR-39-3p mimic.

A10 cells were plated in a 12 well plate at a seeding density of 100,000 cells/well. miR-39-3p (3 nM, 30 nM & 300 nM) was incubated with transfection reagent siPORT Neo FX™ (3 µL) for 10 mins prior to being applied to the cells. The cells were left for 48 h before being washed with PBS, harvested, RNA extracted, quantification was done using qRT-PCR and was normalised to U87 housekeeper gene expression. Data is expressed as RQ values ± RQ max. Data was analysed by performing a one way ANOVA and post-hoc Tukey test relative to the mock control, ***p<0.001. Representative graph of three independent experiments with three biological replicates per condition.

These results indicate that for all the concentrations tested we can reliably detect miR-39-3p expression following the transfection protocol for A10 cells. For each concentration, we could detect miR-39-3p expression and found a

direct correlation between the level of expression of the miR-39-3p observed and the amount applied to the cells, i.e., for a 10 fold increase in concentration we observed a corresponding 10 fold increase in miR-39-3p expression. As the overall aim was to eventually use endogenous therapeutic miRNAs, 30 nM was chosen as a suitable benchmark concentration to use for further testing, based on information given in the manufacturers' protocol and current miRNA literature and the data shown in Figure 4-1 (Cheng *et al.*, 2009a).

Using PLA and SS as model stent materials, we tested the ability for miR-39-3p to be delivered to A10 cells *in vitro*, following application to the surfaces. Thorough washing steps with PBS (3 x 1 mL), which was pipetted directly onto the surfaces, were included in order to mimic the environment that the coating would have to withstand when deploying through the femoral artery, as exposure to the blood flow would inevitably wash off some of the miRNA and cause systemic delivery.

Following the success which collagen had demonstrated for Ad delivery (Chapter 3), collagen entrapment of miRNA was tested for both surfaces. In order to achieve transfection of the miRNA mimic into cells, it was necessary to incubate the miRNA with a transfection reagent siPORT Neo FX™, which is a lipid based formulation that complexes to the miRNA mimic, enabling transfection of the cells.

It was hypothesised that application of the siPORT-mimic complex to the PLA surface could provide a good platform for delivery as the PLA is lipophilic, the lipid based siPORT-mimic complex could therefore adhere to the PLA surface through hydrophobic interactions; providing an environment for efficient adsorption, and delivery. This concept has been demonstrated before by loading PLA with lipophilic drug molecules (Fan *et al.*, 2013).

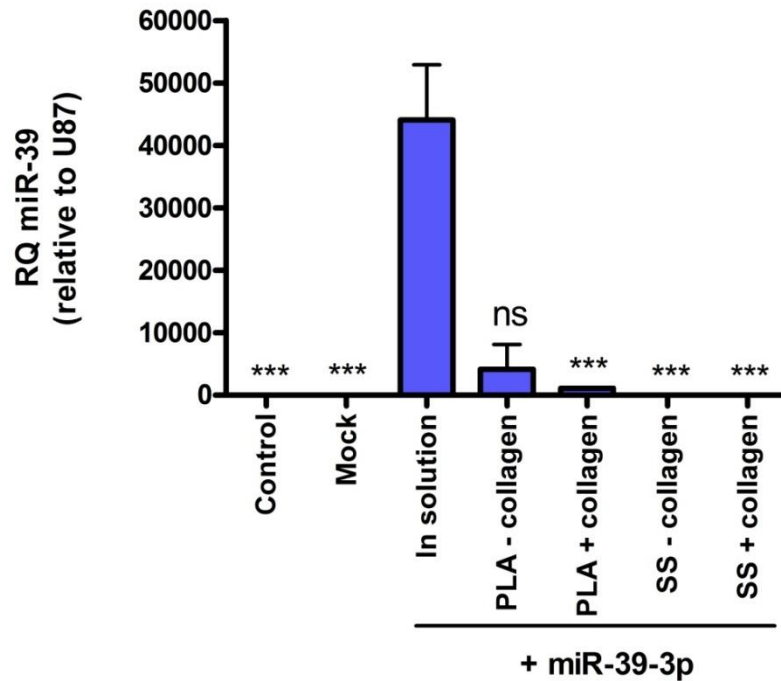


Figure 4-2 miR-39-3p expression in A10 cells transfected with miR-39-3p mimic coated onto PLA and SS surfaces \pm collagen.

A10 cells were plated in a 12 well plate at a seeding density of 100,000 cells/well. miR-39-3p (30 nM) was incubated with transfection reagent siPORT Neo FX™ (3 μ L) for 10 mins and then applied directly onto PLA, SS or directly onto cells. For the collagen coated PLA and SS the miRNA-siPORT complex was mixed with collagen prior to being set onto the PLA surface. Final concentrations of miR-39-3p were 30 nM. All surfaces were washed prior to being placed onto the cells. The cells were left for 48 h before being washed with PBS, harvested, RNA extracted, quantification was done using qRT-PCR and was normalised to U87 housekeeper gene expression. Data is expressed as RQ values \pm RQ max. Data was analysed by performing a one way ANOVA and post-hoc Tukey test relative to the in solution control, *** p <0.001, ns=non-significant. Representative graph of three independent experiments with three biological replicates per condition.

We observed that using the PLA as a surface for delivery of the miRNA-siPORT complex, we can detect expression of the miR-39-3p in the cells, indicating that PLA could be used as a material for miRNA delivery. A comparison of the in solution control to the PLA- collagen shows approximately 10 fold decrease in miR-39-3p expression, this could be due to loss of the miRNA during the washing steps, or the miRNA may be retained within the polymer, a temporal release study would need to be conducted to clarify this. A 4 fold increase in expression of miR-39-3p from the PLA surface compared to the PLA-collagen surface, therefore indicating that unlike the adenovirus, miRNA is retained better on the PLA surface without collagen. Comparison of the SS as a material for miRNA delivery did not show any miR-39-3p expression, indicating that it would not be suitable as a material for this purpose.

Since the overall objective is to deliver therapeutic miRNAs this delivery system from PLA was tested with potential therapeutic miRNAs for prevention of ISR. In order to investigate the role of different miRNAs role within the ISR pathway, it would be useful to upregulate and downregulate a miRNA delivered from stents, to do this miR mimics and miR inhibitors can be used. miR 145 was chosen as the model miRNA to deliver, in both mimic and inhibitor forms. This miRNA was chosen because overexpression of miR-145 has been shown to inhibit proliferation of VSMCs. Conversely, deficiency of miR-145 has been shown to promote the synthetic phenotype of VSMCs which promotes increased VSMC migration (Cordes *et al.*, 2009a, Cheng *et al.*, 2009a, Marx *et al.*, 2011). Both of these systems have been shown *in vitro* using transgenic mice. In our group we have also demonstrated this relationship *in vivo* using a murine stenting model on 145^{-/-} mice which showed a significant reduction in neointima formation when stenting was done on the 145^{-/-} mice, which is contradictory to what would be intuitive following the *in vitro* studies (Robinson, Baker, unpublished). Therefore it would be interesting to further probe the relationship miR-145 has with neointima formation by locally delivering miR-145 and the inhibitor from stent surfaces.

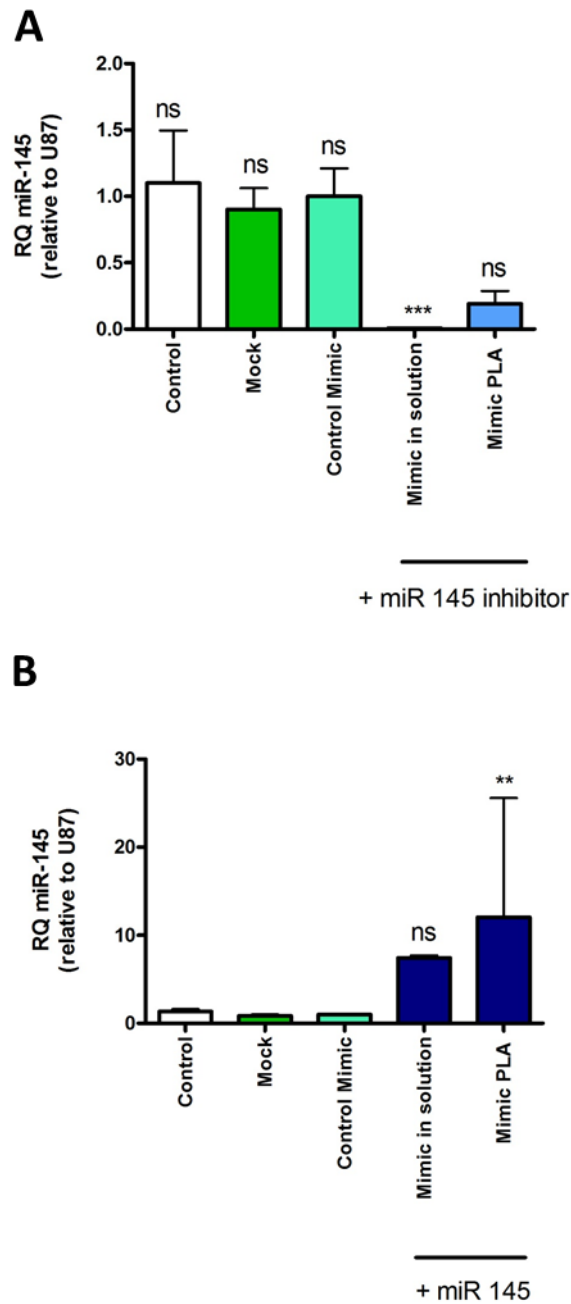


Figure 4-3 miR-145-5p expression in A10 cells transfected with miR-145-5p mimic and miR-145-5p inhibitor coated onto PLA surfaces.

A10 cells were plated in a 12 well plate at a seeding density of 100,000 cells/well. miR-145-5p mimic or inhibitor was incubated with transfection reagent siPORT Neo FX™3 μ L for 10 mins and then applied directly onto PLA or directly onto the cells. Final concentrations of miR-145-5p mimic and inhibitor were 30 nM. All surfaces were washed prior to be being place onto the cells. The cells were left for 48h before being washed with PBS, harvested, RNA extracted, quantification was done using qRT-PCR and was normalised to U87 housekeeper gene expression. Data expressed as RQ values \pm RQ max. Data was analysed by performing a One way ANOVA and post-hoc Tukey test relative to the mock control, *** $p < 0.001$, ** $p < 0.05$, ns=non-significant. Representative graph of three independent experiments with three biological replicates per condition.

Testing of PLA as a candidate delivery material for the siPORT-miRNA (miR-145-5p and miR-145-5p inhibitor) precursor complex was conducted, using the same experimental set up as described for the miR-39-3p (Figure 4-2). It was

observed, that upregulation and downregulation of miR-145-5p could be achieved from the PLA surface when administering the miR-145-5p and miR-145-5p inhibitor respectively (Figure 4-3). A 12 fold increase in miR-145 expression compared to control scramble mimic when using the miR-145 mimic, and a 5 fold decrease in miR-145 expression when delivering the miR-145 inhibitor from the PLA surface was observed.

As detailed in chapter 3, when developing adenovirus eluting stent methodology, moving from *in vitro* delivery on flat discs to *ex vivo* delivery from stent surfaces exposed several logistical problems. Therefore, testing in the *ex vivo* setting was a priority. A preliminary *ex vivo* test was carried out, whereby, mouse aorta were transfected with miR-39-3p, in solution and from the PLA surfaces (Figure 4-4).

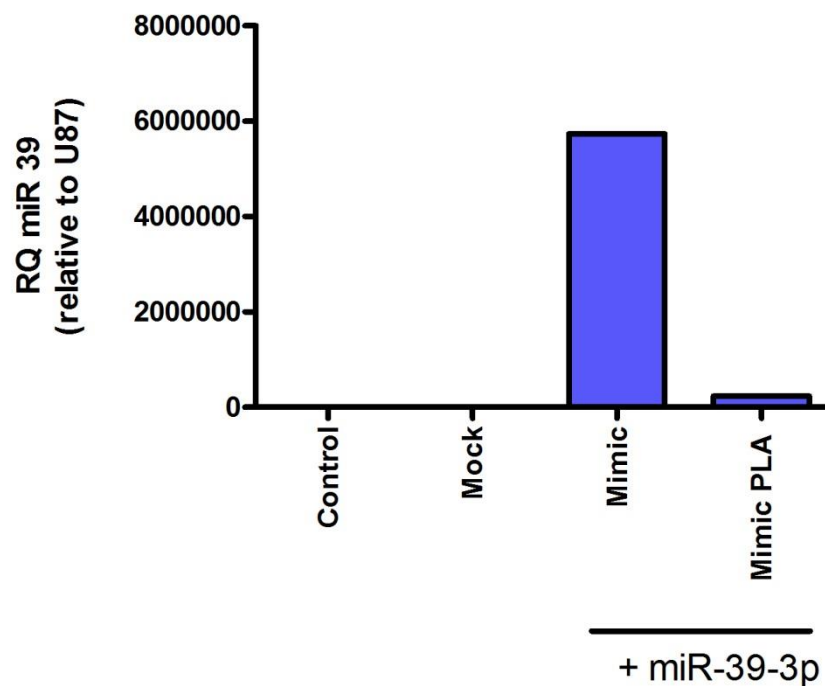


Figure 4-4 *Ex vivo* delivery of miR-39-3p from PLA squares to mice aorta.

Mouse aorta were harvested and placed in 12 well culture dishes. PLA was coated with miR-39-3p-siPORT mix, washed thoroughly with PBS and then placed onto the aortas, or the miR-39-3p was applied directly to the aorta at 30 nM. Aortas were incubated in medium for 48 h then the aortas were homogenised and RNA was extracted from them. Quantification of the miR-39-3p was done by qRT-PCR and normalised to U87 housekeeper gene. Data expressed as RQ values. Preliminary experiment with one condition per aorta.

Delivery of miR-39-3p from PLA surface *ex vivo* to mouse aorta was achieved and detected at high levels as it is a non-endogenous miRNA to mice. Using this non-

endogenous miRNA mimic for delivery provides a good platform to evaluate the delivery system and performance for *in vivo* set-ups.

Murine stents were coated in PLA using the optimised procedure as developed for the adenovirus delivery system, 10% and 15% wt/wt PLA dissolved in chloroform was used to coat the stents, which were then coated with siPORT-miR-39-3p, washed and deployed into the mice aorta *ex vivo*.

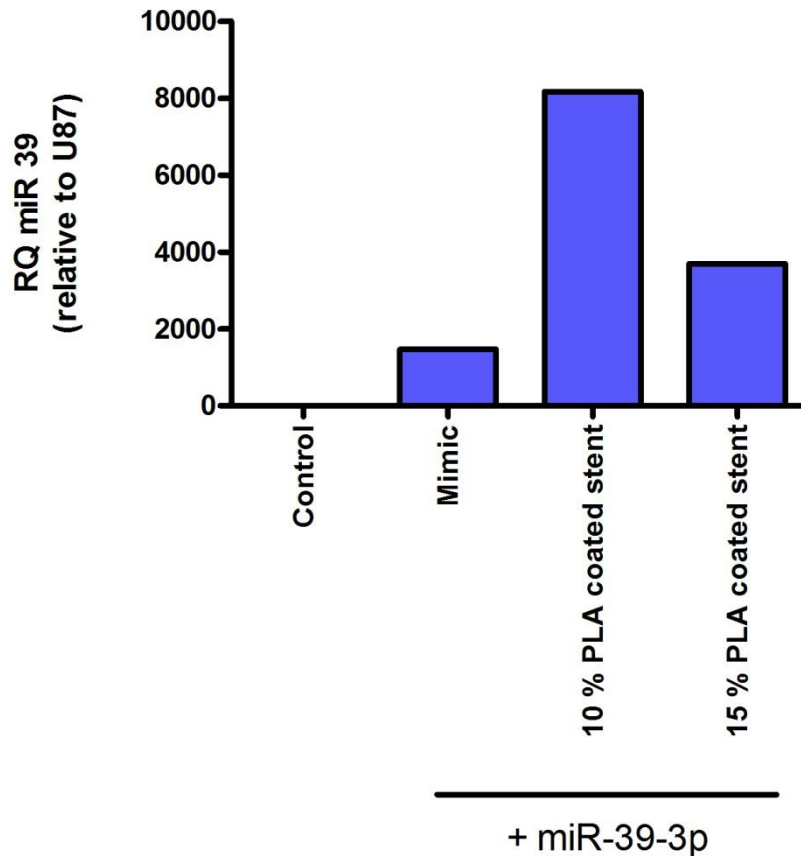


Figure 4-5 *Ex vivo* delivery of miR-39-3p from PLA coated stents to mouse aorta at different PLA concentrations.

Mouse aorta were harvested and placed in 12 well culture dishes. PLA was coated onto murine stents at concentrations 10% and 15% wt/wt PLA dissolved in chloroform with miR-39-3p-siPORT mix, washed thoroughly with PBS and then placed onto the aortas, or the miR-39-3p was applied directly to the aorta at 30 nM. Aortas were incubated in medium for 48 h then the aortas were homogenised and RNA was extracted from them. Quantification of the miR-39-3p was done by qRT-PCR and normalised to U87 housekeeper gene. Data expressed as RQ values. Preliminary experiment with one condition per aorta.

Using the PLA coated stents to deliver the miR-39-3p, we observed higher levels from the PLA coated stents than from the mimic in solution (2 fold increase for 15% PLA coated stent and 4 fold increase for the 10% PLA coated stent), this could be attributed to the direct contact between the stent surface and the mouse aorta and the fact that the stent is locked in place. This therefore

indicates that the localised delivery would be possible using this delivery system. Comparing the two concentrations of PLA, it was observed that 10% w/v PLA in chloroform yields a two fold increase in miR-39-3p expression compared to 15% wt/wt, therefore further testing was carried out using this concentration of PLA for the coating.

Using the preliminary data from the *ex vivo* testing as a reference detailed in Figure 4-4 and Figure 4-5, *ex vivo* testing was now carried out using the optimised PLA concentration of 10% w/v on a bigger scale, with three aortas per condition.

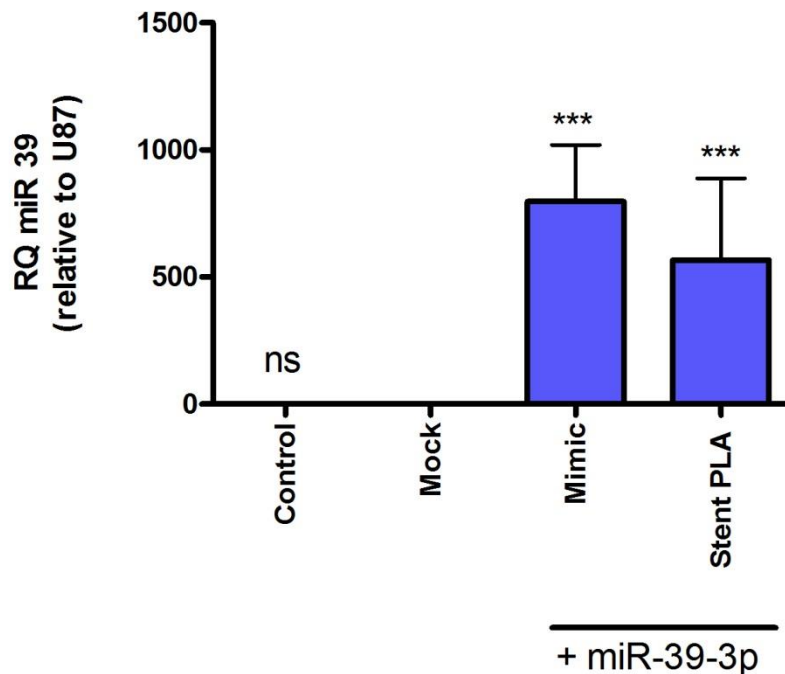


Figure 4-6 *Ex vivo* delivery of miR-39-3p from PLA coated stents to mouse aorta.

Mouse aortas were harvested and placed in 12 well culture dishes. PLA was coated onto murine stents at concentrations 10% wt/wt PLA dissolved in chloroform with miR-39-3p-siPORT mix, washed thoroughly with PBS and then placed onto the aortas, or the miR-39-3p was applied directly to the aorta at 30 nM. Aortas were incubated in medium for 48 h then the aortas were homogenised and RNA was extracted from them. Quantification of the miR-39-3p was done by qRT-PCR and normalised to U87 housekeeper gene. Data is expressed as RQ values \pm RQ max. Data was analysed by performing a One way ANOVA and post-hoc Tukey test relative to the mock control, *** $p < 0.001$, ns=non-significant. Three aortas were treated per condition.

The results from this *ex vivo* study indicate that by using this delivery method we can detect miR-39-3p after 48 h in medium. Using the PLA at this concentration did not cause logistical problems and the stents were all able to fit into the aortas of the mice and be fully expanded. This, therefore, represents a good platform for testing *in vivo* stent models to find out whether the miRNA

coating is able to withstand the procedure of deployment, which is tested in chapter 5.

4.2.2 Using miRNAs to inhibit SMC proliferation as a potential therapeutic for prevention of ISR

As discussed in depth in section 1.3, ISR is caused by the proliferation and migration of SMC in response to the injury caused by stent implantation. A strategy for preventing ISR, therefore, would be to inhibit SMC proliferation, which could be achieved by treatment of the vessel with therapeutic miRNAs. To investigate the biological effects of treating VSMCs with miRNAs on cell proliferation, an EdU (5-ethynyl-2'-deoxyuridine) assay was performed. EdU is a thymidine analogue and therefore incorporates into the DNA during DNA synthesis (Salic and Mitchison, 2008). Detection of the EdU is performed by a reaction of the ethynyl group with an Alexa Fluor® tagged azide through a click reaction (3 + 2 cycloaddition) (Breinbauer and Köhn, 2003, Wang *et al.*, 2003). After labelling the cells, they can then be fixed and analysed using flow cytometry.

The function of miR cluster 99b/let 7e/125a, has been unexplored in the context of the cardiovascular system and for the purposes of inhibiting ISR, it therefore represents a novel potential therapeutic. Other work in the group identified this miRNA cluster as a suitable candidate for this purpose as it was downregulated in a pig vein graft experiment. The cluster has also been associated with suppression of tumour angiogenesis of ovarian cancer cells when over expressed (He *et al.*, 2013). Therefore the miR cluster 99b/let7e/125a was administered to HVSMC *in vitro*, to observe the effect it had on SMC proliferation using the EdU assay as described above.

HVSMC were treated with the miR cluster 99b/let 7e/125a at a concentration of 3 nM. A lentiviral vector expressing the the miR cluster was also administered at 20 MOI. The cells were maintained in 15% FCS MEM for 24 h and then serum starved for 24 h prior to addition and incorporation of the EdU into the newly synthesised DNA. Detection of the EdU was done by employing 'click chemistry' to react an Alexa Fluor™ tagged- azide. Cells were then analysed using FACS.

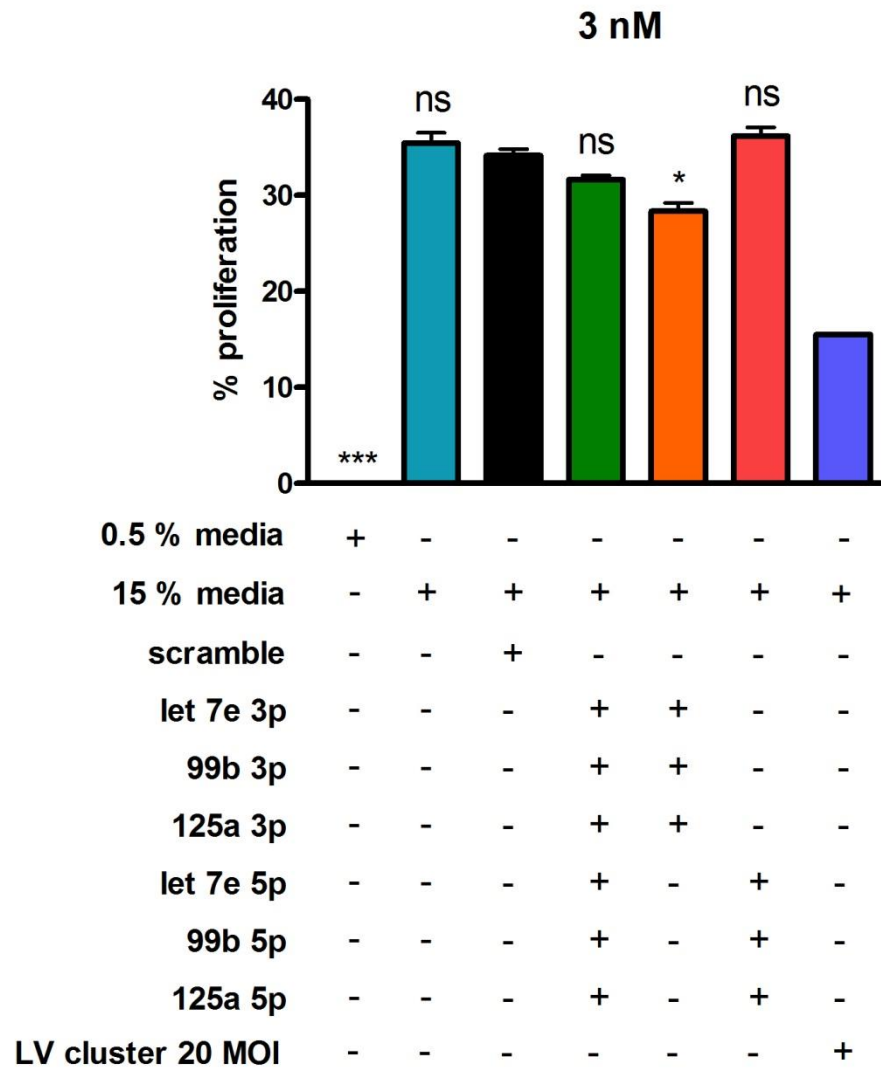


Figure 4-7 EdU Assay measuring the effect of miR cluster 99b/let7e/125a on HVSMC proliferation.

HVSMC were plated in a 12 well plate at a density of 3.5×10^4 cells/well. The cells were transfected with miR cluster 99b/let7e/125a at concentration of 3 nM, using siPORT™ Neo FX™ as a transfection reagent (3 μ L). The cells were treated with both the 3p and the 5p strands, or the 3p and 5p strands separately. LV-miR 99b/let7e/125a was also applied to the cells at a concentration of 20 MOI. The cells were serum starved after 24 h, the EdU was applied on Day 4 and the cells were harvested at Day6. The EdU assay was then performed by labelling with Alexa-Fluor tagged azide® as described in manufacturers protocol. FACS analysis was done on the cells and data analysed using FlowJo software to obtain the %cells proliferating. Representative graph of three independent experiments with each condition having two biological replicates. Data was analysed using a one way ANOVA and post-hoc Tukey test relative to the scramble control (black), *** $p < 0.001$, * $p < 0.05$, ns=non-significant.

Results from the EdU assay indicate a 5% decrease in the %of proliferating cells when treated with the 3p strands of the miR 99b/let 7e/125a cluster, however we did not observe a significant decrease in proliferation for any of the other treatment groups. When treated with the LV-cluster however, a 50% decrease in proliferation was observed, therefore indicating that using the LV to aid delivery and transfection of the miRNA may result in a bigger biological effect for this

purpose. Quantification of the miRNA was also done by RNA extraction and qRT-PCR to confirm that the miRNA was effectively being upregulated.

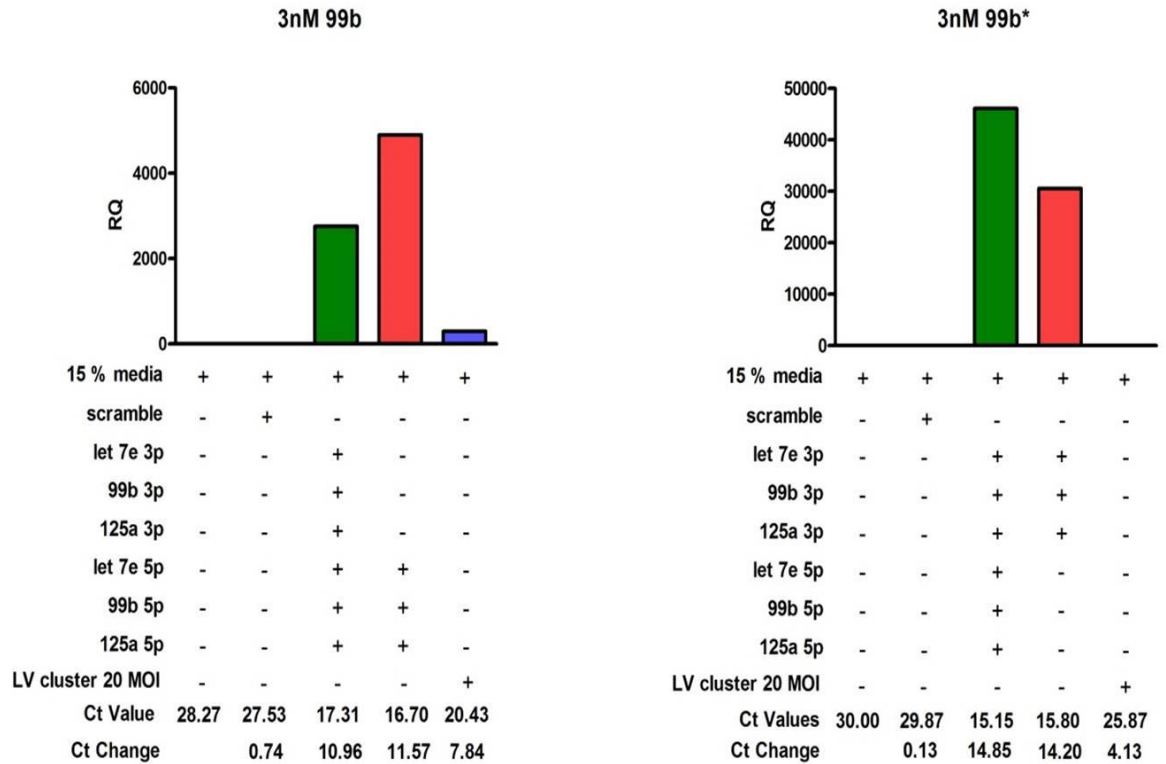


Figure 4-8 Relative expression of miR-99b-3p and 5p strands of HVSMC after 48 h treatment with the miRNA at 3 nM.

RNA was extracted and quantified by qRT-PCR. Data is expressed as RQ relative to expression of housekeeper gene RNU48b. One biological replicate per condition.

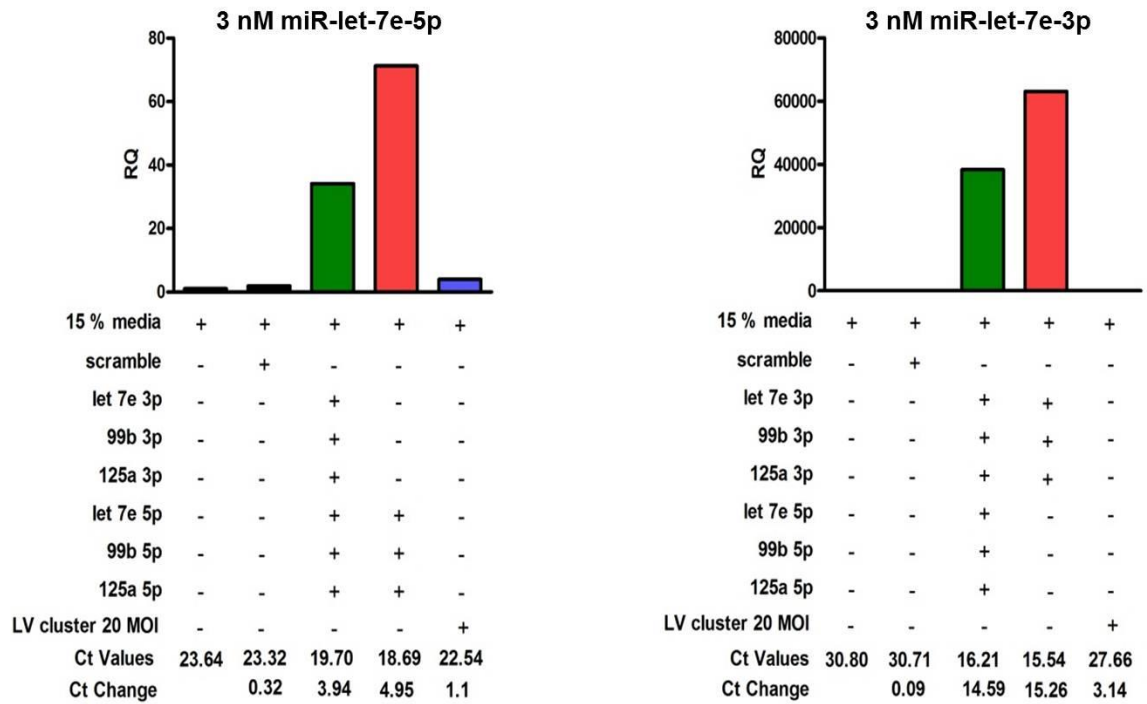


Figure 4-9 Relative expression of miR-let7e-3p and 5p strands of HVSMC after 48 h treatment with the miRNA at 3 nM.

RNA was extracted and quantified by qRT-PCR. Data is expressed as RQ relative to expression of housekeeper gene RNU48b. One biological replicate per condition.

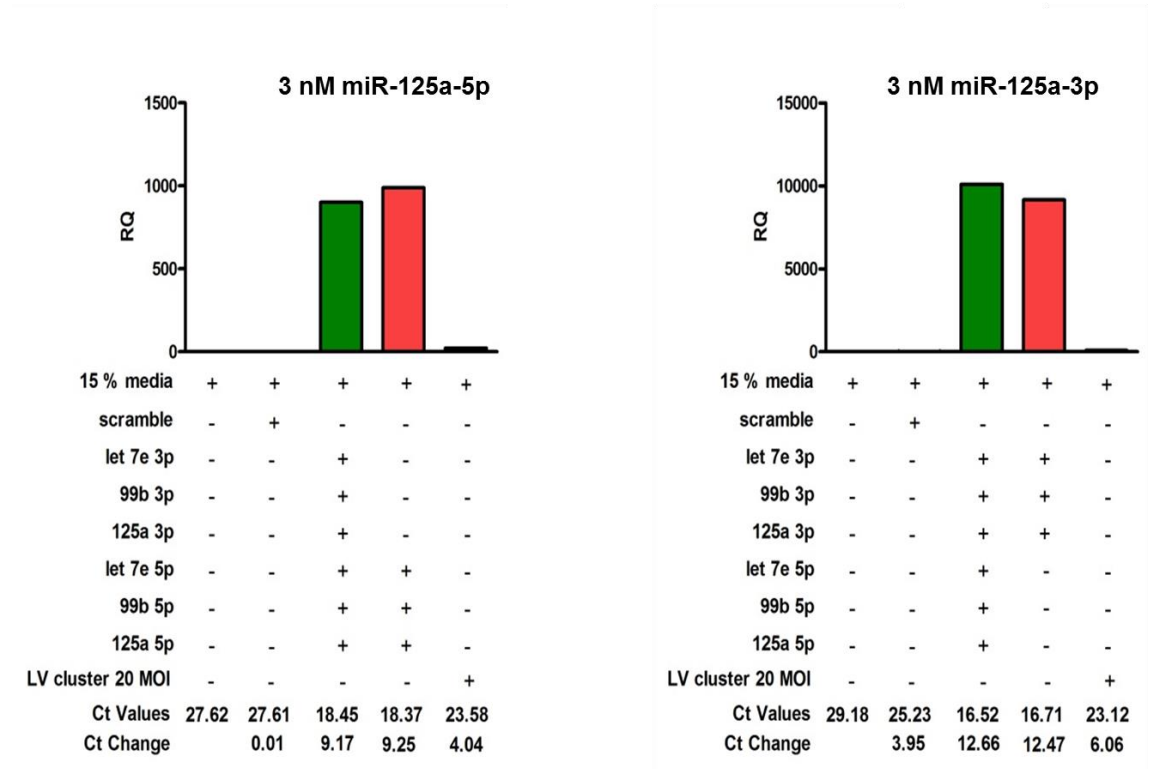


Figure 4-10 Relative expression of miR-125a-3p and 5p strands of HVSMC after 48 h treatment with the miRNA at 3 nM.

RNA was extracted and quantified by qRT-PCR. Data is expressed as RQ relative to expression of housekeeper gene RNU48b. One biological replicate per condition.

From the expression profiles of the miRNAs it can be seen that the miRNAs were overexpressed for both the LV and miR mimic delivery of the cluster (Figure 4-8, Figure 4-9 & Figure 4-10). It is interesting to note that the LV expression of the miRNAs is much less than when treated with the cluster mimics.

4.3 Discussion

In this chapter a method for delivery of miRNA mimics has been developed that is able to deliver miRNA *in vitro* to rat SMC from PLA surfaces, through to delivery from murine stent surfaces *ex vivo*. This method therefore holds much promise for miRNA delivery from stent surfaces in an *in vivo* setting. However, different factors will be present that are not present within the *ex vivo* model, such as blood flow and the logistics of intravascular stent deployment (advancing the stent through the arteries), both of which could result in the miRNA coating becoming detached from the surface prior to deployment. This was compensated for to an extent in the *in vitro* and *ex vivo* model by including extensive washing steps prior to deployment; however exactly how this coating will respond to the demands of an *in vivo* environment will be interesting to find out.

These results agree with the findings detailed in Chapter 3, with respect to PLA performing the best as a material for adherence and delivery of the therapeutic, for miRNA and adenovirus when compared to SS. Collagen encapsulation, which was found to be a useful technique for delivering virus, was not found to be beneficial in the miRNA delivery setting. Instead it was found that the miRNA mimic-siPORT™ complex could be applied directly onto the PLA surface and dried; this coating was able to withstand significant washing steps with PBS, indicating that it might be suitable for *in vivo* applications. Use of transfection reagent siPORT™ Neo FX™, which is a lipid based polyamine was likely to have aided the adherence to the PLA surface, which is hydrophobic in nature, with a contact angle of 80° (Rasal *et al.*, 2010). PLA has been approved by the FDA for use with direct contact with biological fluids and is currently being used as a biodegradable stent material in the clinics, the Abbott Absorb Stent is an example of a commercially available PLA stent (Rasal *et al.*, 2010, Dörr *et al.*, 2014). Using the methodology described in this chapter for coating a BMS with PLA and subsequent miRNA coating steps, could be translatable in the clinical setting and represents a simple methodology for the preparation of miRNA eluting stents.

Non-endogenous miR-39-3p was coated onto stent materials and stent surfaces and tested for delivery *in vitro* with rat A10 cells and *ex vivo* using murine vessels, throughout this testing expression of the miR-39-3p was always

demonstrated, showing clear evidence to support this delivery system as suitable for miRNA mimics. Using miR-39-3p as the miR for delivery allowed for analysis and detection to be straightforward and worked well as a pilot model to show the concept worked.

Testing was also done *in vitro* using miR-145-5p mimic and inhibitor from PLA surfaces to A10 cells, to demonstrate that upregulation and downregulation of miRNAs of interest can be achieved using this system. In the case of miR-145; overexpression of this miRNA has been previously shown to inhibit VSMC proliferation, and therefore represents a potential therapeutic for prevention of ISR (Cordes *et al.*, 2009a). However, observations within our own research group, showed that 145^{-/-} mice exhibited significantly less neointima formation following murine stent deployment (Robinson, Baker, unpublished). The ability to induce overexpression and suppression of miR-145 from local stent delivery would allow further observations on the effect of miR-145 expression on neointima formation and provide more clarity to its exact role.

Another potential miRNA cluster was investigated, miR99b/let7e/125a, which has been previously shown to suppress tumour angiogenesis in ovarian cancer cells when overexpressed (He *et al.*, 2013). It was therefore hypothesised that this miRNA cluster could also be used to prevent ISR by preventing proliferation of VSMC. This was assessed using an EdU assay, which can be used to measure the %proliferating cells. It was found that, by delivering the cluster using a LV vector, a decrease in cell proliferation of 20% was observed. However, when delivering the miRNA as 3p & 5p strands a decrease in proliferation was not observed. Delivering the 3p strands alone, a decrease in proliferation by 7% could be achieved and therefore does show potential for a novel therapeutic for ISR, these findings are in agreement with previous work within our group (Garcia, Baker, unpublished). It is clear however, that the true biological function of this cluster of miRNAs is complex and further investigation is needed.

In order to progress to mouse *ex vivo* stenting, a method was developed for coating the mouse stents with PLA. This was achieved by dissolving the PLA in chloroform, and then coating a thin layer of PLA onto the stent surfaces. Optimisation for the concentration of PLA dissolved in chloroform was performed and it was found that 10% wt/wt worked sufficiently. A technique to achieve a

smooth surface was also needed to ensure that the stent surface was smooth. DCM vaporisation was used to ensure that the PLA was smoothed by dipping the coated stent into a vapour chamber for 5 seconds. Using this method for coating the mouse stent, transfection of miR-39-3p was delivered and detected after 48 h from PLA coated SS mouse stents. Further work, using this model system *in vivo* using the porcine and murine stenting models is detailed in Chapter 5.

The method for coating and delivering miRNA from biodegradable stent surfaces is the first of its kind. To date the only method for miRNA delivery from stent surfaces was published in July 2015, which included a specialised custom microporous stent for delivery of antimir-21 (Wang *et.al.*, 2015). The method presented here therefore represents a more simplified approach, which does not require specialised stents. The use of PLA to as a biodegradable polymer to adhere the miRNA to is novel, and could easily be applied in the context of biodegradable stents.

5 Local delivery of miRNA in murine and porcine *in vivo* stenting models

5.1 Introduction

In order to increase the complexity of the miRNA delivery environment, it was important to establish whether the miRNA eluting stents developed in Chapter 4 would be able to deliver miRNA mimics *in vivo* animal models. There are a number of different stenting models which could be used to this effect.

The murine stent model developed by Ali *et al.* involves stenting the aorta of a mouse, *ex vivo* using a custom-made mouse stent, with the stented section then being excised and grafted into another mouse *in vivo* (Ali *et al.*, 2007). Aside from the logistical advantages of using a mouse stenting model, the main advantage for testing miRNA eluting stents using this model is the scope to extend the methodology so that it can be used on transgenic mice. This would further probe miRNAs function in neointima formation and test the efficacy of miRNA eluting stents for prevention of ISR.

The pig stenting model is a more clinically relevant model, as human stents can be used because artery dimensions are similar between the two species and the stenting operation is the same as with the human stenting deployment procedure.

5.1.1 Aim

The aim of this chapter was:

- To evaluate whether the methodology for miRNA eluting stents could be used to deliver miRNA from stents in murine and porcine *in vivo* stenting models, through detection at 48 h after deployment.

5.2 Results

5.2.1 Transfection of miRNA in murine *in vivo* stenting model

Testing the methodology developed in Chapter 4, for localised delivery of miRNA from stent surfaces to stented arteries, was initially conducted using the murine *in vivo* stenting model. MF1 mice were stented with custom made murine stents, which had been coated with miRNA-39-3p, using the PLA coating methodology as described in Chapter 4. The stents were sterilised by soaking in sterilising solution for 10 minutes prior to coating with the miRNA. The mice were sacrificed at 48 h post deployment, the stented segments were excised for RNA extraction and quantification of the miRNA-39-3p expression was analysed using qRT-PCR (Figure 5-1). A time-point of 48 h was chosen in line with the manufacturer's protocol for miRNA transfection.

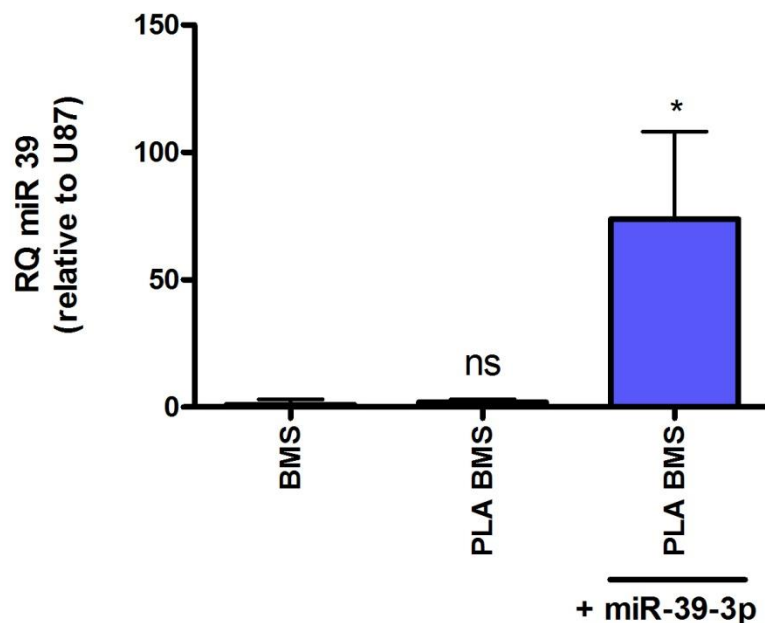


Figure 5-1 Local delivery of miR-39-3p from PLA coated stents to mouse aorta, 48 h after deployment using murine *in vivo* stenting model.

10% wt/wt PLA dissolved in chloroform was coated onto murine stents and dried overnight. miR-39-3p (20 μ M, 1.5 μ L) was added to siPORT (3 μ L) and then applied to the PLA coated stents. Stents were washed in PBS before deployment into the mouse aorta. Mice aortas were harvested at 48 h post deployment, and immediately stored at -80 $^{\circ}$ C. RNA was extracted from the aortas and miR-39-3p expression was quantified by Taqman[®]qRT-PCR. Data is expressed as RQ values \pm RQ max. Data was analysed by performing a One way ANOVA and post-hoc Tukey test relative to the BMS control, * p <0.05, ns=non-significant. n =5 stents/group for PLA BMS +miR-39-3p and n =3 stents/group BMS and BMS PLA control.

miR-39-3p expression was recorded at 48 h from the stented artery, after coating with PLA and the miRNA. This demonstrates that this methodology is

able to withstand deployment procedures and blood flow within the mouse model.

5.2.2 Transfection of miRNA in porcine *in vivo* stenting model

Testing for localised miRNA stent delivery using a larger animal model to allow for a more clinically relevant setting was conducted using the porcine stenting model. Human BMS were initially coated with PLA, followed by siPORT/miRNA and allowed to dry before deploying using the methodology developed in Chapter 4. After 48 h the pigs were sacrificed and the arteries harvested for RNA extraction, and quantification of the locally delivered miRNA was carried out using qRT-PCR.

It was important to identify a suitable housekeeper to allow meaningful comparisons to assess whether delivery of the miRNA had been successful. U6 and miR-103 were tested as potential candidates for the endogenous control on the pig samples, the standard deviation when miR-103 was used across the groups was 0.988735 whereas the standard deviation when U6 was used was 1.800209, therefore, miR-103 was used as a housekeeper for the study (Figure 5-2).

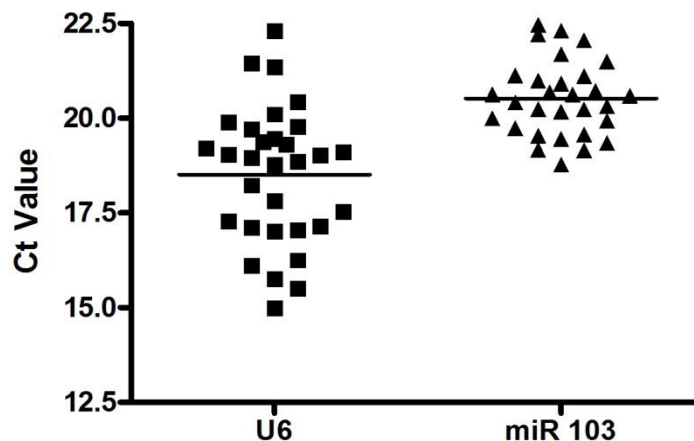


Figure 5-2 Comparison of U6 and miR 103 as endogenous controls for *in vivo* porcine stenting study.

Relative expression of miR-103 and U6 following RNA extraction and quantification by Taqman[®]qRT-PCR from porcine coronary arteries from *in vivo* stenting study. Data is expressed as Ct value, U6 n=31/group, miR-103 n=30/group.

Using the same methodology for coating the stents for the murine *in vivo* study, stents were deployed and harvested and after 48 h. Delivery of miR-39 was observed at this time point, so evaluation as to whether the delivery system worked was straightforward as the expression levels for miR-39 were ~7500 fold above the background levels from the control groups (Figure 5-3).

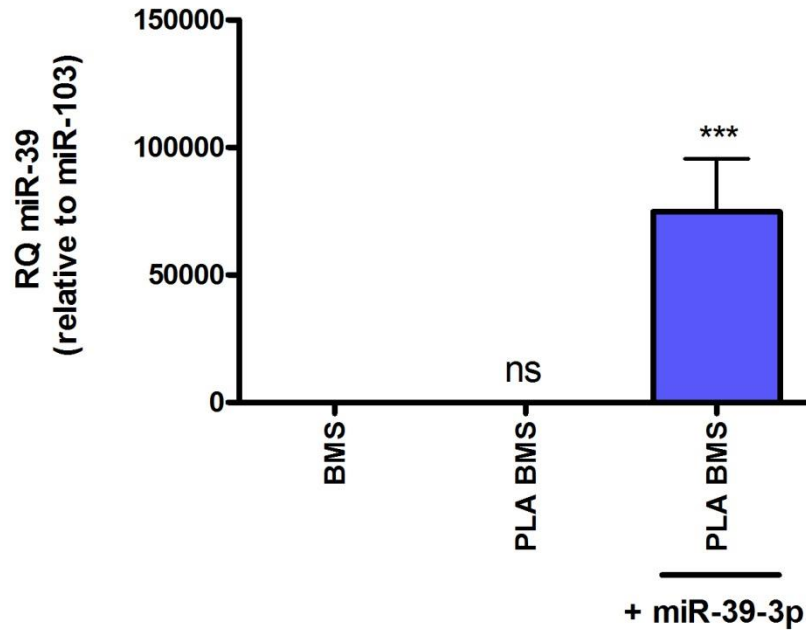


Figure 5-3 Local delivery of miR-39-3p from PLA coated stents to porcine coronary arteries, 48 h after deployment using porcine *in vivo* stenting model.

2.5% wt/wt PLA dissolved in chloroform was coated onto porcine stents and dried overnight. miR-39-3p (20 μ M, 4.5 μ L) was added to siPORT (9 μ L) was then applied to the PLA coated stents. Stents were washed in PBS before deployment into the porcine coronary arteries. Arteries were harvested at 48h post deployment, and immediately stored at -80°C. RNA was extracted from the arteries and miR-39-3p expression was quantified by Taqman[®]qRT-PCR and normalised to miR-103 expression. Data is expressed as RQ values \pm RQ max. Data was analysed by performing a One way ANOVA and post-hoc Tukey test relative to the BMS control, ***p<0.001, ns=non-significant, n=6/group.

Delivery of miRNAs that are relevant to the process of neointima hyperplasia, miR-145-5p and anti-miR-21, were attempted. However, expression of miR-145-5p was not upregulated enough to signify significance within the porcine *in vivo* setting, although the RQ value for PLA BMS miR-145-5p stent was doubled. This could have been due to the fact that miR-145-5p was highly expressed within the artery walls. Ct values for the control groups were, BMS 15.1 and PLA BMS 16.7, therefore saturation of the signal from the miRNA which was delivered from the stent could have occurred (Figure 5-4).

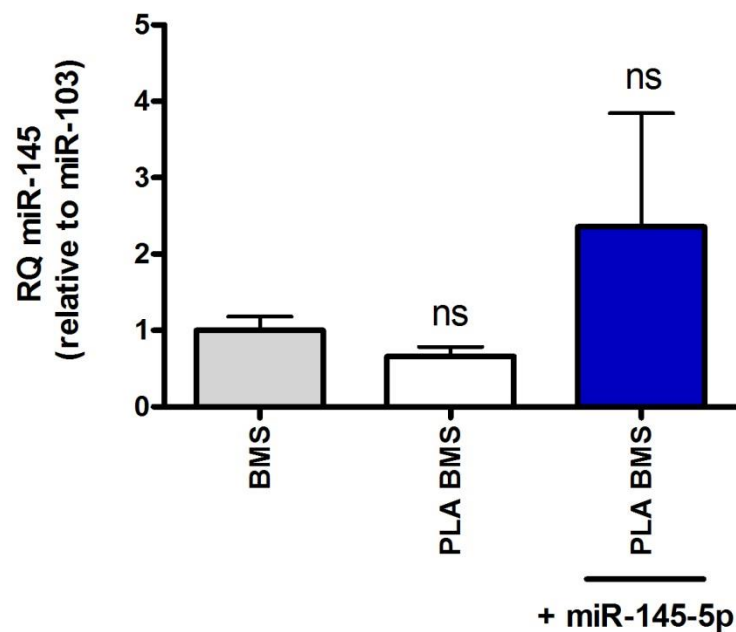


Figure 5-4 Local delivery of miR-145-5p from PLA coated stents to porcine coronary arteries, 48 h after deployment using porcine *in vivo* stenting model.

2.5% wt/wt PLA dissolved in chloroform was coated onto porcine stents and dried overnight. miR-145-5p (20 μ M, 4.5 μ L) was added to siPORT (9 μ L) was then applied to the PLA coated stents. Stents were washed in PBS before deployment into the porcine coronary arteries. Arteries were harvested at 48h post deployment, and immediately stored at -80°C. RNA was extracted from the arteries and miR-145-5p expression was quantified by Taqman[®]qRT-PCR and normalised to miR-103 expression. Data is expressed as RQ values \pm RQ max. Data was analysed by performing a One way ANOVA and post-hoc Tukey test relative to the BMS control, ns=non-significant, n=4 for PLA BMS + miR-145-5p and n=6 for control BMS and PLA BMS groups.

AntimiR-21 was also delivered from the porcine stent surface and the levels of miR-21 were recorded at 48 h post-deployment. Firstly, we noted a change in the miRNA-21 expression profile between the non-stented arteries (NTC) and the control groups (PLA BMS and PLA BMS + S/C), which agrees with other reports which have documented miR-21 release after response to stent deployment and corresponding vessel injury (McDonald *et al.*, 2015). miR-21 expression was decreased by 50% after local delivery of antimiR-21 from the stent surface; however the change was not statistically significant. This study was not highly powered however, with low numbers in the treatment group (n=3) and the scramble control group (n=2), so further testing to elicit whether the trend continued. Increasing the concentration of antimiR-21 could also help to ensure a decrease in miR-21 expression was observed at the 48 h time-point which we could then use to investigate the therapeutic potential and efficacy of this miR-based treatment (Figure 5-5).

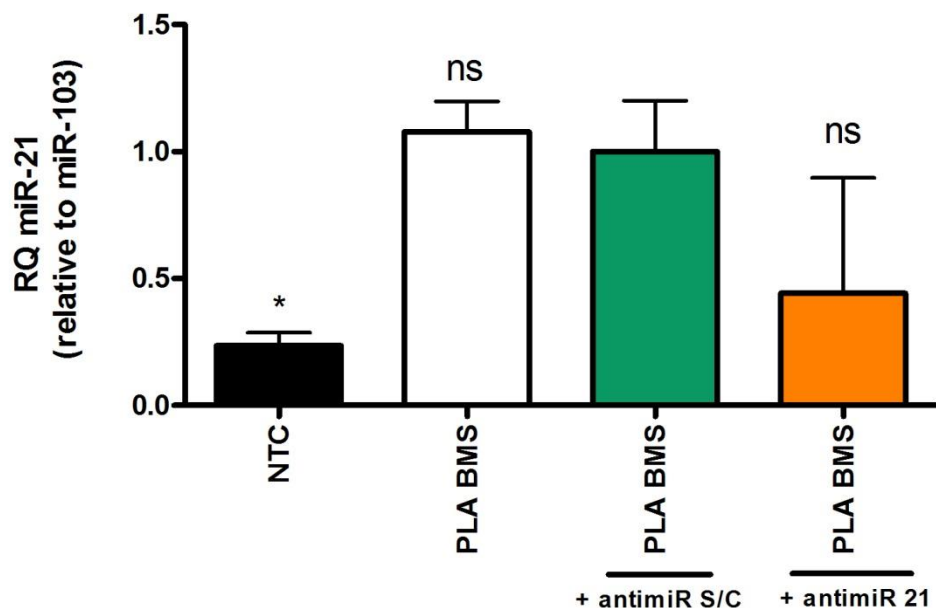


Figure 5-5 Local delivery of antimiR-21 from PLA coated stents to porcine coronary arteries, 48 h after deployment using porcine *in vivo* stenting model.

2.5 % wt/wt PLA dissolved in chloroform was coated onto porcine stents and dried overnight. antimiR-21 (20 μ M, 4.5 μ L) was added to siPORT (9 μ L) was then applied to the PLA coted stents. Stents were washed in PBS before deployment into the porcine coronary arteries. Arteries were harvested at 48h post deployment, and immediately stored at -80°C. RNA was extracted from the arteries and miR-21 expression was quantified by Taqman[®]qRT-PCR and normalised to miR-103 expression. Data is expressed as RQ values \pm RQ max. Data was analysed by performing a One way ANOVA and post-hoc Tukey test relative to the PLA BMS + antimiR scramble control, *p<0.05, ns=non-significant, n=3 for antimiR 21 PLA BMS group, n=2 for antimiR 21 S/C PLA BMS, n=6 for PLA BMS and n=8 for NTC group.

5.3 Discussion

In summary, it has been demonstrated that localised delivery of miRNA from stent surfaces can be achieved in both murine and porcine *in vivo* stenting models, using the technique of coating the BMS stent initially with PLA and then with the miRNA/siPORT. This was clearly demonstrated when using miR-39-3p as a reporter miRNA, as it is non-endogenous to mammals and therefore detection was easier to recognise.

When preliminary studies were conducted delivering antimiR-21 and miR-145-5p from the stent, we did not observe significant differences in miRNA expression between the control groups and the treatment groups. This could be due to a number of reasons. Firstly, since miR-145 is one of the most abundantly expressed miRNAs in arteries, saturation of the miR-145 expression signal could occur as the high background levels of miR-145 could prevent the detection of the miR-145 delivered from the stent being observed. In the case of antimiR-21, the experiment was not highly powered enough to ascertain conclusively whether antimiR-21 could be delivered from the stent and correspond to a decrease in arterial miR-21 expression, so a more highly powered study would aid this. In addition higher concentrations of therapeutic miRNA could be administered to ensure the change in miRNA expression was observed. Finally a method for spray coating the stent with miRNA/siPORT could ensure uniform distribution of miRNA coating (as done with DES) and this could decrease the variability within the treatment groups, which does seem to be an issue to enable consistent results to be generated.

The ability to deliver the miRNA in two different animal models has a lot of future potential for further scientific investigations, as genetically-modified mice could be used to further probe miRNA action on development of ISR. The porcine model however, has the advantage of being much more relevant to the human stent setting. Therefore further investigation using therapeutic miRNAs attached to the surface using this model to see whether alteration of the miRNAs usual expression profile could be altered and most importantly whether a therapeutic response can be monitored would provide a novel therapy for the prevention of ISR.

Recently, the first example of a miRNA eluting stent was published in the rat model, whereby antimiR-21 was delivered from the stent surface which exhibited a decrease in neointima formation (Wang *et al.*, 2015) and also circumvented issues which were present with systemic delivery of the miRNA when delivered intravenously. This has highlighted the advantages of localised delivery and the powerful effects which therapeutic miRNA could have when administered in this way.

Further to the *in vitro* testing detailed in Chapter 4 of miR 99b/let 7e/125a on the effect of VSMC proliferation, a porcine *in vivo* 28 day efficacy study was carried out delivering this cluster from stent surfaces. Although completed, at the time of writing the RNA extractions and analysis of the vessels by optical coherence tomography have not yet been completed. These results will indicate whether or not the cluster miRNA eluting stent would be effective at preventing ISR.

Finally, using a PLA platform for miRNA delivery would enable BMSs to be used as demonstrated in these studies; it also however could be used with the new technology of biodegradable stents which are composed of PLA, to create a transient PLA miRNA eluting stent. This could aid prevention of ISR through miRNA action and then dissolve overtime which would avoid chronic inflammatory responses caused by the stent struts.

To date the work presented here represents the second study detailing methodology for miRNA-eluting stents, with the first study being published a few months before the completion of the writing of this text (Wang *et.al.*, 2015). The methods which have been used here are novel in that they can be universally applied to any BMS, and represent a simple approach for miRNA delivery within this setting. In addition this is the first time that PLA has been used to absorb miRNA onto for use as a miRNA delivery device in the context of coronary stents. Since PLA is a common material for medical implants this technique for miRNA delivery could be applied in different medical contexts.

6 General discussion

6.1 General discussion

This thesis has focused on developing novel methodology for coating stents with adenovirus vectors and miRNA. The aim of the research conducted was to provide systems which would enable localised delivery of Ad vectors/miRNA to the stented region, which would be used to deliver therapeutic Ad vectors/miRNA to prevent ISR, much like the action of drug-eluting stents. In order to develop the coating technology, virus vector Ad5 and *c.elegans* (miR-39-3p) were used as a 'model' virus and miRNA to deliver from the stent/stent material surfaces. Evaluation of Ad delivery was assessed by monitoring viral transduction *in vitro* and *ex vivo* using pig coronary arteries, following the coating of the Ad onto stent material surfaces and stents. Three different techniques for virus coating were tested; PEM formation, covalent attachment and collagen entrapment. Evaluation of miRNA delivery was assessed by monitoring miRNA expression following coating on stent material surfaces and stents, *in vitro*, *ex vivo* and *in vivo* testing in both porcine and murine stenting models.

Linking adenoviruses to surfaces is a significant undertaking. Adenoviruses are complex biological structures and care is needed to preserve the innate biological activity to ensure that the virus is capable of delivering the transgene efficiently, following linkage to the surface. Methods which have been used to create DES cannot therefore be applied to virus linkage methodology as they involve organic solvents required to dissolve the polymer, which would have detrimental effects on the virus biological activity profile. Therefore simple, methods for virus attachment were investigated initially which relied on electrostatic interactions between the negatively charged virus capsid and a positively charged polyelectrolyte layer. To date, a few studies have been reported adherence methods of viruses to stent surfaces using electrostatic interactions. One method used the native adenoviruses net negative charge which could bind to a positively charged phosphorylcholine stent surfaces through electrostatic interactions (Sharif *et al.*, 2008, Johnson *et al.*, 2005b). Similarly a study reported by Saurer *et al.* (2011), demonstrated that poly(electrolyte) multilayers (PEMs), could be used to deliver DNA from stent surfaces *in vitro* through electrostatic interactions. Therefore, it was hypothesised that PEMs could be used to attach virus particles to stent surfaces

via electrostatic interactions, although successful for *in vitro* testing, this technique proved not robust enough to withstand deployment *ex vivo* into rat arteries. This suggested that a more permanent linkage could provide a more suitable delivery system.

Direct covalent linkage of viruses to stent surfaces was attempted by modifying PLA, a biodegradable polymer, which is often used as a stent material. Using this organic biodegradable polymer, allowed access to a wider range of organic chemistry techniques for bio-conjugation of the virus to the polymer surface, which would not be possible if trying to attach directly to SS surfaces. One of the reasons which SS is suitable for its role as an implant material is due to the fact it is very unreactive. Modification of PLA, so that it could react with the virus worked well, although the chemistry involved proved difficult to reliably reproduce and therefore other delivery methods were investigated. This was partly due to restrictions on the solvents and reagents which could be used to ensure that the virus was still biologically active.

One of the advantages of using a covalent modification strategy for direct virus linkage to the surface was for the permanency of the bond, which would be able to withstand the stent deployment procedure. If this strategy was taken further it would be important to incorporate mechanisms for the virus to detach from the surface, enabling the virus to transduce the surrounding cells within its lifespan. Although the PLA is biodegradable and would release the virus particles it may be important to introduce more labile linkages to achieve this and develop this methodology further. Using a variety of different labile linkages could create a system whereby temporal virus elution was achieved by fine-tuning the chemistry, which could be useful for enabling a sustained gene delivery profile.

Methodologies were then investigated which did not require covalent bonding and instead used collagen gel encapsulation. Initial testing revealed that the virus retained its biological activity when encapsulated within the gel and could transduce cells. Better adherence of the collagen gel was demonstrated when deposited directly onto PLA surfaces as opposed to SS. Difficulties were encountered when trying to coat the PLA onto the SS as high %PLA wt/wt dissolved in chloroform were required in order to retain high virus transduction

levels. This created a logistical problem, as when coating the SS stents, high %PLA solutions meant that the stent could no longer fit through the guide catheter and expand fully. Therefore testing using a commercially available PLA stent would be essential for investigating further whether the collagen encapsulation methodology would function *in vivo*.

With both the miRNA and adenovirus eluting stents, future work will need to focus on efficacy studies, in order to demonstrate that therapeutic miRNA/adenovirus can be used to effectively prevent ISR from occurring. The most relevant model to test this in would be the pig *in vivo* stenting model, due to similarities in vessel size, anatomy and the similarity in operational procedures between pigs and humans. Care will need to be given to elucidate whether the miRNA/adenovirus is efficacious as ISR is a complex multi-factorial disease. It will be imperative to ensure that the targets of the relevant adenovirus/miRNA are subsequently upregulated or downregulated as intended. But even after confirmation of target upregulation/downregulation, off-target effects may hinder the desired outcome. For miRNA therapy this poses as a significant problem as they are known to have multiple targets, control over this innate binding ability of the miRNA will therefore be difficult, but key for progression to the human clinical trials.

As mentioned before, until recently miRNA-eluting stents had not previously been reported and at the time of conducting this research no miRNA-eluting stent research literature was available for reference. The success found with the adenovirus collagen encapsulation methodology provided the rationale for investigating whether miRNA delivery could be achieved from these platforms. It was found that the collagen was surplus to requirements and the miRNA could be efficiently delivered *in vitro* from PLA surfaces by direct application onto the surface following mixing with transfection reagent siPORT™ Neo FX™. Although not tested experimentally, it was likely that adherence of the miRNA onto the PLA surface was due to hydrophobic interactions between siPORT™ and the PLA surfaces. This therefore could be used when developing future miRNA delivery systems.

Results from *in vivo* studies, through application of miRNA/siPORT to PLA coated murine and porcine BMS, were very promising. At 48 h, the non-endogenous

c.elegans miR-39-3p that was coated onto the stent surfaces could be detected from the surrounding stented vessel. Initial results also demonstrated that therapeutic miRNAs could be delivered *in vitro* using miR-145-5p and anti-miR-21 *in vivo*, although a more highly powered study would need to be done to supplement these preliminary *in vivo* findings.

Although expression of the *c.elegans* miR-39-3p was observed which provided good evidence that this delivery system was suitable for *in vivo* delivery of miRNA from stent surfaces; when targeting endogenous miRNAs such as miR-145 and miR-21, great variability was observed with expression profiles in both *in vitro* and *in vivo* settings after delivery of the miRNAs and miRNA inhibitors. This could reflect the method for coating the miRNA/siPORT not being uniform enough. In order to progress these delivery systems further, it would be important to implement spray-coating methodology of the miRNA onto the stent surface, to ensure a uniform distribution of the miRNA onto the surface.

Variability introduced from the PLA coating onto the SS stent surfaces, which was done by hand, would also need to be improved by using industrial methods for polymer coatings on stent surfaces, or simply by using a commercially available PLA stent such as the Abbott BioAbsorb scaffold (Abbott, 2015). Although currently this stent is manufactured with everolimus coated onto it, which would inhibit neointima formation. It would therefore be important to obtain a non-anti proliferative drug eluting PLA stent for further studies. Concerns about the manual coating methodology have also been raised for longer term efficacy studies, as the thickness of the coating could cause an increase in neointima formation. Commercial stent struts which are available in the clinic have thicknesses in the range of 60-150 μM (Stefanini *et al.*, 2013), therefore measuring the PLA coating thickness would also needed to be done in order to allow efficacy testing to be done effectively.

In summary, despite these suggested improvements and considerations for further testing of the miRNA eluting stents, the methodology presented here represents a novel way in which miRNAs can be delivered from stent surfaces, which has been shown to deliver miRNA in the porcine and murine *in vivo* models. This is the first of example of miRNA eluting stents using these animal models and the first study to employ the biodegradable polymer PLA in order to

do so. The findings presented here, I hope will form the foundations for a fully functional biodegradable miRNA eluting stent, which will show-case the ability of miRNAs as a new-class of therapeutic for the prevention of ISR.

List of references

- ABBINK, P., LEMCKERT, A. A., EWALD, B. A., LYNCH, D. M., DENHOLTZ, M., SMITS, S., HOLTERMAN, L., DAMEN, I., VOGELS, R. & THORNER, A. R. 2007. Comparative seroprevalence and immunogenicity of six rare serotype recombinant adenovirus vaccine vectors from subgroups B and D. *Journal of virology*, 81, 4654-4663.
- ABBOTT. 2015. Available: <http://www.abbottvascular.com/int/products/corona-ry-intervention/absorb-bioresorbable-scaffold.html>.
- ALEMANY, R. & CURIEL, D. 2001. CAR-binding ablation does not change biodistribution and toxicity of adenoviral vectors. *Gene therapy*, 8, 1347-1353.
- ALEMANY, R., SUZUKI, K. & CURIEL, D. T. 2000. Blood clearance rates of adenovirus type 5 in mice. *Journal of General Virology*, 81, 2605-2609.
- ALFONSO, F. 2010. Treatment of Drug-Eluting Stent Restenosis The New Pilgrimage: Quo Vadis?*. *Journal of the American College of Cardiology*, 55, 2717-2720.
- ALFONSO, F., BYRNE, R. A., RIVERO, F. & KASTRATI, A. 2014. Current Treatment of In-Stent Restenosis. *Journal of the American College of Cardiology*, 63, 2659-2673.
- ALI, Z. A., ALP, N. J., LUPTON, H., ARNOLD, N., BANNISTER, T., HU, Y. H., MUSSA, S., WHEATCROFT, M., GREAVES, D. R., GUNN, J. & CHANNON, K. M. 2007. Increased in-stent stenosis in ApoE knockout mice - Insights from a novel mouse model of balloon angioplasty and

- stenting. *Arteriosclerosis Thrombosis and Vascular Biology*, 27, 833-840.
- ARNBERG, N., KIDD, A. H., EDLUND, K., OLFAT, F. & WADELL, G. 2000. Initial Interactions of Subgenus D Adenoviruses with A549 Cellular Receptors: Sialic Acid versus α Integrins. *Journal of virology*, 74, 7691-7693.
- ATTHOFF, B. & HILBORN, J. 2007. Protein adsorption onto polyester surfaces: Is there a need for surface activation? *Journal of Biomedical Materials Research Part B: Applied Biomaterials*, 80B, 121-130.
- AXEL, D. I., KUNERT, W., GÖGGELMANN, C., OBERHOFF, M., HERDEG, C., KÜTTNER, A., WILD, D. H., BREHM, B. R., RIESSEN, R., KÖVEKER, G. & KARSCH, K. R. 1997. Paclitaxel Inhibits Arterial Smooth Muscle Cell Proliferation and Migration In Vitro and In Vivo Using Local Drug Delivery. *Circulation*, 96, 636-645.
- BABAPULLE, M. N., JOSEPH, L., BÉLISLE, P., BROPHY, J. M. & EISENBERG, M. J. 2004. A hierarchical Bayesian meta-analysis of randomised clinical trials of drug-eluting stents. *The Lancet*, 364, 583-591.
- BAEK, D., VILLEN, J., SHIN, C., CAMARGO, F. D., GYGI, S. P. & BARTEL, D. P. 2008. The impact of microRNAs on protein output. *Nature*, 455, 64-U38.
- BAKER, A. H. 2002. Gene therapy for bypass graft failure and restenosis. *Pathophysiology of haemostasis and thrombosis*, 32, 389-391.
- BAKER, A. H., ZALTSMAN, A. B., GEORGE, S. J. & NEWBY, A. C. 1998. Divergent effects of tissue inhibitor of metalloproteinase-1,-2, or-3 overexpression on rat vascular smooth muscle cell

- invasion, proliferation, and death in vitro. TIMP-3 promotes apoptosis. *Journal of Clinical Investigation*, 101, 1478.
- BARBATO, J. E. & TZENG, E. 2004. Nitric oxide and arterial disease. *Journal of Vascular Surgery*, 40, 187-193.
- BAROUCH, D. H., KIK, S. V., WEVERLING, G. J., DILAN, R., KING, S. L., MAXFIELD, L. F., CLARK, S., BRANDARIZ, K. L., ABBINK, P. & SINANGIL, F. 2011. International seroepidemiology of adenovirus serotypes 5, 26, 35, and 48 in pediatric and adult populations. *Vaccine*, 29, 5203-5209.
- BARTEL, D. P. 2009. MicroRNAs: Target Recognition and Regulatory Functions. *Cell*, 136, 215-233.
- BASSOLS, A. & MASSAGUE, J. 1988. Transforming growth factor beta regulates the expression and structure of extracellular matrix chondroitin/dermatan sulfate proteoglycans. *Journal of Biological Chemistry*, 263, 3039-3045.
- BENTLEY, J. P. 1967. Rate of chondroitin sulfate formation in wound healing. *Annals of surgery*, 165, 186.
- BERGELSON, J. M., CUNNINGHAM, J. A., DROGUETT, G., KURT-JONES, E. A., KRITHIVAS, A., HONG, J. S., HORWITZ, M. S., CROWELL, R. L. & FINBERG, R. W. 1997. Isolation of a common receptor for Coxsackie B viruses and adenoviruses 2 and 5. *Science*, 275, 1320-1323.
- BHF 2015. British Heart Foundation Cardiovascular Disease Statistics
- BIRO, S., FU, Y. M., YU, Z. X. & EPSTEIN, S. E. 1993. Inhibitory effects of antisense oligodeoxynucleotides targeting c-myc mRNA on

- smooth muscle cell proliferation and migration. *Proc Natl Acad Sci U S A*, 90, 654-8.
- BODEN, W. E., O'ROURKE, R. A., TEO, K. K., HARTIGAN, P. M., MARON, D. J., KOSTUK, W. J., KNUDTSON, M., DADA, M., CASPERSON, P., HARRIS, C. L., CHAITMAN, B. R., SHAW, L., GOSSELIN, G., NAWAZ, S., TITLE, L. M., GAU, G., BLAUSTEIN, A. S., BOOTH, D. C., BATES, E. R., SPERTUS, J. A., BERMAN, D. S., MANCINI, G. B. J. & WEINTRAUB, W. S. 2007. Optimal Medical Therapy with or without PCI for Stable Coronary Disease. *New England Journal of Medicine*, 356, 1503-1516.
- BOETTGER, T., BEETZ, N., KOSTIN, S., SCHNEIDER, J., KRUGER, M., HEIN, L. & BRAUN, T. 2009. Acquisition of the contractile phenotype by murine arterial smooth muscle cells depends on the Mir143/145 gene cluster. *Journal of Clinical Investigation*, 119, 2634-2647.
- BORCHERT, G. M., LANIER, W. & DAVIDSON, B. L. 2006. RNA polymerase III transcribes human microRNAs. *Nature Structural & Molecular Biology*, 13, 1097-1101.
- BORING, L., GOSLING, J., CLEARY, M. & CHARO, I. F. 1998. Decreased lesion formation in CCR2^{-/-} mice reveals a role for chemokines in the initiation of atherosclerosis. *Nature*, 394, 894-897.
- BOURANTAS, C. V., ZHANG, Y., FAROOQ, V., GARCIA-GARCIA, H. M., ONUMA, Y. & SERRUYS, P. W. 2012. Bioresorbable Scaffolds: Current Evidence and Ongoing Clinical Trials. *Current Cardiology Reports*, 14, 626-634.
- BRADSHAW, A. C. & BAKER, A. H. 2013. Gene therapy for cardiovascular disease: perspectives

- and potential. *Vascular pharmacology*, 58, 174-181.
- BREINBAUER, R. & KÖHN, M. 2003. Azide–alkyne coupling: a powerful reaction for bioconjugate chemistry. *ChemBioChem*, 4, 1147-1149.
- BRENNECKE, J., STARK, A., RUSSELL, R. B. & COHEN, S. M. 2005. Principles of MicroRNA-target recognition. *Plos Biology*, 3, 404-418.
- BRITO, L. A., CHANDRASEKHAR, S., LITTLE, S. R. & AMIJI, M. M. 2010. Non-viral eNOS gene delivery and transfection with stents for the treatment of restenosis. *Biomed Eng Online*, 9, 56.
- BRODERSEN, P. & VOINNET, O. 2009. Revisiting the principles of microRNA target recognition and mode of action. *Nature Reviews Molecular Cell Biology*, 10, 141-148.
- CAMPBELL, J. H. & CAMPBELL, G. R. 1986. Endothelial cell influences on vascular smooth muscle phenotype. *Annual Review of Physiology*, 48, 295-306.
- CAPODANNO, D., MIANO, M., CINCOTTA, G., CAGGEGI, A., RUPERTO, C., BUCALO, R., SANFILIPPO, A., CAPRANZANO, P. & TAMBURINO, C. EuroSCORE refines the predictive ability of SYNTAX score in patients undergoing left main percutaneous coronary intervention. *American Heart Journal*, 159, 103-109.
- CARLISLE, R. C., DI, Y., CERNY, A. M., SONNEN, A. F.-P., SIM, R. B., GREEN, N. K., SUBR, V., ULBRICH, K., GILBERT, R. J. & FISHER, K. D. 2009. Human erythrocytes bind and inactivate type 5 adenovirus by presenting Coxsackie virus-adenovirus receptor and complement receptor 1. *Blood*, 113, 1909-1918.

- CARTHEW, R. W. & SONTHEIMER, E. J. 2009. Origins and Mechanisms of miRNAs and siRNAs. *Cell*, 136, 642-655.
- CASTELLOT JR, J. J., WRIGHT, T. C. & KARNOVSKY, M. J. Regulation of vascular smooth muscle cell growth by heparin and heparan sulfates. *Seminars in thrombosis and hemostasis*, 1987. 489-503.
- CHAABANE, C., OTSUKA, F., VIRMANI, R. & BOCHATON-PIALLAT, M.-L. 2013. Biological responses in stented arteries. *Cardiovascular Research*, 99, 353-363.
- CHAMBERLAIN, J., GUNN, J., FRANCIS, S. E., HOLT, C. M., ARNOLD, N. D., CUMBERLAND, D. C., FERGUSON, M. W. J. & CROSSMAN, D. C. 2001. TGF β is active, and correlates with activators of TGF β , following porcine coronary angioplasty. *Cardiovascular Research*, 50, 125-136.
- CHEN, M. S., JOHN, J. M., CHEW, D. P., LEE, D. S., ELLIS, S. G. & BHATT, D. L. 2006. Bare metal stent restenosis is not a benign clinical entity. *American Heart Journal*, 151, 1260-1264.
- CHEN, S. F., KAPTURCZAK, M., LOILER, S. A., ZOLOTUKHIN, S., GLUSHAKOVA, O. Y., MADSEN, K. M., SAMULSKI, R. J., HAUSWIRTH, W. W., CAMPBELL-THOMPSON, M., BERNS, K. I., FLOTTE, T. R., ATKINSON, M. A., TISHER, C. C. & AGARWAL, A. 2005. Efficient transduction of vascular endothelial cells with recombinant adeno-associated virus serotype 1 and 5 vectors. *Human Gene Therapy*, 16, 235-247.
- CHENDRIMADA, T. P., GREGORY, R. I., KUMARASWAMY, E., NORMAN, J., COOCH, N., NISHIKURA, K. & SHIEKHATTAR, R. 2005.

- TRBP recruits the Dicer complex to Ago2 for microRNA processing and gene silencing. *Nature*, 436, 740-744.
- CHENG, Y., LIU, X., YANG, J., LIN, Y., XU, D. Z., LU, Q., DEITCH, E. A., HUO, Y., DELPHIN, E. S. & ZHANG, C. 2009a. MicroRNA-145, a novel smooth muscle cell phenotypic marker and modulator, controls vascular neointimal lesion formation. *Circ Res*, 105, 158-66.
- CHENG, Y. H., LIU, X. J., YANG, J., LIN, Y., XU, D. Z., LU, Q., DEITCH, E. A., HUO, Y. Q., DELPHIN, E. S. & ZHANG, C. X. 2009b. MicroRNA-145, a Novel Smooth Muscle Cell Phenotypic Marker and Modulator, Controls Vascular Neointimal Lesion Formation. *Circulation Research*, 105, 158-U113.
- CHOBANIAN, A. V., BAKRIS, G. L., BLACK, H. R., CUSHMAN, W. C., GREEN, L. A., IZZO, J. L., JONES, D. W., MATERSON, B. J., OPARIL, S. & WRIGHT, J. T. 2003. Seventh report of the joint national committee on prevention, detection, evaluation, and treatment of high blood pressure. *Hypertension*, 42, 1206-1252.
- CHUYSINUAN, P., PAVASANT, P. & SUPAPHOL, P. 2012. Preparation and Characterization of Caffeic Acid-Grafted Electrospun Poly (L-Lactic Acid) Fiber Mats for Biomedical Applications. *ACS applied materials & interfaces*, 4, 3031-3040.
- CLOWES, A., CLOWES, M., FINGERLE, J. & REIDY, M. 1989. Kinetics of cellular proliferation after arterial injury. V. Role of acute distension in the induction of smooth muscle proliferation. *Laboratory investigation; a journal of technical methods and pathology*, 60, 360-364.
- CORDES, K. R., SHEEHY, N. T., WHITE, M. P., BERRY, E. C., MORTON, S. U., MUTH, A. N.,

- LEE, T.-H., MIANO, J. M., IVEY, K. N. & SRIVASTAVA, D. 2009a. miR-145 and miR-143 regulate smooth muscle cell fate and plasticity. *Nature*, 460, 705-710.
- CORDES, K. R., SHEEHY, N. T., WHITE, M. P., BERRY, E. C., MORTON, S. U., MUTH, A. N., LEE, T. H., MIANO, J. M., IVEY, K. N. & SRIVASTAVA, D. 2009b. miR-145 and miR-143 regulate smooth muscle cell fate and plasticity. *Nature*, 460, 705-U80.
- COSTA, M. A. & SIMON, D. I. 2005. Molecular basis of restenosis and drug-eluting stents. *Circulation*, 111, 2257-2273.
- DAKIN, R. S., PARKER, A. L., NICKLIN, S. A. & BAKER, A. H. 2015. Efficient transduction of primary vascular cells by the rare adenovirus serotype 49 vector. *Human gene therapy*, 26, 312-319.
- DAVIS, B. N., HILYARD, A. C., LAGNA, G. & HATA, A. 2008. SMAD proteins control DROSHA-mediated microRNA maturation. *Nature*, 454, 56-U2.
- DAVIS, B. N., HILYARD, A. C., NGUYEN, P. H., LAGNA, G. & HATA, A. 2009. Induction of MicroRNA-221 by Platelet-derived Growth Factor Signaling Is Critical for Modulation of Vascular Smooth Muscle Phenotype. *Journal of Biological Chemistry*, 284, 3728-3738.
- DAVIS, E., CAIMENT, F., TORDOIR, X., CAVAILLE, J., FERGUSON-SMITH, A., COCKETT, N., GEORGES, M. & CHARLIER, C. 2005. RNAi-mediated allelic trans-interaction at the imprinted Rtl1/Peg11 locus (vol 15, pg 746, 2005). *Current Biology*, 15, 884-884.
- DE FEYTER, P. J., DE JAEGERE, P. P. & SERRUYS, P. W. 1994. Incidence, predictors, and

- management of acute coronary occlusion after coronary angioplasty. *American heart journal*, 127, 643-651.
- DEUSE, T., ERBEN, R. G., IKENO, F., BEHNISCH, B., BOEGER, R., CONNOLLY, A. J., REICHENSPURNER, H., BERGOW, C., PELLETIER, M. P., ROBBINS, R. C. & SCHREPFER, S. 2008. Introducing the first polymer-free leflunomide eluting stent. *Atherosclerosis*, 200, 126-134.
- DI PAOLO, N. C., MIAO, E. A., IWAKURA, Y., MURALI-KRISHNA, K., ADEREM, A., FLAVELL, R. A., PAPAYANNOPOULOU, T. & SHAYAKHMETOV, D. M. 2009. Virus binding to a plasma membrane receptor triggers interleukin-1 α -mediated proinflammatory macrophage response in vivo. *Immunity*, 31, 110-121.
- DIMITROVA, M., ARNTZ, Y., LAVALLE, P., MEYER, F., WOLF, M., SCHUSTER, C., HAIKEL, Y., VOEGEL, J. C. & OGIER, J. 2007. Adenoviral gene delivery from multilayered polyelectrolyte architectures. *Advanced Functional Materials*, 17, 233-245.
- DISHART, K. L., DENBY, L., GEORGE, S. J., NICKLIN, S. A., YENDLURI, S., TUERK, M. J., KELLEY, M. P., DONAHUE, B. A., NEWBY, A. C., HARDING, T. & BAKER, A. H. 2003. Third-generation lentivirus vectors efficiently transduce and phenotypically modify vascular cells: implications for gene therapy. *Journal of Molecular and Cellular Cardiology*, 35, 739-748.
- DÖRR, O., LIEBETRAU, C., WIEBE, J., HECKER, F., RIXE, J., MÖLLMANN, H., HAMM, C. & NEF, H. 2014. Bioresorbable scaffolds for the treatment of

- in-stent restenosis. *Heart and vessels*, 30, 265-269.
- DOUGLAS, G., VAN KAMPEN, E., HALE, A. B., MCNEILL, E., PATEL, J., CRABTREE, M. J., ALI, Z., HOERR, R. A., ALP, N. J. & CHANNON, K. M. 2013. Endothelial cell repopulation after stenting determines in-stent neointima formation: effects of bare-metal vs. drug-eluting stents and genetic endothelial cell modification. *European Heart Journal*, 34, 3378-3388.
- DUCKERS, H. J., NABEL, E. G. & SERRUYS, P. W. 2007. *Essentials of restenosis: for the interventional cardiologist*, Springer Science & Business Media.
- FAN, T., WU, X. & WU, Y. 2013. Preparation and characterization of cyhalothrin-loaded poly(2-hydroxyethyl methacrylate)-co-poly(lactide) (PHEMA-co-PLA) ultrafine particles. *Journal of Applied Polymer Science*, 129, 1861-1867.
- FARB, A., SANGIORGI, G., CARTER, A. J., WALLEY, V. M., EDWARDS, W. D., SCHWARTZ, R. S. & VIRMANI, R. 1999. Pathology of Acute and Chronic Coronary Stenting in Humans. *Circulation*, 99, 44-52.
- FAROOQ, V., GOGAS, B. D. & SERRUYS, P. W. 2011. Restenosis: Delineating the Numerous Causes of Drug-Eluting Stent Restenosis. *Circulation: Cardiovascular Interventions*, 4, 195-205.
- FAVALORO, R. G. 1968. Saphenous vein autograft replacement of severe segmental coronary artery occlusion: operative technique. *The Annals of thoracic surgery*, 5, 334-339.
- FISCHMAN, D. L., LEON, M. B., BAIM, D. S., SCHATZ, R. A., SAVAGE, M. P., PENN, I.,

- DETRE, K., VELTRI, L., RICCI, D. & NOBUYOSHI, M. 1994. A randomized comparison of coronary-stent placement and balloon angioplasty in the treatment of coronary artery disease. *New England Journal of Medicine*, 331, 496-501.
- FISHBEIN, I., ALFERIEV, I., BAKAY, M., STACHELEK, S. J., SOBOLEWSKI, P., LAI, M. Z., CHOI, H., CHEN, I. W. & LEVY, R. J. 2008. Local delivery of gene vectors from bare-metal stents by use of a biodegradable synthetic complex inhibits in-stent restenosis in rat carotid arteries. *Circulation*, 117, 2096-2103.
- FISHBEIN, I., ALFERIEV, I. S., NYANGUILE, O., GASTER, R., VOHS, J. M., WONG, G. S., FELDERMAN, H., CHEN, I. W., CHOI, H., WILENSKY, R. L. & LEVY, R. J. 2006a. Bisphosphonate-mediated gene vector delivery from the metal surfaces of stents. *Proceedings of the National Academy of Sciences of the United States of America*, 103, 159-164.
- FISHBEIN, I., ALFERIEV, I. S., NYANGUILE, O., GASTER, R., VOHS, J. M., WONG, G. S., FELDERMAN, H., CHEN, I. W., CHOI, H., WILENSKY, R. L. & LEVY, R. J. 2006b. Bisphosphonate-mediated gene vector delivery from the metal surfaces of stents. *Proceedings of the National Academy of Sciences of the United States of America*, 103, 159-164.
- FISHBEIN, I., FORBES, S. P., ADAMO, R. F., CHORNY, M., LEVY, R. J. & ALFERIEV, I. S. 2014. Vascular Gene Transfer from Metallic Stent Surfaces Using Adenoviral Vectors Tethered through Hydrolysable Cross-linkers. *Jove-Journal of Visualized Experiments*, 90, e51653-e51653.

- FLYNT, A. S. & LAI, E. C. 2008. Biological principles of microRNA-mediated regulation: shared themes amid diversity. *Nature Reviews Genetics*, 9, 831-842.
- FOLKMAN, J. & KLAGSBRUN, M. 1987. Angiogenic factors. *Science*, 235, 442-447.
- FOROUGH, R., KOYAMA, N., HASENSTAB, D., LEA, H., CLOWES, M., NIKKARI, S. T. & CLOWES, A. W. 1996. Overexpression of tissue inhibitor of matrix metalloproteinase-1 inhibits vascular smooth muscle cell functions in vitro and in vivo. *Circulation Research*, 79, 812-820.
- FORRESTER, J. S., FISHBEIN, M., HELFANT, R. & FAGIN, J. 1991. A paradigm for restenosis based on cell biology: clues for the development of new preventive therapies. *Journal of the American College of Cardiology*, 17, 758-769.
- FRENCH, B. A., MAZUR, W., ALI, N. M., GESKE, R. S., FINNIGAN, J. P., RODGERS, G. P., ROBERTS, R. & RAIZNER, A. E. 1994. Percutaneous transluminal in vivo gene transfer by recombinant adenovirus in normal porcine coronary arteries, atherosclerotic arteries, and two models of coronary restenosis. *Circulation*, 90, 2402-13.
- FRIEDMAN, R. C., FARH, K. K. H., BURGE, C. B. & BARTEL, D. P. 2009. Most mammalian mRNAs are conserved targets of microRNAs. *Genome Research*, 19, 92-105.
- GAGGAR, A., SHAYAKHMETOV, D. M. & LIEBER, A. 2003. CD46 is a cellular receptor for group B adenoviruses. *Nature medicine*, 9, 1408-1412.
- GAO, M. H., LAI, N. C., MCKIRNAN, D., ROTH, D. A., RUBANYI, G. M., DALTON, N., ROTH, D. M. & HAMMOND, H. K. 2004. Increased regional

- function and perfusion after intracoronary delivery of adenovirus encoding fibroblast growth factor 4: Report of preclinical data. *Human Gene Therapy*, 15, 574-587.
- GEARY, R. L. & CLOWES, A. W. 2007. Epidemiology and pathogenesis of restenosis. *Essentials of restenosis*. Springer.
- GINN, S. L., ALEXANDER, I. E., EDELSTEIN, M. L., ABEDI, M. R. & WIXON, J. 2013. Gene therapy clinical trials worldwide to 2012 an update. *Journal of Gene Medicine*, 15, 65-77.
- GRECH, E. D. 2003. *Percutaneous coronary intervention. I: History and development*.
- GRÜNTZIG, A. 1978. Transluminal dilatation of coronary-artery stenosis. *The Lancet*, 311, 263.
- GU, L., OKADA, Y., CLINTON, S. K., GERARD, C., SUKHOVA, G. K., LIBBY, P. & ROLLINS, B. J. 1998. Absence of Monocyte Chemoattractant Protein-1 Reduces Atherosclerosis in Low Density Lipoprotein Receptor-deficient Mice. *Molecular Cell*, 2, 275-281.
- GUZMAN, R. J., HIRSCHOWITZ, E. A., BRODY, S. L., CRYSTAL, R. G., EPSTEIN, S. E. & FINKEL, T. 1994. In vivo suppression of injury-induced vascular smooth muscle cell accumulation using adenovirus-mediated transfer of the herpes simplex virus thymidine kinase gene. *Proceedings of the National Academy of Sciences*, 91, 10732-10736.
- HACIEN-BEY-ABINA, S. 2003. LMO2-associated clonal T cell proliferation in two patients after gene therapy for SCID-X1 (vol 302, pg 415, 2003). *Science*, 302, 568-568.
- HART, S., COLLINS, L., GUSTAFSSON, K. & FABRE, J. 1997. Integrin-mediated transfection with

- peptides containing arginine-glycine-aspartic acid domains. *Gene therapy*, 4, 1225-1230.
- HART, S., HARBOTTLE, R., COOPER, R., MILLER, A., WILLIAMSON, R. & COUTELLE, C. 1995. Gene delivery and expression mediated by an integrin-binding peptide. *Gene therapy*, 2, 552-554.
- HART, S. L., ARANCIBIA-CARCAMO, C. V., WOLFERT, M. A., MAILHOS, C., O'REILLY, N. J., ALI, R. R., COUTELLE, C., GEORGE, A. J. T., HARBOTTLE, R. P., KNIGHT, A. M., LARKIN, D. F. P., LEVINSKY, R. J., SEYMOUR, L. W., THRASHER, A. J. & KINNON, C. 1998. Lipid-mediated enhancement of transfection by a nonviral integrin-targeting vector. *Human Gene Therapy*, 9, 575-585.
- HAVENGA, M., LEMCKERT, A., GRIMBERGEN, J., VOGELS, R., HUISMAN, L., VALERIO, D., BOUT, A. & QUAX, P. 2001. Improved adenovirus vectors for infection of cardiovascular tissues. *Journal of virology*, 75, 3335-3342.
- HE, J., JING, Y., LI, W., QIAN, X., XU, Q., LI, F.-S., LIU, L.-Z., JIANG, B.-H. & JIANG, Y. 2013. Roles and mechanism of miR-199a and miR-125b in tumor angiogenesis. *PLoS One*, 8, e56647.
- HEDMAN, M., HARTIKAINEN, J., SYVANNE, M., STJERNVALL, J., HEDMAN, A., KIVELA, A., VANNINEN, E., MUSSALO, H., KAUPPILA, E., SIMULA, S., NARVANEN, O., RANTALA, A., PEUHKURINEN, K., NIEMINEN, M. S., LAAKSO, M. & YLA-HERTTUALA, S. 2003. Safety and feasibility of catheter-based local intracoronary vascular endothelial growth factor gene transfer in the prevention of postangioplasty and in-stent restenosis and in the treatment of chronic

- myocardial ischemia - Phase II results of the Kuopio Angiogenesis Trial (KAT). *Circulation*, 107, 2677-2683.
- HEDMAN, M., MUONA, K., HEDMAN, A., KIVELA, A., SYVANNE, M., ERANEN, J., RANTALA, A., STJERNVALL, J., NIEMINEN, M. S., HARTIKAINEN, J. & YLA-HERTTUALA, S. 2009. Eight-year safety follow-up of coronary artery disease patients after local intracoronary VEGF gene transfer. *Gene Therapy*, 16, 629-634.
- HENRY, T. D., GRINES, C. L., WATKINS, M. W., DIB, N., BARBEAU, G., MOREADITH, R., ANDRASZAY, T. & ENGLER, R. L. 2007. Effect of Ad5FGF-4 in patients with angina - An analysis of pooled data from the AGENT-3 and AGENT-4 trials. *Journal of the American College of Cardiology*, 50, 1038-1046.
- HILTUNEN, M. O., LAITINEN, M., TURUNEN, M. P., JELTSCH, M., HARTIKAINEN, J., RISSANEN, T. T., LAUKKANEN, J., NIEMI, M., KOSSILA, M. & HÄKKINEN, T. P. 2000. Intravascular adenovirus-mediated VEGF-C gene transfer reduces neointima formation in balloon-denuded rabbit aorta. *Circulation*, 102, 2262-2268.
- IACONETTI, C., POLIMENI, A., SORRENTINO, S., SABATINO, J., PIRONTI, G., ESPOSITO, G., CURCIO, A. & INDOLFI, C. 2012. Inhibition of miR-92a increases endothelial proliferation and migration in vitro as well as reduces neointimal proliferation in vivo after vascular injury. *Basic Research in Cardiology*, 107, 1-14.
- INDOLFI, C., ESPOSITO, G., STABILE, E., CAVUTO, L., PISANI, A., COPPOLA, C., TORELLA, D., PERRINO, C., DI LORENZO, E., CURCIO, A., PALOMBINI, L. & CHIARIELLO, M. 2000. A new

- rat model of small vessel stenting. *Basic Res Cardiol*, 95, 179-85.
- INDOLFI, C., MONGIARDO, A., CURCIO, A. & TORELLA, D. 2003. Molecular mechanisms of in-stent restenosis and approach to therapy with eluting stents. *Trends Cardiovasc Med*, 13, 142-8.
- IRVINE, S. A., MENG, Q.-H., AFZAL, F., HO, J., WONG, J. B., HAILES, H. C., TABOR, A. B., MCEWAN, J. R. & HART, S. L. 2008. Receptor-targeted nanocomplexes optimized for gene transfer to primary vascular cells and explant cultures of rabbit aorta. *Molecular Therapy*, 16, 508-515.
- JESSUP, M., GREENBERG, B., MANCINI, D., CAPPOLA, T., PAULY, D. F., JASKI, B., YAROSHINSKY, A., ZSEBO, K. M., DITTRICH, H., HAJJAR, R. J. & PERCUTANEOUS, C. U. 2011. Calcium Upregulation by Percutaneous Administration of Gene Therapy in Cardiac Disease (CUPID) A Phase 2 Trial of Intracoronary Gene Therapy of Sarcoplasmic Reticulum Ca²⁺-ATPase in Patients With Advanced Heart Failure. *Circulation*, 124, 304-U113.
- JI, R., CHENG, Y., YUE, J., YANG, J., LIU, X., CHEN, H., DEAN, D. B. & ZHANG, C. 2007a. MicroRNA expression signature and antisense-mediated depletion reveal an essential role of MicroRNA in vascular neointimal lesion formation. *Circ Res*, 100, 1579-88.
- JI, R. R., CHENG, Y. H., YUE, J. M., YANG, J., LIU, X. J., CHEN, H., DEAN, D. B. & ZHANG, C. X. 2007b. MicroRNA expression signature and antisense-mediated depletion reveal an essential role of microRNA in vascular neointimal lesion formation. *Circulation Research*, 100, 1579-1588.

- JOHNSON, T. W., WU, Y. X., HERDEG, C., BAUMBACH, A., NEWBY, A. C., KARSCH, K. R. & OBERHOFF, M. 2005a. Stent-Based Delivery of Tissue Inhibitor of Metalloproteinase-3 Adenovirus Inhibits Neointimal Formation in Porcine Coronary Arteries. *Arteriosclerosis, Thrombosis, and Vascular Biology*, 25, 754-759.
- JOHNSON, T. W., WU, Y. X., HERDEG, C., BAUMBACH, A., NEWBY, A. C., KARSCH, K. R. & OBERHOFF, M. 2005b. Stent-based delivery of tissue inhibitor of metalloproteinase-3 adenovirus inhibits neointimal formation in porcine coronary arteries. *Arteriosclerosis Thrombosis and Vascular Biology*, 25, 754-759.
- JONER, M., FINN, A. V., FARB, A., MONT, E. K., KOLODZIE, F. D., LADICH, E., KUTYS, R., SKORIJA, K., GOLD, H. K. & VIRMANI, R. 2006. Pathology of drug-eluting stents in humans - Delayed healing and late thrombotic risk. *Journal of the American College of Cardiology*, 48, 193-202.
- KAWAMATA, Y., NAGAYAMA, Y., NAKAO, K., MIZUGUCHI, H., HAYAKAWA, T., SATO, T. & ISHII, N. 2002. Receptor-independent augmentation of adenovirus-mediated gene transfer with chitosan in vitro. *Biomaterials*, 23, 4573-4579.
- KHAMIS, H., SHOKRY, K., RAMZY, A. & SAMIR, A. 2014. Bioresorbable Vascular Scaffold (ABSORB BVS); first report in Egyptian patients with 6 month angiographic/IVUS follow up. *The Egyptian Heart Journal*, 66, 227-232.
- KIM, V. N. 2005. MicroRNA biogenesis: Coordinated cropping and dicing. *Nature Reviews Molecular Cell Biology*, 6, 376-385.

- KLUGHERZ, B. D., SONG, C., DEFELICE, S., CUI, X., LU, Z., CONNOLLY, J., HINSON, J. T., WILENSKY, R. L. & LEVY, R. J. 2002a. Gene Delivery to Pig Coronary Arteries from Stents Carrying Antibody-Tethered Adenovirus. *Human Gene Therapy*, 13, 443-454.
- KLUGHERZ, B. D., SONG, C. X., DEFELICE, S., CUI, X. M., LU, Z. B., CONNOLLY, J., HINSON, J. T., WILENSKY, R. L. & LEVY, R. J. 2002b. Gene delivery to pig coronary arteries from stents carrying antibody-tethered adenovirus. *Human Gene Therapy*, 13, 443-454.
- KOCHER, O., GABBIANI, F., GABBIANI, G., REIDY, M., COKAY, M., PETERS, H. & HÜTTNER, I. 1991. Phenotypic features of smooth muscle cells during the evolution of experimental carotid artery intimal thickening. Biochemical and morphologic studies. *Laboratory investigation; a journal of technical methods and pathology*, 65, 459-470.
- KORNOWSKI, R., HONG, M. K., TIO, F. O., BRAMWELL, O., WU, H. & LEON, M. B. 1998. In-Stent Restenosis: Contributions of Inflammatory Responses and Arterial Injury to Neointimal Hyperplasia. *Journal of the American College of Cardiology*, 31, 224-230.
- KRAITZER, A., KLOOG, Y. & ZILBERMAN, M. 2008. Approaches for prevention of restenosis. *Journal of Biomedical Materials Research Part B: Applied Biomaterials*, 85B, 583-603.
- KURO-O, M., NAGAI, R., NAKAHARA, K., KATOH, H., TSAI, R. C., TSUCHIMOCHI, H., YAZAKI, Y., OHKUBO, A. & TAKAKU, F. 1991. cDNA cloning of a myosin heavy chain isoform in embryonic smooth muscle and its expression during vascular

- development and in arteriosclerosis. *Journal of Biological Chemistry*, 266, 3768-73.
- LAGERQVIST, B., JAMES, S. K., STENESTRAND, U., LINDBÄCK, J., NILSSON, T. & WALLENTIN, L. 2007. Long-Term Outcomes with Drug-Eluting Stents versus Bare-Metal Stents in Sweden. *New England Journal of Medicine*, 356, 1009-1019.
- LAW, L. K. & DAVIDSON, B. L. 2005. What does it take to bind CAR? *Molecular Therapy*, 12, 599-609.
- LEE, Y., JEON, K., LEE, J. T., KIM, S. & KIM, V. N. 2002. MicroRNA maturation: stepwise processing and subcellular localization. *Embo Journal*, 21, 4663-4670.
- LEE, Y., KIM, M., HAN, J. J., YEOM, K. H., LEE, S., BAEK, S. H. & KIM, V. N. 2004. MicroRNA genes are transcribed by RNA polymerase II. *Embo Journal*, 23, 4051-4060.
- LEMCKERT, A. A., GRIMBERGEN, J., SMITS, S., HARTKOORN, E., HOLTERMAN, L., BERKHOUT, B., BAROUCH, D. H., VOGELS, R., QUAX, P. & GOUDSMIT, J. 2006. Generation of a novel replication-incompetent adenoviral vector derived from human adenovirus type 49: manufacture on PER. C6 cells, tropism and immunogenicity. *Journal of general virology*, 87, 2891-2899.
- LEUNG, D., GLAGOV, S. & MATHEWS, M. B. 1976. Cyclic stretching stimulates synthesis of matrix components by arterial smooth muscle cells in vitro. *Science*, 191, 475-477.
- LI, E., STUPACK, D., KLEMKE, R., CHERESH, D. A. & NEMEROW, G. R. 1998. Adenovirus Endocytosis via α V Integrins Requires

- Phosphoinositide-3-OH Kinase. *Journal of virology*, 72, 2055-2061.
- LIBBY, P., RIDKER, P. M. & HANSSON, G. K. 2011. Progress and challenges in translating the biology of atherosclerosis. *Nature*, 473, 317-325.
- LOBB, R. R. 1988. Clinical applications of heparin-binding growth factors. *European Journal of Clinical Investigation*, 18, 321-336.
- LUDMAN, P., O'NEILL, D., WHITTAKER, T. & DONALD, A. 2014. British Cardiovascular Intervention Society National Audit of Percutaneous Coronary Interventional Procedures Public Report.
- LUSIS, A. J. 2000. Atherosclerosis. *Nature*, 407, 233-241.
- MACH, F., SAUTY, A., IAROSSE, A. S., SUKHOVA, G. K., NEOTE, K., LIBBY, P. & LUSTER, A. D. 1999. Differential expression of three T lymphocyte-activating CXC chemokines by human atheroma-associated cells. *Journal of Clinical Investigation*, 104, 1041-1050.
- MAHARANA, T., MOHANTY, B. & NEGI, Y. 2009. Melt–solid polycondensation of lactic acid and its biodegradability. *Progress in polymer science*, 34, 99-124.
- MARTIN, K., BRIE, A., SAULNIER, P., PERRICAUDET, M., YEH, P. & VIGNE, E. 2003. Simultaneous CAR-and α V integrin-binding ablation fails to reduce Ad5 liver tropism. *Molecular Therapy*, 8, 485-494.
- MARX, N., WÖHRLE, J., NUSSER, T., WALCHER, D., RINKER, A., HOMBACH, V., KOENIG, W. & HÖHER, M. 2005. Pioglitazone Reduces Neointima Volume After Coronary Stent Implantation: A Randomized, Placebo-Controlled,

- Double-Blind Trial in Nondiabetic Patients. *Circulation*, 112, 2792-2798.
- MARX, S. O., JAYARAMAN, T., GO, L. O. & MARKS, A. R. 1995. Rapamycin-FKBP Inhibits Cell Cycle Regulators of Proliferation in Vascular Smooth Muscle Cells. *Circulation Research*, 76, 412-417.
- MARX, S. O., TOTARY-JAIN, H. & MARKS, A. R. 2011. Vascular smooth muscle cell proliferation in restenosis. *Circulation: Cardiovascular Interventions*, 4, 104-111.
- MAYR, U., ZOU, Y., ZHANG, Z., DIETRICH, H., HU, Y. & XU, Q. 2006. Accelerated Arteriosclerosis of Vein Grafts in Inducible NO Synthase^{-/-} Mice Is Related to Decreased Endothelial Progenitor Cell Repair. *Circulation Research*, 98, 412-420.
- MCDONALD, R. A., HALLIDAY, C. A., MILLER, A. M., DIVER, L. A., DAKIN, R. S., MONTGOMERY, J., MCBRIDE, M. W., KENNEDY, S., MCCLURE, J. D., ROBERTSON, K. E., DOUGLAS, G., CHANNON, K. M., OLDROYD, K. G. & BAKER, A. H. 2015. Reducing In-Stent Restenosis Therapeutic Manipulation of miRNA in Vascular Remodeling and Inflammation. *Journal of the American College of Cardiology*, 65, 2314-2327.
- MCDONALD, R. A., HATA, A., MACLEAN, M. R., MORRELL, N. W. & BAKER, A. H. 2012. MicroRNA and vascular remodelling in acute vascular injury and pulmonary vascular remodelling. *Cardiovasc Res*, 93, 594-604.
- MCDONALD, R. A., WHITE, K. M., WU, J. X., COOLEY, B. C., ROBERTSON, K. E., HALLIDAY, C. A., MCCLURE, J. D., FRANCIS, S., LU, R., KENNEDY, S., GEORGE, S. J., WAN, S., VAN ROOIJ, E. & BAKER, A. H. 2013. miRNA-21 is dysregulated in response to vein grafting in

- multiple models and genetic ablation in mice attenuates neointima formation. *European Heart Journal*, 34, 1636-+.
- MEISTER, G. 2013. Argonaute proteins: functional insights and emerging roles. *Nature Reviews Genetics*, 14, 447-459.
- MENG, Q., IRVINE, S., TAGALAKIS, A., MCANULTY, R., MCEWAN, J. & HART, S. 2013. Inhibition of neointimal hyperplasia in a rabbit vein graft model following non-viral transfection with human iNOS cDNA. *Gene therapy*, 20, 979-986.
- MENG, S., LIU, Z., SHEN, L., GUO, Z., CHOU, L. L., ZHONG, W., DU, Q. & GE, J. 2009a. The effect of a layer-by-layer chitosan–heparin coating on the endothelialization and coagulation properties of a coronary stent system. *Biomaterials*, 30, 2276-2283.
- MENG, S., LIU, Z. J., SHEN, L., GUO, Z., CHOU, L. S. L., ZHONG, W., DU, Q. G. & GE, J. 2009b. The effect of a layer-by-layer chitosan-heparin coating on the endothelialization and coagulation properties of a coronary stent system. *Biomaterials*, 30, 2276-2283.
- MITRA, A. K. & AGRAWAL, D. K. 2006a. In stent restenosis: bane of the stent era. *Journal of Clinical Pathology*, 59, 232-239.
- MITRA, A. K. & AGRAWAL, D. K. 2006b. In stent restenosis: bane of the stent era. *J Clin Pathol*, 59, 232-9.
- MIYOSHI, H., BLOMER, U., TAKAHASHI, M., GAGE, F. H. & VERMA, I. M. 1998. Development of a self-inactivating lentivirus vector. *Journal of Virology*, 72, 8150-8157.
- MOHR, F. W., MORICE, M.-C., KAPPETEIN, A. P., FELDMAN, T. E., STÄHLE, E., COLOMBO, A.,

- MACK, M. J., HOLMES, D. R., MOREL, M.-A. & VAN DYCK, N. 2013. Coronary artery bypass graft surgery versus percutaneous coronary intervention in patients with three-vessel disease and left main coronary disease: 5-year follow-up of the randomised, clinical SYNTAX trial. *The lancet*, 381, 629-638.
- MOLITERNO, D. J. 2005. Healing Achilles—Sirolimus versus Paclitaxel. *New England Journal of Medicine*, 353, 724-727.
- MOSES, J. W., LEON, M. B., POPMA, J. J., FITZGERALD, P. J., HOLMES, D. R., O'SHAUGHNESSY, C., CAPUTO, R. P., KEREIAKES, D. J., WILLIAMS, D. O., TEIRSTEIN, P. S., JAEGER, J. L., KUNTZ, R. E. & INVESTIGATORS, S. 2003. Sirolimus-eluting stents versus standard stents in patients with stenosis in a native coronary artery. *New England Journal of Medicine*, 349, 1315-1323.
- MURUVE, D. A., PÉTRILLI, V., ZAISS, A. K., WHITE, L. R., CLARK, S. A., ROSS, P. J., PARKS, R. J. & TSCHOPP, J. 2008. The inflammasome recognizes cytosolic microbial and host DNA and triggers an innate immune response. *Nature*, 452, 103-107.
- NABEL, E. G. 2002. CDKS and CKIS: Molecular targets for tissue remodelling. *Nat Rev Drug Discov*, 1, 587-598.
- NASHEF, S. A. M., ROQUES, F., MICHEL, P., GAUDUCHEAU, E., LEMESHOW, S., SALAMON, R. & GROUP, T. E. S. S. 1999. European system for cardiac operative risk evaluation (EuroSCORE). *European Journal of Cardio-Thoracic Surgery*, 16, 9-13.

NASHEF, S. A., ROQUES, F., SHARPLES, L. D., NILSSON, J., SMITH, C., GOLDSTONE, A. R. & LOCKOWANDT, U. 2012. Euroscore ii. *European journal of cardio-thoracic surgery*, ezs043.

NHS. 2015. Available:

<http://www.nhs.uk/conditions/Cardiovascular-disease/Pages/Introduction.aspx>.

NICE 2003. Guidance on the use of coronary artery stents.

NICKLIN, S. & BAKER, A. 1999. Simple Methods for Preparing Recombinant Adenoviruses for High-Efficiency Transduction of Vascular Cells. *In*: BAKER, A. (ed.) *Vascular Disease*. Humana Press.

NICKLIN, S. A., BUENING, H., DISHART, K. L., DE ALWIS, M., GIROD, A., HACKER, U., THRASHER, A. J., ALI, R. R., HALLEK, M. & BAKER, A. H. 2001. Efficient and selective AAV2-mediated gene transfer directed to human vascular endothelial cells. *Molecular Therapy*, 4, 174-181.

NIH 2015. What Causes Atherosclerosis?

NIINOMI, M. 2002. Recent metallic materials for biomedical applications. *Metallurgical and materials transactions A*, 33, 477-486.

O'BRIEN, B. & CARROLL, W. 2009. The evolution of cardiovascular stent materials and surfaces in response to clinical drivers: a review. *Acta biomaterialia*, 5, 945-958.

OKA, K., PASTORE, L., KIM, I.-H., MERCHED, A., NOMURA, S., LEE, H.-J., MERCHED-SAUVAGE, M., ARDEN-RILEY, C., LEE, B. & FINEGOLD, M. 2001. Long-Term Stable Correction of Low-Density Lipoprotein Receptor-Deficient Mice With a Helper-Dependent Adenoviral Vector Expressing

- the Very Low-Density Lipoprotein Receptor. *Circulation*, 103, 1274-1281.
- OSHEROV, A. B., GOTHA, L., CHEEMA, A. N., QIANG, B. & STRAUSS, B. H. 2011. Proteins mediating collagen biosynthesis and accumulation in arterial repair: novel targets for anti-restenosis therapy. *Cardiovascular research*, 91, 16-26.
- PARKER, A., WHITE, K., LAVERY, C., CUSTERS, J., WADDINGTON, S. & BAKER, A. 2013. Pseudotyping the adenovirus serotype 5 capsid with both the fibre and penton of serotype 35 enhances vascular smooth muscle cell transduction. *Gene therapy*, 20, 1158-1164.
- PARKES, R., MENG, Q. H., ELENA SIAPATI, K., MCEWAN, J. R. & HART, S. L. 2002. High efficiency transfection of porcine vascular cells in vitro with a synthetic vector system. *The journal of gene medicine*, 4, 292-299.
- PAVINATTO, A., PAVINATTO, F. J. & BARROS-TIMMONS, A. 2009. Electrostatic interactions are not sufficient to account for chitosan bioactivity. *ACS applied materials & interfaces*, 2, 246-251.
- PFISTERER, M., BRUNNER-LA ROCCA, H. P., BUSER, P. T., RICKENBACHER, P., HUNZIKER, P., MUELLER, C., JEGER, R., BADER, F., OSSWALD, S. & KAISER, C. 2006. Late Clinical Events After Clopidogrel Discontinuation May Limit the Benefit of Drug-Eluting Stents An Observational Study of Drug-Eluting Versus Bare-Metal Stents. *Journal of the American College of Cardiology*, 48, 2584-2591.
- RANJZAD, P., SALEM, H. & KINGSTON, P. 2009. Adenovirus-mediated gene transfer of fibromodulin inhibits neointimal hyperplasia in an

- organ culture model of human saphenous vein graft disease. *Gene therapy*, 16, 1154-1162.
- RAPER, S. E., CHIRMULE, N., LEE, F. S., WIVEL, N. A., BAGG, A., GAO, G.-P., WILSON, J. M. & BATSHAW, M. L. 2003. Fatal systemic inflammatory response syndrome in a ornithine transcarbamylase deficient patient following adenoviral gene transfer. *Molecular genetics and metabolism*, 80, 148-158.
- RASAL, R. M., JANORKAR, A. V. & HIRT, D. E. 2010. Poly (lactic acid) modifications. *Progress in polymer science*, 35, 338-356.
- RHOADES, M. W., REINHART, B. J., LIM, L. P., BURGE, C. B., BARTEL, B. & BARTEL, D. P. 2002. Prediction of plant microRNA targets. *Cell*, 110, 513-520.
- RINAUDO, M., PAVLOV, G. & DESBRIERES, J. 1999. Influence of acetic acid concentration on the solubilization of chitosan. *Polymer*, 40, 7029-7032.
- ROBERTSON, K. E., MCDONALD, R. A., OLDROYD, K. G., NICKLIN, S. A. & BAKER, A. H. 2012. Prevention of coronary in-stent restenosis and vein graft failure: Does vascular gene therapy have a role? *Pharmacology & therapeutics*, 136, 23-34.
- ROSENBERG, S. A., AEBERSOLD, P., CORNETTA, K., KASID, A., MORGAN, R. A., MOEN, R., KARSON, E. M., LOTZE, M. T., YANG, J. C., TOPALIAN, S. L., MERINO, M. J., CULVER, K., MILLER, A. D., BLAESE, R. M. & ANDERSON, W. F. 1990. Gene Transfer into Humans — Immunotherapy of Patients with Advanced Melanoma, Using Tumor-Infiltrating Lymphocytes Modified by Retroviral Gene Transduction. *New England Journal of Medicine*, 323, 570-578.

- RUMBAUT, R. E. & THIAGARAJAN, P. 2010. Platelet-Vessel Wall Interactions in Hemostasis and Thrombosis. *Colloquium Series on Integrated Systems Physiology: From Molecule to Function*, 2, 1-75.
- RUSSELL, W. 2009. Adenoviruses: update on structure and function. *Journal of General Virology*, 90, 1-20.
- RUTANEN, J., TURUNEN, A. M., TEITTINEN, M., RISSANEN, T. T., HEIKURA, T., KOPONEN, J. K., GRUCHALA, M., INKALA, M., JAUHAINEN, S., HILTUNEN, M. O., TURUNEN, M. P., STACKER, S. A., ACHEN, M. G. & YLA-HERTTUALA, S. 2005. Gene transfer using the mature form of VEGF-D reduces neointimal thickening through nitric oxide-dependent mechanism. *Gene Ther*, 12, 980-987.
- SALIC, A. & MITCHISON, T. J. 2008. A chemical method for fast and sensitive detection of DNA synthesis in vivo. *Proceedings of the National Academy of Sciences*, 105, 2415-2420.
- SANBORN, T. A., FAXON, D., HAUDENSCHILD, C., GOTTSMAN, S. & RYAN, T. 1983. The mechanism of transluminal angioplasty: evidence for formation of aneurysms in experimental atherosclerosis. *Circulation*, 68, 1136-1140.
- SANTULLI, G., WRONSKA, A., URYU, K., DIACOVO, T. G., GAO, M., MARX, S. O., KITAJEWSKI, J., CHILTON, J. M., AKAT, K. M. & TUSCHL, T. 2014. A selective microRNA-based strategy inhibits restenosis while preserving endothelial function. *The Journal of clinical investigation*, 124, 4102.
- SAURER, E. M., JEWELL, C. M., ROENNEBURG, D. A., BECHLER, S. L., TORREALBA, J. R.,

- HACKER, T. A. & LYNN, D. M. 2013. Polyelectrolyte Multilayers Promote Stent-Mediated Delivery of DNA to Vascular Tissue. *Biomacromolecules*, 14, 1696-1704.
- SAURER, E. M., YAMANOUCHI, D., LIU, B. & LYNN, D. M. 2011. Delivery of plasmid DNA to vascular tissue in vivo using catheter balloons coated with polyelectrolyte multilayers. *Biomaterials*, 32, 610-618.
- SCHMITTGEN, T. D. & LIVAK, K. J. 2008. Analyzing real-time PCR data by the comparative CT method. *Nat. Protocols*, 3, 1101-1108.
- SCHOENHAGEN, P., ZIADA, K. M., VINCE, D. G., NISSEN, S. E. & TUZCU, E. M. 2001. Arterial remodeling and coronary artery disease: the concept of "dilated" versus "obstructive" coronary atherosclerosis. *Journal of the American College of Cardiology*, 38, 297-306
- SCHOGGINS, J. W. & FALCK-PEDERSEN, E. 2006. Fiber and penton base capsid modifications yield diminished adenovirus type 5 transduction and proinflammatory gene expression with retention of antigen-specific humoral immunity. *Journal of virology*, 80, 10634-10644.
- SELBACH, M., SCHWANHAUSSER, B., THIERFELDER, N., FANG, Z., KHANIN, R. & RAJEWSKY, N. 2008. Widespread changes in protein synthesis induced by microRNAs. *Nature*, 455, 58-63.
- SERRUYS, P. W., DE JAEGERE, P., KIEMENEIJ, F., MACAYA, C., RUTSCH, W., HEYNDRICKX, G., EMANUELSSON, H., MARCO, J., LEGRAND, V. & MATERNE, P. 1994. A comparison of balloon-expandable-stent implantation with balloon angioplasty in patients with coronary artery

- disease. *New England Journal of Medicine*, 331, 489-495.
- SERRUYS, P. W., GARCIA-GARCIA, H. M. & ONUMA, Y. 2012. From metallic cages to transient bioresorbable scaffolds: change in paradigm of coronary revascularization in the upcoming decade? *European Heart Journal*, 33, 16-25.
- SERRUYS, P. W., MORICE, M.-C., KAPPETEIN, A. P., COLOMBO, A., HOLMES, D. R., MACK, M. J., STÄHLE, E., FELDMAN, T. E., VAN DEN BRAND, M., BASS, E. J., VAN DYCK, N., LEADLEY, K., DAWKINS, K. D. & MOHR, F. W. 2009. Percutaneous Coronary Intervention versus Coronary-Artery Bypass Grafting for Severe Coronary Artery Disease. *New England Journal of Medicine*, 360, 961-972.
- SHARIF, F., HYNES, S. O., COONEY, R., HOWARD, L., MCMAHON, J., DALY, K., CROWLEY, J., BARRY, F. & O'BRIEN, T. 2008. Gene-eluting stents: adenovirus-mediated delivery of eNOS to the blood vessel wall accelerates re-endothelialization and inhibits restenosis. *Molecular Therapy*, 16, 1674-80.
- SHARIF, F., HYNES, S. O., MCCULLAGH, K., GANLEY, S., GREISER, U., MCHUGH, P., CROWLEY, J., BARRY, F. & O'BRIEN, T. 2012. Gene-eluting stents: non-viral, liposome-based gene delivery of eNOS to the blood vessel wall in vivo results in enhanced endothelialization but does not reduce restenosis in a hypercholesterolemic model. *Gene therapy*, 19, 321-328.
- SHARIF, F., HYNES, S. O., MCMAHON, J., COONEY, R., CONROY, S., DOCKERY, P., DUFFY, G.,

- DALY, K., CROWLEY, J., BARTLETT, J. S. & O'BRIEN, T. 2006. Gene-Eluting Stents: Comparison of Adenoviral and Adeno- Associated Viral Gene Delivery to the Blood Vessel Wall In Vivo. *Human Gene Therapy*, 17, 741-750.
- SHEDDEN, L., OLDROYD, K. & CONNOLLY, P. 2009. Current issues in coronary stent technology. *Proceedings of the Institution of Mechanical Engineers, Part H: Journal of Engineering in Medicine*, 223, 515-524.
- SHIROTA, T., YASUI, H., SHIMOKAWA, H. & MATSUDA, T. 2003. Fabrication of endothelial progenitor cell (EPC)-seeded intravascular stent devices and in vitro endothelialization on hybrid vascular tissue. *Biomaterials*, 24, 2295-2302.
- SIGWART, U., PUEL, J., MIRKOVITCH, V., JOFFRE, F. & KAPPENBERGER, L. 1987. Intravascular stents to prevent occlusion and re-stenosis after transluminal angioplasty. *New England Journal of Medicine*, 316, 701-706.
- SIMARI, R. D., SAN, H., REKHTER, M., OHNO, T., GORDON, D., NABEL, G. J. & NABEL, E. G. 1996. Regulation of cellular proliferation and intimal formation following balloon injury in atherosclerotic rabbit arteries. *Journal of Clinical Investigation*, 98, 225.
- SMITH JR, S., DOVE, J., JACOBS, A., KENNEDY, J., KEREIAKES, D., KERN, M., KUNTZ, R., POPMA, J., SCHAFF, H. & WILLIAMS, D. 2001. Society for Cardiac Angiography and Interventions. ACC/AHA guidelines for percutaneous coronary intervention (revision of the 1993 PTCA guidelines)-executive summary: a report of the American College of Cardiology/American Heart Association task force on practice guidelines (Committee to revise the

1993 guidelines for percutaneous transluminal coronary angioplasty) endorsed by the Society for Cardiac Angiography and Interventions.

Circulation, 103, 3019-3041.

SPARANO, J. A., BERNARDO, P., STEPHENSON, P., GRADISHAR, W. J., INGLE, J. N., ZUCKER, S. & DAVIDSON, N. E. 2004. Randomized Phase III Trial of Marimastat Versus Placebo in Patients With Metastatic Breast Cancer Who Have Responding or Stable Disease After First-Line Chemotherapy: Eastern Cooperative Oncology Group Trial E2196. *Journal of Clinical Oncology*, 22, 4683-4690.

SPRUGEL, K., MCPHERSON, J., CLOWES, A. & ROSS, R. 1987. Effects of growth factors in vivo. I. Cell ingrowth into porous subcutaneous chambers. *The American journal of pathology*, 129, 601.

STEFANINI, G. G., TANIWAKI, M. & WINDECKER, S. 2013. Coronary stents: novel developments. *Heart*, 100, 1051-1061.

STONE, D., LIU, Y., SHAYAKHMETOV, D., LI, Z.-Y., NI, S. & LIEBER, A. 2007a. Adenovirus-platelet interaction in blood causes virus sequestration to the reticuloendothelial system of the liver. *Journal of virology*, 81, 4866-4871.

STONE, G. W., ELLIS, S. G., COX, D. A., HERMILLER, J., O'SHAUGHNESSY, C., MANN, J. T., TURCO, M., CAPUTO, R., BERGIN, P., GREENBERG, J., POPMA, J. J., RUSSELL, M. E. & INVESTIGATORS, T.-I. 2004. A polymer-based, paclitaxel-eluting stent in patients with coronary artery disease. *New England Journal of Medicine*, 350, 221-231.

- STONE, G. W., MOSES, J. W., ELLIS, S. G., SCHOFFER, J., DAWKINS, K. D., MORICE, M.-C., COLOMBO, A., SCHAMPAERT, E., GRUBE, E. & KIRTANE, A. J. 2007b. Safety and efficacy of sirolimus-and paclitaxel-eluting coronary stents. *New England Journal of Medicine*, 356, 998-1008.
- SU, C.-H., WU, Y.-J., WANG, H.-H. & YEH, H.-I. 2012. Nonviral gene therapy targeting cardiovascular system. *American Journal of Physiology-Heart and Circulatory Physiology*, 303, H629-H638.
- SUMIDA, S. M., TRUITT, D. M., LEMCKERT, A. A. C., VOGELS, R., CUSTERS, J. H. H. V., ADDO, M. M., LOCKMAN, S., PETER, T., PEYERL, F. W., KISHKO, M. G., JACKSON, S. S., GORGONE, D. A., LIFTON, M. A., ESSEX, M., WALKER, B. D., GOUDSMIT, J., HAVENGA, M. J. E. & BAROUCH, D. H. 2005. Neutralizing Antibodies to Adenovirus Serotype 5 Vaccine Vectors Are Directed Primarily against the Adenovirus Hexon Protein. *The Journal of Immunology*, 174, 7179-7185.
- SUMMERFORD, C. & SAMULSKI, R. J. 1998. Membrane-associated heparan sulfate proteoglycan is a receptor for adeno-associated virus type 2 virions. *Journal of Virology*, 72, 1438-1445.
- TANNER, F. C., YANG, Z.-Y., DUCKERS, E., GORDON, D., NABEL, G. J. & NABEL, E. G. 1998. Expression of Cyclin-Dependent Kinase Inhibitors in Vascular Disease. *Circulation Research*, 82, 396-403.
- VON BURKERSRODA, F., SCHEDL, L. & GÖPFERICH, A. 2002. Why degradable polymers undergo surface erosion or bulk erosion. *Biomaterials*, 23, 4221-4231.

- VIRMANI, R., FARB, A., GUAGLIUMI, G. & KOLODZIE, F. D. 2004. Drug-eluting stents: caution and concerns for long-term outcome. *Coronary artery disease*, 15, 313-318.
- VOLPERS, C. & KOCHANNEK, S. 2004. Adenoviral vectors for gene transfer and therapy. *The Journal of Gene Medicine*, 6, S164-S171.
- VON SEGGERN, D. J., KEHLER, J., ENDO, R. I. & NEMEROW, G. R. 1998. Complementation of a fibre mutant adenovirus by packaging cell lines stably expressing the adenovirus type 5 fibre protein. *Journal of General Virology*, 79, 1461-1468.
- WADDINGTON, S. N., MCVEY, J. H., BHELLA, D., PARKER, A. L., BARKER, K., ATODA, H., PINK, R., BUCKLEY, S. M., GREIG, J. A. & DENBY, L. 2008. Adenovirus serotype 5 hexon mediates liver gene transfer. *Cell*, 132, 397-409.
- WALKER, L. N., BOWEN-POPE, D. F., ROSS, R. & REIDY, M. A. 1986. Production of platelet-derived growth factor-like molecules by cultured arterial smooth muscle cells accompanies proliferation after arterial injury. *Proceedings of the National Academy of Sciences of the United States of America*, 83, 7311-7315.
- WANG, B. B., LI, S. Q., QI, H. H., CHOWDHURY, D., SHI, Y. & NOVINA, C. D. 2009. Distinct passenger strand and mRNA cleavage activities of human Argonaute proteins. *Nature Structural & Molecular Biology*, 16, 1259-U76.
- WANG, D., DEUSE, T., STUBBENDORFF, M., CHERNOGUBOVA, E., ERBEN, R. G., EKEN, S. M., JIN, H., HEEGER, C., BEHNISCH, B., REICHENSPURNER, H., ROBBINS, R. C., SPIN, J. M., TSAO, P. S., MAEGDEFESSEL, L. &

- SCHREPFER, S. 2015. Coronary Allograft Arteriosclerosis: Local MicroRNA Modulation Using a Novel Anti-Mir-21-Eluting Stent Prevents in-Stent Restenosis. *Journal of Heart and Lung Transplantation*, 34, S39-S39.
- WANG, J. C. & BENNETT, M. 2012. Aging and Atherosclerosis: Mechanisms, Functional Consequences, and Potential Therapeutics for Cellular Senescence. *Circulation Research*, 111, 245-259.
- WANG, Q., CHAN, T. R., HILGRAF, R., FOKIN, V. V., SHARPLESS, K. B. & FINN, M. 2003. Bioconjugation by copper (I)-catalyzed azide-alkyne [3+ 2] cycloaddition. *Journal of the American Chemical Society*, 125, 3192-3193.
- WELT, F. G. & ROGERS, C. 2002. Inflammation and restenosis in the stent era. *Arteriosclerosis, thrombosis, and vascular biology*, 22, 1769-1776.
- WHO 2015. World Health Organisation Cardiovascular diseases (CVDs), Fact Sheet 317.
- WICKHAM, T. J., MATHIAS, P., CHERESH, D. A. & NEMEROW, G. R. 1993. Integrins $\alpha v \beta 3$ and $\alpha v \beta 5$ promote adenovirus internalization but not virus attachment. *Cell*, 73, 309-319.
- WIEBE, J., NEF, H. M. & HAMM, C. W. 2014. Current Status of Bioresorbable Scaffolds in the Treatment of Coronary Artery Disease. *Journal of the American College of Cardiology*, 64, 2541-2551.
- WILEY. 2015. *Vectors used in gene therapy trials worldwide* [Online]. Available: <http://www.abedia.com/wiley/vectors.php>.
- WILLIAMS, P. D., RANJZAD, P., KAKAR, S. J. & KINGSTON, P. A. 2010. Development of Viral Vectors for Use in Cardiovascular Gene Therapy. *Viruses-Basel*, 2, 334-371.

- WINDECKER, S., KOLH, P., ALFONSO, F., COLLET, J.-P., CREMER, J., FALK, V., FILIPPATOS, G., HAMM, C., HEAD, S. J. & JÜNI, P. 2014. 2014 ESC/EACTS Guidelines on myocardial revascularization. *European heart journal*, ehu278.
- WORGALL, S., WOLFF, G., FALCK-PEDERSEN, E. & CRYSTAL, R. G. 1997. Innate immune mechanisms dominate elimination of adenoviral vectors following in vivo administration. *Human gene therapy*, 8, 37-44.
- WORK, L. M., NICKLIN, S. A., BRAIN, N. J. R., DISHART, K. L., VON SEGGERN, D. J., HALLEK, M., BUNING, H. & BAKER, A. H. 2004. Development of efficient viral vectors selective for vascular smooth muscle cells. *Molecular Therapy*, 9, 198-208.
- WU, Z. J., ASOKAN, A. & SAMULSKI, R. J. 2006. Adeno-associated virus serotypes: Vector toolkit for human gene therapy. *Molecular Therapy*, 14, 316-327.
- YANG, J., WAN, Y., TU, C., CAI, Q., BEI, J. & WANG, S. 2003. Enhancing the cell affinity of macroporous poly(L-lactide) cell scaffold by a convenient surface modification method. *Polymer International*, 52, 1892-1899.
- YEH, R. W., NORMAND, S.-L. T., WOLF, R. E., JONES, P. G., HO, K. K., COHEN, D. J., CUTLIP, D. E., MAURI, L., KUGELMASS, A. D. & AMIN, A. P. 2011. Predicting the restenosis benefit of drug-eluting versus bare metal stents in percutaneous coronary intervention. *Circulation*, 124, 1557-1564.
- YI, R., QIN, Y., MACARA, I. G. & CULLEN, B. R. 2003. Exportin-5 mediates the nuclear export of pre-

- microRNAs and short hairpin RNAs. *Genes & Development*, 17, 3011-3016.
- YIN, K. & AGRAWAL, D. 2014. Gene therapy for in-stent restenosis: Targets and delivery system. *Current Research: Cardiology*, 1, 93-101.
- YOO, P. J., NAM, K. T., BELCHER, A. M. & HAMMOND, P. T. 2008. Solvent-assisted patterning of polyelectrolyte multilayers and selective deposition of virus assemblies. *Nano letters*, 8, 1081-1089.
- ZENG, Y., YI, R. & CULLEN, B. R. 2003. MicroRNAs and small interfering RNAs can inhibit mRNA expression by similar mechanisms. *Proceedings of the National Academy of Sciences of the United States of America*, 100, 9779-9784.
- ZHANG, Y., WANG, Z. J. & GEMEINHART, R. A. 2013. Progress in microRNA delivery. *Journal of Controlled Release*, 172, 962-974.
- ZHONG, H., LEI, X., QIN, L., WANG, J. & HUNG, T. 2011. Augmentation of adenovirus 5 vector-mediated gene transduction under physiological pH conditions by a chitosan/NaHCO₃ solution. *Gene Ther*, 18, 232-239.